



Universiteit  
Leiden  
The Netherlands

## Computed tomography coronary angiography : from quantification of coronary atherosclerosis to risk stratification of patients

Graaf, M.A. de

### Citation

Graaf, M. A. de. (2016, November 8). *Computed tomography coronary angiography : from quantification of coronary atherosclerosis to risk stratification of patients*. Retrieved from <https://hdl.handle.net/1887/43967>

Version: Not Applicable (or Unknown)

License: [Licence agreement concerning inclusion of doctoral thesis in the Institutional Repository of the University of Leiden](#)

Downloaded from: <https://hdl.handle.net/1887/43967>

**Note:** To cite this publication please use the final published version (if applicable).

Cover Page



Universiteit Leiden



The handle <http://hdl.handle.net/1887/43967> holds various files of this Leiden University dissertation

**Author:** Graaf, Michiel A. de

**Title:** Computed tomography coronary angiography : from quantification of coronary atherosclerosis to risk stratification of patients

**Issue Date:** 2016-11-08

**Computed tomography coronary angiography:  
From quantification of coronary atherosclerosis  
to risk stratification of patients**

The research described in this thesis was performed at the Department of Cardiology of the Leiden University Medical Center, Leiden, The Netherlands

Lay-out: Optima Grafische Communicatie

Printed by: Optima Grafische Communicatie

ISBN: 978-94-6169-939-8

Financial support for the costs associated with the publication of this thesis was gratefully received from: Amgen, Bayer, Biotronik, Medis medical imaging systems, Pfizer, Sanofi, Servier

Financial support by the Dutch Heart Foundation for the publication of this thesis is gratefully acknowledged.

# **Computed tomography coronary angiography: From quantification of coronary atherosclerosis to risk stratification of patients**

## **Proefschrift**

Ter verkrijging van  
de graad van Doctor aan de Universiteit Leiden,  
op gezag van Rector Magnificus prof.mr. C.J.J.M. Stolker,  
volgens besluit van het College van Promoties  
te verdedigen op

dinsdag 8 november 2016 klokke 13.45 uur

Door

Michiel Alexander de Graaf  
Geboren te Woerden in 1988

**Promotores**

Prof. dr. Jeroen J. Bax

Prof. dr. J. Wouter Jukema

**Co-promotor**

Dr. Arthur J. Scholte

**Promotiecommissie**

- Prof. dr. ir. B.P.F. Lelieveldt
- Prof. dr. ir. J.H.C. Reiber
- Prof. dr. M.J. Schalij
- Prof. dr. W. J. Niessen
- Prof. dr. J. Knuuti
- Prof. dr. L-F. de Geus-Oei

(Erasmus MC)

(Turku, PET Centre, Finland)

# Thesis outline

<b>Chapter 1</b>	General introduction and outline	9
<b>Chapter 2</b>	Computed tomography angiography and other applications of CT	17
<b>Part 1</b>	Quantitative assessment of coronary atherosclerosis on coronary CTA	55
<b>Chapter 3</b>	High coronary plaque load: a heavy burden.	57
<b>Chapter 4</b>	Automatic quantification and characterization of coronary atherosclerosis with computed tomography coronary angiography: cross-correlation with intravascular ultrasound virtual histology.	65
<b>Chapter 5</b>	Enhanced characterization of calcified areas in intravascular ultrasound virtual histology images by quantification of the acoustic shadow: validation against computed tomography coronary angiography.	89
<b>Chapter 6</b>	Automatic detection and quantification of the Agatston coronary artery calcium score on contrast computed tomography angiography.	107
<b>Chapter 7</b>	Automated quantitative coronary computed tomography correlates of myocardial ischaemia on gated myocardial perfusion SPECT.	127
<b>Chapter 8</b>	Feasibility of an automated quantitative computed tomography angiography-derived risk score for risk stratification of patients with suspected coronary artery disease.	147
<b>Chapter 9</b>	Feasibility of automated quantitative assessment of serial computed tomography angiography to detect changes in coronary atherosclerosis.	167
<b>Part 2</b>	Clinical aspects coronary CTA in high risk diabetic patients without chest pain syndrome	185
<b>Chapter 10</b>	Changes in ischaemia as assessed with single-photon emission computed tomography myocardial perfusion imaging in high-risk patients with diabetes without cardiac symptoms: relation with coronary atherosclerosis on computed tomography coronary angiography.	187

<b>Chapter 11</b> Prognostic value of coronary computed tomography angiography in high risk diabetic patients without chest pain syndrome.	205
<b>Chapter 12</b> Summary and conclusions	229
<b>Chapter 13</b> Samenvatting en conclusies	237
List of publications	245
Dankwoord	251
Curriculum Vitae	253





# Chapter 1

General introduction and outline



## Introduction

Around 1970 computed tomography (CT) entered the field of clinical imaging tools. In those days both the spatial and temporal resolution of CT were insufficient for cardiac imaging. With the introduction of 4-slice CT in the late 1990s, visualization of coronary arteries became feasible. Nowadays computed tomography coronary angiography (CTA) is considered a suitable non-invasive method for the assessments of coronary atherosclerosis; its clinical applicability is widely incorporated in current guidelines.<sup>1,2</sup> Coronary stenosis severity on CTA is strongly correlated with invasive coronary angiography, and the diagnostic accuracy for the presence of coronary artery disease (CAD) is excellent. Especially the high sensitivity (~ 98%) allows for accurate rule-out of disease in patients with suspected CAD.<sup>3</sup> Additionally, the prognostic value of CTA has been established in the past years.<sup>4</sup> The prognosis of patients is decreased with increasing number of obstructive ( $\geq 50\%$  stenosis) lesions.<sup>5</sup> Most importantly, the prognosis of patients without CAD on coronary CTA is excellent. Moreover, it has been noted, that also the presence of non-obstructive CAD is associated with impaired prognosis.<sup>6</sup> This has led to an increasing interest in the clinical value of coronary atherosclerosis burden in addition to only assessing the presence of obstructive CAD. On coronary CTA, plaque composition can also be assessed. Traditionally, coronary plaque is classified as non-calcified, partially plaque or calcified plaque. In several studies, the prognostic implications of the presence of different plaque types have been established.<sup>7,8</sup> Patients with non-calcified and partially calcified plaque have a worse prognosis compared to patients with only calcified plaques. Currently the field of research in cardiac CT is shifting towards assessment of overall atherosclerotic burden and incorporating additional features of coronary CTA, besides obstructive CAD, for risk stratification of patients.

### **Quantification of coronary atherosclerosis.**

In current practice the assessment of CAD on coronary CTA is performed visually. However, for accurate and reproducible assessment of the dimension and composition of coronary atherosclerosis, a quantitative approach would be favorable. Recently, novel software algorithms have become available which allow for such a quantitative analysis.<sup>9</sup> Using this software, the burden of coronary atherosclerosis, the three-dimensional dimensions (i.e. diameters and volumes) and the exact degree of stenosis can be quantified. Moreover, this software allows for assessment of composition of coronary atherosclerosis using Hounsfield Unit (HU) thresholds. The accuracy of this software for quantification of atherosclerosis dimensions has been recently established.<sup>10</sup>

This thesis further investigates the accuracy of this software, especially for quantification of coronary plaque composition. Additionally, the clinical value of this quantification algorithm will be explored.

### **Diabetic patients without chest pain syndrome.**

Cardiovascular death is the main cause of death in patients with diabetes mellitus (DM).<sup>11</sup> Additionally, patients with DM often have silent myocardial ischemia and CAD in an advanced stage before becoming manifest.<sup>12</sup> However, in these patients traditional cardiovascular risk factors fail to accurately predict diabetic patients' risk.<sup>13</sup> In the past years the value of different imaging modalities in the specific setting of asymptomatic patients with DM has been addressed.<sup>14</sup>

This thesis explores the prognostic value of coronary CTA in these high risk diabetic patients. Furthermore, the change in ischemia over-time is investigated, focusing on the role of coronary CTA to predict these changes.

## **Outline**

This thesis focuses on the clinical value of quantification of coronary atherosclerosis on coronary CTA. Moreover, the value of coronary CTA in high risk diabetic patients without chest pain syndrome in clinical practice is assessed. This thesis is preceded by **Chapter 2** which provides an overview of the clinical use of computed tomography coronary angiography (CTA) and the application in acute cardiac care.

**Part 1** of this thesis focuses on the quantitative assessment of coronary atherosclerosis on coronary CTA.

**Chapter 3** describes the different imaging techniques for analysis of coronary atherosclerosis. In **Chapter 4** the feasibility of an automatic algorithm for coronary atherosclerotic tissue characterization is established and compared to IVUS VH.

**Chapter 5** continues the study of Chapter 4 and discusses a novel method to enhance the characterization of calcified areas in IVUS VH by quantification of the acoustic shadow. This acoustic shadow is the result of the inability of the IVUS signal to penetrate calcium, and considered a major limitation of this technique. **Chapter 6** assesses the accuracy of a novel algorithm to automatically detect and quantify the Agatston coronary artery calcium score on contrast CTA. In **Chapter 7** the parameters of coronary atherosclerosis as derived from quantitative coronary computed tomography (QCT) are correlated to the presence of myocardial ischemia on gated myocardial perfusion single photon emission computed tomography (SPECT). In **Chapter 8**, a novel CTA risk score is introduced which integrates the location, severity

and composition of coronary atherosclerosis on CTA in one score. The value of this automated QCT-derived risk score for risk stratification is assessed in patients with suspected coronary artery disease. In **Chapter 9**, the value of CTA for serial imaging of coronary atherosclerosis is investigated. For this purpose, QCT is performed in patients who underwent serial CTA with a 2-year interval.

**Part 2** of this thesis focuses on the clinical aspects of coronary atherosclerosis on coronary CTA in high risk diabetic patients without chest pain syndrome.

**Chapter 10** investigates the changes in ischemia over time as assessed with SPECT myocardial perfusion imaging in relation to characteristics of coronary atherosclerosis on coronary CTA. In **Chapter 11** the long-term prognostic value of coronary CTA in high risk diabetic patients without cardiac symptoms is assessed.

## References

- (1) Montalescot G, Sechtem U, Achenbach S *et al.* 2013 ESC guidelines on the management of stable coronary artery disease: The Task Force on the management of stable coronary artery disease of the European Society of Cardiology. *Eur Heart J* 2013 August 30.
- (2) Taylor AJ, Cerqueira M, Hodgson JM *et al.* ACCF/SCCT/ACR/AHA/ASE/ASNC/NASCI/SCAI/SCMR 2010 appropriate use criteria for cardiac computed tomography. A report of the American College of Cardiology Foundation Appropriate Use Criteria Task Force, the Society of Cardiovascular Computed Tomography, the American College of Radiology, the American Heart Association, the American Society of Echocardiography, the American Society of Nuclear Cardiology, the North American Society for Cardiovascular Imaging, the Society for Cardiovascular Angiography and Interventions, and the Society for Cardiovascular Magnetic Resonance. *J Am Coll Cardiol* 2010 November 23;56(22):1864-94.
- (3) von Ballmoos MW, Haring B, Juillerat P, Alkadhi H. Meta-analysis: diagnostic performance of low-radiation-dose coronary computed tomography angiography. *Ann Intern Med* 2011 March 15;154(6):413-20.
- (4) Bamberg F, Sommer WH, Hoffmann V *et al.* Meta-analysis and systematic review of the long-term predictive value of assessment of coronary atherosclerosis by contrast-enhanced coronary computed tomography angiography. *J Am Coll Cardiol* 2011 June 14;57(24):2426-36.
- (5) Min JK, Shaw LJ, Devereux RB *et al.* Prognostic value of multidetector coronary computed tomographic angiography for prediction of all-cause mortality. *J Am Coll Cardiol* 2007 September 18;50(12):1161-70.
- (6) Lin FY, Shaw LJ, Dunning AM *et al.* Mortality risk in symptomatic patients with nonobstructive coronary artery disease: a prospective 2-center study of 2,583 patients undergoing 64-detector row coronary computed tomographic angiography. *J Am Coll Cardiol* 2011 July 26;58(5):510-9.
- (7) Gaemperli O, Valenta I, Schepis T *et al.* Coronary 64-slice CT angiography predicts outcome in patients with known or suspected coronary artery disease. *Eur Radiol* 2008 June;18(6):1162-73.
- (8) van Werkhoven JM, Schuijff JD, Gaemperli O *et al.* Incremental prognostic value of multi-slice computed tomography coronary angiography over coronary artery calcium scoring in patients with suspected coronary artery disease. *Eur Heart J* 2009 November;30(21):2622-9.
- (9) Boogers MJ, Broersen A, van Velzen JE *et al.* Automated quantification of coronary plaque with computed tomography: comparison with intravascular ultrasound using a dedicated registration algorithm for fusion-based quantification. *Eur Heart J* 2012 April;33(8):1007-16.
- (10) Voros S, Rinehart S, Qian Z *et al.* Coronary atherosclerosis imaging by coronary CT angiography: current status, correlation with intravascular interrogation and meta-analysis. *JACC Cardiovasc Imaging* 2011 May;4(5):537-48.
- (11) Morrish NJ, Wang SL, Stevens LK, Fuller JH, Keen H. Mortality and causes of death in the WHO Multinational Study of Vascular Disease in Diabetes. *Diabetologia* 2001 September;44 Suppl 2:S14-S21.
- (12) Zellweger MJ, Hachamovitch R, Kang X *et al.* Prognostic relevance of symptoms versus objective evidence of coronary artery disease in diabetic patients. *Eur Heart J* 2004 April;25(7):543-50.
- (13) van Dieren S, Beulens JW, Kengne AP *et al.* Prediction models for the risk of cardiovascular disease in patients with type 2 diabetes: a systematic review. *Heart* 2012 March;98(5):360-9.

- (14) Bax JJ, Young LH, Frye RL, Bonow RO, Steinberg HO, Barrett EJ. Screening for coronary artery disease in patients with diabetes. *Diabetes Care* 2007 October;30(10):2729-36.



# Chapter 2

## Computed tomography angiography and other applications of CT

de Graaf MA, Scholte AJ, Kroft LJ, Bax JJ.

*The ESC Textbook of Intensive and Acute Cardiac Care 2nd edition Oxford University Press, 2015*

## Abstract

Patients presenting with acute chest pain constitute a common and important diagnostic challenge. This has increased interest in using computed tomography (CT) for non-invasive visualization of coronary artery disease in patients presenting with acute chest pain to the emergency department; particularly the subset of patients who are suspect of having an acute coronary syndrome, but without typical ECG changes and normal troponin levels at presentation. As a result of the rapid developments in coronary CT angiography technology, high diagnostic accuracies for excluding coronary artery disease can be obtained. It has been shown that these patients can be discharged safely. The accuracy for detecting a significant coronary artery stenosis is also high, but the presence of coronary artery atherosclerosis or stenosis does not necessarily imply that the cause of the chest pain is related to coronary artery disease. Moreover, the non-invasive detection of coronary artery disease by CT has been shown to relate with an increased use of subsequent invasive coronary angiography and revascularization, and further studies are needed to define which patients benefit from invasive evaluation following coronary CT angiography. Conversely, the implementation of coronary CT angiography can significantly reduce the length of hospital stay, with a significant cost reduction.

Additionally, CT is an excellent modality in patients whose symptoms suggest other causes of acute chest pain such as aortic aneurysm, aortic dissection, or pulmonary embolism. Furthermore, acquisition of the coronary arteries, thoracic aorta, and pulmonary arteries in a single CT examination is feasible, allowing 'triple rule-out' (exclusion of aortic dissection, pulmonary embolism and coronary artery disease). Finally, other applications such as the evaluation of coronary artery plaque composition, myocardial function and perfusion or fractional flow reserve are currently being developed and may also become valuable in the setting of acute chest pain in the future.

## Introduction

The present chapter is an update of the previous book chapter.<sup>1</sup> Those parts on which new literature is available have been updated, whereas other parts have been inserted unchanged. Since the introduction of CT in the early 1970s the technique has evolved into an essential imaging tool in general medicine. With this technique, non-invasive high resolution cross-sectional imaging of internal structures such as the brain, thorax and abdomen was permitted, thereby gradually replacing the more invasive radiographic techniques.<sup>2</sup> Moreover, CT angiography has evolved as a very accurate tool for visualization of the aorta and pulmonary arteries. However, high-quality imaging of the coronary arteries remained challenging because of their small vessel size, movement, and tortuous anatomy requiring high temporal, spatial and contrast resolution. In the late 1990s, the first 4-slice spiral CT scanner was developed with sufficient resolution to allow visualization of the coronary arteries, establishing the potential of multi-slice CT for detecting significant coronary artery stenosis in comparison to invasive coronary angiography (ICA).<sup>3-5</sup> Since then, multi-slice CT coronary angiography has developed into a promising non-invasive alternative to ICA. With each successive generation of scanners from 4-slice to the present 64-, 256- and 320- slice scanners, temporal and spatial resolution improved markedly due to faster gantry rotation times, thinner detectors, and volumetric coverage. These new developments currently allow motion-free visualization of the entire coronary artery tree with high diagnostic accuracy for detecting coronary artery stenosis.<sup>6,7</sup> Thanks to these rapid developments, interest has been raised in using CT for the evaluation of patients presenting with acute chest pain. In the intensive cardiac care unit (ICCU), acute chest pain is the most common clinical presentation of coronary artery disease (CAD). The diagnosis of acute coronary syndrome (ACS) is straightforward in high risk patients with typical chest pain, typical ECG changes, and elevation of serum cardiac markers (enzymes), whereas it is difficult in patients presenting with atypical chest pain, non-diagnostic or normal ECG, and normal markers on presentation. Indeed, up to 8 % of patients with ACS are misdiagnosed and inappropriately discharged home.<sup>8</sup> Conversely, only a minority of 'low risk' patients (i.e. those with initially normal ECGs and cardiac enzymes) actually suffer from myocardial ischemia.<sup>9</sup> Therefore, the conventional approach for patients with acute chest pain leads to many unnecessary hospital admissions and is both time-consuming and expensive and thus, resource-intensive. Therefore, a non-invasive and rapid examination to establish or exclude CAD as the underlying cause of symptoms could substantially improve the clinical care of patients admitted to the ICCU, reducing hospital admissions and costs. This chapter focuses on the evolving role of coronary CT angiography (CTA) (including coronary artery calcium (CAC) scoring) in the diagnosis of patients presenting

with acute chest pain. An overview of a wide range of other CT applications is also provided, including triple rule-out, evaluation of plaque composition, myocardial function, and perfusion.

## **CT coronary angiography: patient preparation, acquisition, post-processing**

CT is an imaging modality which has an X-ray source (tube) and detectors on opposite sides of a gantry that continuously rotates around the patient. During the CT scan the patient is moved through the gantry. Subsequently, the X-ray source emits photons collimated into a fan beam which are, after partial absorption and dispersion, reabsorbed by the detectors. Computer systems process these data into three-dimensional (3D) volumetric information, which can be transferred to CT workstations and evaluated using multiple post-processing techniques.

### **Patient preparation**

Proper patient preparation is important for obtaining diagnostic image quality. Therefore, before referring a patient for coronary CTA, a short patient history should be obtained. Overall, a history of a severe allergic reaction to contrast agents, impaired renal function (glomerular filtration rate  $<30$  mL/min), presence of atrial fibrillation, and pregnancy are considered contraindications. The patient should refrain from food and liquids preferably 3 hours before the examination, to prevent nausea as a reaction to the contrast agent. Moreover, a low and stable heart rate in the range of approximately 50–60 beats/min is preferred during image acquisition. To achieve a low and stable heart rate, a  $\beta$ -blocker is frequently administered prior to the examination, unless contraindicated. Preferably, sublingual nitrates (0.4mg) are administered to the patient. The resulting vasodilatation facilitates the assessment of small coronary arteries.<sup>10</sup> Lastly, to ensure rapid delivery of the contrast agent bolus for coronary CTA, an intravenous catheter should be present for delivery of the contrast agent, preferably in the right antecubital vein (18–20 gauge).

### **Acquisition**

The scan range of the current 64-slice scanners is not large enough to cover the entire heart in one rotation and therefore several heart cycles are needed to image the entire heart. To compensate for cardiac motion and synchronize the start of the systole, ECG gating is needed to obtain phase-compatible images. Currently, the majority of cardiac CTs are acquired using prospective triggering, in which the start of scanning is triggered by the preceding R-wave. Most often the scan is triggered in

the relatively motion-free phase of mid diastole (70–80 % of the R–R interval) to minimize motion artefacts. Depending on the scanner type, imaging can be performed in helical ('spiral') mode with continuous table movement and modulated acquisition, or in step-and-shoot mode with multiple volumetric acquisitions reconstructed into a single data set. A wide-volume detector allows full cardiac acquisition in a single gantry rotation, e.g. a 256- or 320-detector-row scanner that allows a maximum of 16 cm scan range in a single rotation.<sup>11, 12</sup> Novel dual-source CT scanners, equipped with two X-ray tubes and two detectors at a 90 degree angle provide high temporal resolution. As a result, these scanners are able to produce images of high quality in patients with high heart rates. Besides, with these 64-slice dual-source CT scanners, using a high-pitch spiral technique, the entire heart can be depicted in one cardiac cycle with ultra-low radiation dose (<1mSv).<sup>13</sup>

For CAC scoring, a low-dose ECG triggered non-contrast-enhanced scan is performed before the contrast-enhanced CT examination and reconstructed to 3-mm slices. Additionally, this scan can be used to determine the proper location and scan range for coronary CT imaging. For a regular CTA, a rapid infusion of 60–100 mL of contrast material with a flow rate of 5 mL/s is used, followed by a saline flush. Typical scan parameters are a pitch of 0.375, rotation time of 333–500 ms, tube voltage of 100 or 120 kV and tube current of 300-500 mA (depending on body mass index). However, with novel iterative reconstruction algorithms, lower radiation exposure can be achieved by lowering tube voltage and current with preserved image quality. When using a bolus-triggered start of the CT scan, the start is automatically initiated if the preset contrast-enhancement threshold level in the descending aorta is reached. Alternatively, a test bolus injection can be used to determine the contrast transit time. Subsequently, data acquisition is performed at half-inspiratory breath hold of approximately 10 s.

### Post-processing

After data acquisition, images are reconstructed and sent to a dedicated workstation for post-processing. Commonly, coronary CTA data sets are reconstructed with continuous images using thin increments (typically 0.5–0.6 mm slice thickness). For post-processing, various types of algorithms are available.

- The thin axial slices, as depicted in Figure 1, are considered the source information of CT imaging. Accordingly, the cardiac structures and coronary arteries can easily be evaluated by scrolling through the images in axial direction.
- Curved multiplanar reconstructions (MPR) allow visualization of the entire coronary artery in a single image which is useful for depicting the entire coronary lumen and evaluating degree of stenosis.

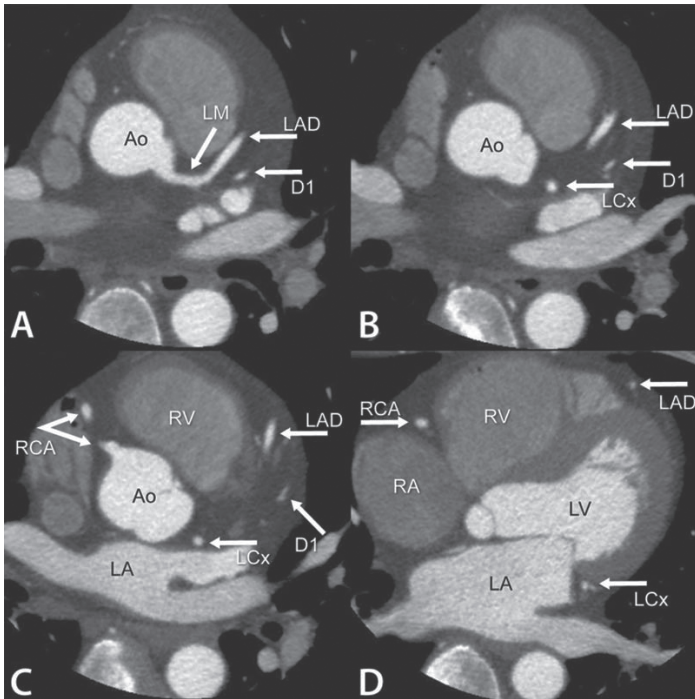


**Figure 1. Typical example of axial contrast-enhanced images.**

This image with a 0.5-mm slice thickness, can be used to evaluate cardiac structures (such as the left ventricle (LV), left atrium (LA), right ventricle (RV), and aorta (Ao)) and coronary arteries by scrolling through the slices in the cranio-caudal direction. Four images have been selected to demonstrate the anatomy of the heart. A. Axial image showing the left main (LM) coronary artery at the level of the ostium which arises from the left coronary cusp and bifurcates first into the left anterior descending coronary artery (LAD). B. Slightly more distal axial image showing the left circumflex coronary artery (LCx) and the first diagonal branch (D1) which has originated from the LAD. C. Axial image demonstrating the origin of the right coronary artery (RCA) from the right coronary cusp and the mid segments of the LCx, LAD, and D1. (D) Axial image at midventricular level which shows the mid segment of the right coronary artery (RCA) and distal segments of the LAD and LCx (the latter is seen in the left atrio-ventricular groove).

- Maximum intensity projections (MIP) can be reconstructed which represent a series of contiguous CT slices stacked into a single image ('slab'). Moreover, MIPs are very suitable for assessment of longer length of vessel segments and may facilitate in evaluating the degree of stenosis.
- 3D volume rendering provides a 3D image of the heart and vessels. An excellent overview of the coronary anatomy is provided, although 3D volume rendering is generally not used for assessing the stenosis severity. Figure 2 provides an example of a 3D volume rendered image.

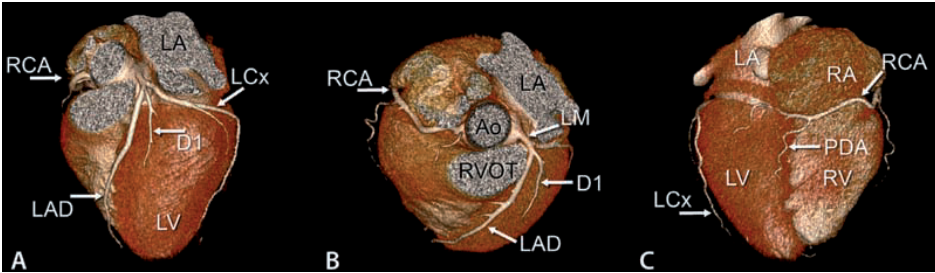


**Figure 2. Surface-rendered volumetric 3D images of the coronary arteries and side branches.**

This type of image provides a 3D overview of the coronary artery tree and their relative position to the underlying cardiac structures, including the left ventricle (LV) and right ventricle (RV). A. Anterior view of the left circulation demonstrating the left anterior descending coronary artery (LAD) with first diagonal branch (D1). In addition, the left circumflex coronary artery (LCx) can be identified. The left atrium (LA), aorta (Ao), and right ventricular outflow tract (RVOT) can be also appreciated in this view. B. Cranial view demonstrating a volume-rendered image of right coronary artery (RCA) and left main coronary artery (LM) and their main branches originating from the right and left coronary cusp, respectively. C. Posterior view of the RCA and the posterior descending coronary artery (PDA).

## Interpretation of coronary artery disease on coronary CT angiography

A systematic approach is important when evaluating a coronary CTA. If CAC scoring has been performed, the Agatston score is reported on a patient and vessel basis. Thereafter, the coronary CTA is interpreted to assess coronary atherosclerosis and stenosis severity. In addition to the analysis of the coronary arteries, the entire scan range should be examined to detect potential extra-cardiac findings.

### Coronary artery calcium score

For quantification of the coronary calcifications, the Agatston method (a method that multiplies the calcified area by a density factor based on the highest Hounsfield values within this area) is routinely used.<sup>14</sup> Total CAC scores are generally stratified into normal (zero calcium), mild (1–100), moderate (101–400), and severe (> 400).<sup>15</sup> Several population based studies have demonstrated that the CAC score increases with higher age, thereby reflecting the natural progression of atherosclerosis. In addition, men tend to have higher CAC scores than women of similar age. Therefore, the CAC score should be ranked in percentiles according to the distribution within age and gender<sup>16, 17</sup> Although newer quantification methods have been introduced (calcified volume (mm<sup>3</sup>) and mass (mg) measurements), these metrics are not commonly used in clinical practice.<sup>18</sup> With novel algorithms the quantification of CAC on contrast enhanced scans is feasible.<sup>19</sup> However, these techniques are currently not used in clinical practice.

## Coronary CT angiography

With regard to the coronary CTA, the quality of the scan should be mentioned as this influences the diagnostic certainty of the study. Findings are commonly reported similar to the reporting of invasive coronary angiography (ICA). Typically, each coronary segment of the American Heart Association 17-segment model<sup>20</sup> is described as normal, mild (<30% wall irregularities), non-significant (30–50% stenosis), significant (>50% stenosis), severe stenosis (> 70%), and occlusion. In addition to stenosis severity, the plaque composition of each lesion should be described as non-calcified, calcified, or mixed (i.e. a combination of calcified and non-calcified plaque). Presence and patency of stents and bypasses are reported, if evaluable. Segments that are uninterpretable due to severe calcifications, motion, or breathing artefacts should be mentioned as such in the report.

## Extra-cardiac findings

Beyond evaluating the coronary arteries, other cardiac findings and/or extra-cardiac findings may be identified during coronary CTA. Interestingly, extra-cardiac findings provide an explanation for chest pain complaints in 4–8% of patients or may be incidental findings not related to chest complaints.<sup>21, 22</sup> Clinically important findings that require immediate therapy, intervention, additional diagnosis, or follow-up are reported in approximately 13% of cardiac CT examinations.<sup>23, 24</sup> These include suspected malignancy which may necessitate immediate therapeutic actions, or the presence of acute pulmonary embolism or pneumonia.<sup>21, 25-27</sup> Incidental lung cancers are found in 0.24% of patients.<sup>23</sup> For coronary artery assessment, a zoomed-in small field of view focused on the heart is reconstructed to obtain maximal spatial resolution for evaluation. However, this focused view reveals only 36% of the total chest volume, whereas 70% of the total chest volume has been exposed to radiation.<sup>27</sup> Substantially more significant extra-cardiac pathology is found on maximum full-field reconstructions than on small-field reconstructions.<sup>23</sup> Therefore the maximum full-field reconstructions should be reviewed for optimal identification of extra-cardiac pathology.<sup>21, 23, 25, 27, 28</sup>

# Patients with non-acute chest pain

## Coronary artery calcium score

It has been widely verified that the presence of coronary artery calcification only occurs in the presence of coronary artery atherosclerosis.<sup>29</sup> Both electron beam CT (EBCT) and multi-slice CT have been used over the past years for the noninvasive evaluation of coronary artery calcifications, both demonstrating high sensitivities

for the detection of CAD indicating that a large proportion of patients with CAD are accurately detected by CAC scoring.<sup>17, 30</sup> The relation between the presence of obstructive CAD and the presence and extent of CAC has been extensively studied.<sup>31</sup> The CAC score has a high sensitivity and negative predictive value for the presence of obstructive CAD, but its specificity is limited.<sup>31, 32</sup> The high negative predictive value indicates that patients without CAC virtually never have obstructive CAD. In contrast, the lower specificity indicates that patients without obstructive CAD still often present with CAC. For instance, Haberl *et al.* evaluated 1,764 patients who underwent both EBCT (CAC score) and ICA. The absence of CAC was associated with an extremely low probability of disease (<1%) and thus highly accurate to exclude obstructive CAD. However, specificity was only 23% in men and 40% in women. Therefore, the technique may be more suited to provide an estimate of total plaque burden rather than stenosis severity.

Furthermore, numerous investigations have shown that the extent of CAC provides prognostic information. CAC scoring has therefore been proposed as a tool for cardiac risk stratification. Several large trials have reported that elevated CAC scores have predictive value for cardiovascular events, both independently and incrementally to cardiovascular risk factors.<sup>33, 34</sup> Budoff *et al.* assessed the prognostic value of CAC scoring in 25,253 asymptomatic individuals over a mean follow-up period of 6.8 years. The survival of individuals without CAC was excellent (99.6%), with a gradual reduction in survival rates with increasing CAC score.<sup>33</sup>

### **Coronary CT angiography**

With the current generation 64-slice CT scanners, with improved temporal and spatial resolution, a good diagnostic accuracy for detection of obstructive CAD has been reported, both for the proximal as well as the distal part of the coronary arteries. In comparison with ICA, a high sensitivity (85–99%) and high specificity (83–90%) has been reported for the detection of obstructive stenoses.<sup>6, 7</sup> More importantly, as demonstrated by the high negative predictive value, coronary CTA is an excellent tool to exclude significant CAD. This implies that in the presence of normal coronary arteries on coronary CTA, no further testing is required and patients can be reassured. The positive predictive value however, is lower (64–93%), and the severity of atherosclerotic lesions is frequently overestimated on coronary CTA.

Recently, new low-radiation-dose algorithms have been introduced, which resulted in a significant reduction in radiation. A meta-analysis of these studies confirmed the diagnostic accuracy<sup>35</sup>; pooled data from 15 studies (with varying novel CT scanners) included 960 patients, reported a sensitivity of 100% with a specificity of 89%. The NPV was 99%, with a PPV of 93%, indicating overestimation of stenosis severity in 7% of patients. Moreover, the diagnostic performance of coronary CTA is influenced

by the pretest likelihood of obstructive CAD. Indeed, as shown in Table 1, the benefit from CT is highest in patients with a low to intermediate pretest likelihood for CAD due to the high accuracy to exclude obstructive CAD.<sup>36</sup>

In line with these observations, Henneman *et al.* demonstrated that coronary CTA was able to exclude coronary artery atherosclerosis in 58% of patients with low pretest likelihood of CAD, with no need for further routine visits to the outpatient clinic.<sup>37</sup> Conversely, coronary CTA demonstrated atherosclerosis and/or stenosis in 83% of patients with a high pretest likelihood of CAD. These patients may thus benefit more from non-invasive testing for ischemia and/or direct ICA with fractional flow reserve assessment, to determine optimal therapy (medical management or revascularization). Indeed the recent European Society of Cardiology guidelines for stable CAD indicate that coronary CTA is particularly useful in patients with low-intermediate pretest likelihood of CAD (recommendation class IIa).<sup>38</sup>

In addition to the diagnostic value, coronary CTA provides prognostic information. Chow *et al.* reported in the CONFIRM (Coronary CT Angiography Evaluation for Clinical Outcomes) registry (with 14,064 patients in 12 different centers) that a normal coronary CTA was associated with an annual mortality rate of 0.65% over a mean follow-up of 22.5 months (Figure 3).<sup>39</sup> Conversely, patients with obstructive CAD had an annual mortality rate of 2.9%, which increased to almost 5% in patients with 3-vessel, left-main and or proximal LAD disease. It is important to realize that the annual mortality in the CONFIRM registry was only 1.1%, indicating a relatively low risk population.

A recent meta-analysis by Bamberg *et al.* focused on the prognostic value of coronary CTA, and included 9 studies with 3,760 patients with an average follow-up varying from 14 to 78 months.<sup>40</sup>

The overall event rate was 6.8%, but it should be noted that two-third of the events were coronary revascularizations. (Early) Revascularization is not an ideal end-point since the findings on coronary CTA may have triggered the revascularization. Patients with a normal coronary CTA had an event rate of 0.4%. Patients with obstructive CAD had a 6-fold increased risk for death, infarction or ACS. Importantly, a significant

**Table 1. Diagnostic accuracy of 64-slice coronary CT angiography for detection of significant stenosis ( $\geq 50\%$ ) categorized according to pretest probability.**

Pretest probability	N	Sens(%)	Spec(%)	PPV(%)	NPV(%)
Low	66	100	93	78	100
Intermediate	83	100	84	80	100
High	105	98	74	93	89

Data adapted from Meijboom *et al.*<sup>36</sup>

Abbreviations: NPV: negative predictive value, Sens: sensitivity, Spec: specificity, PPV: positive predictive value

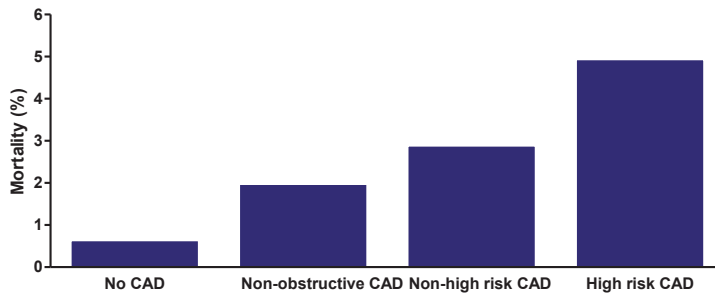


**Figure 3. Bar graph illustrating the prognostic value of coronary CTA for the prediction of all-cause mortality.**

Non-obstructive CAD was defined as <50% stenosis, non-high risk CAD was defined as  $\geq 50\%$  stenosis and high risk CAD included left main stenosis ( $\geq 50\%$ ) or 3-vessel disease ( $\geq 70\%$ ) or 2-vessel disease ( $\geq 70\%$ ) including the proximal left anterior descending artery.

CAD: coronary artery disease

Adapted from Chow, *Circulation Cardiovascular Imaging* 2011

stenosis on coronary CTA remained predictive of events after correction for CAC score and cardiovascular risk factors.

## Patients with suspected acute coronary syndrome

### Coronary artery calcium score

The prognostic value of the CAC score has been widely established in patients with stable angina, but some studies evaluated the use of CAC score in patients with acute chest pain. Earlier studies with EBCT reported a high negative predictive value of the CAC score, demonstrating that patients with a CAC score of 0 had an excellent prognosis.<sup>41-43</sup> Georgiou *et al.* reported in 192 patients with acute chest pain that the absence of coronary artery calcifications had a very low risk for future cardiac events (<1%), whereas the presence of CAC was a strong predictor of events<sup>41</sup>. More recently, Nabi and co-workers reported on the use of CAC score in 1031 patients with acute chest pain using 16-slice CT.<sup>44</sup> In the 625 (61%) patients with zero CAC score, the cardiac event rate was <1%, whereas the event rate increased in parallel with an increasing CAC score. The various prognostic studies using CAC score in patients with acute chest pain and/or suspected ACS are summarized in Table 2. The results of six studies, with a total of 3035 patients were included in the pooled analysis.<sup>45</sup> In total, 62% of patients with acute chest pain or suspected ACS presented with a CAC score of 0 (indicating relatively low risk populations). However, there was a large variation in incidence of CAC score of zero between studies, ranging from 36%

**Table 2. Diagnostic accuracy of a coronary artery calcium score of 0 for the prediction of acute coronary syndrome or events.**

Author	N	No. (%) CAC=0	Follow-up	Sens(%)	Spec(%)	PPV(%)	NPV(%)
Chang et al <sup>48</sup>	1047	795 (76)	Prospective, 30 days	67	77	4	99
Georgiou et al <sup>41</sup>	192	76 (40)	Prospective, 50 ± 10 months	97	64	48	97
Hoffman et al <sup>51</sup>	368	197 (54)	Prospective, 6 months	97	58	18	99
Laudon et al <sup>42</sup>	263	133 (51)	Prospective, 6 months	97	57	23	99
McLaughlin et al <sup>43</sup>	134	48 (36)	Prospective, 30 days	88	37	8	98
Nabi et al <sup>44</sup>	1031	625 (61)	Prospective, 6 months	94	62	7	99
Pooled *	3035	1874(62)	-	93	65	14	99

\*Data adapted from Tota-Maharaj *et al.*<sup>45</sup>

Abbreviations: CAC: coronary artery calcium, NPV: negative predictive value, Sens: sensitivity, Spec: specificity, PPV: positive predictive value

to 76%. The pooled analysis demonstrated a negative predictive value of 99% for the occurrence of future events. In contrast, the positive predictive value was only 14%. The long-term prognostic value of CAC score patients with suspected ACS has also been evaluated. Forouzandeh and colleagues acquired long-term follow-up data (median 3.3 years) in 760 patients presenting with acute chest pain who underwent 16-slice CT.<sup>46</sup> Events occurred in 45 (6%) patients; the long-term event rate was 0.4% in patients without CAC, and increased to 11% in patients with a CAC score >400. Although a CAC score of zero has been associated with an excellent prognosis, it has simultaneously been observed that patients with ACS or acute infarction can present without CAC in the culprit vessel<sup>47</sup>. Thus, particularly in the acute setting, the absence of CAC may not always imply the absence of atherosclerotic plaque. This was demonstrated by Chang *et al* showing that obstructive atherosclerosis was present in 17 of 795 (2%) patients with a suspected ACS and CAC 0.<sup>48</sup> In addition, 12% of the patients with a CAC 0 had non-obstructive CAD. Accordingly, Biegel *et al.* performed coronary CTA in 785 consecutive patients with acute chest pain.<sup>49</sup> Of the 255 patients with CAC score 0, significant CAD was observed on ICA in 2.7% of patients. Figure 4 provides an example of a patient with an obstructive non-calcified plaque despite a CAC score of zero.

### Coronary CT angiography

Previous studies have demonstrated that coronary CTA has a high sensitivity and specificity for the detection of CAD compared to ICA in patient with stable CAD. More importantly, due to the high negative predictive value, coronary CTA can reliably exclude significant CAD, which is of potential value in patients presenting with

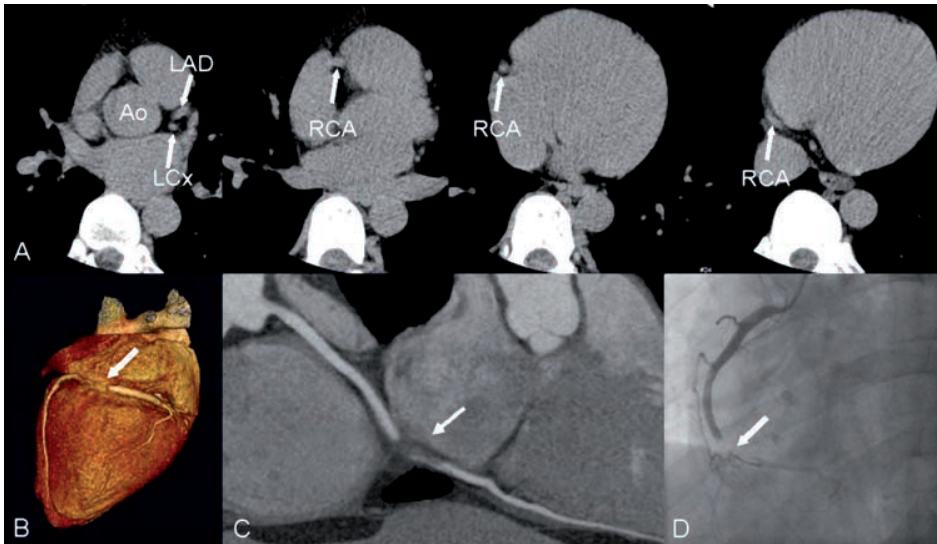


**Figure 4.** Example of a patient presenting with suspected ACS.

In this patient coronary artery calcium (CAC) scoring and contrast-enhanced coronary CT angiography were performed to exclude CAD. Although the CAC score was zero (A), an obstructive non-calcified plaque with a superimposed thrombus in the right coronary artery (RCA) was detected on coronary CT angiography (B, C). The volume-rendered 3D reconstruction (B) and curved multi-planar reconstruction (C) show an occlusion in the mid segment of the RCA (white arrows). (D) This finding was confirmed on invasive coronary angiography (white arrow). Ao, aorta; LAD, left anterior descending coronary artery; LCx, left circumflex coronary artery. From Henneman MM, Schuijff JD, Pundziute G, *et al.* Noninvasive evaluation with multislice computed tomography in suspected acute coronary syndrome: plaque morphology on multislice computed tomography versus CAC score. *J Am Coll Cardiol* 2008; **52** (3):216–222, with permission.

suspected ACS in the emergency room, but without specific ECG abnormalities and serum troponin levels in the normal range on admission. Limited studies are available that assess the diagnostic value of coronary CTA for the detection of significant CAD compared to ICA in patients presenting with suspected ACS. Meijboom *et al.* evaluated 104 patients with non-ST elevation ACS using 64-slice CTA compared with ICA.<sup>36</sup> In total 88 patients (85%) presented with significant CAD on ICA. Reported sensitivity and specificity of coronary CTA for detecting or excluding significant coronary artery stenosis were 100% and 75% respectively. Figure 5 shows an example of a patient presenting with suspected ACS with a significant stenosis in the RCA. More importantly, several investigations have addressed the predictive value of coronary CTA for the detection of ACS in patients with acute chest pain. Table 3 demonstrates the diagnostic accuracy of coronary CTA for the detection of ACS. In the most of these studies ACS is defined as either acute myocardial infarction or unstable angina pectoris according to the ACC/AHA-criteria<sup>50</sup>, preferably with evidence of myocardial

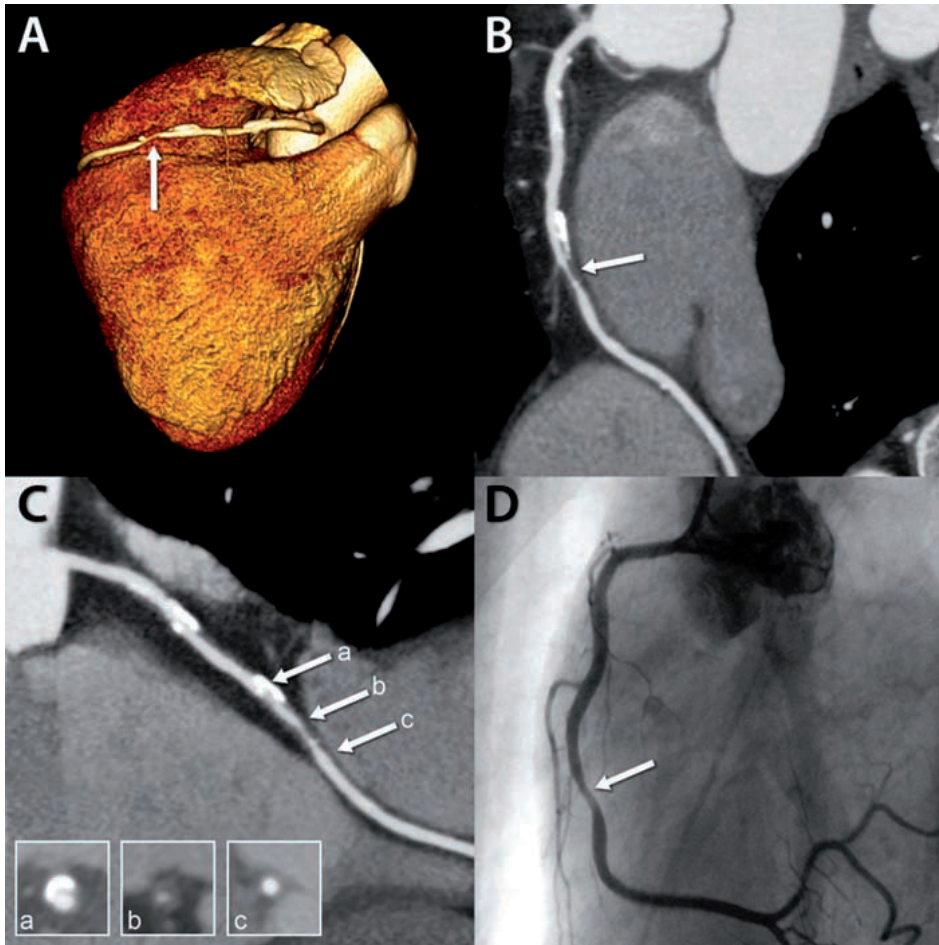


**Figure 5.** Example of non-invasive coronary angiography with CT in a patient presenting with suspected ACS.

In (A), a 3D volume-rendered reconstruction is provided, showing a large dominant right coronary artery (RCA) with signs of luminal narrowing (white arrow). B. A curved multiplanar reconstruction (MPR) of the RCA is shown demonstrating the presence of significant luminal narrowing in the mid segment (arrow). C. Another curved MPR in a different view, revealing the presence of significant stenosis (arrows). Cross-sectional CT images (inlays) show the presence of calcified plaque proximal to the stenosis (a), exclusively non-calcified plaque within the stenosis (b), and no coronary plaque distal from the stenosis (c). D. Conventional coronary angiography confirming the presence of significant luminal narrowing of the RCA (arrow).

ischemia on functional testing.<sup>51</sup> In the ROMICAT I study, 368 patients presenting with chest pain and possible ACS (but normal initial troponin and non-ischemic ECG) underwent 64-slice CTA.<sup>51</sup> Of these 368 patients, 8% eventually developed an ACS according to the definition described above. On 64-slice CT, 183 did not have any coronary atherosclerosis (no CAD), whereas 117 had non-obstructive coronary artery

Table 3. Diagnostic accuracy of CTA for the detection of acute coronary syndrome.

Author	N	Pre-test probability	% ACS	% patients negative CTA	Definition ACS	Sens(%) (TP/(TP+FN))	Spec(%) (TN/(TN+FP))	PPV(%) (TP/(TP+FP))	NPV(%) (TN/(TN+FN))
White <i>et al.</i> <sup>89</sup>	69	Low - high	17	82	Clinical	83 (10/12)	96 (55/57)	83 (10/12)	96 (55/57)
Gallagher <i>et al.</i> <sup>103</sup>	85	Low	8	86	Clinical	86 (6/7)	92 (72/78)	50 (6/12)	99 (72/73)
Hoffman <i>et al.</i> <sup>104</sup>	40	All	13	65	Clinical	100 (5/5)	74 (26/35)	38 (5/14)	100 (26/26)
Hoffman <i>et al.</i> <sup>105</sup>	103	Low	14	71	Clinical	100 (14/14)	82 (73/89)	47 (14/30)	100 (73/73)
Olivetti <i>et al.</i> <sup>106</sup>	31	Low- Intermediate	58	52	ICA	83 (15/18)	100 (13/13)	100 (15/15)	81 (13/16)
Sato <i>et al.</i> <sup>107</sup>	31	Low	71	29	Clinical	95 (21/22)	89 (8/9)	95 (21/22)	89 (8/9)
Goldstein <i>et al.</i> <sup>54</sup>	99	Low	8	89	Clinical	100 (8/8)	97 (88/91)	73 (8/11)	100 (88/88)
Meijboom <i>et al.</i> <sup>36</sup>	33	Low <sup>†</sup>	85	12	ICA	100 (28/28)	75 (4/5)	96 (28/29)	100 (4/4)
Rubinshtein <i>et al.</i> <sup>108</sup>	58	Intermediate	34	60	Clinical	100 (20/20)	92 (35/38)	87 (20/23)	100 (35/35)
Hoffman <i>et al.</i> <sup>51</sup>	368	Low	8	82	Clinical	77 (24/31)	84 (293/337)	35 (24/68)	98 (293/300)
Meta-analysis *	917	-	16	72	-	92 (151/165)	89 (667/752)	64 (151/236)	98 (667/681)

<sup>†</sup> Only a portion of patients with low risk were included in this meta-analysis

\* Meta-analysis adapted from Vanhoenacker *et al.*<sup>109</sup>

Abbreviations: ACS: acute coronary syndrome, FN: false negative, FP: false positive, ICA: invasive coronary angiography, NPV: negative predictive value, Sens: sensitivity, Spec: specificity, TN: true negative, TP: true positive, PPV: positive predictive value

stenoses. Of these 300 patients, only 7 (2%) were diagnosed with ACS, yielding a NPV of 98%. Conversely, 68 patients had obstructive CAD on CTA, and 24 developed an ACS; accordingly the PPV was 35%. Similarly, Gallagher *et al.* evaluated 85 patients with suspected ACS using 64-slice CTA; 73 patients had non-obstructive or no CAD on the CT scan and 1 of these developed an ACS, resulting in a NPV of 99%. On the other hand, 6 of the 12 patients with obstructive CAD on the CT scan developed an ACS, yielding a PPV of 50%. Meta-analysis combining the results of 10 studies with a total of 917 patients confirmed a NPV of 98%, with a lower PPV of 64%. The high NPV permits rule out of future development of ACS. In contrast, significant CAD on coronary CTA has lower predictive value for the development of ACS. These observations indicate that absence of significant CAD on coronary CTA can rule out development of ACS, but the presence of significant CAD does not indicate that these patients will always develop an ACS.

In addition, coronary CTA has been used for prediction of short- and long-term outcome of patients presenting to the emergency room with suspected ACS. In the ROMICAT I study, none of the 300 patients with a 'negative coronary CTA' (defined as no coronary atherosclerosis or non-obstructive CAD) experienced a subsequent cardiovascular event during a 6 months follow-up period.<sup>51</sup> Based on these initial observations, subsequent studies have focused on the potential implementation of coronary CTA in management of patients presenting to the emergency room with suspected ACS (but with normal troponins and non-ischemic ECG). For example, Lit *et al.* performed a randomized controlled trial (RCT) in 1370 patients with suspected ACS.<sup>52</sup> Patients were randomized to either CTA or standard care. Of the 908 patients referred for CTA, 640 (70%) had a negative CTA (no atherosclerosis or non-significant CAD). These patients were discharged, and none of these patients died, or presented with myocardial infarction within the next 30 days.

At present, four large RCTs have been conducted to assess the value of a CTA-based strategy compared to standard care. The results of these four trials have been pooled in a meta-analysis by Hulthen *et al.*<sup>53</sup> This meta-analysis included the results of 1,869 patients undergoing coronary CTA and 1,397 patients receiving standard care. Of the 1,869 patients undergoing CTA, only 4.2% had a significant coronary artery stenosis ( $\geq 70\%$  luminal narrowing) on CTA. None of the patients died during the trials. In total, 142 (7.6%) of the patients in the coronary CTA group underwent ICA, of which 76 (4.1%) were revascularized. Patients referred to coronary CTA more often underwent ICA than patients receiving standard care. As depicted in Figure 6, the ICA referral rate was 6.3% in patients receiving standard care as compared to 8.4% in patients randomized to CTA ( $P = 0.003$ ). The absolute increase in ICA for a coronary CTA based strategy was 21 per 1,000 patients.<sup>53</sup> Of interest, the majority of these downstream referrals for ICA were during the index hospitalization. Similar to the

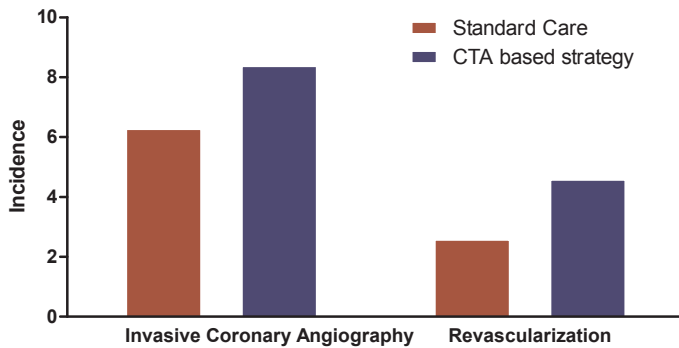


**Figure 6.** Difference in referral rate for invasive coronary angiography and subsequent revascularization between patients randomized to either a coronary CTA based strategy or standard care.

Adapted from Hulthen *et al.*<sup>53</sup>

increase in ICA in the coronary CTA group, a significant increase in revascularization was observed in this group (both PCI and CABG). The revascularization rate was 2.6% in patients receiving standard care as compared to 4.6% in patients randomized to coronary CTA ( $P = 0.004$ ). The absolute increase in revascularization for a coronary CTA based strategy was 20 per 1,000 patients.

The information from these 4 RCTs underscores the value of coronary CTA in the emergency room for patients presenting with acute chest pain, suspect of ACS in the emergency room, namely exclusion of CAD. At the same time however, this approach is associated with an increased use of ICA and subsequent revascularization.

At the same time, the coronary CTA based strategy resulted in a significant reduction in the length of stay (emergency department or hospital stay) by 3.4–11.6 hours as compared to patients receiving standard care.<sup>52, 54-56</sup> For example, 50% of the patients randomized to coronary CTA in the ROMICAT II study could be safely discharged within 8.6 hours as compared to 26.7 hours for the patients receiving standard care (Figure 7).<sup>55</sup> Moreover, a coronary CTA based strategy positively affected emergency department costs: in three of the four trials a significant reduction in costs was observed in the group of patients randomized to CTA, ranging from \$286 to \$1321.

The number of post discharge hospitalizations for ACS is extremely low in these 4 trials (ranging from 0 to 3.1%), which further supports the safety of coronary CTA guided discharge of patients.

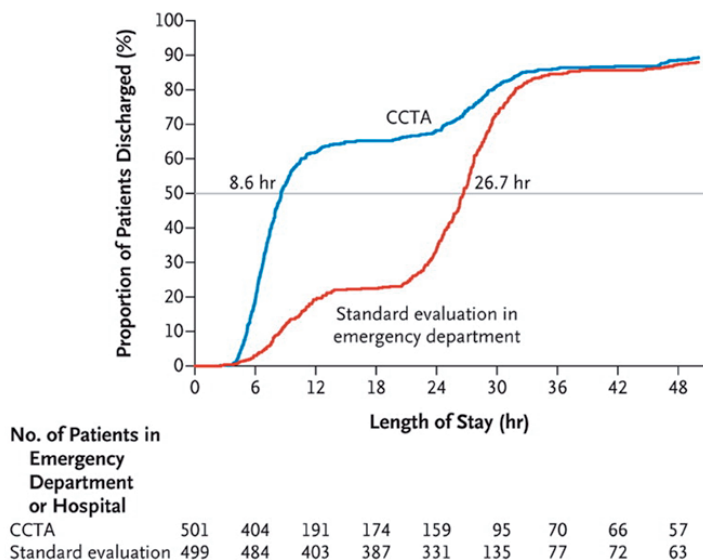


**Figure 7. Difference in length of hospital stay between patients referred to CTA of standard care.**  
 The horizontal line indicated the median length of stay in both study groups which was significantly different.

From: Hoffmann *et al.* NEJM. 2011

## CT angiography of aorta and pulmonary arteries

Non-cardiac causes of acute chest pain concerning vascular structures in the thorax such as in acute aortic syndrome and pulmonary embolism can be easily visualized by CT. CT angiography of other vascular beds than the heart is less complex if non-ECG gating techniques are used. ECG gating may be used to improve image quality. In addition, contrast enhancement in the blood pool is required to visualize the vascular structures, and thus intravenous contrast is still needed. Several common principles should be applied to all imaging protocols to provide optimal diagnostic image quality such as bolus timing for optimization of contrast delivery in the vessel, fast high resolution acquisition, and administration of approximately 60–120 mL of contrast material (dependent on patient size, contrast agent used, and scanner type) injected at rapid infusion rates (4–5 mL/s).

Because of the availability, excellent image quality with good spatial resolution, high sensitivity, and fast imaging speed, multi-slice CT has become the first-choice imaging tool for the evaluation of acute aortic syndrome<sup>57</sup> and traumatic aortic pathology.<sup>58</sup> multi-slice CT is also widely used in the evaluation of non-acute pathology such as aneurysm or aortic coarctation, inflammatory and infective aortic disease, and after aortic surgery.<sup>59</sup>

Acute aortic syndrome encompasses a variety of life-threatening conditions that require emergency diagnosis and management, including aortic dissection (AD) (see Figure 8), intramural hematoma (IMH), penetrating aortic ulcer (PAU) and symptomatic aortic aneurysm.

If a patient presents with suspected acute aortic syndrome, the CT protocol should include a non-contrast enhanced scan from the proximal part of the arch vessels to the diaphragm, followed by CTA from the proximal part of the arch vessels to the femoral arteries. The non-contrast scan is to evaluate possible presence of an IMH as aortic wall thrombus.<sup>59</sup> IMH of the ascending aorta is clinically regarded at high risk for complication (evolving into dissection) and death, and surgery is usually indicated.<sup>60</sup>

PAU is usually located in the mid-descending thoracic aorta, where it presents as a mushroom-like contrast outpouching beyond the expected contours of the aortic lumen. PAU represents an atherosclerotic ulceration that penetrates the internal elastic lamina allowing hematoma formation within the aortic media, and may develop into IMH, aortic dissection, or vessel rupture.<sup>61</sup>

### Thoracic aortic aneurysm

Aneurysm is defined as a permanent localized dilatation of an artery, having at least a 50% increase in diameter as compared with the normal diameter.<sup>60</sup> In general, an ascending aortic diameter equal to or greater than 4 cm (in an individual less than 60 years old) is considered an aneurysm. The size of the thoracic aorta increases with age and depends on sex and body size. The normal ascending aorta diameter is approximately 27 mm in 20-years old and 36 mm in 80-years old.<sup>60</sup> Thoracic aortic

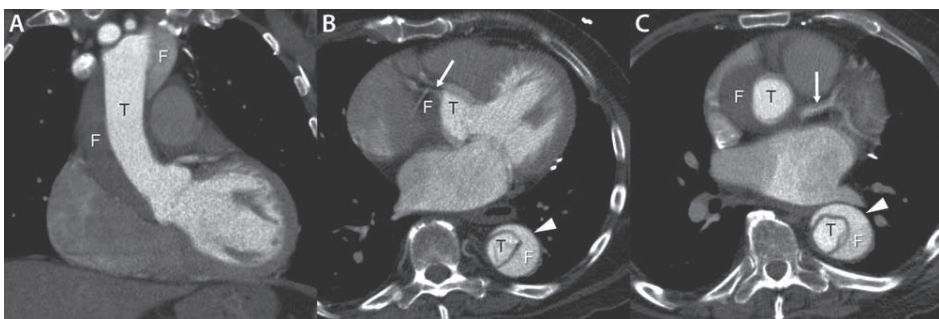


**Figure 8. Thoracic CT angiography showing a type A aortic dissection(A).**

The right coronary artery is contrast enhanced and has its origin from the true lumen (arrow, B). The right coronary artery has double appearance due to motion artefacts in this non-ECG gated scan. The left main coronary artery stem (arrow, C) is also contrast enhanced and had its origin from the true lumen. Carotid and subclavian arteries as well as the visceral arteries all had their origin from the true lumen. Note the almost complete disruption between the true and false lumen of the descending aorta (arrowheads B, C). F, false lumen; T, true lumen.

aneurysms can be true or false aneurysms. In a true aneurysm all three layers of the vessel wall are involved (intima, media, and adventitia) and is characterized by a fusiform shape. In a false aneurysm (or pseudo-aneurysm), the intima is disrupted and the blood is contained by the adventitia. Atherosclerosis is the most frequent cause of thoracic aneurysms (70%). Several genetic syndromes, vasculitis, and inflammatory diseases are also associated with aortic aneurysm and dissection.

Asymptomatic patients with an ascending aorta or sinus diameter larger than 5.5 cm, a growth rate more than 0.5 cm per year in aorta aneurysm less than 5.5 cm, and patients with genetically mediated syndromes and thoracic aorta aneurysm exceeding 4.0 to 5.0 cm, are candidates for elective surgical repair. Symptomatic patients suggestive of expansion of a thoracic aneurysm should be evaluated for prompt surgical intervention.<sup>60</sup>

CT angiography is the most robust tool for evaluating aortic aneurysms and some key features should be evaluated when using CT such as the maximal aortic diameter, presence of thrombus, shape and extent of the aneurysm, involvement of aortic branches, relationship to adjacent structures, and presence of aortic calcifications. In 23% of cases a thoracic aneurysm coexists with an abdominal aortic aneurysm, and thus evaluation of the entire aorta is indicated. Most importantly, CT shows excellent accuracy for characterizing important features of aneurysms.<sup>62</sup>

### **Pulmonary embolism**

The well-known Wells' clinical decision rule is used to risk stratify patients suspected of pulmonary embolism.<sup>63</sup> This is a scoring method based on various clinical risk factors and stratifies patients as low, intermediate, or high risk. If a patient has a score of 4 or more, further testing is required. In routine clinical practice, multi-slice CT pulmonary angiography has become the first-choice imaging method for evaluating the pulmonary arteries when pulmonary embolism is suspected (see Figure 9).<sup>64</sup> A normal CT pulmonary angiography can safely exclude pulmonary embolism without need for additional tests.<sup>65</sup> On CT, pulmonary emboli are shown as filling defects of the contrast-enhanced central or segmental pulmonary arteries. In patients with pulmonary embolism, cloth burden is related to right ventricular dysfunction, where the measure of a right to left ventricular diameter ratio exceeding 1.0 is at risk for short term death.<sup>66</sup>

### **Triple rule-out CT**

The concept of the 'triple rule-out' protocol is to simultaneously exclude all three potentially life-threatening causes of acute chest pain (ACS or infarction, acute aortic dissection or syndrome, and pulmonary embolism) in a single CT examination. A triple rule-out scan protocol includes coverage of the entire thorax cavity including

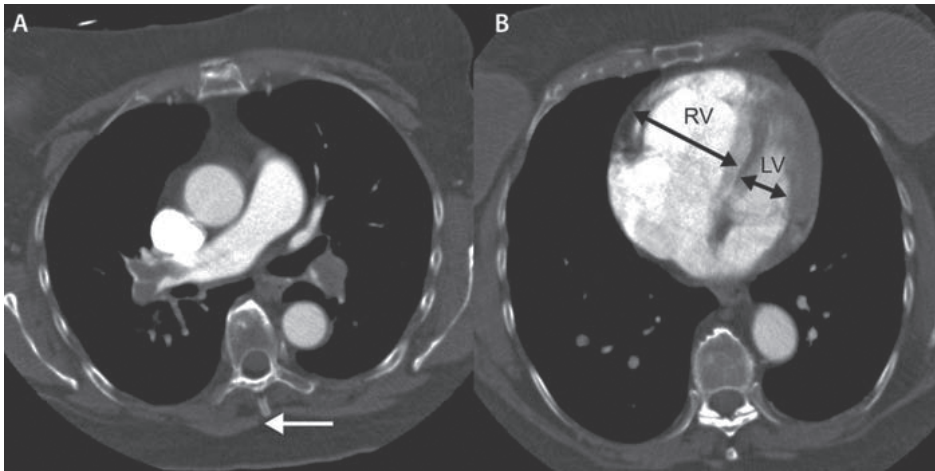


**Figure 9. Patient with acute pulmonary embolism and high embolus load.**

Massive emboli in the left and right pulmonary arteries can be observed (arrows, A). Note severe dilatation of the right ventricle (RV, B) with interventricular septum shift to the left and compression of the left ventricle (LV) due to high embolus load. Normally the RV diameter does not exceed that of the LV.

the aortic arch. State-of-the-art 64-slice scanners with wide anatomical coverage are able to scan the entire thorax including the pulmonary arteries, thoracic aorta, and coronary arteries in a single breath hold of approximately 15–20 s. An important technical challenge of a triple rule-out scan protocol is to ensure that high contrast enhancement is present simultaneously in both the pulmonary and systemic circulation to evaluate the pulmonary arteries and aorta including the coronary arteries. Injection protocols should be adapted to scanner type and acquisition settings.

Triple rule-out approach may improve the triage of patients presenting to the emergency department with acute chest pain, and provide a faster algorithm to make a diagnosis. However, it is crucial that patients should be carefully selected to ensure the appropriate use of a triple rule-out CT protocol. If the triple rule-out protocol involves retrospective gating of the entire thorax, radiation dose is high, even more than the radiation dose observed in dedicated coronary CT angiography.<sup>67, 68</sup> Prospective gating techniques strongly reduce radiation dose, but may not be applied effectively in patients with high or irregular heart rates. Therefore, patients with symptoms highly suggestive for ACS, acute pulmonary embolism, or acute aortic dissection, should be referred for a work-up specifically designed for this purpose (such as ICA if a patient has a high risk for ACS). As discussed before, the presence of a significant stenosis on coronary CTA does not automatically confirm the presence of ACS. In the remaining patients with uncertain cause of chest pain, a triple rule-out protocol can be considered.

Initial studies suggest that a triple rule-out CTA protocol for evaluation of patients with acute chest pain is feasible and that quantitative parameters of image quality may be comparable to the conventional, dedicated coronary and pulmonary CTA protocol.<sup>69, 70</sup> A study evaluating the diagnostic value of triple rule-out with 64-slice CT in 55 patients admitted to the emergency department demonstrated that this technique facilitated the differential diagnosis of chest pain.<sup>70</sup> Furthermore, the triple rule-out protocol could potentially identify a subset of patients with acute chest pain who can safely be discharged from the emergency department without adverse events during a 30-day follow-up.<sup>71</sup> A recent study in 100 patients with acute chest pain and an intermediate cardiac risk profile used either coronary CTA or a triple rule-out protocol in case of elevated D-dimer levels. Based on a negative coronary CTA or triple rule-out findings, 60 of 100 patients were discharged the same day, without major cardiac events at 90-days follow up. Also, those patients with significant coronary artery stenosis were identified.<sup>72</sup> The use of this protocol in intermediate cardiac risk profile patients was calculated to reduce the number of hospitalized patients and total health costs.<sup>73</sup> Indeed, more RCTs are needed to determine how the triple rule-out protocol is best applied to improve clinical decision making and justified use.

## Technical developments

### Coronary artery plaque quantification

Currently, assessment of stenosis severity on coronary CTA is performed visually. This requires however significant experience and is characterized by limited reproducibility.<sup>74</sup> Novel software tools have become available to (automatically) quantify stenosis severity on CTA, so-called quantitative CTA (QCT).<sup>75, 76</sup> These algorithms usually consist of various steps. First, the coronary tree is extracted from the CTA dataset and a multiplanar reformation is created of each coronary artery or side branch. Thereafter, the lumen and vessel wall are delineated on these MPR images. Based on these segmented contours, the severity of coronary artery stenosis can be quantified, but also the amount of coronary atherosclerosis (the plaque burden) can be derived (see Figure 10.) Previous investigations using QCT have demonstrated a good agreement between stenosis severity as assessed with QCT compared to ICA and intravascular ultrasound (IVUS).<sup>75, 76</sup> It was also shown that stenosis severity derived from QCT was related with the presence of ischemia on SPECT perfusion imaging.<sup>77</sup> Besides these geometrical parameters, it is also feasible to automatically assess and quantify coronary plaque composition with QCT. In a head-to-head comparison between QCT and IVUS with virtual histology, a good agreement was shown for assessment of different plaque types (calcified, mixed or non-calcified).<sup>78</sup> QCT will improve

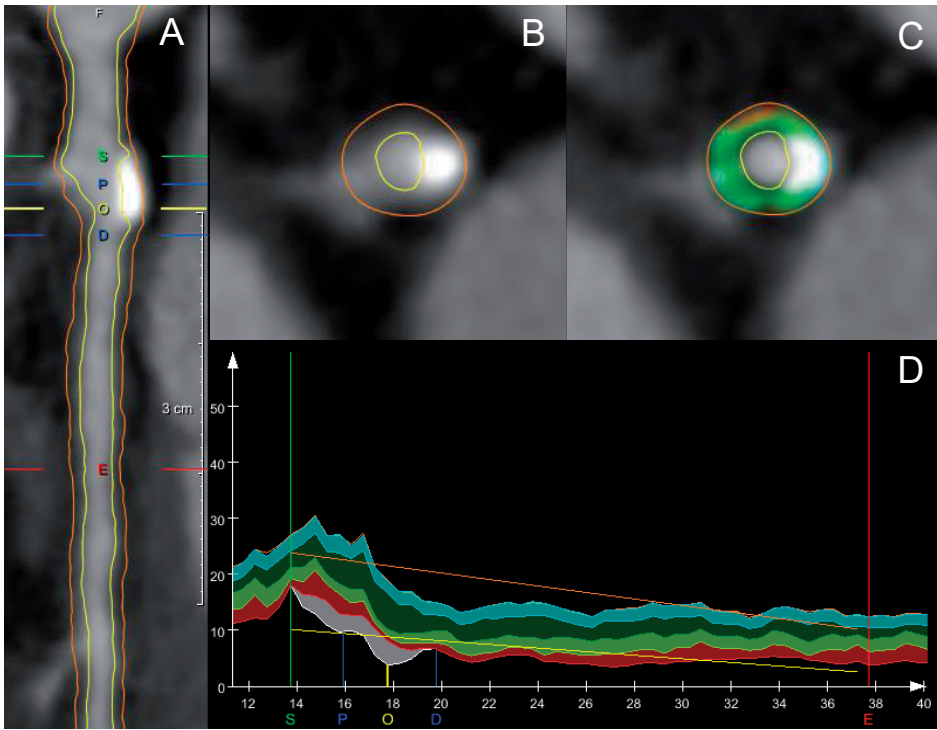


**Figure 10.** Example of quantitative CTA analysis of a 48 year old male patient referred for the evaluation of stable chest pain.

Panel A demonstrates a stretched multiplanar reformation (MPR) of the LAD with a calcified lesion. QCT was used to detect both lumen (yellow) and vessel wall (orange) contours. Longitudinal lumen and vessel wall contours are shown in panel A; whereas transversal lumen and vessel wall contours at the level of the minimal lumen area (MLA) are shown in panel B. Panel C shows the quantification of coronary plaque constitution. Calcium is labeled in white, fibrotic tissue labeled in dark green, fibro-fatty tissue in light green and necrotic core labeled in red. Quantification of the calcified lesion was performed using proximal (green) and distal (red) reference markers as well as lumen (yellow) and vessel wall (orange) reference lines, as illustrated in panel D. In this graph, the x-axis represents the distance from the coronary ostium in mm. The y-axis represents the area of either the lumen (lower part of graph) or the vessel wall (upper part of graph) in mm<sup>2</sup>. The part between the two graphs shows the plaque constitution. Stenosis severity was quantified as 35%.

quantification of coronary stenosis and assessment of plaque composition and may be of particular value in serial evaluations to assess a potential effect of medication on atherosclerosis progression/regression and plaque composition.<sup>79</sup> Recently, the incremental predictive value of these QCT parameters (over visual interpretation) for development of a subsequent ACS, has been established.<sup>80</sup> Versteysen *et al.* compared the coronary CTA results in 25 patients who subsequently developed an ACS (over a mean follow-up period of 26 months) to 101 control patients without events. In the patients who developed an ACS, the total plaque volume, the plaque burden and the

non-calcified plaque volume were significantly larger. Moreover, these quantitative CTA parameters provided incremental prognostic value over the clinical risk profile and the visual interpretation of the coronary CTA results.

### **Developments in CT scanners**

The technology of the CT scanners is evolving rapidly. With the introduction of 256- and 320-slice scanners complete volume coverage of the heart becomes possible in a single heartbeat,<sup>11, 12</sup> This may potentially reduce motion artefacts, particularly in patients with irregular heart rates or rhythm abnormalities. Moreover, dual-source CT scanners with  $2 \times 128$  detector rows have been introduced and these systems demonstrated a high temporal resolution of 75 ms (approximately half of the temporal resolution of the fastest 64-slice scanners) making possible to freeze cardiac motion and obtain diagnostic quality images of the coronary arteries regardless of heart rate or rhythm. Initial studies with dual-source coronary CT in patients presenting with chest pain have reported high negative predictive values approaching 100%, enabling to reliably excluded coronary artery stenoses also in patients with higher heart rates.<sup>81</sup> Very recently, high-pitch ECG triggered ('Flash Spiral') dual-source CT scanners have shown promising results.<sup>13</sup> The novelty of this technique lies in the very high pitch which results in fast image acquisition without cardiac motion artefacts and a very low radiation exposure ( $<1$  mSv).<sup>13</sup> Currently only limited data in selected patients are available with these newer scanners, and larger studies are needed to determine the value of these novel equipment in routine clinical practice.

## **Novel applications of cardiac CT**

### **Assessment of coronary artery plaque composition**

Since coronary CTA allows for the visualization of the coronary vessel wall, coronary atherosclerosis on coronary CTA can be further characterized (beyond stenosis severity), permitting assessment of plaque composition. The plaques can be divided into non-calcified, calcified and mixed plaques. Interestingly, coronary plaque composition has been linked to clinical presentation: patients presenting with an ACS were shown to have more non-calcified and/or mixed plaques in the coronary arteries, whereas patients with stable CAD present with more calcified plaques.<sup>82</sup> In addition, it has been suggested that plaque composition may provide prognostic information.

Specifically, non-calcified plaques with low attenuation values, positive remodeling, and spotty calcifications have been associated with subsequent development of ACS.<sup>83</sup> Moreover, Gaemperli *et al.* evaluated 220 patients with known or suspected CAD using 64-slice coronary CTA and demonstrated worse outcome of patients with

mixed or non-calcified plaques.<sup>84</sup> This was further confirmed by Hou *et al.* in 4,425 patients with suspected CAD with a follow-up period of nearly 3 years. The authors demonstrated that patients with non-calcified plaque were at 5 times higher risk for the combination of death, infarction or revascularization, as compared to patients with calcified plaques, and the risk of patients with mixed plaques was nearly 10 times higher.<sup>85</sup> Interestingly, it was shown in 163 patients with chest pain and suspected CAD that mixed plaques were also correlated with the presence of ischemia on SPECT perfusion imaging.<sup>86</sup>

### **Evaluation of myocardial perfusion**

Recent developments in CT scanner technology have enabled evaluation of left ventricular myocardial contrast attenuation enabling CT myocardial perfusion imaging (of the left ventricle). This functional information is of particular importance to determine the hemodynamical significance of intermediate coronary artery stenoses (around 50% luminal narrowing). Standard CT perfusion (CTP) protocols include a rest study for the evaluation of the coronary arteries and the resting myocardial perfusion, followed by an adenosine-induced stress study to determine the stress perfusion.<sup>87</sup> Similar to perfusion imaging with SPECT or magnetic resonance imaging (MRI), reversible or fixed perfusion defects can be detected indicating ischemia or scar tissue respectively.<sup>88-91</sup> A major advantage of CTP is the combination of coronary artery anatomy (CTA) and function (CTP) in one examination. Blankstein *et al.* demonstrated with 64-slice CT that an adenosine stress CT protocol can identify stress-induced myocardial perfusion defects with a diagnostic accuracy comparable to SPECT.<sup>92</sup> Additionally, the average radiation required in this protocol was similar to the radiation dose of SPECT perfusion imaging. It is anticipated that with improved dose reduction protocols, the radiation dose will be reduced significantly. Recent studies have indicated an improved diagnostic accuracy for CTP compared to coronary CTA alone for the detection of myocardial ischemia.<sup>87, 93</sup> George *et al.* demonstrated in 53 patients with an intermediate to high pre-test likelihood of CAD that the diagnostic accuracy of CTP to predict reversible ischemia on SPECT was higher than coronary CTA.<sup>87</sup>

### **Evaluation of myocardial infarction**

Over recent years, MRI has been successfully employed to image the presence of infarcted myocardium with delayed contrast enhancement imaging. However, several studies have demonstrated that the presence of infarction can be also identified on CT.<sup>88</sup> Because of the pharmacokinetics of the contrast material, a difference between the accumulation of contrast in infarcted and normal myocardium can be visualized. Accordingly, early hypo-enhancement can be observed on the CT images during the first pass of contrast medium at the area of infarcted myocardium. In addition,

delayed hyper-enhancement of infarcted tissue can be detected similarly to MRI. Good correlations between infarct imaging with CT and other imaging modalities such as MRI and SPECT imaging have been demonstrated.<sup>88-90</sup> Moreover, a good correlation between enhancement patterns (both early hypo-enhancement and late hyper-enhancement) and recovery of myocardial function at a follow-up of 3 months post-infarction was reported, suggesting that CT may be useful to predict functional recovery after infarction.<sup>91</sup> However, it is important to realize that in general, delayed enhancement imaging with CT requires additional imaging and thus involves additional radiation exposure. Also, a larger amount of contrast agent is required for delayed enhancement imaging as compared to imaging the coronary arteries alone.

### Fractional flow reserve (FFR)

It has been shown in the FAME (FFR vs. Angiography for multivessel evaluation) trial that revascularization guided by invasive assessment of FFR is superior in terms of outcome over revascularization driven by angiographic stenosis severity.<sup>94</sup> This observation highlights that functional (ischemia) assessment may be preferred over anatomical assessment (stenosis severity) to guide the need for revascularization. Invasive assessment of FFR however, may not be the first choice in patients with stable chest pain, and a non-invasive approach may be preferred. With the application of computational fluid dynamics and complex mathematical calculations, novel software tools allow for the non-invasive assessment of FFR from coronary CTA datasets (FFR<sub>CT</sub>) without additional imaging, modification of CT acquisition protocols, or administration of medication.<sup>95</sup> An example of this approach (as compared to ICA and

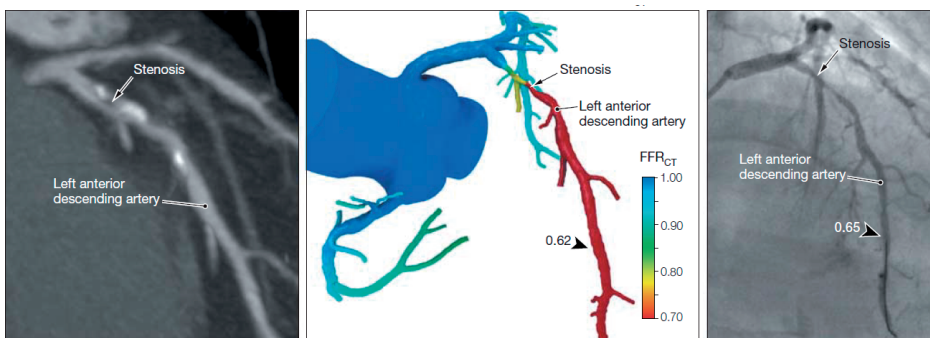


**Figure 11. Case example of FFR<sub>CT</sub> with corresponding invasive coronary angiogram.**

Multipanar reformat of a coronary CT angiogram demonstrating obstructive stenosis of the proximal portion of the left anterior descending (LAD) coronary artery and a computed fractional flow reserve (FFR<sub>CT</sub>) value of 0.62, indicating ischemia. Invasive coronary angiography demonstrates obstructive stenosis of the proximal portion of the LAD and measured fractional flow reserve (FFR) values of 0.65, indicating ischemia.

From: Min *et al.*, JAMA 2012

invasive FFR) is shown in Figure 11. In the DISCOVER FLOW (diagnosis of ischemia-causing stenoses obtained via noninvasive fractional flow reserve) trial, Koo *et al.* have demonstrated good agreement between FFRct and invasive FFR in 103 patients in whom 159 coronary arteries were evaluated.<sup>96</sup> At present, FFRct is not suitable for implementation in the daily practice since FFRct calculations are time consuming (calculation of FFRct may require up to 5 hours) and requires sophisticated computation which is not available in routine clinical imaging departments.<sup>96</sup>

### **Transluminal attenuation gradient**

Another method to improve assessment of the hemodynamic significance of a coronary stenosis with CTA could be the calculation of the transluminal attenuation gradient (TAG).<sup>97</sup> For this purpose a MPR is generated of each coronary. Along the center-line of this MPR the luminal intensity is measured at 1 mm increments. TAG is then defined as the slope of the regression line of the decrease in luminal intensity from the proximal to the distal part of the coronary (Figure 12). A steep decrease in intensity (i.e. a more negative TAG) was associated with the presence of an obstructive lesion in that coronary.<sup>97</sup> Recently Wong *et al.* have reported the incremental value of TAG measurements on 320-row CTA over CTA alone for the prediction of invasive FFR significant lesions.<sup>98</sup> However, until present the exact clinical value of TAG is unknown and requires further trials and investigations.

### **Evaluation of myocardial function**

Besides assessment of the coronary arteries, cardiac CT imaging also permits assessment of left ventricular volumes and function. If data have been collected during the whole cardiac cycle, images can be retrospectively reconstructed in several phases to derive left ventricular ejection fraction from the left ventricular volumes. Indeed, numerous studies have shown that global left ventricular function assessed by CT correlates well with echocardiography and MRI, although CT appeared to minimally overestimate end-systolic volume and may thus slightly underestimate left ventricular ejection fraction.<sup>99, 100</sup> In addition, regional wall motion abnormalities can be reliably evaluated as compared to MRI.<sup>101</sup> However, as images should be acquired throughout the cardiac cycle, left ventricular function protocols are associated with increased radiation exposure and CT may not be the first choice technique, but could be considered as an alternative for patients who are not suitable to undergo MRI.<sup>102</sup>

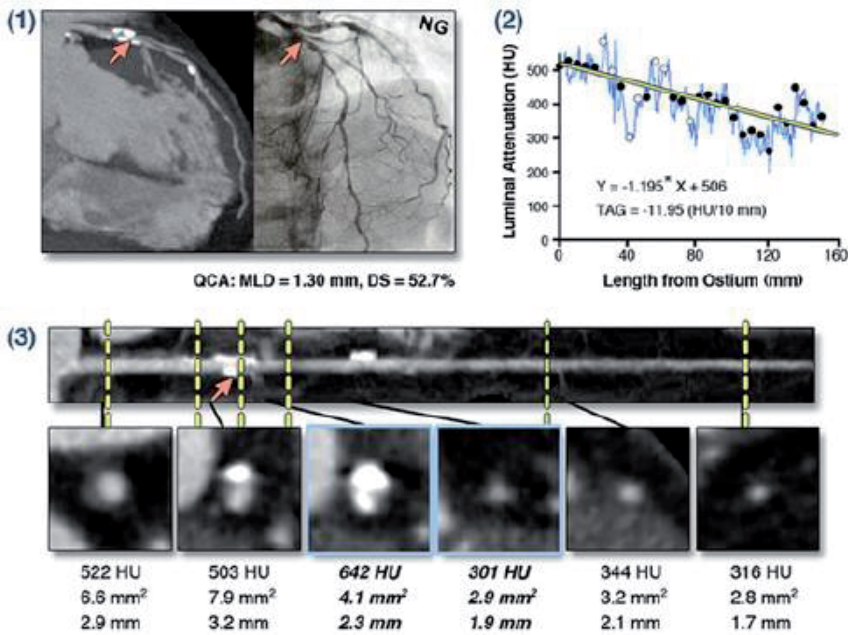


**Figure 12. Patient example of transluminal attenuation gradient (TAG) calculation.**

Panel 1: Coronary CTA demonstrates calcified lesions in the proximal LAD coronary artery and moderate stenosis in the mid LAD trajectory, confirmed by invasive coronary angiography.

Panel 2: Luminal attenuation plot. Black dots represent 5-mm intervals at which intraluminal attenuation (in Hounsfield units, HU) and luminal area (in mm<sup>2</sup>) were measured. TAG is shown by the yellow line and was -11.95 (HU/10mm).

Panel 3: Axial and representative cross-sectional views of coronary CTA.

MLD: minimal lumen diameter, QCA: quantitative coronary angiography

From: Choi *et al.*, JACC: cardiovascular imaging 2011

## Conclusion

Patients presenting with acute chest pain to the emergency room, suspect for an ACS but without the diagnostic ECG and troponin criteria. This poses an important dilemma in clinical cardiology: on the one hand, this population constitutes a large number of patients with a low prevalence of ACS, but on the other hand a substantial number of patients appear to develop an ACS once discharged. Coronary CT angiography is a feasible technique for non-invasive, fast, and accurate exclusion of obstructive CAD in patients presenting with acute chest pain. Moreover, a normal coronary CTA permits safe discharge with good short- to mid-term prognosis. This has increased interest in using CT for non-invasive assessment of CAD in the emergency department, and in addition the technique can evaluate the presence/absence of other causes of acute chest pain such as aortic aneurysm, aortic dissection, or pulmonary embolism.

Four RCTs have been performed comparing a CT-based approach in the emergency room versus a standard of care approach. These trials confirmed the value of coronary CTA to exclude CAD, with good outcome after discharge, and a reduction in hospital stay and costs. At the same time, an increase in ICA and revascularization rate was observed in patients with CAD on coronary CTA; this warrants further studies to determine the precise relation between the coronary CTA findings and referral for ICA. Finally, other applications such as the evaluation of coronary artery plaque composition, myocardial function and perfusion or fractional flow reserve are currently being developed and may also become valuable in the setting of acute chest pain in the future.

## References

- (1) van Velzen JE, Schuif JD, Kroft LJ, Bax JJ. CT angiography and other applications of CT. In: Tubaro M, Danchin N, Filippatos G, Goldstein P, Vranckx P, Zahger D (eds.) *The ESC textbook of acute and intensive cardiac care*. 1st ed. Oxford: Oxford University Press; 2011. pp. 200–12.
- (2) Hounsfield GN. Computerized transverse axial scanning (tomography). 1. Description of system. *Br J Radiol* 1973 December; 46 (552): 1016–22.
- (3) Knez A, Becker CR, Leber A *et al.* Usefulness of multislice spiral computed tomography angiography for determination of coronary artery stenoses. *Am J Cardiol* 2001 November 15; 88 (10): 1191–4.
- (4) Nieman K, Oudkerk M, Rensing BJ *et al.* Coronary angiography with multi-slice computed tomography. *Lancet* 2001 February 24; 357 (9256): 599–3.
- (5) Achenbach S, Giesler T, Ropers D *et al.* Detection of coronary artery stenoses by contrast-enhanced, retrospectively electrocardiographically-gated, multislice spiral computed tomography. *Circulation* 2001 May 29; 103 (21): 2535–8.
- (6) Budoff MJ, Dowe D, Jollis JG *et al.* Diagnostic performance of 64-multidetector row coronary computed tomographic angiography for evaluation of coronary artery stenosis in individuals without known coronary artery disease: results from the prospective multicenter ACCURACY (Assessment by Coronary Computed Tomographic Angiography of Individuals Undergoing Invasive Coronary Angiography) trial. *J Am Coll Cardiol* 2008 November 18; 52 (21): 1724–32.
- (7) Miller JM, Rochitte CE, Dewey M *et al.* Diagnostic performance of coronary angiography by 64-row CT. *N Engl J Med* 2008 November 27; 359 (22): 2324–36.
- (8) Lee TH, Goldman L. Evaluation of the patient with acute chest pain. *N Engl J Med* 2000 April; 20; 342 (16): 1187–95.
- (9) Reilly BM, Evans AT, Schaidt JJ *et al.* Impact of a clinical decision rule on hospital triage of patients with suspected acute cardiac ischemia in the emergency department. *JAMA* 2002 July 17; 288 (3): 342–50.
- (10) Klass O, Mutlu S, Hohl K *et al.* Multidetector computed tomography coronary angiography: sublingual nitroglycerine improves image quality significantly because of peripheral coronary vasodilatation. *J Comput Assist Tomogr* 2009 March; 33 (2): 199–3.
- (11) Dewey M, Zimmermann E, Deissenrieder F *et al.* Noninvasive coronary angiography by 320-row computed tomography with lower radiation exposure and maintained diagnostic accuracy: comparison of results with cardiac catheterization in a head-to-head pilot investigation. *Circulation* 2009 September 8; 120 (10): 867–75.
- (12) Petcherski O, Gaspar T, Halon DA *et al.* Diagnostic accuracy of 256-row computed tomographic angiography for detection of obstructive coronary artery disease using invasive quantitative coronary angiography as reference standard. *Am J Cardiol* 2013 February 15; 111 (4): 510–5.
- (13) Achenbach S, Marwan M, Ropers D *et al.* Coronary computed tomography angiography with a consistent dose below 1 mSv using prospectively electrocardiogram-triggered high-pitch spiral acquisition. *Eur Heart J* 2010 February; 31 (3): 340–6.
- (14) Agatston AS, Janowitz WR, Hildner FJ, Zusmer NR, Viamonte M, Jr, Detrano R. Quantification of coronary artery calcium using ultrafast computed tomography. *J Am Coll Cardiol* 1990 March 15; 15 (4): 827–32.

- (15) Greenland P, Bonow RO, Brundage BH *et al.* ACCF/AHA 2007 clinical expert consensus document on coronary artery calcium scoring by computed tomography in global cardiovascular risk assessment and in evaluation of patients with chest pain: a report of the American College of Cardiology Foundation Clinical Expert Consensus Task Force (ACCF/AHA Writing Committee to Update the 2000 Expert Consensus Document on Electron Beam Computed Tomography) developed in collaboration with the Society of Atherosclerosis Imaging and Prevention and the Society of Cardiovascular Computed Tomography. *J Am Coll Cardiol* 2007 January 23; 49 (3): 378–2.
- (16) Hoff JA, Chomka EV, Krainik AJ, Daviglius M, Rich S, Kondos GT. Age and gender distributions of coronary artery calcium detected by electron beam tomography in 35,246 adults. *Am J Cardiol* 2001 June 15; 87 (12): 1335–9.
- (17) McClelland RL, Chung H, Detrano R, Post W, Kronmal RA. Distribution of coronary artery calcium by race, gender, and age: results from the Multi-Ethnic Study of Atherosclerosis (MESA). *Circulation* 2006 January 3; 113 (1): 30–7.
- (18) Becker CR, Majeed A, Crispin A *et al.* CT measurement of coronary calcium mass: impact on global cardiac risk assessment. *Eur Radiol* 2005 January; 15 (1): 96–101.
- (19) Bischoff B, Kantert C, Meyer T *et al.* Cardiovascular risk assessment based on the quantification of coronary calcium in contrast-enhanced coronary computed tomography angiography. *Eur Heart J Cardiovasc Imaging* 2012 June; 13 (6): 468–75.
- (20) Austen WG, Edwards JE, Frye RL *et al.* A reporting system on patients evaluated for coronary artery disease. Report of the Ad Hoc Committee for Grading of Coronary Artery Disease, Council on Cardiovascular Surgery, American Heart Association. *Circulation* 1975 April; 51 (4 Suppl): 5–40.
- (21) Lehman SJ, Abbara S, Cury RC *et al.* Significance of cardiac computed tomography incidental findings in acute chest pain. *Am J Med* 2009 June; 122 (6): 543–9.
- (22) Onuma Y, Tanabe K, Nakazawa G *et al.* Noncardiac findings in cardiac imaging with multidetector computed tomography. *J Am Coll Cardiol* 2006 July 18; 48 (2): 402–6.
- (23) Earls JP. The pros and cons of searching for extracardiac findings at cardiac CT: studies should be reconstructed in the maximum field of view and adequately reviewed to detect pathologic findings. *Radiology* 2011 November; 261 (2): 342–6.
- (24) Buckens CF, Verkooijen HM, Gondrie MJ, Jairam P, Mali WP, van der Graaf Y. Unrequested findings on cardiac computed tomography: looking beyond the heart. *PLoS One* 2012; 7 (4): e 32184.
- (25) Aglan I, Jodocy D, Hiehs S *et al.* Clinical relevance and scope of accidental extracoronary findings in coronary computed tomography angiography: a cardiac versus thoracic FOV study. *Eur J Radiol* 2010 April; 74 (1): 166–74.
- (26) Chia PL, Kaw G, Wansaicheong G, Ho KT. Prevalence of non-cardiac findings in a large series of patients undergoing cardiac multi-detector computed tomography scans. *Int J Cardiovasc Imaging* 2009 June; 25 (5): 537–43.
- (27) Haller S, Kaiser C, Buser P, Bongartz G, Bremerich J. Coronary artery imaging with contrast-enhanced MDCT: extracardiac findings. *AJR Am J Roentgenol* 2006 July; 187 (1): 105–10.
- (28) Kirsch J, Araoz PA, Steinberg FB, Fletcher JG, McCollough CH, Williamson EE. Prevalence and significance of incidental extracardiac findings at 64-multidetector coronary CTA. *J Thorac Imaging* 2007 November; 22 (4): 330–4.

- (29) Margolis JR, Chen JT, Kong Y, Peter RH, Behar VS, Kisslo JA. The diagnostic and prognostic significance of coronary artery calcification. A report of 800 cases. *Radiology* 1980 December; 137 (3): 609–16.
- (30) Rumberger JA, Simons DB, Fitzpatrick LA, Sheedy PF, Schwartz RS. Coronary artery calcium area by electron-beam computed tomography and coronary atherosclerotic plaque area. A histopathologic correlative study. *Circulation* 1995 October 15; 92 (8): 2157–62.
- (31) Haberl R, Becker A, Leber A *et al.* Correlation of coronary calcification and angiographically documented stenoses in patients with suspected coronary artery disease: results of 1,764 patients. *J Am Coll Cardiol* 2001 February; 37 (2): 451–7.
- (32) Budoff MJ, Diamond GA, Raggi P *et al.* Continuous probabilistic prediction of angiographically significant coronary artery disease using electron beam tomography. *Circulation* 2002 April 16; 105 (15): 1791–6.
- (33) Budoff MJ, Shaw LJ, Liu ST *et al.* Long-term prognosis associated with coronary calcification: observations from a registry of 25,253 patients. *J Am Coll Cardiol* 2007 May 8; 49 (18): 1860–70.
- (34) Greenland P, LaBree L, Azen SP, Doherty TM, Detrano RC. Coronary artery calcium score combined with Framingham score for risk prediction in asymptomatic individuals. *JAMA* 2004 January 14; 291 (2): 210–5.
- (35) von Ballmoos MW, Haring B, Juillerat P, Alkadhi H. Meta-analysis: diagnostic performance of low-radiation-dose coronary computed tomography angiography. *Ann Intern Med* 2011 March 15; 154 (6): 413–20.
- (36) Meijboom WB, Mollet NR, Van Mieghem CA *et al.* 64-Slice CT coronary angiography in patients with non-ST elevation acute coronary syndrome. *Heart* 2007 November; 93 (11): 1386–92.
- (37) Henneman MM, Schuijf JD, van Werkhoven JM *et al.* Multi-slice computed tomography coronary angiography for ruling out suspected coronary artery disease: what is the prevalence of a normal study in a general clinical population? *Eur Heart J* 2008 August; 29 (16): 2006–13.
- (38) Montalescot G, Sechtem U, Achenbach S *et al.* 2013 ESC guidelines on the management of stable coronary artery disease: the Task Force on the management of stable coronary artery disease of the European Society of Cardiology. *Eur Heart J* 2013; **34**:2949–3003.
- (39) Chow BJ, Small G, Yam Y *et al.* Incremental prognostic value of cardiac computed tomography in coronary artery disease using CONFIRM: COroNary computed tomography angiography evaluation for clinical outcomes: an International Multicenter registry. *Circ Cardiovasc Imaging* 2011 September; 4 (5): 463–72.
- (40) Bamberg F, Sommer WH, Hoffmann V *et al.* Meta-analysis and systematic review of the long-term predictive value of assessment of coronary atherosclerosis by contrast-enhanced coronary computed tomography angiography. *J Am Coll Cardiol* 2011 June 14; 57 (24): 2426–36.
- (41) Georgiou D, Budoff MJ, Kaufer E, Kennedy JM, Lu B, Brundage BH. Screening patients with chest pain in the emergency department using electron beam tomography: a follow-up study. *J Am Coll Cardiol* 2001 July; 38 (1): 105–10.
- (42) Laudon DA, Behrenbeck TR, Wood CM *et al.* Computed tomographic coronary artery calcium assessment for evaluating chest pain in the emergency department: long-term outcome of a prospective blind study. *Mayo Clin Proc* 2010 April; 85 (4): 314–22.
- (43) McLaughlin VV, Balogh T, Rich S. Utility of electron beam computed tomography to stratify patients presenting to the emergency room with chest pain. *Am J Cardiol* 1999 August 1; 84 (3): 327–8, A8.

- (44) Nabi F, Chang SM, Pratt CM *et al.* Coronary artery calcium scoring in the emergency department: identifying which patients with chest pain can be safely discharged home. *Ann Emerg Med* 2010 September; 56 (3): 220–9.
- (45) Tota-Maharaj R, McEvoy JW, Blaha MJ, Silverman MG, Nasir K, Blumenthal RS. Utility of coronary artery calcium scoring in the evaluation of patients with chest pain. *Crit Pathw Cardiol* 2012 September; 11 (3): 99–106.
- (46) Forouzandeh F, Chang SM, Muhyieddeen K *et al.* Does quantifying epicardial and intrathoracic fat with noncontrast computed tomography improve risk stratification beyond calcium scoring alone? *Circ Cardiovasc Imaging* 2013 January 1; 6 (1): 58–66.
- (47) Shemesh J, Stroh CI, Tenenbaum A *et al.* Comparison of coronary calcium in stable angina pectoris and in first acute myocardial infarction utilizing double helical computerized tomography. *Am J Cardiol* 1998 February 1; 81 (3): 271–5.
- (48) Chang AM, Le J, Matsuura AC, Litt HI, Hollander JE. Does coronary artery calcium scoring add to the predictive value of coronary computed tomography angiography for adverse cardiovascular events in low-risk chest pain patients? *Acad Emerg Med* 2011 October; 18 (10): 1065–71.
- (49) Beigel R, Oieru D, Goitein O *et al.* Usefulness of routine use of multidetector coronary computed tomography in the ‘fast track’ evaluation of patients with acute chest pain. *Am J Cardiol* 2009 June 1; 103 (11): 1481–6.
- (50) Braunwald E, Antman EM, Beasley JW *et al.* ACC/AHA 2002 guideline update for the management of patients with unstable angina and non-ST-segment elevation myocardial infarction—summary article: a report of the American College of Cardiology/American Heart Association task force on practice guidelines (Committee on the Management of Patients With Unstable Angina). *J Am Coll Cardiol* 2002 October 2; 40 (7): 1366–74.
- (51) Hoffmann U, Bamberg F, Chae CU *et al.* Coronary computed tomography angiography for early triage of patients with acute chest pain: the ROMICAT (Rule Out Myocardial Infarction using Computer Assisted Tomography) trial. *J Am Coll Cardiol* 2009 May 5; 53 (18): 1642–50.
- (52) Litt HI, Gatsonis C, Snyder B *et al.* CT angiography for safe discharge of patients with possible acute coronary syndromes. *N Engl J Med* 2012 April 12; 366 (15): 1393–3.
- (53) Hulten E, Pickett C, Bittencourt MS *et al.* Outcomes after coronary computed tomography angiography in the emergency department: a systematic review and meta-analysis of randomized, controlled trials. *J Am Coll Cardiol* 2013 February 26; 61 (8): 880–92.
- (54) Goldstein JA, Gallagher MJ, O’Neill WW, Ross MA, O’Neil BJ, Raff GL. A randomized controlled trial of multi-slice coronary computed tomography for evaluation of acute chest pain. *J Am Coll Cardiol* 2007 February 27; 49 (8): 863–71.
- (55) Hoffmann U, Truong QA, Schoenfeld DA *et al.* Coronary CT angiography versus standard evaluation in acute chest pain. *N Engl J Med* 2012 July 26; 367 (4): 299–8.
- (56) Goldstein JA, Chinnaiyan KM, Abidov A *et al.* The CT-STAT (Coronary Computed Tomographic Angiography for Systematic Triage of Acute Chest Pain Patients to Treatment) trial. *J Am Coll Cardiol* 2011 September 27; 58 (14): 1414–22.
- (57) Chiu KW, Lakshminarayan R, Ettles DF. Acute aortic syndrome: CT findings. *Clin Radiol* 2013 July; 68 (7): 741–8.
- (58) Steenburg SD, Ravenel JG. Acute traumatic thoracic aortic injuries: experience with 64-MDCT. *AJR Am J Roentgenol* 2008 November; 191 (5): 1564–9.
- (59) Holloway BJ, Rosewarne D, Jones RG. Imaging of thoracic aortic disease. *Br J Radiol* 2011; **84** Spec No 3: S338–54.

- (60) Hiratzka LF, Bakris GL, Beckman JA *et al.* 2010 ACCF/AHA/AATS/ACR/ASA/SCA/SCAI/SIR/STS/SVM Guidelines for the diagnosis and management of patients with thoracic aortic disease. A Report of the American College of Cardiology Foundation/American Heart Association Task Force on Practice Guidelines, American Association for Thoracic Surgery, American College of Radiology, American Stroke Association, Society of Cardiovascular Anesthesiologists, Society for Cardiovascular Angiography and Interventions, Society of Interventional Radiology, Society of Thoracic Surgeons, and Society for Vascular Medicine. *J Am Coll Cardiol* 2010 April 6; 55 (14): e27–e 129.
- (61) Stanson AW, Kazmier FJ, Hollier LH *et al.* Penetrating atherosclerotic ulcers of the thoracic aorta: natural history and clinicopathologic correlations. *Ann Vasc Surg* 1986 May; 1 (1): 15–23.
- (62) Hartnell GG. Imaging of aortic aneurysms and dissection: CT and MRI. *J Thorac Imaging* 2001 January; 16 (1): 35–46.
- (63) Wells PS, Anderson DR, Ginsberg J. Assessment of deep vein thrombosis or pulmonary embolism by the combined use of clinical model and noninvasive diagnostic tests. *Semin Thromb Hemost* 2000; 26 (6): 643–56.
- (64) Remy-Jardin M, Pistolesi M, Goodman LR *et al.* Management of suspected acute pulmonary embolism in the era of CT angiography: a statement from the Fleischner Society. *Radiology* 2007 November; 245 (2): 315–29.
- (65) Mos IC, Klok FA, Kroft LJ, de RA, Dekkers OM, Huisman MV. Safety of ruling out acute pulmonary embolism by normal computed tomography pulmonary angiography in patients with an indication for computed tomography: systematic review and meta-analysis. *J Thromb Haemost* 2009 September; 7 (9): 1491–8.
- (66) Furlan A, Aghayev A, Chang CC *et al.* Short-term mortality in acute pulmonary embolism: clot burden and signs of right heart dysfunction at CT pulmonary angiography. *Radiology* 2012 October; 265 (1): 283–93.
- (67) McCollough CH, Primak AN, Saba O *et al.* Dose performance of a 64-channel dual-source CT scanner. *Radiology* 2007 June; 243 (3): 775–84.
- (68) Hausleiter J, Meyer T, Hadamitzky M *et al.* Radiation dose estimates from cardiac multislice computed tomography in daily practice: impact of different scanning protocols on effective dose estimates. *Circulation* 2006 March 14; 113 (10): 1305–10.
- (69) White CS, Kuo D, Kelemen M *et al.* Chest pain evaluation in the emergency department: can MDCT provide a comprehensive evaluation? *AJR Am J Roentgenol* 2005 August; 185 (2): 533–40.
- (70) Johnson TR, Nikolaou K, Wintersperger BJ *et al.* ECG-gated 64-MDCT angiography in the differential diagnosis of acute chest pain. *AJR Am J Roentgenol* 2007 January; 188 (1): 76–82.
- (71) Takakuwa KM, Halpern EJ. Evaluation of a “triple rule-out” coronary CT angiography protocol: use of 64-Section CT in low-to-moderate risk emergency department patients suspected of having acute coronary syndrome. *Radiology* 2008 August; 248 (2): 438–46.
- (72) Gruettner J, Fink C, Walter T *et al.* Coronary computed tomography and triple rule out CT in patients with acute chest pain and an intermediate cardiac risk profile. Part 1: impact on patient management. *Eur J Radiol* 2013 January; 82 (1): 100–5.
- (73) Henzler T, Gruettner J, Meyer M *et al.* Coronary computed tomography and triple rule out CT in patients with acute chest pain and an intermediate cardiac risk for acute coronary syndrome: part 2: economic aspects. *Eur J Radiol* 2013 January; 82 (1): 106–11.

- (74) Hoffmann H, Frieler K, Hamm B, Dewey M. Intra- and interobserver variability in detection and assessment of calcified and noncalcified coronary artery plaques using 64-slice computed tomography: variability in coronary plaque measurement using MSCT. *Int J Cardiovasc Imaging* 2008 October; 24 (7): 735–42.
- (75) Boogers MJ, Broersen A, van Velzen JE *et al.* Automated quantification of coronary plaque with computed tomography: comparison with intravascular ultrasound using a dedicated registration algorithm for fusion-based quantification. *Eur Heart J* 2012 April; 33 (8): 1007–16.
- (76) Voros S, Rinehart S, Qian Z *et al.* Prospective validation of standardized, 3-dimensional, quantitative coronary computed tomographic plaque measurements using radiofrequency backscatter intravascular ultrasound as reference standard in intermediate coronary arterial lesions: results from the ATLANTA (assessment of tissue characteristics, lesion morphology, and hemodynamics by angiography with fractional flow reserve, intravascular ultrasound and virtual histology, and noninvasive computed tomography in atherosclerotic plaques) I study. *JACC Cardiovasc Interv* 2011 February; 4 (2): 198–8.
- (77) de Graaf MA, El-Naggar HM, Boogers MJ *et al.* Automated quantitative coronary computed tomography correlates of myocardial ischaemia on gated myocardial perfusion SPECT. *Eur J Nucl Med Mol Imaging* 2013; **40**:1171–80.
- (78) de Graaf MA, Broersen A, Kitslaar PH *et al.* Automatic quantification and characterization of coronary atherosclerosis with computed tomography coronary angiography: cross-correlation with intravascular ultrasound virtual histology. *Int J Cardiovasc Imaging* 2013; **29**:1177–90.
- (79) Papadopoulou SL, Garcia-Garcia HM, Rossi A *et al.* Reproducibility of computed tomography angiography data analysis using semiautomated plaque quantification software: implications for the design of longitudinal studies. *Int J Cardiovasc Imaging* 2013; **29**:1095–104.
- (80) Versteyleen MO, Kietselaer BL, Dagnelie PC *et al.* Additive value of semiautomated quantification of coronary artery disease using cardiac computed tomographic angiography to predict future acute coronary syndrome. *J Am Coll Cardiol* 2013 June 4; 61 (22): 2296–5.
- (81) Westwood ME, Raatz HD, Misso K *et al.* Systematic review of the accuracy of dual-source cardiac CT for detection of arterial stenosis in difficult to image patient groups. *Radiology* 2013 May; 267 (2): 387–95.
- (82) Pundziute G, Schuijff JD, Jukema JW *et al.* Evaluation of plaque characteristics in acute coronary syndromes: non-invasive assessment with multi-slice computed tomography and invasive evaluation with intravascular ultrasound radiofrequency data analysis. *Eur Heart J* 2008 October; 29 (19): 2373–81.
- (83) Motoyama S, Sarai M, Harigaya H *et al.* Computed tomographic angiography characteristics of atherosclerotic plaques subsequently resulting in acute coronary syndrome. *J Am Coll Cardiol* 2009 June 30; 54 (1): 49–57.
- (84) Gaemperli O, Valenta I, Schepis T *et al.* Coronary 64-slice CT angiography predicts outcome in patients with known or suspected coronary artery disease. *Eur Radiol* 2008 June; 18 (6): 1162–73.
- (85) Hou ZH, Lu B, Gao Y *et al.* Prognostic value of coronary CT angiography and calcium score for major adverse cardiac events in outpatients. *JACC Cardiovasc Imaging* 2012 October; 5 (10): 990–9.
- (86) Lin F, Shaw LJ, Berman DS *et al.* Multidetector computed tomography coronary artery plaque predictors of stress-induced myocardial ischemia by SPECT. *Atherosclerosis* 2008 April; 197 (2): 700–9.

- (87) George RT, Arbab-Zadeh A, Miller JM *et al.* Computed tomography myocardial perfusion imaging with 320-row detector computed tomography accurately detects myocardial ischemia in patients with obstructive coronary artery disease. *Circ Cardiovasc Imaging* 2012 May 1; 5 (3): 333–40.
- (88) Henneman MM, Schuijf JD, Dibbets-Schneider P *et al.* Comparison of multislice computed tomography to gated single-photon emission computed tomography for imaging of healed myocardial infarcts. *Am J Cardiol* 2008 January 15; 101 (2): 144–8.
- (89) Gerber BL, Belge B, Legros GJ *et al.* Characterization of acute and chronic myocardial infarcts by multidetector computed tomography: comparison with contrast-enhanced magnetic resonance. *Circulation* 2006 February 14; 113 (6): 823–33.
- (90) Mahnken AH, Koos R, Katoh M *et al.* Assessment of myocardial viability in reperfused acute myocardial infarction using 16-slice computed tomography in comparison to magnetic resonance imaging. *J Am Coll Cardiol* 2005 June 21; 45 (12): 2042–7.
- (91) Lessick J, Dragu R, Mutlak D *et al.* Is functional improvement after myocardial infarction predicted with myocardial enhancement patterns at multidetector CT? *Radiology* 2007 September; 244 (3): 736–44.
- (92) Blankstein R, Shtruman LD, Rogers IS *et al.* Adenosine-induced stress myocardial perfusion imaging using dual-source cardiac computed tomography. *J Am Coll Cardiol* 2009 September 15; 54 (12): 1072–84.
- (93) Feuchtnner GM, Plank F, Pena C *et al.* Evaluation of myocardial CT perfusion in patients presenting with acute chest pain to the emergency department: comparison with SPECT-myocardial perfusion imaging. *Heart* 2012 October; 98 (20): 1510–7.
- (94) Tonino PA, De BB, Pijls NH *et al.* Fractional flow reserve versus angiography for guiding percutaneous coronary intervention. *N Engl J Med* 2009 January 15; 360 (3): 213–24.
- (95) Kim HJ, Vignon-Clementel IE, Coogan JS, Figueroa CA, Jansen KE, Taylor CA. Patient-specific modeling of blood flow and pressure in human coronary arteries. *Ann Biomed Eng* 2010 October; 38 (10): 3195–9.
- (96) Koo BK, Erglis A, Doh JH *et al.* Diagnosis of ischemia-causing coronary stenoses by noninvasive fractional flow reserve computed from coronary computed tomographic angiograms. Results from the prospective multicenter DISCOVER-FLOW (Diagnosis of Ischemia-Causing Stenoses Obtained Via Noninvasive Fractional Flow Reserve) study. *J Am Coll Cardiol* 2011 November 1; 58 (19): 1989–97.
- (97) Choi JH, Min JK, Labounty TM *et al.* Intracoronary transluminal attenuation gradient in coronary CT angiography for determining coronary artery stenosis. *JACC Cardiovasc Imaging* 2011 November; 4 (11): 1149–57.
- (98) Wong DT, Ko BS, Cameron JD *et al.* Transluminal attenuation gradient in coronary computed tomography angiography is a novel noninvasive approach to the identification of functionally significant coronary artery stenosis: a comparison with fractional flow reserve. *J Am Coll Cardiol* 2013 March 26; 61 (12): 1271–9.
- (99) Dewey M, Muller M, Eddicks S *et al.* Evaluation of global and regional left ventricular function with 16-slice computed tomography, biplane cineventriculography, and two-dimensional transthoracic echocardiography: comparison with magnetic resonance imaging. *J Am Coll Cardiol* 2006 November 21; 48 (10): 2034–44.
- (100) Wu YW, Tadamura E, Yamamuro M *et al.* Estimation of global and regional cardiac function using 64-slice computed tomography: a comparison study with echocardiography, gated-SPECT and cardiovascular magnetic resonance. *Int J Cardiol* 2008 August 1; 128 (1): 69–76.

- (101) Annuar BR, Liew CK, Chin SP *et al.* Assessment of global and regional left ventricular function using 64-slice multislice computed tomography and 2D echocardiography: a comparison with cardiac magnetic resonance. *Eur J Radiol* 2008 January; 65 (1): 112–9.
- (102) Taylor AJ, Cerqueira M, Hodgson JM *et al.* ACCF/SCCT/ACR/AHA/ASE/ASNC/NASCI/SCAI/SCMR 2010 appropriate use criteria for cardiac computed tomography. A report of the American College of Cardiology Foundation Appropriate Use Criteria Task Force, the Society of Cardiovascular Computed Tomography, the American College of Radiology, the American Heart Association, the American Society of Echocardiography, the American Society of Nuclear Cardiology, the North American Society for Cardiovascular Imaging, the Society for Cardiovascular Angiography and Interventions, and the Society for Cardiovascular Magnetic Resonance. *J Am Coll Cardiol* 2010 November 23; 56 (22): 1864–94.
- (103) Gallagher MJ, Ross MA, Raff GL, Goldstein JA, O'Neill WW, O'Neil B. The diagnostic accuracy of 64-slice computed tomography coronary angiography compared with stress nuclear imaging in emergency department low-risk chest pain patients. *Ann Emerg Med* 2007 February; 49 (2): 125–36.
- (104) Hoffmann U, Pena AJ, Moselewski F *et al.* MDCT in early triage of patients with acute chest pain. *AJR Am J Roentgenol* 2006 November; 187 (5): 1240–7.
- (105) Hoffmann U, Nagurney JT, Moselewski F *et al.* Coronary multidetector computed tomography in the assessment of patients with acute chest pain. *Circulation* 2006 November 21; 114 (21): 2251–60.
- (106) Olivetti L, Mazza G, Volpi D, Costa F, Ferrari O, Pirelli S. Multislice CT in emergency room management of patients with chest pain and medium-low probability of acute coronary syndrome. *Radiol Med* 2006 December; 111 (8): 1054–63.
- (107) Sato Y, Matsumoto N, Ichikawa M *et al.* Efficacy of multislice computed tomography for the detection of acute coronary syndrome in the emergency department. *Circ J* 2005 September; 69 (9): 1047–51.
- (108) Rubinshtein R, Halon DA, Gaspar T *et al.* Usefulness of 64-slice cardiac computed tomographic angiography for diagnosing acute coronary syndromes and predicting clinical outcome in emergency department patients with chest pain of uncertain origin. *Circulation* 2007 April 3; 115 (13): 1762–8.
- (109) Vanhoenacker PK, Decramer I, Bladt O, Sarno G, Bevernage C, Wijns W. Detection of non-ST-elevation myocardial infarction and unstable angina in the acute setting: meta-analysis of diagnostic performance of multi-detector computed tomographic angiography. *BMC Cardiovasc Disord* 2007;7:39.



# Part 1

Quantitative assessment of coronary atherosclerosis on coronary CTA



# Chapter 3

## High coronary plaque load: a heavy burden

de Graaf MA, Jukema JW.

*European Heart Journal* 2013;34:3168-3170



*This editorial refers to: “Coronary Atheroma Volume and Cardiovascular Events During Maximally Intensive Statin Therapy” by Puri et al. published in European Heart Journal in November 2013*

Hydroxymethylglutaryl (HMG) CoA-Reductase inhibitors or statins play an important role in the primary and secondary prevention of coronary heart disease. By inhibiting the enzyme HMG-CoA reductase, statins lower the production of cholesterol in the liver, resulting in lower LDL cholesterol levels. Besides lowering cholesterol levels, statin therapy slows down plaque progression and in some patients even cause plaque regression.

In the beginning of the 90's the first trials were initiated to assess the effect of statin therapy on plaque dynamics. Randomized trials, like MARS and REGRESS, used (quantitative) invasive coronary angiography (ICA) to assess luminal stenosis characteristics. Since ICA only allows assessment of the coronary lumen, differences in minimal lumen diameters (MLD) and mean segment diameters (MSD) between baseline and follow-up were assessed as a measurement of coronary plaque change.<sup>1,2</sup> These early studies demonstrated that moderate dose statin therapy on average reduces plaque progression. Importantly, this was associated with a reduction of major adverse cardiovascular events (MACE). Of note, it was shown that the beneficial effect of statin therapy is more pronounced in more severe lesions.<sup>1</sup>

A relative shortcoming of these studies was the inability of ICA to visualize true coronary atherosclerotic burden. Around the same time as the first angiographic studies with statin therapy were executed, a novel method for the assessment of coronary plaque burden was designed; intracoronary ultrasound (ICUS), nowadays known as intravascular ultrasound (IVUS). This invasive method uses ultrasound to create two dimensional tomographic images of the coronary lumen and vessel wall morphology.<sup>3</sup> Since then IVUS is frequently used for coronary plaque assessment and has been widely validated for serial plaque imaging.<sup>4</sup> IVUS is able to visualize true atherosclerotic burden with a high resolution and could be of value, not only for prognostic implications, but also to provide novel insights in the mechanisms of plaque dynamics in patients receiving statin therapy. In the future, non-invasive, serial assessment of coronary atherosclerosis could be feasible using quantitative computed tomography coronary angiography (QCT).<sup>5</sup> Figure 1 demonstrates the difference in coronary plaque assessment between ICA, IVUS and QCT.

In this issue of the European Heart Journal Puri *et al.* present the results of a novel sub-study of the SATURN trial. In this study, 1039 patients underwent serial IVUS before and after 24 months of statin therapy. Patients were randomized to the highest dose of either rosuvastatin (40mg) or atorvastatin (80mg), which is currently the most intensive statin regimen used in clinical practice. Serial IVUS was performed in a

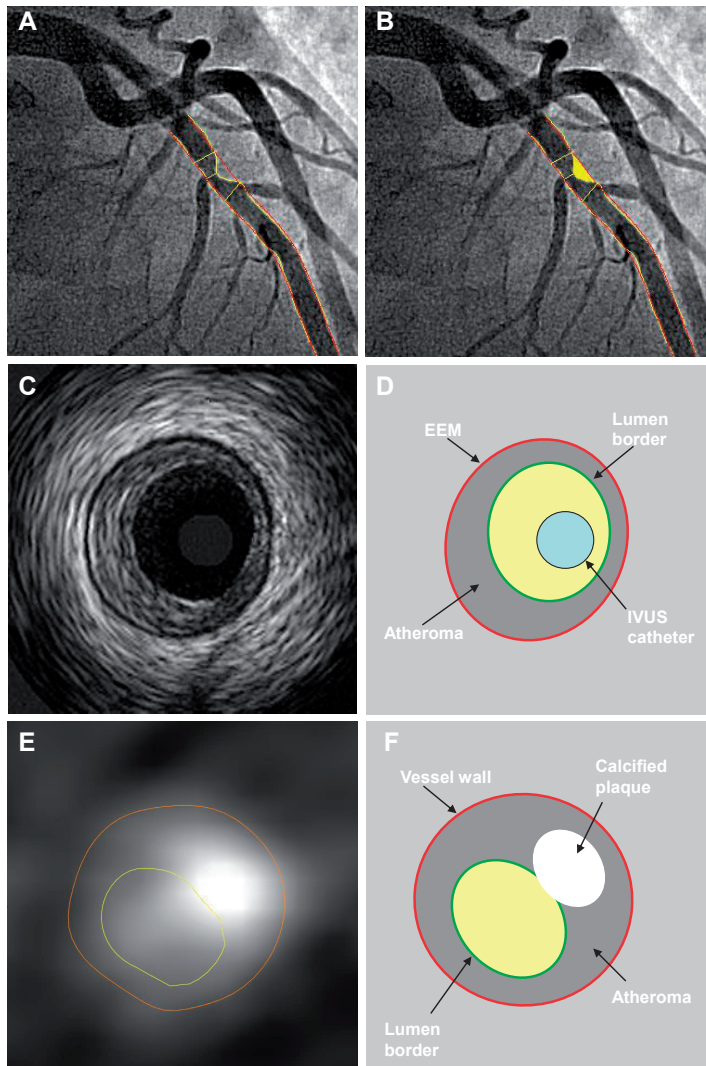


**Figure 1. Difference in coronary plaque assessment between IVUS , invasive coronary angiography (ICA) and quantitative computed tomography coronary angiography (QCT).**

Panel A demonstrates quantitative coronary angiography (Qangio XA version 7, Medis medical image systems B.V.). After delineation of the contrast-filled lumen the percentage stenosis can be calculated. The yellow area in Panel B represents the coronary plaque. However, since the vessel wall cannot be depicted on ICA this is a derived parameter. Panel C demonstrates a cross-sectional IVUS image of a coronary artery. This view allows assessment of coronary atherosclerosis. After segmentation of the EEM and lumen contours as demonstrated in Panel D, the plaque burden can be assessed. Panel E represent a cross-section of a QCT analysis of a coronary artery (Qangio CT research edition version 1.3.6., Medis medical image systems B.V.). In a similar fashion as IVUS, the lumen and vessel wall are segmented (Panel F). Thereafter, coronary plaque burden can be calculated. In addition, QCT allows for characterization of coronary atherosclerosis.

Abbreviations: EEM: external elastic membrane, IVUS: Intravascular Ultrasound

single coronary, without significant luminal stenosis or previous revascularization. The authors investigated the prognostic influence of baseline percentage atheroma volume (PAV) on: a) MACE b) lipid levels at baseline and follow-up and c) coronary plaque progression. It was demonstrated that PAV at baseline is associated with the occurrence of MACE during 2 years follow-up. The incidence of MACE in patients in the lowest quartile of PAV was 5.1% and was significantly increased stepwise per PAV quartile (5.1%, 5.7%, 7.9% and 12% respectively,  $p=0.001$ ). This relation remained significant after correction for baseline risk factors. Of particular interest, neither LDL cholesterol levels at baseline or after high dose statin treatment could independently predict MACE. Thereafter, the correlation between PAV at baseline and plaque progression on IVUS was assessed. As expected, patients with PAV above median demonstrated a greater reduction in PAV at 12 months follow-up. Accordingly, in these patients lumen volume was significantly more increased after therapy compared to patients with PAV below median. However, no significant differences in vessel wall volume were observed between the two groups. Thus, patients with heavy disease burden at baseline benefit relatively more from aggressive/high dose statin therapy with regard to plaque regression, compared to patients with a light disease burden, confirming the older ICA results with modest dose statin therapy

One of the most striking results of this study is the fact that LDL levels at baseline or after statin treatment showed no predictive value for MACE. This could lead to doubt about the beneficial effect of LDL-lowering therapy. However, as also discussed by the authors, there is overwhelming evidence for the beneficial effects of statin therapy on plaque progression and MACE.<sup>6</sup> As demonstrated by IVUS in the REVERSAL-trial, there is a significant association between the amount of LDL-cholesterol reduction due to statin therapy and slowed progression of atherosclerosis (as assessed by PAV). Currently, statin therapy is so fundamentally established in daily practice, its beneficial effect is beyond doubt. Even though it has been demonstrated that in patients receiving statin therapy LDL cholesterol levels have no additional prognostic value, further lowering of LDL cholesterol levels with novel PCSK9 monoclonal antibodies could further reduce the residual risk in these patients.<sup>7, 8</sup> These drugs are currently investigated in trial to assess the safety and efficacy.

Recently, evidence has become available suggesting that the effect of statin therapy on prognosis is not solely mediated through lowering of LDL-cholesterol but also so-called “pleiotropic effects” play an important role. These molecular mechanisms seem to be in part independent of LDL-lowering. Examples of these pleiotropic effects are: improvement of endothelial function, stabilization of atherosclerotic plaques and decreasing oxidative stress and inflammation.<sup>9</sup> Indeed, recent studies have demonstrated that in addition to decrease in PAV, statin therapy leads to stabilization of

coronary atherosclerosis. Nozue *et al* performed IVUS Virtual Histology (IVUS-VH) in 39 patients during PCI and after 8 and 48 months of statin therapy. An increase in negative remodeling and calcified plaque was observed during follow-up suggesting stabilization of coronary plaque.<sup>10</sup> This was further confirmed by Taguchi *et al*, in 120 ACS patients receiving statin therapy who underwent serial IVUS. Both in patients showing plaque progression or regression, the amount of necrotic core, associated with plaque vulnerability, was significantly decreased after 8 to 10 months of statin therapy.<sup>11</sup> In the SATURN sub-study, Puri *et al*. demonstrated that plaque regression was most pronounced in patients with PAV above the median. These patients presented with an unfavorable risk profile at baseline. It seems that the most diseased patients benefit the most from aggressive therapy. This was in line with a recent study that comparing plaque regression by statin therapy in patients with stable CAD and ACS demonstrated the most benefit of statin therapy in ACS patients.<sup>12</sup> Unfortunately, the study by Puri *et al*. lacks further insight in the prognostic value of PAV changes by statin therapy. This would be an interesting topic, worth further investigation.

In conclusion, statin therapy lowers PAV and as a result improves prognosis. These beneficial effects are more pronounced in patients with a PAV above the median. Despite aggressive/high dose statin therapy, a high atherosclerotic plaque burden still remains a heavy burden and novel treatment modalities should be developed to further reduce residual risk.

## References

- (1) Blankenhorn DH, Azen SP, Krams DM, Mack WJ, Cashin-Hemphill L, Hodis HN, DeBoer LW, Mahler PR, Masteller MJ, Vailas LI, Alaupovic P, Hirsch LJ. Coronary angiographic changes with lovastatin therapy. The Monitored Atherosclerosis Regression Study (MARS). *Ann Intern Med* 1993;119(10):969-976.
- (2) Jukema JW, Bruschke AV, van Boven AJ, Reiber JH, Bal ET, Zwinderman AH, Jansen H, Boerma GJ, van Rappard FM, Lie KI, . Effects of lipid lowering by pravastatin on progression and regression of coronary artery disease in symptomatic men with normal to moderately elevated serum cholesterol levels. The Regression Growth Evaluation Statin Study (REGRESS). *Circulation* 1995;91(10):2528-2540.
- (3) Yock PG, Linker DT, Angelsen BA. Two-dimensional intravascular ultrasound: technical development and initial clinical experience. *J Am Soc Echocardiogr* 1989;2(4):296-304.
- (4) Nicholls SJ, Sipahi I, Schoenhagen P, Crowe T, Tuzcu EM, Nissen SE. Application of intravascular ultrasound in anti-atherosclerotic drug development. *Nat Rev Drug Discov* 2006;5(6):485-492.
- (5) Boogers MJ, Broersen A, van Velzen JE, de Graaf FR, El-Naggar HM, Kitslaar PH, Dijkstra J, Delgado V, Boersma E, de RA, Schuijf JD, Schalij MJ, Reiber JH, Bax JJ, Jukema JW. Automated quantification of coronary plaque with computed tomography: comparison with intravascular ultrasound using a dedicated registration algorithm for fusion-based quantification. *Eur Heart J* 2012;33(8):1007-1016.
- (6) Anderson KM, Castelli WP, Levy D. Cholesterol and mortality. 30 years of follow-up from the Framingham study. *JAMA* 1987;257(16):2176-2180.
- (7) Liem AH, van de Woestijne AP, Roeters van Lennep HW, Zwinderman AH, van der Steeg WA, Jukema JW. ApoB/A1 and LDL-C/HDL-C and the prediction of cardiovascular risk in statin-treated patients. *Curr Med Res Opin* 2008;24(2):359-364.
- (8) Koren MJ, Scott R, Kim JB, Knusel B, Liu T, Lei L, Bolognese M, Wasserman SM. Efficacy, safety, and tolerability of a monoclonal antibody to proprotein convertase subtilisin/kexin type 9 as monotherapy in patients with hypercholesterolaemia (MENDEL): a randomised, double-blind, placebo-controlled, phase 2 study. *Lancet* 2012;380(9858):1995-2006.
- (9) Liao JK, Laufs U. Pleiotropic effects of statins. *Annu Rev Pharmacol Toxicol* 2005;45:89-118.:89-118.
- (10) Nozue T, Fukui K, Yamamoto S, Kunishima T, Umezawa S, Onishi Y, Tohyama S, Hibi K, Sozu T, Terashima M, Michishita I. Time course of statin-induced changes in coronary atherosclerosis using intravascular ultrasound with virtual histology. *Coron Artery Dis* 2013.
- (11) Taguchi I, Oda K, Yoneda S, Kageyama M, Kanaya T, Toyoda S, Abe S, Node K, Inoue T. Evaluation of serial changes in tissue characteristics during statin-induced plaque regression using virtual histology-intravascular ultrasound studies. *Am J Cardiol* 2013;111(9):1246-1252.
- (12) Nozue T, Yamamoto S, Tohyama S, Fukui K, Umezawa S, Onishi Y, Kunishima T, Sato A, Nozato T, Miyake S, Takeyama Y, Morino Y, Yamauchi T, Muramatsu T, Hibi K, Terashima M, Michishita I. Comparison of change in coronary atherosclerosis in patients with stable versus unstable angina pectoris receiving statin therapy (from the Treatment With Statin on Atheroma Regression Evaluated by Intravascular Ultrasound With Virtual Histology [TRUTH] study). *Am J Cardiol* 2013;111(7):923-929.



# Chapter 4

## Automatic quantification and characterization of coronary atherosclerosis with computed tomography coronary angiography: cross-correlation with intravascular ultrasound virtual histology

de Graaf MA, Broersen A, Kitslaar PH, Roos CJ, Dijkstra J, Lelieveldt BP, Jukema JW, Schalij MJ, Delgado V, Bax JJ, Reiber JH, Scholte AJ.

*International Journal of Cardiovascular Imaging* 2013;29:1177-1190

## Abstract

**Purpose:** Plaque constitution on CTA is associated with prognosis. At present only visual assessment of plaque constitution is possible. An accurate automatic, quantitative approach for CTA plaque constitution assessment would improve reproducibility and allows higher accuracy. The present study assessed the feasibility of a fully automatic and quantitative analysis of atherosclerosis on CTA. Clinically derived CTA and IVUS VH datasets were used to investigate the correlation between quantitatively automatically derived CTA parameters and IVUS VH.

**Methods:** A total of 57 patients underwent CTA prior to IVUS VH. First, quantitative CTA (QCT) was performed. Per lesion stenosis parameters and plaque volumes were assessed. Using predefined HU thresholds, CTA plaque volume was differentiated in 4 different plaque types necrotic core (NC), dense calcium (DC), fibrotic (FI) and fibro-fatty tissue (FF). At the identical level of the coronary, the same parameters were derived from IVUS VH. Bland-Altman analyses were performed to assess the agreement between QCT and IVUS VH.

**Results:** Assessment of plaque volume using QCT in 108 lesions showed excellent correlation with IVUS VH ( $r = 0.928$ ,  $P < 0.001$ ) (Figure 1). The correlation of both FF and FI volume on IVUS VH and QCT was good ( $r = 0.714$ ,  $P < 0.001$  and  $r = 0.695$ ,  $P < 0.001$  respectively) with corresponding bias and 95% limits of agreement of  $24 \text{ mm}^3$  (-42 ; 90) and  $7.7 \text{ mm}^3$  (-54 ; 70). Furthermore, NC and DC were well-correlated in both modalities ( $r = 0.523$ ,  $P < 0.001$ ) and ( $r = 0.736$ ,  $P < 0.001$ ).

**Conclusion:** Automatic, quantitative CTA tissue characterization is feasible using a dedicated software tool.

## Introduction

Computed tomography coronary angiography (CTA) is a well established non-invasive method for the assessment of coronary atherosclerosis. At present, there is a rich amount of data confirming the correlation between stenosis degree on CTA and invasive coronary angiography.<sup>1,2</sup> Moreover, several studies have demonstrated the prognostic value of stenosis degree as assessed by CTA in the occurrence of adverse cardiovascular events.<sup>3,4</sup> In addition to the assessment of stenosis degree, CTA allows *in vivo* characterization of coronary atherosclerotic plaque to differentiate non-calcified, calcified and mixed plaque. These CTA plaque types have been associated with prognosis.<sup>5</sup> Besides, several additional plaque characteristics on CTA have been associated with plaque vulnerability (e.g. positive remodeling, spotty calcification, low attenuation plaque).<sup>6</sup>

Ultimately, CTA stenosis degree and plaque constitution can be derived by a fully automatic, quantitative approach, allowing high accuracy and good reproducibility. Previously, semi-automated methods to characterize plaque on CTA have been described.<sup>7,8</sup> However, a dedicated fully automatic quantitative CTA plaque characterization tool to assess plaque constitution is currently unavailable.

The present study assessed the feasibility of an automatic and quantitative analysis of CTA data. In this study, clinically derived CTA and intravascular ultrasound virtual histology (IVUS VH) datasets were used to investigate the correlation between quantitatively, automatically derived CTA parameters and IVUS VH. For this assessment, IVUS VH was defined as the golden standard since it is an approved method for the *in-vivo* assessment of coronary plaque characteristics and has been well validated against histopathology.<sup>9</sup> IVUS VH allows for the assessment of plaque vulnerability and is associated with outcome.<sup>10</sup> The correlation between CTA plaque characteristics and intravascular ultrasound virtual histology (IVUS VH) has previously been described.<sup>11-13</sup>

In this investigation automatic, quantitative assessed stenosis degree and plaque constitution on CTA were compared to IVUS VH. For this purpose, a dedicated 3-dimensional registration algorithm was used, allowing a slice-by-slice comparison of both modalities. In short, the aim of the present study was 1) to perform an automatic quantitative CTA analysis of stenosis degree and plaque constitution and 2) to validate this against IVUS VH.

## Methods

### Patient population

The patient population consisted of 57 patients who presented with chest pain at the outpatient clinic (Leiden, the Netherlands) and underwent CTA, followed by clinically referred invasive coronary angiography (ICA). In addition, IVUS VH was performed to further evaluate the severity and extent of coronary artery disease.

CTA images were acquired using either a 64-slice CT scanner (Aquilion 64, Toshiba Medical System, Otawara, Japan) or a 320-row volumetric scanner (Aquilion ONE, Toshiba Medical System, Otawara, Japan). Non-ionic contrast material (Iomeron 400, Bracco, Milan Italy or Ultravist 370, Bayer Schering Pharma AG Berlin, Germany) was administered with an amount of 80-110 ml followed by a saline flush with a flow rate of 5 ml/s. Contra-indications for CTA were: 1) renal insufficiency (glomerular filtration rate < 30 ml/min); 2) known allergy to iodine contrast material; and 3) pregnancy. Only scans with adequate image quality were included for the current analysis. The effective dose was calculated using a conversion factor of 0.014 mSv/(mGy x cm)

IVUS VH examinations were acquired during conventional ICA using a dedicated IVUS console (S5<sup>tm</sup> Imaging system Volcano Corporation, rancho, Cordova, CA, USA) in combination with a 20MHz, 2,9 F phased-array IVUS Catheter (Eagle Eye, Volcano Corporation, Rancho Cordova, CA, USA). Motorized pullback was performed at a constant speed of 0.5 mm/s until the IVUS catheter reached the guiding catheter. Exclusion criteria for IVUS VH were severe stenosis, (subtotal) vessel occlusion or vessel tortuosity.

Clinical data were prospectively entered into the departmental Cardiology Information System (EPD-Vision, Leiden University Medical Center) and retrospectively analyzed. In each patient, the presence of CAD risk factors was recorded.

The feasibility of quantitative CTA analysis software to assess stenosis severity has been reported previously.<sup>14</sup> For the current analysis, the most recent update of this program was used, which allows fully automatic, quantitative assessment of both stenosis severity and plaque constitution (QAngioCT Research Edition version 1.3.6, Medis Medical Imaging Systems, Leiden, the Netherlands). In all patients quantitative computed tomography (QCT) was performed to determine lumen and vessel wall borders. Subsequently, using a dedicated 3-dimensional registration algorithm, CTA images were registered with the corresponding IVUS VH run as shown in Figure 1. Thereafter, automatic lesion quantification was performed in both modalities to assess stenosis parameters and plaque constitution. Finally, the correlations for all parameters (Table 1) between the both modalities were assessed.

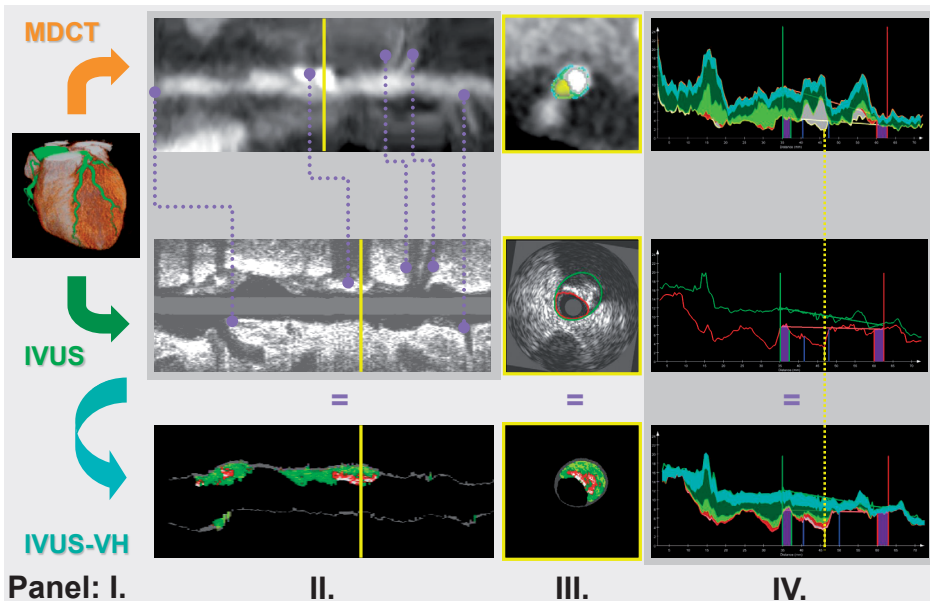


**Figure 1. Schematic illustration of the characterization of coronary plaque on CTA: cross-correlation with IVUS VH.**

First, the 3-dimensional centerline was generated from the CTA data set using an automatic tree extraction algorithm (Panel I). Using a unique registration a complete pullback series of IVUS images was mapped on the CTA volume using true anatomical markers (Panel II). Fully automatic lumen and vessel wall contour detection was performed for both imaging modalities (Panel III). Finally, fusion-based quantification of atherosclerotic lesions was based on the lumen and vessel wall contours as well as the corresponding reference lines (estimate of normal tapering of the coronary artery), as shown in panel IV. At the level of the minimal lumen area (MLA) (yellow lines), stenosis parameters, could be calculated for both imaging techniques. Additionally, plaque volumes and plaque types were derived for the whole coronary artery lesion, ranging from the proximal to distal lesion marker (blue markers). Fibrotic tissue was labeled in dark green, Fibro-fatty tissue in light green, dense calcium in white and necrotic core was labeled in red.

## Quantitative CTA analysis

### Lumen and vessel wall detection.

First, an automatic tree extraction algorithm was used to obtain all the 3-dimensional centerlines of the coronary tree.<sup>15</sup> Based on these centerlines, straightened multi-planar reformatted (MPR) volumes were created of those vessels of which an IVUS VH examination was available. Next, the lumen border contours and vessel wall borders were assessed according to the previously reported method.<sup>14</sup> This method uses spatial first- and second-derivative gradient filters in longitudinal cross sections in combination with knowledge of the expected CTA intensity values in the arteries. Thereafter lumen and vessel contour are detected in the individual transversal

**Table 1. QCT derived parameters and their corresponding definitions.**

<b>QCT parameter</b>	<b>Definition</b>
Lesion length (mm)	The distance between the proximal and distal ends of the coronary lesion
Lumen volume (mm <sup>3</sup> )	Total volume of the lumen between the proximal and distal ends of the coronary lesion
Vessel wall volume(mm <sup>3</sup> )	Total volume of the vessel wall between the proximal and distal ends of the coronary lesion
Plaque volume(mm <sup>3</sup> )	Total volume of plaque wall between the proximal and distal ends of the coronary lesion. Defined as vessel wall volume – lumen volume
Minimal Lumen Area (MLA) (mm <sup>2</sup> )	The minimal lumen area at the point of maximal obstruction.
Percentage lumen area stenosis at the level of the MLA (%)	$1 - (MLA/\text{corresponding reference lumen area}) \times 100\%$

cross-sections perpendicular to the centerlines, whereby the locations from the longitudinal analyses are taken into account. This method is insensitive to differences in attenuation values between data sets and independent of window and level settings.

### **Plaque constitution.**

Two approaches for tissue (plaque) classification were implemented. The first used predefined fixed intensity cut-off values on the Hounsfield Units (HU) to assess plaque constitution. Currently, different cut-off values are available in the literature, which are obtained by comparing CTA with IVUS VH or histological examination.<sup>6, 16</sup> For the current analysis, the fixed HU cut-off values used for classifying were: -30 – 75, for necrotic core, 76 – 130 for fibro-fatty, 131 – 350 for fibrotic, and 351+ for dense calcium. These values were initially based on the paper by Brodoefel *et al.* and empirically optimized using three representative training sets.<sup>16</sup>

The second approach used an adaptive threshold based on the principle that plaque attenuation values are influenced by luminal contrast densities.<sup>17, 18</sup> Therefore, in this approach, the HU thresholds are adapted according to lumen attenuation values. This method is based on two principles.

The first principle is the decrease in lumen intensity from the proximal to the distal part of the coronary artery. The intensity cut-off values are adapted by the same linear, decreasing trend along the vessel.

The second principle is that the lumen intensities are lower in the parts of a severe stenosis and higher in the parts with severe calcified lesions due to blooming artifacts. Therefore, intensity cut-off values are locally compensated by subtracting a percentage of the difference to correct for the cut-off values in these locations. These dynamic thresholds were automatically derived and are user independent. The

inter- and intra observer variability for the lumen and vessel segmentation have been previously described.<sup>19, 20</sup> The assessment of plaque constitution was performed fully automatically.

### **Cross-correlation with IVUS VH**

To validate the results of the QCT analysis, CTA images were compared to IVUS VH images of the corresponding artery. IVUS VH lumen and vessel wall contours were generated using QCU (QCU- CMS 4.59, Medis, Leiden, The Netherlands). A dedicated software tool was used to fuse the CTA and IVUS VH images as previously described.<sup>14</sup> First using anatomical landmarks (side-branches, ostia, calcified plaques) the IVUS VH images were mapped on the longitudinal CTA centerline. Secondly, the IVUS VH cross-sectional images were translated and rotated to fit onto the corresponding CTA cross-section. This 3-dimensional registration method allows correction of deviations in IVUS VH caused by inconstant motorized pullback speed and enables a slice-by slice comparison of the coronary artery.

In both modalities, CTA and IVUS VH, lesions are manually defined by placing reference locations at non-diseased, non-bifurcated proximal and distal parts of the segment of interest. A slope is automatically defined between these reference locations which represent an estimate of the normal proximal-to-distal tapering of the segment of interest. Consecutively, using the reference slope, the minimal lumen area (MLA) as well as the proximal and distal ends of a lesion were automatically assessed as shown in Figure 1. Subsequently, a number of parameters were derived from QCT and IVUS VH in each analyzed coronary lesion as described in Table 1.

In addition to coronary arteries with atherosclerotic lesions, a vessel-based analysis of non-diseased coronary arteries was performed in the mid part of the coronary artery. In these non-diseased vessels, lumen and plaque volumes were assessed in both modalities. Since no plaque was present in these vessels, no comparison of plaque characteristics was performed.

### **Statistical analysis**

Continuous data are presented as mean  $\pm$  SD if normally distributed or as median (interquartile range (IQR)) if non-normally distributed. Categorical data are presented as absolute numbers and percentages. A comparison was made between QCT and IVUS VH parameters on a lesion basis. Bland-Altman analyses were performed to assess the bias and the limits of agreement for the comparison between QCT and IVUS VH (GraphPad Prism software, version 5.01, GraphPad software Inc, San Diego, California, MA, USA). Bland-Altman analyses represent the difference of each pair plotted against the average value of each pair. Additionally, to correct for intra-patient correlation linear mixed models were used. The differences for each parameter be-

tween QCT and IVUS VH was calculated and entered as a dependent value. For this analysis, the 95% confidence intervals (95% CI) were calculated. Furthermore, the feasibility of QCT to assess luminal parameters in non-diseased segments was assessed in all plaque free segments.

## Results

For this study, 61 patients with diagnostic quality of the CTA were selected. In 4 of these 61 patients (7%) image quality was still insufficient to perform tissue characterization. The remaining 57 patients were included in this study. These 57 patients underwent CTA using either a 320-row volumetric ( $n = 41$ ) or a 64-row helical scanner ( $n = 16$ ). Median time between CTA and IVUS VH was 2 (IQR 0 – 64) days. The effective dose of the CTA acquired on 320-row CTA was  $6.5 \pm 4.0$  mSv, The mean radiation dose for 64-slice CT performed in our centre has been previously described ( $18.1 \pm 5.9$  mSv)<sup>21</sup>. Baseline characteristics are described in Table 2; the mean age was  $57.8 \pm 11.5$  years and 68% of patients were male. In these 57 patients an IVUS VH run was available of 138 vessels; 29 of these vessels were unsuitable for further analysis because of the presence of a stent ( $n = 11$ ) or insufficient quality of either the IVUS VH run ( $n = 6$ ), the CTA extraction ( $n = 7$ ) or other technical limitations ( $n = 5$ ). For the final analysis, 109 vessels were used of which 69 revealed atherosclerosis, whereas 40 vessels did not. In these 69 diseased vessels, 108 lesions were identified. These 108 lesions were used for the lesion based comparison.

### Coronary plaque volume

The results of the comparison of coronary plaque volumes (per lesion) are depicted in Figure 2. There was an excellent correlation between vessel volume on QCT and vessel volume on IVUS VH ( $r = 0.957$ ,  $P < 0.001$ ). Based on linear mixed models, vessel volume was significantly overestimated on QCT as compared to IVUS VH, median vessel volume ( $242 \text{ mm}^3$  (IQR 152 – 371) vs.  $238 \text{ mm}^3$  (IQR 141 – 331), respectively, 95% CI of the mean difference ranging from 5.3 to  $24.8 \text{ mm}^3$ ,  $P = 0.003$ ). Bland-Altman analysis demonstrated a bias of  $15 \text{ mm}^3$  with 95% limits of agreement ranging from  $-84.9$  to  $115 \text{ mm}^3$ . The correlation between lumen volume on QCT and IVUS was excellent ( $r = 0.917$ ,  $P < 0.001$ ). QCT significantly underestimated the lumen volume: the median volume was  $92 \text{ mm}^3$  (IQR 60 – 136) on QCT compared to  $111 \text{ mm}^3$  (IQR 64 – 163) on IVUS VH (95 CI of the mean difference ranging from  $-28.3$  to  $-14.6 \text{ mm}^3$ ,  $P < 0.001$ ). The bias of the Bland-Altman analysis of lumen volume was  $-21.5 \text{ mm}^3$  with 95% limits of agreement from  $-92.3$  to  $39.4 \text{ mm}^3$ . Accordingly, the correlation between plaque volume measured with both modalities was similar

**Table 2. Baseline characteristics of study population (n=57).**

Men	39 (68)
Age (years)	57.8 ± 11.5
Calcium score	69 (0 – 287) (range 0 – 3247)
Known CAD	11 (19)
<b>Risk Factors</b>	
Diabetes	14 (25)
Hypertension †	38 (67)
Hypercholesterolemia ‡	27 (47)
Smoking	20 (35)
Obesity (BMI ≥ 30 kg/m <sup>2</sup> )	14 (25)
Positive family history*	25 (44)
<b>Medication</b>	
Beta-blockade	29 (51)
ACE inhibitor / AT II blockade	30 (53)
Diuretics	19 (33)
Nitrate	11 (19)
Calcium antagonist	10 (18)

Data are represented as mean ± SD, median (interquartile range) or as number and percentages of patients.

†Defined as systolic blood pressure ≥140 mmHg or diastolic blood pressure ≥90 mmHg or the use of antihypertensive medication. ‡Serum total cholesterol ≥230 mg/dL or serum triglycerides ≥200 mg/dL or treatment with lipid lowering drugs.

\*Defined as the presence of coronary artery disease in first-degree family members at <55 years in men and <65 years in women.

Abbreviations: CAD, coronary artery disease; BMI, body mass index; ACE, angiotensin converting enzyme; AT II, angiotensin II

( $r = 0.928$ ,  $P < 0.001$ ). QCT overestimated plaque volume with a bias of  $36.5 \text{ mm}^3$  ( $P < 0.001$ ) with limits of agreement of  $-48.8$  to  $121.9 \text{ mm}^3$ .

### Coronary stenosis parameters

Good correlations were observed for the assessment of minimal lumen area (MLA) and lumen area stenosis,  $r = 0.836$  and  $r = 0.701$ , respectively. However MLA was underestimated on CTA, as demonstrated by a bias of  $-1.62 \text{ mm}^2$  with 95% limits of agreement ranging from  $-5.54$  to  $2.30 \text{ mm}^2$ . Median MLA on QCT was  $4.3 \text{ mm}^2$  (IQR 3.12 - 5.83) compared to  $5.20 \text{ mm}^2$  (IQR 3.75 – 7.90) on IVUS VH (95% CI of mean difference ranging from  $-2$  to  $-1.2 \text{ mm}^2$ ,  $P < 0.001$ ). In contrast, area stenosis was

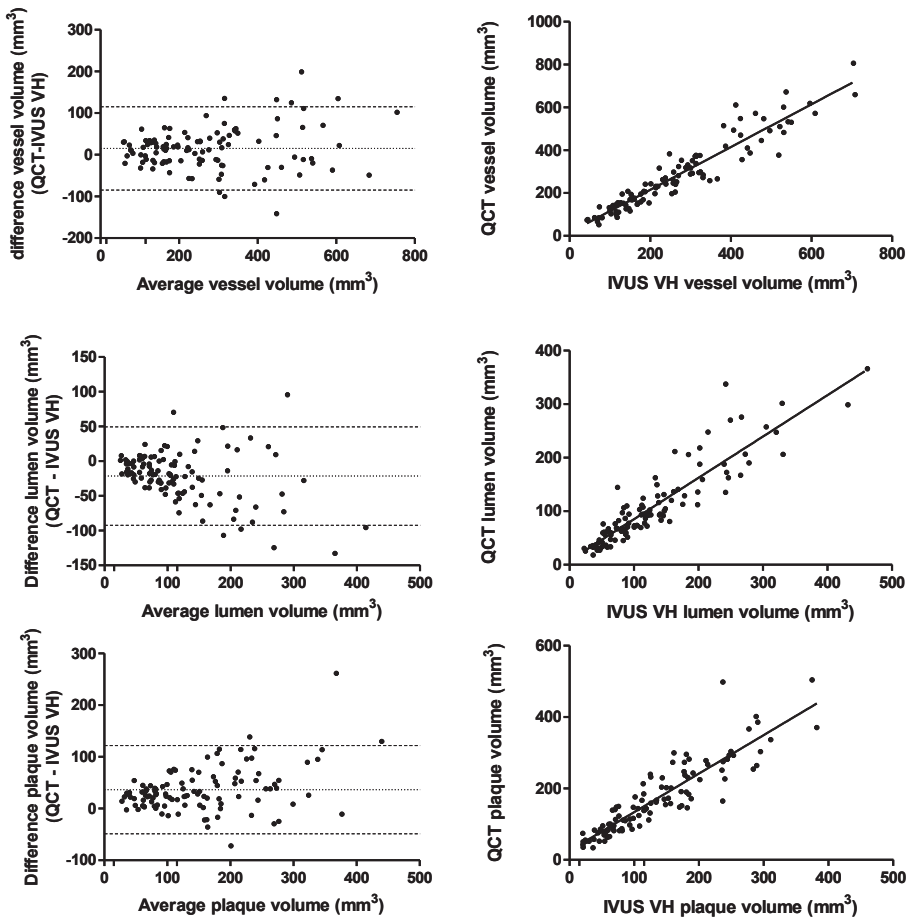


Figure 2. Bland-Altman analyses of vessel volume, lumen volume and plaque volume,.

significantly overestimated on QCT (median 42.8% (IQR 32.22 – 55.12)) compared to IVUS VH (median 40.06% (IQR 28.66 – 50.49) (95% CI of mean difference ranging from 0.7 to 5.6 %,  $P = 0.01$ ). Bland-Altman analysis demonstrated a bias of 3.17 % with limits of agreement ranging from -21.61 to 27.96 %

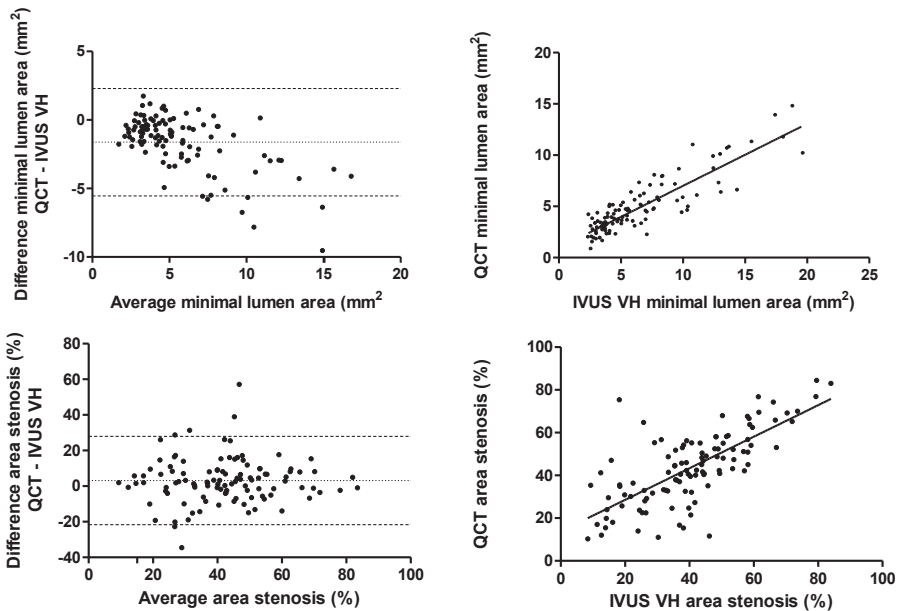
### Coronary plaque constitution

The results of both fixed and dynamic threshold CTA tissue classifier are demonstrated in Table 3. Bland-Altman analyses of the two different CTA tissue classifier methods are depicted in Figures 3 and 4 respectively.

**Table 3. Results of QCT plaque constitution assessment : cross-correlation with IVUS VH (n=108).**

	IVUS VH Median (IQR) (mm <sup>3</sup> )	QCT Median (IQR) (mm <sup>3</sup> )	95 % CI of mean difference	P-value	Correlation coefficient	Bias (mm <sup>3</sup> )	Lower 95% LOA (mm <sup>3</sup> )	Upper 95% LOA (mm <sup>3</sup> )
<b>Fixed threshold</b>								
Fibrotic	39.7(19.9-67.3)	43.2 (23.1-76.1)	1.6 ; 13.8	0.013	0.695, <0.001	7.7	-54.8	70.2
Fibro-fatty	9.3(4.9–19.4)	25.9 (16.0-41.6)	13.3 ; 19.0	<0.001	0.714, <0.001	24.4	-41.8	90.7
Necrotic core	11.8(6.0–22.3)	22.8 (14.7-38.9)	10.4 ; 19.1	<0.001	0.523, <0.001	14.8	-29.7	59.2
Dense calcium	5.4(1.7–11.6)	7.6 (2.1-24.9)	6.6 ; 15.9	<0.001	0.736, <0.001	11.3	-36.4	59.0
<b>Dynamic threshold</b>								
Fibrotic	As above	55.7(36.1-94.9)	15.0 ; 25.9	<0.001	0.787, <0.001	20.4	-35.7	76.6
Fibro-fatty	"	28.3(16.2-45.9)	16.7 ; 23.6	<0.001	0.704, <0.001	20.2	-15.2	55.6
Necrotic core	"	11.0(5.6-24.7)	-1.6 ; 3.6	0.458	0.479, <0.001	1.0	-25.9	27.9
Dense calcium	"	6.95(0.9-18.9)	4,5 ; 12.5	<0.001	0.733, <0.001	8.5	-32.5	49.5

IVUS VH, Intravascular Ultrasound Virtual Histology, QCT, quantitative computed tomography, LOA, Limits of agreement, IQR interquartile range

**Figure 3. Bland-Altman analyses of minimal lumen area (MLA) and percentage area stenosis.**

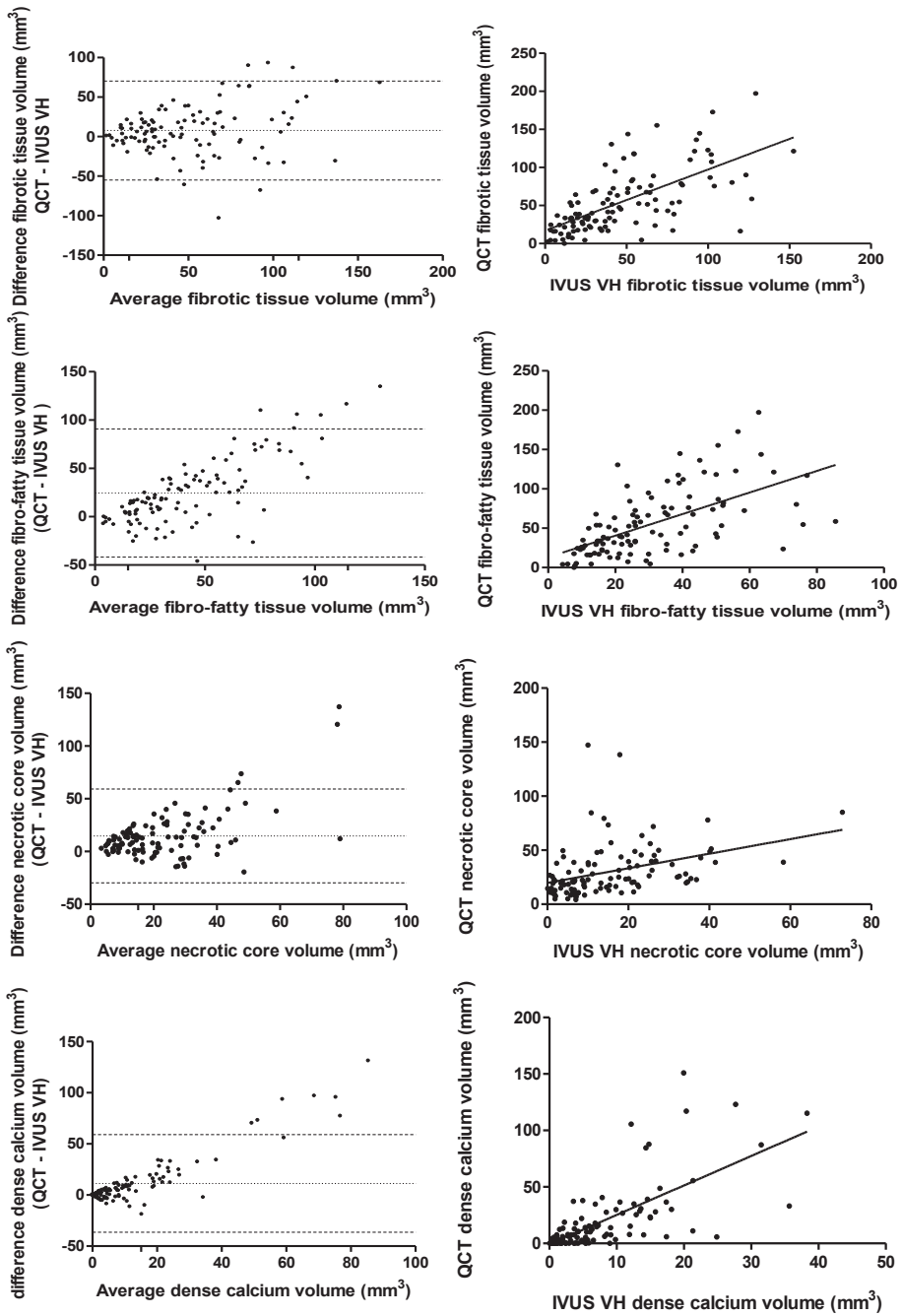


**Figure 4. Bland-Altman analyses of plaque constitution as assessed using fixed thresholds.**  
 Comparison between QCT and IVUS VH for fibrotic tissue, fibro-fatty tissue, necrotic core and dense calcium volumes.

**Method 1: fixed thresholds.**

On a lesion basis, good correlations were observed for volumes of fibrotic tissue ( $r = 0.695$ ,  $p < 0.001$ ), fibro-fatty tissue ( $r = 0.714$ ,  $p < 0.001$ ), necrotic core ( $r = 0.523$ ,  $p < 0.001$ ) and dense calcium ( $r = 0.736$ ,  $p < 0.001$ ). Bland-Altman analysis, as depicted in Figure 3 and described in Table 3, demonstrated a significant overestimation of the volumes of all four plaque types by QCT. For necrotic core, bias was  $11.3 \text{ mm}^3$  with limits of agreement ranging from  $-29.7$  to  $59.2 \text{ mm}^3$ . The smallest bias was observed for fibrotic tissue ( $7.7 \text{ mm}^3$ ) with limits of agreement ranging from  $-54.8$  to  $70.2 \text{ mm}^3$ .

**Method 2: dynamic thresholds.**

The results of the dynamic CTA tissue classifier are described in Table 3. The volumes of dense calcium, fibrotic and fibro-fatty volumes were all significantly overestimated by QCT ( $P < 0.001$ .) No significant differences were observed in necrotic core volumes between both modalities ( $P = 0.481$ ). In Figure 5, the Bland-Altman analysis of the dynamic tissue classifier is depicted. The narrowest limits of agreement were observed for necrotic core volume ranging from  $-25.9$  to  $27.9 \text{ mm}^3$  with a bias of  $1.0 \text{ mm}^3$ . However, the correlation coefficient for necrotic core ( $r = 0.479$ ,  $P < 0.001$ ) was smaller compared to the other three plaque types. In Figure 6 an example is demonstrated of CTA plaque constitution assessment of a coronary lesion using the two different methods.

**Non-diseased coronary arteries**

In non-diseased coronary arteries ( $n = 40$ ), vessel, lumen and plaque volume on QCT were significantly correlated with IVUS VH ( $r = 0.947$ ,  $r = 0.920$  and  $r = 0.738$ , respectively ( $p < 0.001$ )). However median vessel volume was significantly overestimated on QCT as compared to IVUS VH ( $410 \text{ mm}^3$  (IQR 250 - 616) versus  $408 \text{ mm}^3$  (IQR 236 - 550)) (95% CI of the mean difference ranging from  $25.5$  to  $85.5 \text{ mm}^3$ ,  $p = 0.001$ )). Lumen volumes were significantly smaller on QCT as compared to IVUS VH (median  $190 \text{ mm}^3$  (IQR 92 - 303) versus median  $283 \text{ mm}^3$  (IQR 147 - 422)) (95% CI of the mean difference ranging from  $-90.3$  to  $-40.5 \text{ mm}^3$ ,  $p < 0.001$ )). Accordingly, plaque volume on QCT was significantly higher (median  $236 \text{ mm}^3$  (IQR 157 - 324)) as compared to IVUS VH (median  $112 \text{ mm}^3$  (IQR 66 - 153)).

**Discussion**

The present study has demonstrated the feasibility of a fully automatic, quantitative analysis of CTA images for the assessment of coronary artery stenosis severity and

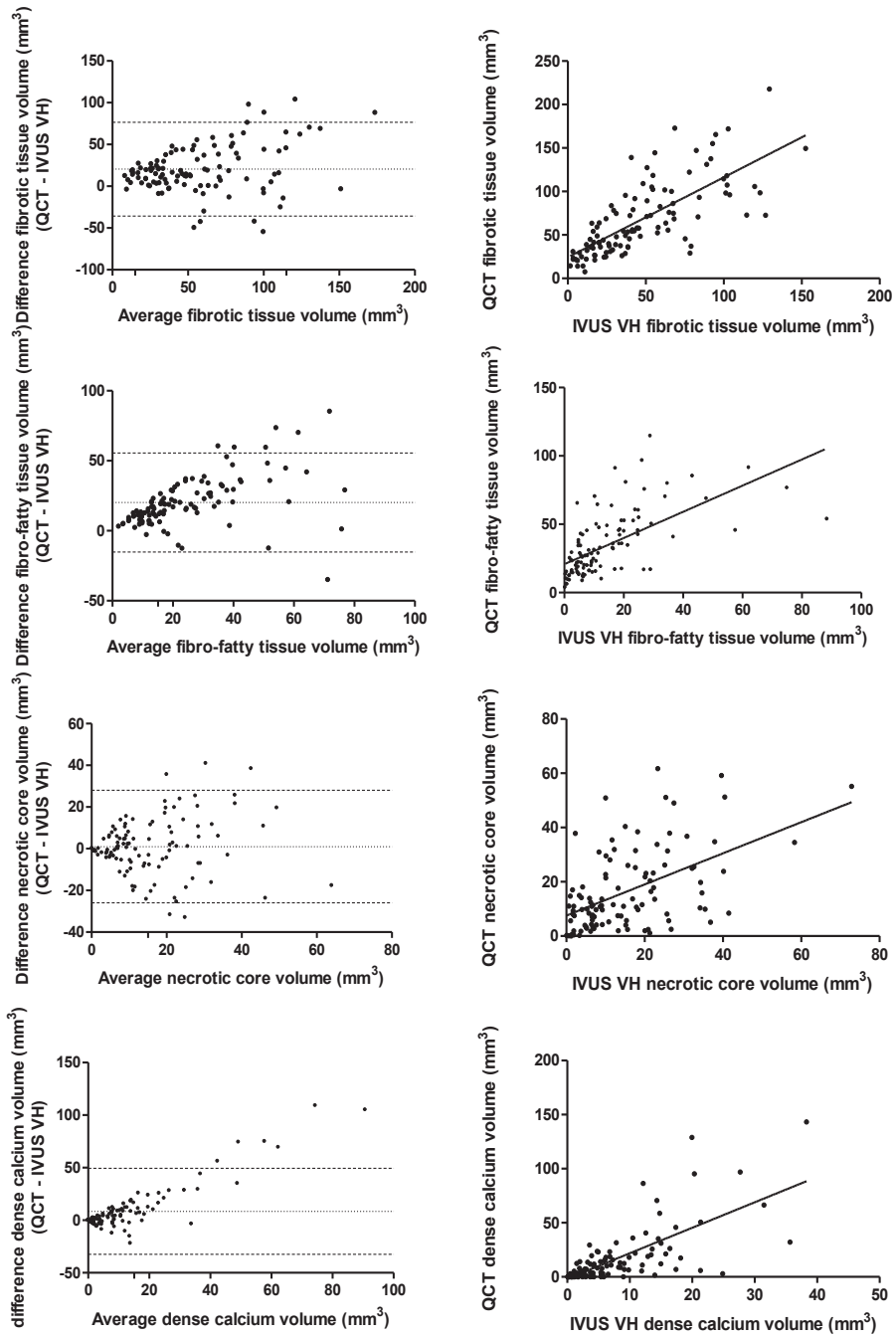


**Figure 5. Bland-Altman analyses of plaque constitution as assessed using dynamic thresholds.** Comparison between QCT and IVUS VH for fibrotic tissue, fibro-fatty tissue, necrotic core and dense calcium volumes.

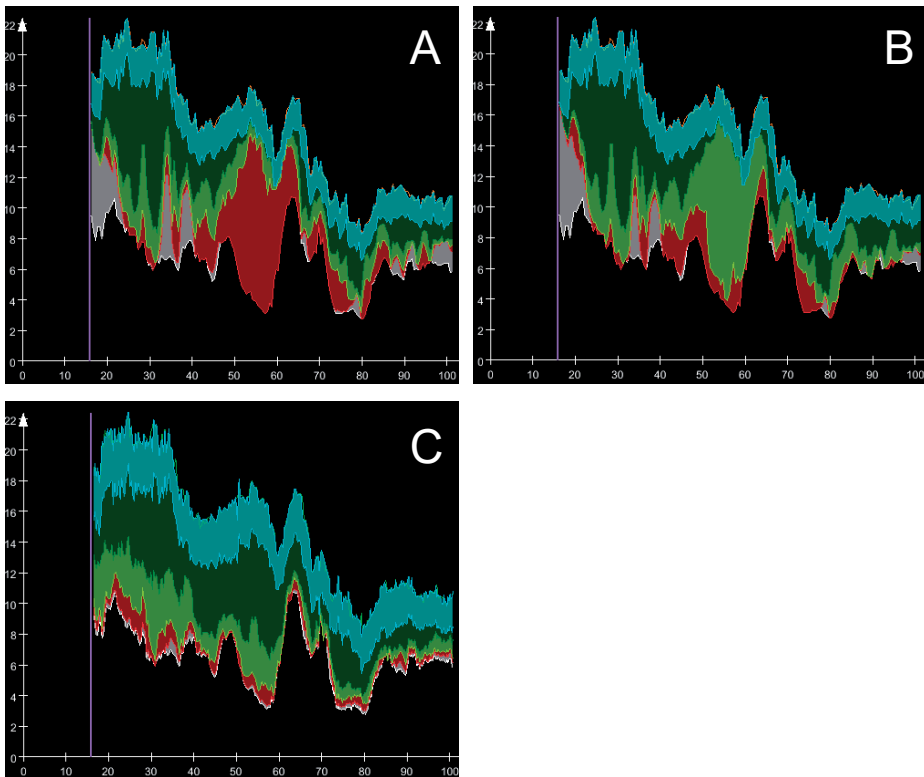


**Figure 6. An example of a coronary lesion, plaque constitution is assessed using two methods of tissue characterization.**

The x-axis represents the distance from the coronary ostium in mm. The y-axis represents the area of either the lumen (lower part of graph) or the vessel wall (upper part of graph) in mm<sup>2</sup>. The part between the two graphs shows the plaque constitution using a color code with fibrotic tissue labeled in dark green, fibro-fatty tissue in light green, dense calcium in white and necrotic core labeled in red. Plaque constitution is assessed using either method 1 (Panel A) or method 2 (Panel B). In Panel C the corresponding IVUS VH data is shown. The use of method 2 correlated better with IVUS VH compared to method 1.

plaque constitution. Using a dedicated 3-dimensional registration algorithm a slice-by-slice comparison was made between QCT and IVUS VH. Very good correlations were observed for lumen, vessel and plaque volume between QCT and IVUS VH. Still, lumen volume was slightly underestimated and vessel volume slightly overestimated on QCT. The assessment of MLA and lumen area stenosis using QCT correlated well with IVUS VH ( $r = 0.836$  and  $r = 0.701$ , respectively).

In addition, the performance of two different approaches for tissue characterization was evaluated. The differentiation of coronary plaque volume in fibrous, fibro-fatty, necrotic core and dense calcium on QCT correlated well with IVUS VH. The dynamic

threshold approach performed better compared to the fixed threshold approach, as demonstrated by more narrow limits of agreement on the Bland-Altman analyses.

### **Coronary stenosis assessment**

CTA is a suitable method for the non-invasive evaluation of coronary atherosclerosis. Beyond the assessment of luminal narrowing it allows for the visualization of coronary plaque. The prognostic value of CTA has been extensively reported and CTA is commonly used in clinical practice to rule out atherosclerosis in patients with low-to-intermediate pre-test likelihood of CAD.<sup>22</sup> Currently, CTA datasets are mainly visually analyzed to assess luminal narrowing. This visual approach requires an experienced observer, is subjected to interobserver variability and has lesser reproducibility. In the literature a quantitative analysis of CTA datasets on luminal narrowing and plaque constitution has been proposed as an objective and accurate method for analyzing CTA images. Several previous studies have reported different quantitative assessments of CTA images<sup>7, 8, 12, 23</sup>. These studies have shown wide variety in results, mainly caused by differences in CTA contour detection algorithms. In the present study, good correlations were observed for the assessment of plaque volume ( $r = 0.928$ ), lumen volume ( $r = 0.917$ ) and vessel volume ( $r = 0.957$ ). Vessel volume was slightly overestimated, whereas lumen volume was underestimated resulting in overestimation of plaque volume. In line with the present findings, Bruining *et al.*<sup>24</sup> have demonstrated an overestimation of coronary plaque volume. In 48 patients, the investigators compared a quantitative CTA analysis with limited manual interference to IVUS. In contrast to the present investigation, the authors report an underestimation of coronary vessel wall volume. This discrepancy is potentially caused by differences in the vessel wall detection algorithm. In the future, the assessment of coronary plaque volume on CTA could be applied as a non-invasive method for the investigation of plaque regression or progression in patients or to assess the effect of medical therapy. In addition to coronary volume parameters, the ability of QCT to assess stenosis severity was investigated. Despite an overestimation on QCT for lumen area stenosis, good correlations were observed compared to IVUS VH. The method applied in the present study is best comparable to the ATLANTA study.<sup>12</sup> In this prospective study 50 patients were enrolled. In 50 lesions, a quantitative analysis of CTA datasets was performed and compared with IVUS VH. Similar to the present findings an overestimation of MLA and an overestimation of plaque volume was observed.

### **Coronary plaque constitution**

Beyond establishing luminal narrowing, CTA allows for the assessment of coronary plaque constitution. Previous studies have indicated the correlation between CTA plaque characteristics and plaque vulnerability.<sup>6</sup> Also, the prognostic value of CTA

plaque constitution has been reported.<sup>25</sup> Potentially, an accurate, quantitative assessment of coronary plaque constitution could provide more detail on the relation between plaque vulnerability and plaque constitution on CTA. However, at present an automatic, quantitative assessment of plaque constitution is unavailable. Previous studies have assessed mean HU of coronary plaques on CTA in different plaque types as assessed with IVUS (e.g. hypo or hyperechogenic).<sup>26</sup> In contrast, the present study has used predefined HU thresholds to compare the four different plaque volumes with both modalities. In previous investigations the feasibility of manual or semi-automatic quantitative CTA plaque constitution analyses has been assessed using IVUS VH as a reference.<sup>7, 12</sup> However, data is lacking evaluating a direct slice-by-slice comparison between automatically, quantitatively assessed plaque constitution and IVUS VH.

Two different methods were applied for the quantitative analysis of plaque constitution.

#### **Method 1: fixed thresholds.**

The first method used fixed, predefined HU thresholds to differentiate coronary plaque volume in four different plaque types. This method has been applied in previous investigations.<sup>7, 12</sup> In the present study, significant correlations were observed for all four plaque components. Still, an overestimation of plaque volume was noted for all different components on QCT. However, corresponding bias on Bland-Altman analysis were small for all components. These results are in line with previous reports. Indeed, using an automated vessel segmentation algorithm in 50 patients, Voros *et al.*<sup>12</sup> demonstrated small difference, but wide limits of agreement for the assessment of plaque constitution on CTA compared to IVUS VH. In contrast, in a study by Brodoefel *et al.*<sup>7</sup> in 14 patients, a comparison was made between plaque constitution on CTA and IVUS VH. The authors reported a good correlation for overall plaque volume; however, no significant correlation could be demonstrated for different plaque types.

#### **Method 2: dynamic thresholds.**

Recently, Dalager<sup>17</sup> *et al.* have demonstrated that differences in luminal intensities have an effect on the attenuation values inside the plaque. A decrease in luminal intensity was associated with lower coronary plaque HU. Besides, Choi *et al.*<sup>27</sup> have shown that coronary stenosis severity has an effect on luminal intensities. A significant decrease in luminal HU was observed at the location of a severe obstruction. It can therefore be expected that at the location of a severe stenosis different thresholds apply for the assessment of plaque constitution. These two previously described mechanisms formed the basis of the second approach on tissue characterization. A dynamic threshold algorithm was applied which automatically adapt HU thresholds

based on the luminal intensity values at the level of the plaque. This was previously proposed in a review by Akram *et al.*<sup>18</sup> suggesting that it is quite important for the implementation of plaque segmentation algorithms to take local attenuation values into consideration. For this reason a dynamic tissue characterization algorithm was implemented. As demonstrated, the performance of the dynamic threshold approach was superior to a fixed threshold approach. For all four plaque types, limits of agreement of Bland-Altman analyses were smaller for the dynamic threshold approach. This indicated that there is indeed an effect of luminal intensities on coronary plaque HU. An accurate characterization of coronary plaque requires a method which accounts for these differences. Possibly, more sophisticated algorithms to account for local difference in plaque attenuation values could be established. This would require further studies into local differences in attenuation values.

Recently, the influence of 100kV scanning on plaque constitution assessment became a topic of interest. In the present study none of the patients were scanned using 100kV. In a recent publication by Horiguchi *et al.*<sup>28</sup> using in vitro models the authors demonstrated equal performance of 100 kV in 120 Kv in soft plaque densitometry. In contrast, the intracoronary CT values were approximately 50 HU higher in 100 kV scans compared to 120kV scans. Potentially, applying the dynamic threshold algorithm used in the present study could correct for these intracoronary density differences and would allow for more accurate tissue characterization.

### **Clinical implications**

At present the clinical value of quantitative CTA plaque constitution assessment has yet to be established. Although a reasonable correlation was observed for the assessment of coronary plaque constitution between QCT and IVUS VH, there still is a large variability in different plaque volumes between both modalities. It is unlikely that full agreement of coronary plaque constitution between QCT and IVUS VH will be achieved. To appreciate the prognostic value of quantitatively assessed plaque constitution on CTA, future studies are needed.

### **Limitations**

Although the present study demonstrated that automatic quantification of coronary plaque is feasible, some limitations need to be considered. For the present study only scans with sufficient quality were included. Therefore, the value of QCT in scans with severe noise or motion artifacts is unknown. The present analysis was a single-center, single-vendor study. An analysis of CTA datasets acquired by different CT-scanners could provide additional valuable insight. IVUS VH was used as the gold standard. However, two limitations of this technique need to be considered. First, the radial resolution of IVUS VH is limited to 100µm, allowing less accurate assessment of

coronary plaque. Secondly, coronary calcium creates an acoustic shadow on IVUS VH caused by the inability of the echo signal to penetrate calcium. Although, plaque located behind calcifications is labeled on IVUS VH, the accuracy of characterizing tissue surrounding dense calcium is unknown. Potentially this leads to an underestimation of calcium volume on IVUS VH. In addition, a direct comparison between QCT plaque characterization and histopathology could provide further insights into the pathophysiology of CTA plaque constitution.

## **Conclusions**

The present study has demonstrated the feasibility of automatic, quantitative analysis of CTA images. QCT demonstrated excellent correlations for the assessment of plaque volume and stenosis parameters as compared to IVUS VH. Furthermore, plaque constitution was well-correlated between both modalities. In a direct comparison between a fixed threshold approach and a dynamic threshold approach for the quantification of plaque type volume, the dynamic threshold performed better as shown by better correlations with IVUS VH.

## References

- (1) Budoff MJ, Dowe D, Jollis JG *et al.* Diagnostic performance of 64-multidetector row coronary computed tomographic angiography for evaluation of coronary artery stenosis in individuals without known coronary artery disease: results from the prospective multicenter ACCURACY (Assessment by Coronary Computed Tomographic Angiography of Individuals Undergoing Invasive Coronary Angiography) trial. *J Am Coll Cardiol* 2008 November 18;52(21):1724-32.
- (2) Miller JM, Rochitte CE, Dewey M *et al.* Diagnostic performance of coronary angiography by 64-row CT. *N Engl J Med* 2008 November 27;359(22):2324-36.
- (3) Chow BJ, Small G, Yam Y *et al.* Incremental prognostic value of cardiac computed tomography in coronary artery disease using CONFIRM: COroNary computed tomography angiography evaluation for clinical outcomes: an International Multicenter registry. *Circ Cardiovasc Imaging* 2011 September;4(5):463-72.
- (4) Min JK, Shaw LJ, Devereux RB *et al.* Prognostic value of multidetector coronary computed tomographic angiography for prediction of all-cause mortality. *J Am Coll Cardiol* 2007 September 18;50(12):1161-70.
- (5) Min JK, Feignoux J, Treutenaere J, Laperche T, Sablayrolles J. The prognostic value of multidetector coronary CT angiography for the prediction of major adverse cardiovascular events: a multicenter observational cohort study. *Int J Cardiovasc Imaging* 2010 August;26(6):721-8.
- (6) Motoyama S, Sarai M, Harigaya H *et al.* Computed tomographic angiography characteristics of atherosclerotic plaques subsequently resulting in acute coronary syndrome. *J Am Coll Cardiol* 2009 June 30;54(1):49-57.
- (7) Brodoefel H, Burgstahler C, Heuschmid M *et al.* Accuracy of dual-source CT in the characterisation of non-calcified plaque: use of a colour-coded analysis compared with virtual histology intravascular ultrasound. *Br J Radiol* 2009 October;82(982):805-12.
- (8) Otsuka M, Bruining N, Van Pelt NC *et al.* Quantification of coronary plaque by 64-slice computed tomography: a comparison with quantitative intracoronary ultrasound. *Invest Radiol* 2008 May;43(5):314-21.
- (9) Nair A, Kuban BD, Tuzcu EM, Schoenhagen P, Nissen SE, Vince DG. Coronary plaque classification with intravascular ultrasound radiofrequency data analysis. *Circulation* 2002 October 22;106(17):2200-6.
- (10) Stone GW, Maehara A, Lansky AJ *et al.* A prospective natural-history study of coronary atherosclerosis. *N Engl J Med* 2011 January;20;364(3):226-35.
- (11) Pundziute G, Schuijff JD, Jukema JW *et al.* Head-to-head comparison of coronary plaque evaluation between multislice computed tomography and intravascular ultrasound radiofrequency data analysis. *JACC Cardiovasc Interv* 2008 April;1(2):176-82.
- (12) Voros S, Rinehart S, Qian Z *et al.* Prospective validation of standardized, 3-dimensional, quantitative coronary computed tomographic plaque measurements using radiofrequency backscatter intravascular ultrasound as reference standard in intermediate coronary arterial lesions: results from the ATLANTA (assessment of tissue characteristics, lesion morphology, and hemodynamics by angiography with fractional flow reserve, intravascular ultrasound and virtual histology, and noninvasive computed tomography in atherosclerotic plaques) I study. *JACC Cardiovasc Interv* 2011 February;4(2):198-208.
- (13) Sarno G, Vanhoenacker P, Decramer I *et al.* Characterisation of the "vulnerable" coronary plaque by multi-detector computed tomography: a correlative study with intravascular

- ultrasound-derived radiofrequency analysis of plaque composition. *EuroIntervention* 2008 November;4(3):318-23.
- (14) Boogers MJ, Broersen A, van Velzen JE *et al.* Automated quantification of coronary plaque with computed tomography: comparison with intravascular ultrasound using a dedicated registration algorithm for fusion-based quantification. *Eur Heart J* 2012 April;33(8):1007-16.
  - (15) Yang G, Kitslaar P, Frenay M *et al.* Automatic centerline extraction of coronary arteries in coronary computed tomographic angiography. *Int J Cardiovasc Imaging* 2012 April;28(4):921-33.
  - (16) Brodoefel H, Reimann A, Heuschmid M *et al.* Characterization of coronary atherosclerosis by dual-source computed tomography and HU-based color mapping: a pilot study. *Eur Radiol* 2008 November;18(11):2466-74.
  - (17) Dalager MG, Bottcher M, Andersen G *et al.* Impact of luminal density on plaque classification by CT coronary angiography. *Int J Cardiovasc Imaging* 2011 April;27(4):593-600.
  - (18) Akram K, Rinehart S, Voros S. Coronary arterial atherosclerotic plaque imaging by contrast-enhanced computed tomography: fantasy or reality? *J Nucl Cardiol* 2008 November;15(6):818-29.
  - (19) Boogers MJ, Broersen A, van Velzen JE *et al.* Automated quantification of coronary plaque with computed tomography: comparison with intravascular ultrasound using a dedicated registration algorithm for fusion-based quantification. 2012 April;33(8):1007-16.
  - (20) Papadopoulou SL, Garcia-Garcia HM, Rossi A *et al.* Reproducibility of computed tomography angiography data analysis using semiautomated plaque quantification software: implications for the design of longitudinal studies. *Int J Cardiovasc Imaging* 2012 December 7.
  - (21) van Velzen JE, Schuijff JD, de Graaf FR *et al.* Diagnostic performance of non-invasive multi-detector computed tomography coronary angiography to detect coronary artery disease using different endpoints: detection of significant stenosis vs. detection of atherosclerosis. *Eur Heart J* 2011 March;32(5):637-45.
  - (22) Taylor AJ, Cerqueira M, Hodgson JM *et al.* ACCF/SCCT/ACR/AHA/ASE/ASNC/NASCI/SCAI/SCMR 2010 Appropriate Use Criteria for Cardiac Computed Tomography. A Report of the American College of Cardiology Foundation Appropriate Use Criteria Task Force, the Society of Cardiovascular Computed Tomography, the American College of Radiology, the American Heart Association, the American Society of Echocardiography, the American Society of Nuclear Cardiology, the North American Society for Cardiovascular Imaging, the Society for Cardiovascular Angiography and Interventions, and the Society for Cardiovascular Magnetic Resonance. *J Cardiovasc Comput Tomogr* 2010 November;4(6):407-33.
  - (23) Leber AW, Becker A, Knez A *et al.* Accuracy of 64-slice computed tomography to classify and quantify plaque volumes in the proximal coronary system: a comparative study using intravascular ultrasound. *J Am Coll Cardiol* 2006 February 7;47(3):672-7.
  - (24) Bruining N, Roelandt JR, Palumbo A *et al.* Reproducible coronary plaque quantification by multislice computed tomography. *Catheter Cardiovasc Interv* 2007 May 1;69(6):857-65.
  - (25) Miszalski-Jamka T, Klimeczek P, Banyas R *et al.* The composition and extent of coronary artery plaque detected by multislice computed tomographic angiography provides incremental prognostic value in patients with suspected coronary artery disease. *Int J Cardiovasc Imaging* 2012 March;28(3):621-31.
  - (26) Pohle K, Achenbach S, Macneill B *et al.* Characterization of non-calcified coronary atherosclerotic plaque by multi-detector row CT: comparison to IVUS. *Atherosclerosis* 2007 January;190(1):174-80.

#### Chapter 4

- (27) Choi JH, Min JK, Labounty TM *et al.* Intracoronary transluminal attenuation gradient in coronary CT angiography for determining coronary artery stenosis. *JACC Cardiovasc Imaging* 2011 November;4(11):1149-57.
- (28) Horiguchi J, Fujioka C, Kiguchi M, Yamamoto H, Shen Y, Kihara Y. In vitro measurement of CT density and estimation of stenosis related to coronary soft plaque at 100 kV and 120 kV on ECG-triggered scan. *Eur J Radiol* 2011 February;77(2):294-8.





# Chapter 5

## Enhanced characterization of calcified areas in intravascular ultrasound virtual histology images by quantification of the acoustic shadow: validation against computed tomography coronary angiography

de Graaf MA, Broersen A, Eggermont J, Wolterbeek R, Kitslaar PH, Dijkstra J, Bax JJ, Reiber JH, Scholte AJ

(Shared first authorship)

*International Journal of Cardiovascular Imaging* 2015;32:543-552

## Abstract

**Purpose:** We enhance intravascular ultrasound virtual histology (VH) tissue characterization by fully automatic quantification of the acoustic shadow behind calcified plaque. VH is unable to characterize atherosclerosis located behind calcifications. In this study, the quantified acoustic shadows are considered calcified to approximate the real dense calcium (DC) plaque volume.

**Methods:** In total, 57 patients with 108 coronary lesions were included. A novel post-processing step is applied on the VH images to quantify the acoustic shadow and enhance the VH results. The VH and enhanced VH results are compared to quantitative computed tomography angiography (QTA) plaque characterization as reference standard.

**Results:** The correlation of the plaque types between enhanced VH and QTA differs significantly from the correlation with unenhanced VH. For DC, the correlation improved from 0.733 to 0.818. Instead of an underestimation of DC in VH with a bias of  $8.5 \text{ mm}^3$ , there was a smaller overestimation of  $1.1 \text{ mm}^3$  in the enhanced VH.

**Conclusion:** Although tissue characterization within the acoustic shadow in VH is difficult, the novel algorithm improved the DC tissue characterization. This algorithm contributes to accurate assessment of calcium on VH and could be applied in clinical studies.

## Introduction

Intravascular ultrasound Virtual Histology™ (IVUS VH) is considered to be the gold standard for in vivo assessment of coronary plaque characteristics.<sup>1,2</sup> However, a limitation of this technique is the ability of the ultrasound signal to fully penetrate calcified tissue, resulting in an acoustic shadow behind calcified tissue.<sup>3</sup> Therefore, IVUS only visualizes the leading edge of calcium, due to a nearly total reflection of the echo signal. Moreover, tissue located behind large calcifications with a clearly edged acoustic shadow cannot be classified accurately and determination of the extent of the calcifications and other plaque characteristics is not possible.<sup>4</sup> Even though the accuracy is unknown, IVUS based tissue characterization methods such as VH® (Volcano) or iMap™ (Boston Scientific) provide classifications of the plaque in these acoustic shadow areas.<sup>5</sup> However, coronary atherosclerosis in the acoustic shadow is rarely classified as dense calcium (DC). This may lead to underestimating the DC area and overestimating of other plaque components. We hypothesized that most of the tissue in the acoustic shadow is DC and aim to compensate for the underestimated calcified areas in VH.

Therefore, a novel masking algorithm was developed in which a fully automatic post-processing step is applied on the VH images to quantify the acoustic shadow behind calcified areas. The quantified regions are modified and added to the total DC volume. To validate this new post-processing step, the enhanced VH (eVH) results are compared to plaque characteristics obtained with computed tomography angiography (CTA).

## Methods

The study population consisted of a previously described patient cohort of 57 patients with chest pain.<sup>6</sup> In brief, all patients underwent CTA followed by clinically referred invasive coronary angiography (ICA) and IVUS VH. The Institutional Review Board of the Leiden University Medical Center approved this retrospective evaluation of clinically collected data, and waived the need for written informed consent.

### IVUS Virtual Histology

#### Acquisition and quantification.

The examinations were acquired during conventional ICA using a dedicated IVUS console (S5<sup>im</sup> Imaging system Volcano Corporation, Rancho Cordova, CA, USA) in combination with a 20MHz, 2.9 F phased-array IVUS Catheter (Eagle Eye, Volcano

Corporation, Rancho Cordova, CA, USA). All IVUS lumen and vessel wall delineations were quantified with QCU-CMS-Research v4.69 (research version of QIvus, developed by the Leiden University Medical Center). Additionally, the tissue region between the lumen and vessel wall was characterized by the integrated Volcano VH software in the following plaque types: necrotic core (NC), dense calcium (DC), fibrotic tissue (FI) and fibro-fatty tissue (FF).

### Post-processing of the acoustic shadow.

A novel automatic method was developed to combine VH tissue characterization with an acoustic shadow detection method in order to quantify calcified plaque behind the acoustic shadow. This is performed in five automatic steps as shown in Figure 1:

- 1) The potential acoustic shadow regions are determined for each transversal IVUS frame by dividing it into two-degree wide wedges, resulting in 180 wedges.
- 2) For every wedge, the mean and maximum grayscale intensities of the plaque area are compared to the corresponding mean and maximum grayscale intensities of four predefined layers located outside of the external elastic membrane (0-0.2 mm, 0.2-0.5 mm, 0.5-1.0 mm and 1.0-2.0 mm). If the mean and maximum grayscale intensity of each layer is less than the corresponding mean and maximum grayscale intensities of the plaque area, the wedge is marked as potential acoustic shadow.
- 3) Every transversal frame is analysed per one degree along a virtual polar scan-line. If the sum of grayscale intensities from the lumen border up to and including the VH determined dense calcium region is larger than 20% of the sum of all grayscale intensity values of the scan-line, the angle is marked as an acoustic shadow angle.
- 4) A mask is constructed based on the marked acoustic shadow angles covering all pixels behind the dense calcified regions as shown in Figure 1D.

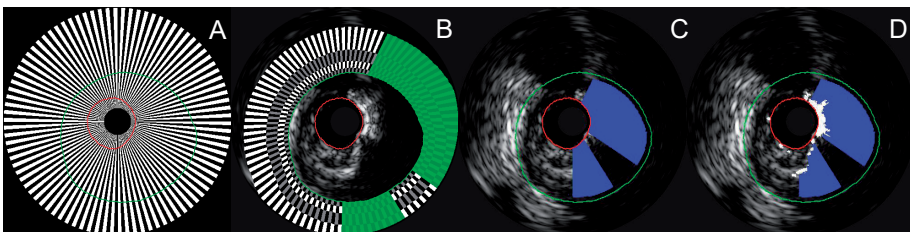


**Figure 1: The automatic post-processing steps on the IVUS VH.**

A) The first step shows the 180 wedges. B) shows the second step with the four predefined layers in grey and white and in green the potential acoustic shadows. C) shows the third step with shadows in blue where the calcium regions are larger than 20%. D) shows the final masks with the calcified regions in white.

- 5) The area and volume of the masked areas are quantified and added to the total DC area and DC volume.

## **Computed tomography coronary angiography**

### **Acquisition.**

Of the 57 patients, 16 CTA exams were acquired using a 64-row helical CT scanner (Aquilion 64, Toshiba Medical System, Otawara, Japan) and 41 from a 320-row volumetric scanner (Aquilion ONE, Toshiba Medical System, Otawara, Japan). The scan protocol was previously described.<sup>7,8</sup> Scans with poor image quality were excluded for the current analysis.

### **Quantification of coronary atherosclerosis.**

CAD on CTA was quantified using dedicated software (QAngio CT Research Edition v1.3.6, Medis medical imaging systems bv, Leiden, the Netherlands). The validity of this software tool for the segmentation of the coronary anatomy was previously established.<sup>9</sup> For characterization of CAD, two different approaches are available in the software. One approach with predefined fixed intensity cut-off values on the Hounsfield Units (HU) and an adaptive approach where cut-off values are adapted according to lumen attenuation. In the present analysis the adaptive threshold for CTA plaque constitution was used as the reference standard.<sup>6</sup> This adaptive threshold is based on the principle that plaque intensity is influenced by luminal contrast densities and decrease from the proximal to the distal part of the vessel. Therefore, in this automatic- and user-independent approach, the HU cut-off values of the different plaque types are adapted according to lumen intensity. First, a linear trend line is fitted through the mean lumen intensity. Next, the threshold for NC is defined as 200 HU below this estimate with a maximum of 75 HU and the DC threshold is defined as 100 HU above this estimate with a maximum of 450 HU. The threshold between FI and FF is set on 20% of the difference between the NC and DC threshold. This way, the intensity cut-off values are adapted by the same linear, decreasing trend along the vessel (see Figure 2). Additionally, because the lumen intensity is lower in parts of a severe stenosis, the NC cut-off value is locally decreased with 125% of the difference between the estimate and the real lumen intensities. In contrast, lumen intensity is higher in calcified parts due to blooming artefacts. Therefore, the DC cut-off value is locally increased with 25% of the difference between the estimate and the real lumen intensities.

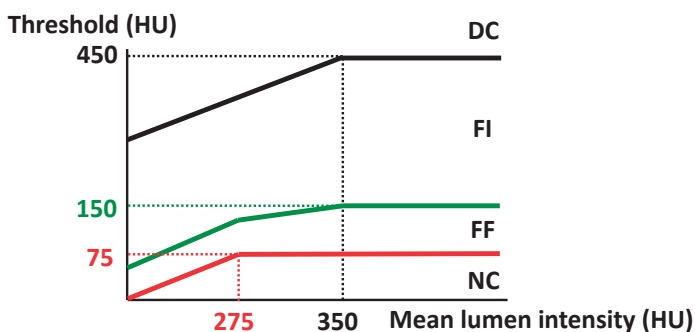


**Figure 2: The adaptive threshold scheme.**

The graphs shows the thresholds in HU (above the black line is DC, above the green line is FI, above the red line is FF and below the red line is NC) that are used for each measured mean lumen intensity on the x-axis for each cross-sectional CTA image. For example, if the mean lumen intensity is more than 350 HU, everything below 75 HU is NC, between 76 and 150 is FF, between 151 and 450 is FI and above 451 is DC.

### Comparison between VH and CTA

To compare the VH data with the CTA data a previously described comparison algorithm was used.<sup>6</sup> All transversal IVUS images were matched and fused with the corresponding transversal CTA images using anatomical landmarks (side-branches, ostia, and calcified plaques) as shown in Figure 3. The plaque volumes of all different plaque components in the lesions in each corresponding artery were assessed. Both the original VH images and the post-processed, eVH images were compared to QCT as shown in Figure 4.

### Statistical analysis

Statistical analyses were performed with the use of SPSS software (version 20.0, SPSS Inc., Chicago, IL, USA). First, the absolute plaque volumes of each plaque type on VH and eVH were compared. Second, both the VH and eVH plaque parameters were compared to QCT. For this purpose, the Spearman correlations were calculated. Moreover, the absolute median differences between QCT and VH or eVH were established. Thereafter, Bland–Altman plots were made to assess the bias and the limits of agreement for the comparison between VH and CTA (GraphPad Prism software, version 5.01, San Diego, California, USA). These plots show the difference of each pair plotted against the average value of each pair. Additionally, the Pitman-Morgan test of variances was used to demonstrate if the variances in the comparisons of QCT with VH with and without post-processing were significantly different.<sup>10</sup> The Pitman-Morgan test takes the correlation between two variances into account. A P-value  $\leq 0.05$  was considered statistically significant.

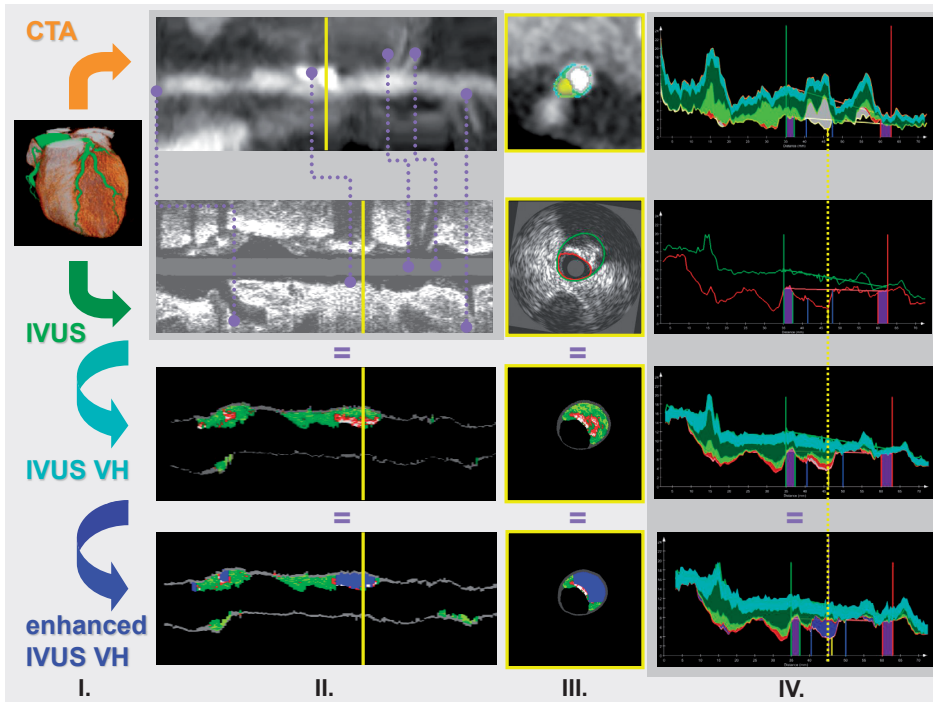


**Figure 3: Schematic illustration of the comparison of VH and eVH with QCT.**

First, the centerline was generated from the CTA data set (I). IVUS images are fused with the CTA volume using anatomical landmarks (II). Lumen and vessel wall contours were detected for both imaging modalities (III). Finally, lesions were quantified on the segmented plaque as shown in panel IV. Plaque volumes and plaque types were derived for the whole lesion, ranging from the proximal to distal lesion marker (blue markers). Both VH and eVH were compared to QCT.

## Results

Baseline patient characteristics were previously described.<sup>6</sup> For this analysis, 109 vessels were used of which 69 revealed atherosclerosis, whereas 40 vessels did not. In these 69 diseased vessels, 108 lesions were identified. These 108 lesions were used for the present lesion based comparison.

### Plaque classification on VH compared to eVH

The quantification results of both VH and eVH are depicted in Table 1. On VH median FI volume was 39.7(19.9-67.3) mm<sup>3</sup>, while applying the novel algorithm decreased the median FI volume to 37.6(16.8-61.5) mm<sup>3</sup>, ( $P < 0.001$ ). Similarly, the total volume of FF decreased from 9.3(4.9-19.4) mm<sup>3</sup> to 7.9(4.1-16.9) mm<sup>3</sup>, ( $P < 0.001$ ). Also, NC volume decreased from 11.8(6.0-22.3) mm<sup>3</sup> to 10.1(4.2-18.8) mm<sup>3</sup>, ( $P < 0.001$ ).

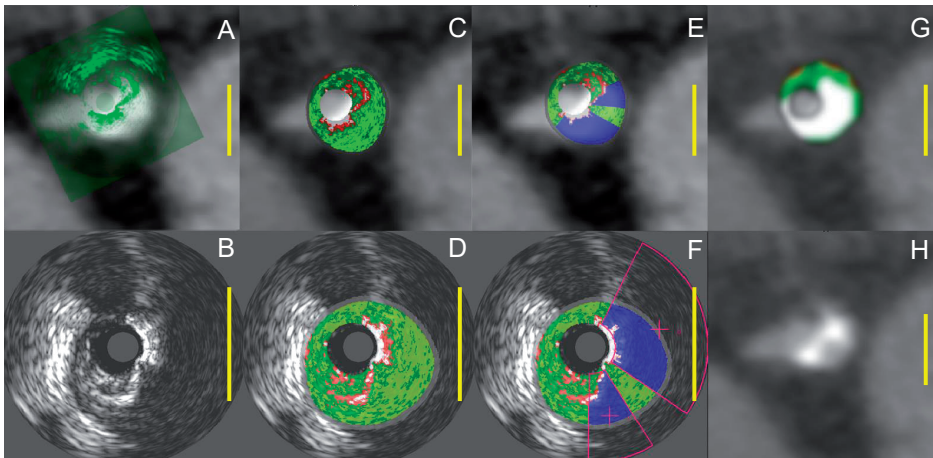


**Figure 4: Example of the registered images after fusion.**

The yellow scale bars represent 5 mm. A) CTA image with IVUS overlay B) in green correctly translated and rotated on the CTA image. C) contains the corresponding VH overlay from D) and similarly E) contains the eVH image from F). The QCT tissue overlay is shown in G) from the CTA image in H) Note that all overlays are mirrored in the top row for a correct fusion. The overlays in C-G have five color codes: red (NC), light-green (FF), dark-green (FI), white (DC), and blue for the masked areas. There is a nice correspondence between the masked areas in E) and the two calcified areas with high intensities in H) with in between a calcified area with lower intensity, more similar to the luminal contrast intensity in the bifurcating artery. This example shows that the DC area in VH is underestimated when compared to the DC area in the tissue overlay in G). Adding the blue quantified acoustic shadow to the total DC volume in eVH will approximate the DC volume in QCT.

**Table 1: Absolute differences between VH vs eVH plaque constitution compared to QCT plaque constitution (n=108).**

	VH median (IQR) (mm <sup>3</sup> )	QCT median (IQR) (mm <sup>3</sup> )	95% CI of mean differences	P-value
<b>Fibrotic</b>	39.7(19.9-67.3)	55.7(36.1-94.9)	15.0;25.9	<0.001
<b>Enhanced fibrotic</b>	37.6(16.8-61.5)		18.5;30.2	<0.001
<b>Fibro fatty</b>	9.3(4.9-19.4)	28.3(16.2-45.9)	16.7;23.6	<0.001
<b>Enhanced fibro fatty</b>	7.9(4.1-16.9)		19.4;25.9	<0.001
<b>Necrotic core</b>	11.8(6.0-22.3)	11.0(5.6-24.7)	-1.6;3.6	0.458
<b>Enhanced necrotic core</b>	10.1(4.2-18.8)		1.1;6.3	0.006
<b>Dense calcium</b>	5.4(1.7-11.6)	6.95(0.9-18.9)	4.5;12.5	<0.001
<b>Enhanced dense calcium</b>	10.0(3.0-22.8)		-3.6;1.5	0.401

eHV, Enhanced Virtual Histology; CI, confidence interval; IQR, interquartile range; VH, virtual histology; QCT, quantitative computed tomography

In the total population, the volume of DC in VH was 815.22 mm<sup>3</sup>. An acoustic shadow was detected in 106 of the 108(98%) lesions. The quantified acoustic shadow resulted in a total volume of 1033.93 mm<sup>3</sup>. These quantified areas were added to

the DC volumes providing a total enhanced DC volume of 1949.15 mm<sup>3</sup>. Overall, the median DC volume increased from 5.4(1.7-11.6) mm<sup>3</sup> to 10.0(3.0-22.8) mm<sup>3</sup>, (P<0.001).

### **Plaque classification on QCT**

The QCT plaque quantification results were previously described.<sup>6</sup> In brief, on QCT, the median FI volume was 55.7(36.1-94.9) mm<sup>3</sup>, the median FF volume was 28.3(16.2-45.9) mm<sup>3</sup>, the median volume of NC was 11.0(5.6-24.7) mm<sup>3</sup> and the DC volume was 6.95(0.9-18.9) mm<sup>3</sup>.

### **Comparison of VH and eVH to QCT plaque classification**

To validate the novel algorithm, the VH and eVH data were compared to QCT. The results of this comparison are demonstrated in Table 1.

#### **Absolute differences.**

The median DC volume was significantly underestimated by VH compared to QCT (5.4(1.7-11.6) mm<sup>3</sup>, vs. 6.95(0.9-18.9) mm<sup>3</sup> P<0.001). After applying the novel algorithm to the VH data, there was no significant difference between the DC volume on both modalities 10.0(3.0-22.8) mm<sup>3</sup> for eVH vs. 6.95(0.9-18.9) mm<sup>3</sup> for QCT, P=0.401). However, for NC a significant difference between QCT and eVH was observed (11.0(5.6-24.7) mm<sup>3</sup> on QCT vs 10.1(4.2-18.8) mm<sup>3</sup> on eVH P=0.006). For FI and FF a significant difference was observed for both VH and eVH compared to QCT.

#### **Correlation and agreement.**

For all four plaque types there was difference in correlation between QCT and VH compared to QCT and eVH after applying the novel algorithm (Table 2). The largest change in correlation between VH and QCT was observed for DC. Adding the quantified area to the DC volume improved the correlation with QCT from 0.733 to 0.818. The correlations of the other plaque types changed less if the novel algorithm was applied to the VH data.

The results of the corresponding Bland-Altman plots for the DC volume of both VH and eVH compared to QCT are shown in Table 2 and depicted in Figure 5. Without masking, DC volume in VH was underestimated with a bias of 8.5 mm<sup>3</sup> compared to the QCT. After applying the masking tool it was overestimated with a bias of -1.1 mm<sup>3</sup>. The masking is especially useful on cases with large DC volumes as shown in Figure 5 where the systematic error in the large DC volumes is smaller for eVH. The last column in Table 2 depicts the statistical significance of the difference in variances between the two comparisons (i.e. QCT vs. VH and QCT vs. eVH). As demonstrated with the Pitman-Morgan test of variances, the agreement in DC volume between

**Table 2: Correlation and agreement of VH vs eVH plaque constitution compared to QCT plaque constitution (n=108).**

	<b>Correlation (Spearman)</b>	<b>Bias (mm<sup>3</sup>)</b>	<b>Lower 95% LOA (mm<sup>3</sup>)</b>	<b>Upper 95% LOA (mm<sup>3</sup>)</b>	<b>Difference in variance (P-values Pitman's test)</b>
<b>Fibrotic</b>	0.787,<0.001	20.4	-35.7	76.6	<0.01
<b>Enhanced fibrotic</b>	0.750,<0.001	24.3	-54.6	77.8	
<b>Fibro fatty</b>	0.704,<0.001	20.2	-15.2	55.6	0.05
<b>Enhanced fibro fatty</b>	0.728,<0.001	22.6	-7.3	44.5	
<b>Necrotic core</b>	0.479,<0.001	1.0	-25.9	27.9	0.76
<b>Enhanced necrotic core</b>	0.425,<0.001	3.7	-26.4	61.4	
<b>Dense calcium</b>	0.733,<0.001	8.5	-32.5	49.5	<0.001
<b>Enhanced dense calcium</b>	0.818 <0.001	-1.1	-28.3	31.7	

VH, virtual histology; LOA, limits of agreement; QCT, quantitative computed tomography

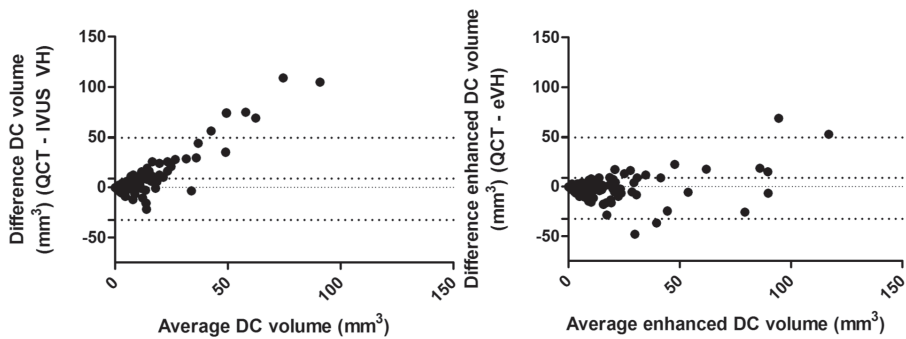


**Figure 5: Bland-Altman plots for both the DC volume of VH and DC volume of eVH compared with QCT.**

VH and QCT was significantly improved by applying the masking tool ( $P < 0.001$ ). Similarly, there was a significant change in variance for the FF and FI between VH and eVH compared to QCT. However, for these plaque types the agreement of QCT was better with VH than with eVH. For NC, there was no significant difference in variances between QCT vs. VH and QCT vs. enhanced VH. An example of a coronary lesion and the resulting comparison between QCT and VH without and with the enhanced plaque quantification is shown in Figure 6.

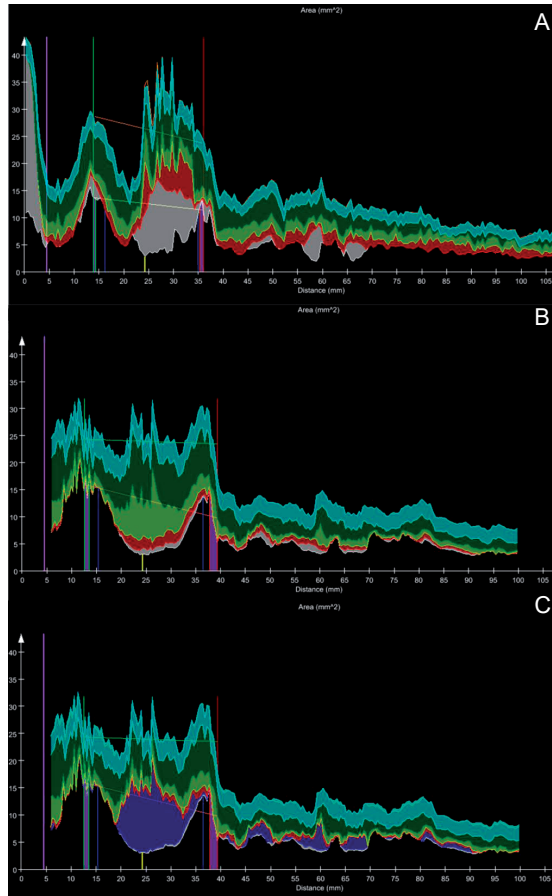


**Figure 6: Quantification of plaque volumes along the vessel.**

A) An example of a coronary lesion in CTA. The x-axis represents the distance from the coronary ostium in mm. The y-axis represents the area of either the lumen (lower part of graph) or the vessel wall (upper part of graph) in  $\text{mm}^2$ . The part between the two graphs shows the plaque constitution using a color code. In the corresponding VH data is shown in B) and in C) the results with the quantified shadows in blue. The enhanced quantification has better correspondence with the CTA analysis after adding the quantified shadow areas to the DC.

## Discussion

This study presents the results of a novel post-processing step on VH data to compensate for the limited ability of IVUS to penetrate dense calcified tissue. The novel algorithm detects, masks, and quantifies the acoustic shadow behind calcium. By adding the quantified acoustic shadows to the total DC volume, the correlation between DC volumes on VH and QCT improves significantly. Moreover, the agreement between both modalities improved significantly, from an underestimation in VH to a

small overestimation of DC volume in the enhanced VH. However, for FI and FF the agreement with QCT was reduced after applying the novel algorithm.

### **Acoustic shadow**

The limited ability of the echo-signal to penetrate coronary calcium results in two problems.<sup>5</sup> Firstly, the outer vessel boundaries located in the acoustic shadow are difficult to segment and need to be manually adjusted. This potentially leads to observer bias. However, an experienced observer can manually overcome this problem. Secondly and most important, the noise in the acoustic shadow is classified as coronary atherosclerosis by RF based methods as VH or iMap™(Boston Scientific).<sup>11</sup> Ideally, an acoustic shadow should be completely dark in B-mode IVUS images due to the greatly limited ability of the ultrasound signal to penetrate the calcified plaque. Current software tools fail to identify these acoustic shadows and quantify the tissue within the acoustic shadow. These regions are characterized mainly as FI or FF by VH or characterized mainly as necrotic tissue by iMap. The validity of this quantification is unknown. Recent echogenicity methods solve this problem by classifying the acoustic shadows behind calcifications as 'unknown'.<sup>12</sup> The acoustic shadow can be delineated manually, but is very time consuming. Moreover, a manual approach is susceptible to inter- and intra-observer variability for determining and masking the regions in the acoustic shadows. Bayturan *et al.* investigated a novel type of 'attenuated plaque' which occurs in the absence of DC.<sup>13</sup> Attenuated plaque was defined as hypoechoic plaque with deep ultrasonic attenuation (shadow) despite the absence of DC and is associated with high risk lesions. The acoustic shadow behind this attenuated plaque can also be detected by this post-processing procedure by using step 4 to differentiate between attenuated shadow regions and shadow regions resulting from DC as classified by VH or for example by echogenicity if there is no VH available.<sup>14</sup>

### **Novel algorithm**

For the present study a novel algorithm was developed to automatically detect and quantify the regions of acoustic shadow. Our hypothesis is that most of the tissue in the acoustic shadow is DC, or at least a larger volume than is detected with IVUS VH. To compensate for the suspected underestimation of DC within these regions, the quantified areas were added to the total DC volume. Although the corrected DC volumes in eVH show improved bias and correlation with QCT, the post-processing step does not detect any additional DC but selects regions without enough signal for reliable tissue characterization. Adding the quantified acoustic shadows to the overall DC volume, could result in overestimating DC in VH because not all plaque within the acoustic shadow is calcified. However, excluding the quantified shadows from the VH results will result in larger underestimation of the DC volume, because

all DC areas located in the acoustic shadow (i.e. calcifications located behind other calcified areas) will be excluded as well. Moreover, a thin or non-dense calcified plaque would allow for penetration of the acoustic signal and would likely not result in an acoustic shadow.

### **Coronary artery calcium on IVUS**

Coronary calcium, as assessed with different imaging modalities, is a representation of overall atherosclerotic burden. The prognostic value of coronary artery calcifications has been widely established.<sup>15</sup> Therefore, accurate assessment of coronary calcium on IVUS is of value in clinical practice. Calcifications on IVUS are strongly correlated with overall coronary plaque burden, but show limited correlation with stenosis severity.<sup>16</sup>

Besides sole DC, the relation between DC and necrotic core (considered a vulnerable plaque type) is of clinical value. Previous studies addressed the prognostic value of the NC/DC ratio on IVUS VH. On IVUS VH the ratio between NC and DC was the only significant parameter associated with cardiovascular risk factors for sudden coronary death in men.<sup>17</sup> Moreover, the NC/DC ratio was positively associated with a high-risk acute coronary syndrome presentation.<sup>18</sup> Indeed, ruptured plaques have a smaller calcium arch, and relatively more deep calcium than superficial calcium compared to non-ruptured plaques.<sup>19</sup>

The influence of coronary calcium on atherosclerotic plaque characterization with VH is an ongoing topic of debate.<sup>20</sup> Some studies suggest that coronary calcium on VH is surrounded by an area of artefact incorrectly quantified as NC.<sup>21</sup> This was confirmed by Pu *et al.* in a study with 131 coronary lesions, combining VH with near-infrared spectroscopy (NIRS).<sup>22</sup> In all lesions with calcified plaque, NC was present on VH. However, in these calcified plaques no relation was observed between percentage NC of VH and lipid core burden index on NIRS, suggesting an overestimation of NC in VH due to the artefact caused by calcium. By masking the regions behind the DC in the acoustic shadow, the median NC volume decreases compared to VH which potentially could improve the relation with NIRS. Furthermore, Thim *et al.* found no correlation between NC size determined by IVUS VH and real histology.<sup>23</sup> Although they did not include histological examples with large calcifications and acoustic shadows on the corresponding VH images, they suggest that the NC tissue detection in VH and the presence of calcifications are linked. A similar assessment of DC by VH and real histology is needed to provide further insights in this approach of enhancing VH results.

In addition to the relation with clinical presentation, coronary calcium influences the local response to medical therapy for plaque regression. Bruining *et al.* performed IVUS in 118 patients randomized to treatment with perindopril or placebo.<sup>24</sup> Patients

with little calcium showed plaque regression on perindopril treatment, whereas patients with moderate calcium showed no change in atherosclerosis. This led to the concept that coronary calcium content should be considered in quantitative analysis of therapy effect in atherosclerosis regression studies and need accurate assessment.

By quantifying the acoustic shadow, the presented algorithm can enhance the assessment of DC in VH. By applying the algorithm, there is a small trade-off in the agreement of NC, but there is no significant difference in NC variance between VH and eVH as shown in the last column of Table 2. Potentially, this novel tool provides better applicability of VH for DC assessment.

## Limitations

Although results of the presented study show that the VH results can be enhanced to improve correlation and bias of DC with QCT, there are some limitations. The post-processing step was applied on VH data and analyses from a single-centre. The influence of the post-processing step on the output of different IVUS catheters/vendors is unknown, specifically if iMap would benefit in the same degree of this approach.<sup>11</sup> The agreement for FI and FF became less with the novel algorithm. However, for clinical purpose accurate assessment of DC and NC is of greater value. Both NC and DC on VH are associated with ACS presentation or plaque rupture, whereas FI and FF are not.<sup>1,25</sup>

For this comparison, the QCT was used as the gold standard. However, the segmentation of plaque areas and the tissue classification in QCT is influenced by blooming artefacts. Also, bias between both modalities is always present because of the difference in segmented plaque volumes. QCT overestimates the plaque volume by an underestimation of the lumen volume and a slight overestimation of vessel wall volume compared with IVUS.<sup>6</sup> A direct comparison between the plaque characterization in VH and OCT or histopathology could provide further insights into the distribution of DC in areas within the acoustic shadows.<sup>26</sup>

## Conclusion

Although tissue characterization within the acoustic shadow in VH is unreliable, an automatic post-processing step to quantify the acoustic shadow in order to add these regions to the calcified tissue enhances the agreement with QCT DC characterization.

## References

- (1) Nasu K, Tsuchikane E, Katoh O, Vince DG, Virmani R, Surmely JF, Murata A, Takeda Y, Ito T, Ehara M, Matsubara T, Terashima M, Suzuki T (2006) Accuracy of in vivo coronary plaque morphology assessment a validation study of in vivo virtual histology compared with in vitro histopathology. *J Am Coll Cardiol.* 47:2405–2412
- (2) Stone GW, Maehara A, Lansky AJ, Bruyne B de, Cristea E, Mintz GS, Mehran R, McPherson J, Farhat N, Marso SP, Parise H, Templin B, White R, Zhang Z, Serruys PW (2011) A Prospective Natural-History Study of Coronary Atherosclerosis. *N Engl J Med.* 364:226–235
- (3) Mintz GS, Missel E (2009) What is behind the calcium? The relationship between calcium and necrotic core on virtual histology analyses: reply. *Eur Heart J.* 30:125–126
- (4) Mintz GS, Nissen SE, Anderson WD, Bailey SR, Erbel R, Fitzgerald PJ, Pinto FJ, Rosenfield K, Siegel RJ, Tuzcu EM, Yock PG (2001) American college of cardiology clinical expert consensus document on standards for acquisition, measurement and reporting of intravascular ultrasound studies (IVUS). *J Am Coll Cardiol.* 37:1478–1492
- (5) García-García HM, Gogas BD, Serruys PW, Bruining N (2011) IVUS-based imaging modalities for tissue characterization: similarities and differences. *Int J Cardiovasc Imaging.* 27:215–224
- (6) Graaf MA de, Broersen A, Kitslaar PH, Roos CJ, Dijkstra J, Lelieveldt BPF, Jukema JW, Schalij MJ, Delgado V, Bax JJ, Reiber JHC, Scholte AJ (2013) Automatic quantification and characterization of coronary atherosclerosis with computed tomography coronary angiography: cross-correlation with intravascular ultrasound virtual histology. *Int J Cardiovasc Imaging.* 29:1177–1190
- (7) Graaf FR de, Schuijff JD, Velzen JE van, Kroft LJ, Roos A de, Reiber JH, Boersma E, Schalij MJ, Spanó F, Jukema JW, Wall EE van der, Bax JJ (2010) Diagnostic accuracy of 320-row multidetector computed tomography coronary angiography in the non-invasive evaluation of significant coronary artery disease. *Eur Heart J.* 31:1908–1915
- (8) Werkhoven JM van, Schuijff JD, Gaemperli O, Jukema JW, Kroft LJ, Boersma E, Pazhenkottil A, Valenta I, Pundziute G, Roos A de, Wall EE van der, Kaufmann PA, Bax JJ (2009) Incremental prognostic value of multi-slice computed tomography coronary angiography over coronary artery calcium scoring in patients with suspected coronary artery disease. *Eur Heart J.* 30:2622–2629
- (9) Papadopoulou SL, Garcia-Garcia HM, Rossi A, Girasis C, Dharampal AS, Kitslaar PH, Krestin GP, Feyter PJ de (2013) Reproducibility of computed tomography angiography data analysis using semiautomated plaque quantification software: implications for the design of longitudinal studies. *Int J Cardiovasc Imaging.* 29:1095–1104
- (10) Pitman EG (1939) A note on normal correlation. *Biometrika.* 31:9–12
- (11) Shin E-S, Garcia-Garcia HM, Ligthart JMR, Witberg K, Schultz C, Steen AFW van der, Serruys PW (2011) In vivo findings of tissue characteristics using iMap IVUS and Virtual Histology IVUS. *EuroIntervention.* 6:1017–1019
- (12) Bruining N, Verheye S, Knaapen M, Somers P, Roelandt JR, Regar E, Heller I, Winter S de, Ligthart J, Van Langenhove G, Feijter PJ de, Serruys PW, Hamers R (2007) Three-dimensional and quantitative analysis of atherosclerotic plaque composition by automated differential echogenicity. *Catheter Cardiovasc Interv.* 70:968–978
- (13) Bayturan O, Tuzcu EM, Nicholls SJ, Balog C, Lavoie A, Uno K, Crowe TD, Magyar WA, Woloski K, Kapadia S, Nissen SE, Schoenhagen P (2009) Attenuated Plaque at Nonculprit Lesions

- in Patients Enrolled in Intravascular Ultrasound Atherosclerosis Progression Trials. *J Am Coll Cardiol Interv.* 2:672–678
- (14) Campos CM, Ishibashi Y, Eggermont J, Nakatani S, Cho YK, Dijkstra J, Reiber JHC, Sheehy A, Lane J, Kamberi M, Rapoza R, Perkins L, Garcia-Garcia HM, Onuma Y, Serruys PW (2015) Echogenicity as a surrogate for bioresorbable everolimus-eluting scaffold degradation: analysis at 1-, 3-, 6-, 12-, 18-, 24-, 30-, 36- and 42-month follow-up in a porcine model. *Int J Cardiovasc Imaging.* 31:471–482
  - (15) Budoff MJ, Shaw LJ, Liu ST, Weinstein SR, Mosler TP, Tseng PH, Flores FR, Callister TQ, Raggi P, Berman DS (2007) Long-term prognosis associated with coronary calcification: observations from a registry of 25,253 patients. *J Am Coll Cardiol.* 49:1860–1870
  - (16) Mintz GS, Pichard AD, Popma JJ, Kent KM, Satler LF, Bucher TA, Leon MB (1997) Determinants and Correlates of Target Lesion Calcium in Coronary Artery Disease: A Clinical, Angiographic and Intravascular Ultrasound Study. *J Am Coll Cardiol.* 29:268–274
  - (17) Missel E, Mintz GS, Carlier SG, Qian J, Shan S, Castellanos C, Kaple R, Biro S, Fahy M, Moses JW, Stone GW, Leon MB (2008) In vivo virtual histology intravascular ultrasound correlates of risk factors for sudden coronary death in men: results from the prospective, multi-centre virtual histology intravascular ultrasound registry. *Eur Heart J.* 29:2141–2147
  - (18) Missel E, Mintz GS, Carlier SG, Sano K, Qian J, Kaple RK, Castellanos C, Dangas G, Mehran R, Moses JW, Stone GW, Leon MB (2008) Necrotic Core and Its Ratio to Dense Calcium Are Predictors of High-Risk Non-ST-Elevation Acute Coronary Syndrome. *Am J Cardiol.* 101:573–578
  - (19) Fujii K, Carlier SG, Mintz GS, Wijns W, Colombo A, Böse D, Erbel R, Jr J de RC, Kimura M, Sano K, Costa RA, Lui J, Stone GW, Moses JW, Leony MB (2005) Association of Plaque Characterization by Intravascular Ultrasound Virtual Histology and Arterial Remodeling. *Am J Cardiol.* 96:1476–1483
  - (20) Murray SW, Palmer ND (2009) What is behind the calcium? The relationship between calcium and necrotic core on virtual histology analyses. *Eur Heart J.* 30:125–126
  - (21) Sales FJ, Falcão BA, Falcão JL, Ribeiro EE, Perin MA, Horta PE, Spadaro AG, Ambrose JA, Martinez EE, Furuie SS, Lemos PA (2010) Evaluation of plaque composition by intravascular ultrasound “virtual histology”: the impact of dense calcium on the measurement of necrotic tissue. *EuroIntervention.* 6:394–399
  - (22) Pu J, Mintz GS, Brilakis ES, Banerjee S, Abdel-Karim A-RR, Maini B, Biro S, Lee J-B, Stone GW, Weisz G, Maehara A (2012) In vivo characterization of coronary plaques: novel findings from comparing greyscale and virtual histology intravascular ultrasound and near-infrared spectroscopy. *Eur Heart J.* 33:372–383
  - (23) Thim T, Hagensen MK, Wallace-Bradley D, Granada JF, Kaluza GL, Drouet L, Paaske WP, Botker HE, Falk E (2010) Unreliable assessment of necrotic core by virtual histology intravascular ultrasound in porcine coronary artery diseasemen. *Circ Cardiovasc Imaging.* 3:384–391
  - (24) Bruining N, Winter S de, Roelandt JRTC, Rodriguez-Granillo GA, Heller I, Domburg RT van, Hamers R, Feijter PJ de (2009) Coronary calcium significantly affects quantitative analysis of coronary ultrasound: importance for atherosclerosis progression/regression studies. *Coron Artery Dis.* 20:409–414
  - (25) Shah PK (2003) Mechanisms of plaque vulnerability and rupture. *J Am Coll Cardiol.* 41:S15–S22
  - (26) Rasheed Q, Dhawale PJ, Anderson J, Hodgson JM (1995) Intracoronary ultrasound-defined plaque composition: Computer-aided plaque characterization and correlation with histologic samples obtained during directional coronary atherectomy. *Am Heart J.* 129:631–637





# Chapter 6

## Automatic detection and quantification of the Agatston coronary artery calcium score on contrast computed tomography angiography

de Graaf MA, Ahmed W, Broersen A, Kitslaar PH, Oost E, Dijkstra J, Bax JJ, Reiber JH, Scholte AJ

(Shared first authorship)

*International Journal of Cardiovascular Imaging* 2015;31:151-161

## Abstract

**Purpose:** Potentially, Agatston coronary artery calcium (CAC) score could be calculated on contrast CTA. This will make a separate non-contrast CT scan superfluous. This study aims to assess the performance of a novel fully automatic algorithm to detect and quantify the Agatston CAC score in contrast CTA images.

**Methods:** From a clinical registry, 20 patients were randomly selected for each CAC category (i.e. 0,1-99,100-399,400-999,≥1000). The Agatston CAC score on non-contrast CT was calculated manually, while the novel algorithm was used to automatically detect and quantify Agatston CAC score in contrast CTA images. The resulting Agatston CAC scores were validated against the non-contrast images.

**Results:** A total of 100 patients ( $60 \pm 11$  years, 63 men) were included. The median CAC score on non-contrast CT was 145 (IQR 5-760), whereas the contrast CTA CAC score was 170 (IQR 23-594) ( $P=0.004$ ). The automatically computed CAC score showed a high correlation ( $R=0.949$ ;  $P<0.001$ ) and intra-class correlation ( $R=0.863$ ;  $P<0.001$ ) with non-contrast CT CAC score. Moreover, agreement within CAC categories was good (Kappa 0.588).

**Conclusion:** Fully automatic detection of Agatston CAC score on contrast CTA is feasible and showed high correlation with non-contrast CT CAC score. This could imply a radiation dose reduction and time saving by omitting the non-contrast scan.

## Introduction

Coronary artery disease (CAD) is one of the leading causes of death worldwide.<sup>1</sup> Coronary artery calcium (CAC) is a representative marker of the overall coronary atherosclerosis burden.<sup>2</sup> The amount of coronary artery calcium is routinely detected and quantified on a non-contrast computed tomography (CT) scan according to the Agatston scoring approach.<sup>3, 4</sup> This Agatston CAC score has been demonstrated to have prognostic value for cardiovascular events, independent of age, ethnicity and sex.<sup>5-10</sup> However, for the estimation of severity and extent of coronary stenosis a contrast computed tomography coronary angiography (CTA) has to be performed.<sup>11, 12</sup> This technique allows evaluation of coronary stenosis with good accuracy compared to invasive coronary angiography.<sup>13-16</sup> Moreover, contrast CTA provides accurate visualization of the coronary vessel wall and allows assessment of coronary plaque constitution.

In current clinical practice, a non-contrast CT scan is often performed to quantify the Agatston CAC score. Subsequently, depending on the clinical question, a contrast CTA scan is performed to assess coronary stenosis severity. While the non-contrast CT scan and contrast CTA are performed separately, they both contribute to radiation exposure.<sup>17</sup> Since calcified lesions can be distinguished on contrast CTA, it is conceivable that contrast CTA images could be used to detect coronary calcium and calculate the Agatston score. If Agatston CAC score calculation on contrast CTA images is accurately achievable, it could result in making a separate non-contrast CT scan superfluous, hence resulting in a decrease in cost, time and radiation exposure. Previous studies have addressed this topic, aiming to assess the potential of software tools to quantify CAC on CTA datasets, however, these algorithms required (partial) manual interference or provided moderate results.<sup>18-22</sup> Recently, using a novel software algorithm, fully automatic quantification of the Agatston CAC score on contrast CT has become feasible. However, the accuracy of this tool has yet to be determined.

Therefore, the aim of this present study was to 1) assess the feasibility of a novel tool to fully automatically detect and quantify CAC in contrast CTA images, and calculate the Agatston CAC scores and 2) to compare the derived Agatston scores with Agatston CAC scores obtained from traditional non-contrast CT scans and assess the agreement per Agatston CAC score risk category. 3) The contribution of the non-contrast CT to the overall radiation exposure was calculated.

## Methods

### Patients and study protocol

The population consisted of 100 patients from an ongoing clinical registry. Per Agatston CAC score risk categories (i.e. 0, 1-99, 100-399, 400-999,  $\geq 1000$ ), 20 patients, with sufficient image quality of the non-contrast CT and the contrast CTA, were randomly selected to ensure an equal distribution. These patients had known or suspected CAD and were clinically referred for the evaluation of chest pain to the Leiden University Medical Center, between 2008 and 2012. All patients underwent a non-contrast CT scan followed by a contrast CTA.

Patients with previous, myocardial infarction, percutaneous coronary intervention (PCI) or coronary artery bypass graft surgery (CABG) were excluded. The clinical data were prospectively entered into the departmental Cardiology Information System (EPD-Vision©, Leiden University Medical Center, the Netherlands) and retrospectively analyzed. The Institutional Review Board of the Leiden University Medical Center approved this retrospective evaluation of clinically collected data, and waived the need for written informed consent.

### Cardiac CT and CTA acquisition

Patients were scanned with either a 64-slice CT scanner (Aquilion 64, Toshiba Medical System, Otowara, Japan) or a 320-row volumetric scanner (Aquilion ONE, Toshiba Medical System, Otowara, Japan). Contra-indications for CTA were, 1) impaired renal function (glomerular filtration rate  $< 60$ ), 2) pregnancy, 3) (supra-) ventricular arrhythmias, 4) known allergy to contrast agent, 5) severe claustrophobia. Prior to CT examination, beta-blocking medication was administered if the heart rate was  $\geq 65$  beats per minutes, unless contra-indicated. Patients received 0.4 mg of nitrates sublingual prior to the scan. Non-contrast CT and contrast CTA were performed according to standard clinical practice.<sup>23, 24</sup> For assessment of the CAC-score on non-contrast CT, images with a 3mm slice-thickness were reconstructed. Scan parameters for 64-slice CTA were 400ms gantry rotation time, collimation of 64x0.5mm, tube voltage of 100-135 kV and tube current of 250-350mA, depending on body mass index. Scan parameters for 320-row CTA were 350ms gantry rotation time, collimation of 320 x0.5mm, tube voltage of 100-135 kV and tube current of 400-580mA, depending on body mass index. Images were acquired prospectively and reconstructed at 75% and at the best phase of the R-R interval.<sup>25</sup> Radiation dose was calculated with a dose-length product conversion factor of 0.014 mSv/(mGy x cm).<sup>26</sup>

### **Quantification of Agatston CAC score on non-contrast CT scan**

The standard non-contrast CT scan was made to manually assess the total amount of CAC in the coronary arteries, defined according to the Agatston CAC-scoring method. To analyze the CAC score, the collected images were transferred to a workstation for evaluation using dedicated post-processing software (CalcSore v1.1.1 by Medis specials bv). Coronary calcified lesions were manually selected and quantified in non-contrast CT scans with a threshold of 130 Hounsfield Unit (HU).

### **Quantification of Agatston CAC score on contrast CTA**

Prior to coronary artery calcium quantification, image quality of both non-contrast CT and contrast CTA was assessed using the following ordinal scale: good image quality, moderate image quality or poor image quality. Image data sets without motion artefacts or increased image noise were evaluated as good quality datasets with motion artefacts or increased image noise were classified as moderate. Clinically non-diagnostic scans were classified as poor image quality and were excluded.

A novel algorithm for fully automatic detection and quantification of the calcium volume and Agatston CAC score on the contrast CTA datasets was developed. The Agatston CAC score was automatically derived in the following steps:

1. The coronary tree was automatically extracted from the CTA dataset using a 3D vessel-tracking algorithm.<sup>27</sup>
2. Using an automatic tree labeling algorithm, the segments of the coronary tree were automatically labeled according the AHA 17-segment model.<sup>27-29</sup> Subsequently, the four main coronaries, i.e., right coronary artery (RCA), left main (LM) artery, left anterior descending (LAD) artery and left circumflex (LCx) artery and corresponding side-branches were identified based on this labeling result. Multi-planar reformations (MPRs) were created based on the centerlines of the detected coronaries. An experienced observer verified the extracted and labeled coronary tree.
3. To automatically detect and quantify CAC, a novel algorithm was used to identify the presence of calcium in the coronary arteries. A reference trend line on the lumen intensity values along the centerline was fitted for each individual vessel, ranging from the proximal to the distal part of the vessel. After this, only the pixels near the centerline with intensity values higher than the reference trend line are considered to be calcified and selected for further processing using an advanced region growing scheme (Figure 1.)
4. All detected calcified pixels in the MPRs are projected back into the original volume. Any emerging gaps within projected spots are filled if needed. Next, the volume is resampled to have a slice thickness of 3 mm.

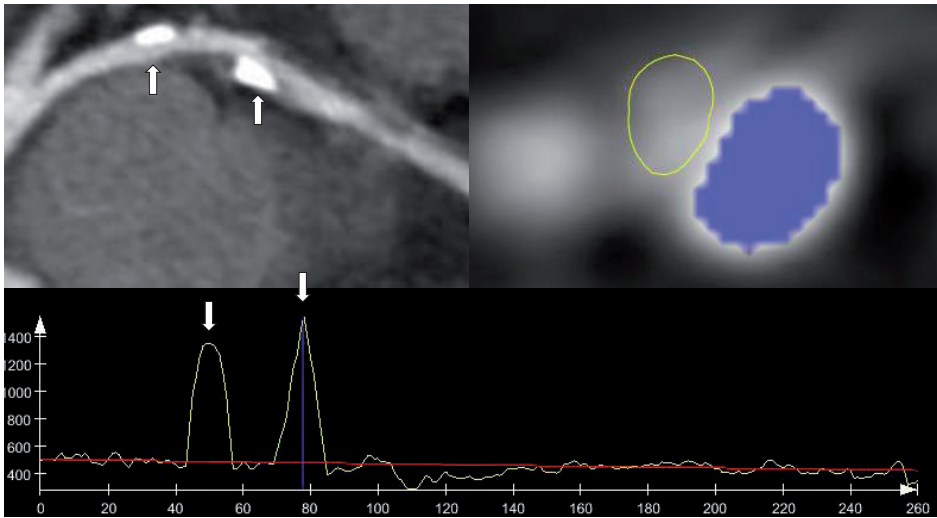


**Figure 1. Method for automatic coronary calcium detection.**

Example of the method for automatic coronary calcium detection. Panel A shows an MPR with two calcified coronary lesions (white arrows). Panel C demonstrates the luminal intensities plot. The x-axis represents the distance from the coronary ostium, the y-axis represents the peak intensity along the centerline (HU). The red line is the trendline of this plot. Large deviations from this trendline are considered coronary calcium (white arrows) Panel B demonstrates a cross-sectional view of the coronary artery with the detected coronary calcium marked in blue. The yellow line indicates the coronary lumen border.

- Based on the detected CAC volumes for each of the four main coronaries and side-branches, the Agatston CAC score was automatically calculated using a predefined conversion factor of 2.74.<sup>19</sup>

An example of the automatic CAC assessment on contrast CTA with corresponding non-contrast CT reference is depicted in Figure 2.

First, the Agatston CAC scores derived from contrast CTA using the novel software tool were compared to the Agatston CAC score from non-contrast CT as a reference. Second, differences in performance of the software per coronary vessel were assessed. Third, the agreement between the two methods per Agatston CAC score risk category was assessed. Last, the contribution of the non-contrast CT to the overall radiation exposure was calculated.

### Statistical analysis

Continuous data are presented as mean  $\pm$  SD if normally distributed or as median (interquartile range, IQR) if non-normally distributed. Categorical data are presented as absolute numbers and percentages. A comparison was made between the non-contrast CT Agatston CAC score and the contrast CTA Agatston CAC score. Non-

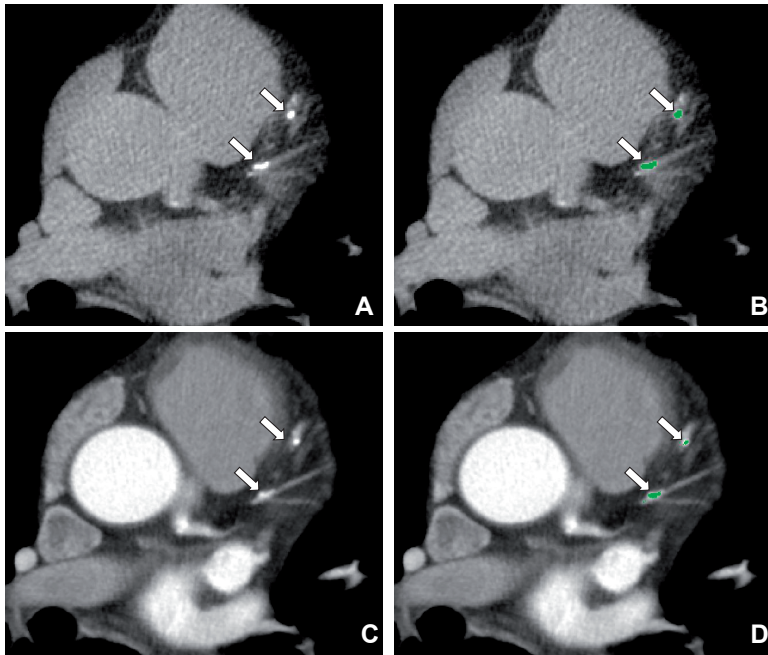


**Figure 2. Patient example of coronary calcium detection with both methods.**

A 66 year old male patient with calcified coronary plaque in the LAD. Panel A illustrates the coronary artery calcium (CAC) on the non-contrast CT scan (arrows). Panel B depicts the manual detection of the calcified lesions on the same non-contrast CT scan. Panel C shows CAC in the same patient on the contrast CTA scan. Panel D depicts the automatic detection and quantification of the calcium on the contrast CTA scan with a novel fully automatic algorithm. The Agatston CAC score was 63 on the non-contrast CT scan and 58 on the contrast CTA scan as assessed with the fully automatic algorithm.

parametric tests were used to compare the absolute difference between the CAC score derived from non-contrast CT scan and contrast CTA. A non-parametric correlation (Spearman) and intra-class correlation (ICC) were used to calculate the correlation between the two methods. An ICC less than 0.4 indicated poor correlation, an ICC between 0.4 and 0.75 indicated fair to good correlation, and an ICC greater than 0.75 indicated excellent correlation.<sup>30</sup> Thereafter, the Bland-Altman method was used to assess the limits of agreement for the Agatston CAC score between the two methods.<sup>31</sup> The Bland-Altman was calculated for both absolute and percentage differences. For clarity, a magnified view of the Bland-Altman plot with an X-axis range up to 1000 was provided. The agreement within the Agatston CAC score risk categories, was evaluated using the weighted kappa ( $k$ ) statistics. Poor, fair-to-good and excellent were defined by a  $k$ -value of  $<0.4$ , between 0.4 and 0.75, and  $>0.75$ , respectively.<sup>32</sup> All statistical tests were two-sided and a P-value  $<0.05$  was considered statistically

significant. All statistical analyses were performed with SPSS software (Version 20.0, SPSS Inc., Chicago, Illinois).

## Results

### Patient population

The total patient population consisted of 100 patients with a mean age of  $60 \pm 11$  years and 63 patients (63%) were male. The clinical baseline characteristics of the patients are listed in Table 1. Hypercholesterolemia was observed in 33% of patients, and 21% of patients presented with obesity. Of the 100 scans, 54 were classified as good; the remaining 46 were classified as moderate quality.

**Table 1. Patient characteristics.**

Baseline characteristics	Total (N = 100)
Age (yrs)	60 ± 11
Gender (% male)	63 (63%)
Cardiovascular risk factors	
Hypertension†	38 (38%)
Hypercholesterolemia‡	33 (33%)
Diabetes mellitus	31 (31%)
Family history of CAD*	33 (33%)
Current Smoker	15 (15%)
Obesity (BMI ≥ 30 kg/ m <sup>2</sup> )	21 (21%)
Agatston CAC score (non-contrast CT) images)	606 ± 997
	=-
	145 (IQR 5 – 760)

Data are represented as mean ± SD, median (interquartile range) or as number and percentages of patients.

†Defined as systolic blood pressure ≥140 mmHg or diastolic blood pressure ≥90 mmHg or the use of antihypertensive medication.

‡Serum total cholesterol ≥230 mg/dL or serum triglycerides ≥200 mg/dL or treatment with lipid lowering drugs.

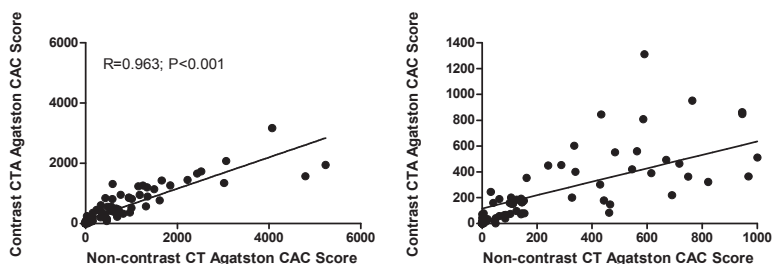
\*Defined as the presence of coronary artery disease in first-degree family members at <55 years in men and <65 years in women.

Abbreviations: BMI: body mass index, CAD: coronary artery disease, CAC: coronary artery calcium, CT: computed tomography, IQR: interquartile range.

**Table 2. Agreement between the Agatston CAC score derived from non-contrast CT and contrast CTA per coronary vessel.**

Coronary artery	Non-contrast Agatston CAC score Median (IQR)	Contrast CTA Agatston CAC score Median (IQR)	P-value	Correlation (R), (P-value)	ICC, (P-value)
LM	0 (0-37)	0 (0-13)	0.160	0.513, (P<0.001)	0.757, (P<0.001)
LAD	83 (1-369)	86 (0-281)	0.371	0.894, (P<0.001)	0.854, (P<0.001)
RCA	16 (0-251)	33 (0-150)	0.001	0.827, (P<0.001)	0.793, (P<0.001)
LCX	4 (0-53)	11 (0-65)	0.703	0.754, (P<0.001)	0.851, (P<0.001)
<b>Total</b>	<b>145 (5-760)</b>	<b>170 (23-594)</b>	<b>0.004</b>	<b>0.949, (P&lt;0.001)</b>	<b>0.863, (P&lt;0.001)</b>

Abbreviations: CT: computed tomography, CTA: computed tomography coronary angiography, ICC: Intra-class correlation, IQR: Interquartile Range, CX: circumflex artery, LAD: Left anterior descending artery, LM: Left main, RCA: Right coronary artery.

**Figure 3. Correlation between non-contrast CT Agatston CAC score and contrast CTA Agatston CAC score.**

The left figure shows the full range scatter plot. The right figure shows a magnified view of the non-contrast CT Agatston CAC score up to 1000.

### Agreement between non-contrast CT and contrast CTA Agatston CAC score

The median Agatston CAC score on non-contrast CT was lower compared to the Agatston CAC score on contrast CTA (145(IQR 5-760) and 170(IQR 23-594),  $P=0.004$ , respectively) (Table 2). Overall, the median difference was 0 (-217-35).

The correlation between the non-contrast CT- and contrast CTA Agatston CAC score is displayed in Figure 3. The Agatston CAC score on non-contrast CT was highly correlated with the contrast CTA Agatston CAC score ( $R=0.949$ ,  $P<0.001$  and  $ICC=0.863$ ,  $P<0.001$ ). The correlation was similar between scans of good image quality ( $R=0.934$ ) and moderate image quality ( $R=0.949$ ). The correlation was similar for patients scanned with 100kV ( $n=13$ ),  $R=0.994$ ,  $P<0.001$ , 120 kV ( $n=72$ ),  $R=0.935$ ,

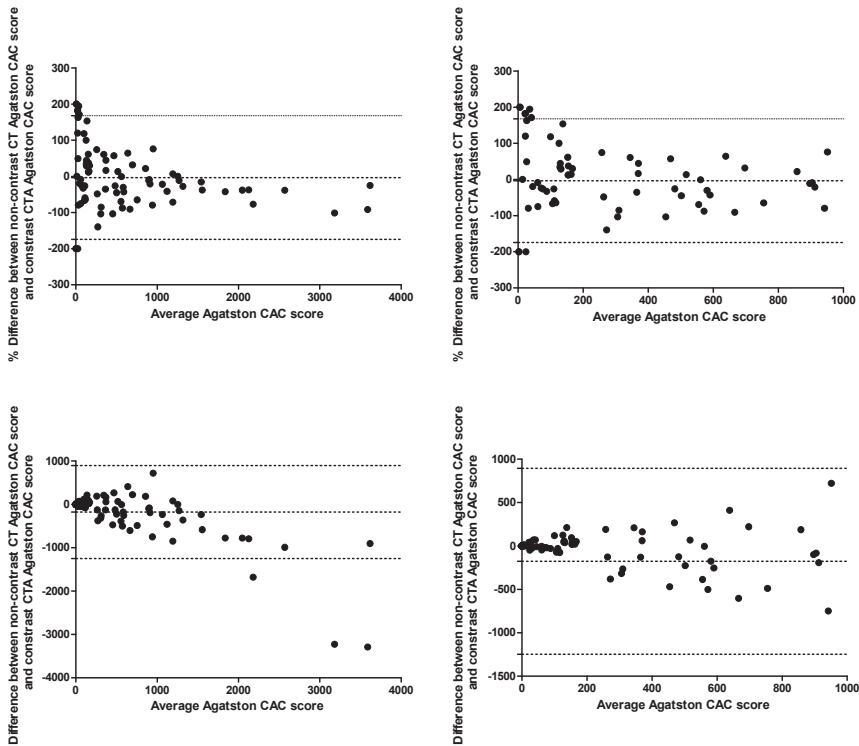


**Figure 4. Bland-Altman of non-contrast CT Agatston CAC score and contrast CTA Agatston CAC score.** The left panel shows the Bland-Altman plot. Dotted vertical lines represent the bias with corresponding 95% limits of agreement. The right panel shows a magnified view of the same Bland-Altman plot with an X-axis range of 1000. In the two upper panels the Y-axis represents the percentage difference of the Agatston CAC score between the two methods. In the lower two panels the Y-axis represents the absolute difference.

$P < 0.001$ , or 135 kV ( $n = 15$ ),  $R = 0.960$ ,  $P < 0.001$ . For all three kV settings the ICC between the non-contrast CT and contrast CTA CAC score was 0.784.

The Bland-Altman analysis of the Agatston CAC score as assessed with both methods is shown in Figure 4. The non-contrast CT Agatston CAC score was lower compared to the contrast CTA Agatston CAC score as demonstrated by a bias of -176 with 95%-limits of agreement ranging from -1248 to 896. The bias on a percentage basis was 3% with 95%-limits of agreement ranging from -174% to -168%. As demonstrated in the Bland-Altman analysis the absolute error increases with increasing CAC-scores (lower panels). However, on a percentage basis this trend is not observed (upper panels).

The per-vessel analysis, as described in Table 2, demonstrated similar results. Correlations for LAD, RCA and LCX were 0.894, 0.827 and 0.754, respectively ( $P < 0.001$ ).

However, the correlation for LM CAC score was lower ( $R=0.513$ ,  $P<0.001$ ) compared to the correlation for the overall CAC score. Except for RCA, there were no significant absolute differences between non-contrast CT Agatston CAC score and contrast CTA Agatston CAC score per vessel.

### Agreement within Agatston CAC score risk categories

The agreement between the two methods within the traditional Agatston CAC score risk categories was assessed and depicted in Table 3. The fully automatic algorithm used on contrast CTA classified 67/100 patients (67%) in the same cardiovascular risk category compared with the non-contrast CT Agatston CAC score. Of the remaining 33 (33%) patients, 10 (10%) shifted to a higher category and 23 (23%) to a lower category. Importantly, of the 20 patients with a non-contrast CT Agatston CAC score of 0, 18 (90%) patients were accurately classified as CAC score of 0 on the contrast scan. Only two patients shifted to a higher category, these patient had a contrast CTA Agatston CAC score of 11 and 14. Furthermore, in the CAC score category of 1-99, 14 (70%) patients remained in the same category while 3 (15%) patients shifted to a lower category and 3 (15%) patients to a higher category. In the category 100-399, 11 (55%) patients remained in the same category, while 5 (25%) patients shifted to a lower category of 1-99 and 4 (20%) patients shifted to a higher category of 400-999. Of the 20 patients in the category 400-999, 10 (50%) patients remained in the same category after calcium scoring on CTA images, while 9 (45%) patients shifted to a

**Table 3. Agreement within CAC score risk categories between the contrast CTA Agatston CAC score and the non-contrast CT Agatston score.**

		Non-contrast CT Agatston CAC score						
		Category	0	1-99	100-399	400-999	≥1000	Total
<b>Contrast CTA Agatston CAC score</b>	<b>0</b>		<u>18</u>	3	0	0	0	21
	<b>1-99</b>		2	<u>14</u>	5	1	0	22
	<b>100-399</b>		0	3	<u>11</u>	8	0	22
	<b>400-999</b>		0	0	4	<u>10</u>	6	20
	<b>≥1000</b>		0	0	0	1	<u>14</u>	15
	<b>Total</b>		20	20	20	20	20	100
		<b>Same</b>	<u>18</u>	<u>14</u>	<u>11</u>	<u>10</u>	<u>14</u>	<u>67</u>
		<b>Shift up</b>	2	3	4	1	0	10
		<b>Shift down</b>	0	3	5	9	6	23

The underlined numbers indicate agreement between both methods.

Abbreviations: CAC: coronary artery calcium, CT: computed tomography, CTA: computed tomography coronary angiography.

lower category and 1 (5%) patient to a higher category of  $\geq 1000$ . Lastly, 6 (30%) patient in the risk category of  $\geq 1000$ , shifted to a lower category. Overall, the agreement within the Agatston CAC score risk categories was good ( $k=0.588$ ). This was the same for scans with good ( $k=0.578$ ) and fair ( $k=0.586$ ) image quality.

### **Radiation dose**

In total, the mean radiation dose was  $9.10 \pm 5.78$  mSv. For non-contrast CT the radiation dose was  $1.39 \pm 0.39$  mSv and for the contrast CTA  $7.60 \pm 5.78$  mSv. On average, the radiation dose of the non-contrast CT was 20% of the total radiation exposure.

## **Discussion**

The present study assessed the feasibility and accuracy of a novel software tool for fully automatic detection of CAC and subsequent quantification of the Agatston CAC score on contrast CTA images. The automatic algorithm was evaluated by using the non-contrast CT Agatston CAC score as a reference standard. The Agatston CAC score derived from contrast CTA was well-correlated with non-contrast CT Agatston CAC score. Moreover, even though a third of the patients were reclassified in a different CAC-risk category, the overall agreement within the traditional Agatston CAC score risk categories was good, thus providing accurate assessment of cardiovascular risk in correspondence with the Agatston CAC score derived from non-contrast CT. Based on these results, the novel software tool allows for accurate quantification of CAC on contrast CTA and could thus provide an important prognostic and well validated marker of risk. Omitting the non-contrast CT from the scan protocol could have potentially reduced the radiation exposure in this study cohort by 20%.

### **Contrast CTA conversion factor**

Different voxel size, contrast attenuation and applied threshold for calcium scoring influences the Agatston CAC score between the non-contrast CT images and contrast CTA.<sup>20, 21, 25, 33, 34</sup> To adapt for this difference, a conversion factor is required. This factor was previously established by Mylonas *et al.*<sup>19</sup> For this purpose, 92 patients underwent both a non-contrast CT scan and contrast CTA scan to measure CAC. Using linear regression analysis, a conversion factor of 2.74 for the CAC score on contrast CTA was established. A subsequent validation study in 47 patients, revealed an excellent correlation between Agatston CAC score derived from non-contrast CT and contrast CTA after applying the predefined conversion factor. The same conversion factor was used in the present study to calculate the Agatston CAC score on contrast CTA.

## Different methods for quantification of CAC score on contrast CTA

Several previous studies have focused on the feasibility of assessing and computing the CAC scores from contrast CTA images.<sup>18-22,35</sup> The main challenge in all these studies was to establish an accurate method to differentiate between CAC and coronary artery luminal contrast.

### Manual delineation of CAC.

Manually segmentation of CAC from the contrast filled lumen by delineating the calcified spots was performed by Bijl *et al.* in 100 patients, of which 50 presented without CAC<sup>36</sup>. To derive the Agatston CAC score from contrast CTA images, calcifications were manually delineated and thereafter quantified with a HU threshold of 130 for each voxel within the marked area. The CAC score, derived from the contrast CTA, was well correlated with non-contrast CT CAC score. Similar to the present study, in only a small number of patients with a non-contrast CAC score of zero, CAC was detected on contrast CTA. Even though manual input was needed, the inter-observer agreement was as excellent for the CTA-derived Agatston scores.

### Fixed HU thresholds.

Another method to differentiate between CAC and contrast was sought in increasing the HU threshold for CAC detection hence avoiding the need for manually drawn contours. Glodny *et al.* used a detection threshold of 600 HU to compute the Agatston CAC on CTA images.<sup>20</sup> Although the increased attenuation threshold revealed an excellent correlation for the Agatston CAC score between non-contrast CT and contrast CTA, an overall underestimation of the calcium scoring in CTA images was observed. The authors provide no detail on the CAC-risk categories. In contrast, Hong *et al.* selected 50 patients to derive a Agatston CAC score on contrast CTA images, with a detection threshold of 350 HU.<sup>21</sup> In this study, the CAC score on contrast CTA was significantly overestimated. The under- and overestimation of the Agatston CAC score in the previous studies can be the result of inadequate threshold definitions in some patients. Luminal contrast could have exceeded the HU threshold level, thereby being detected as coronary artery calcium, or vice-versa, CAC being mistakenly characterized as luminal contrast.

### Patient specific HU thresholds.

Previous publications have indicated that HU threshold for coronary plaque quantification are dependent on luminal contrast intensity and CT scan protocol.<sup>33, 37</sup> To account for this, a scan (or patient) specific threshold could be preferable. Mylonas *et al.* determined the HU threshold for CAC scoring based on contrast attenuation.<sup>19</sup> For this purpose, the calcium detection threshold was set at aortic attenuation (HU)

+ 2 standard deviations (SD). In this study, an excellent correlation was observed between CAC score on contrast CTA and non-contrast CT. Moreover, 83% of patients were classified in the same CAC risk category. However, this method needed manual threshold determination and manual CAC selection.

Similarly, Bischoff *et al.* used 150% of the mean attenuation (HU) in the ascending aorta as a threshold.<sup>22</sup> An excellent correlation was observed between CAC score based on contrast CTA compared to non-contrast CT and >90% of patients were classified in the same CAC risk category. However, manual interference forms part of the method; the study used a manual threshold determination and semi-automated system for CAC scoring.

### **Advanced algorithms.**

In the present study, a novel HU adaptive algorithm was used. This trend-line based algorithm facilitates patient specific calcium detection that adapts itself to the contrast attenuation. Similar to the present study, Ebersbergen *et al.* described a tool to fully automatically derive coronary artery calcium scores from contrast CTA studies in a cohort of 127 patients.<sup>35</sup> This study used an automated model-based image processing algorithm, whereas the present study used an algorithm based on HU intensities. Ebersbergen *et al.* demonstrated no significant difference in Agatston CAC scores between non-contrast CT calcium scoring and contrast coronary CTA. Moreover, a significant relation was noted between both methods as well as good agreement within the CAC score risk categories. Similar to our study, the approach of Ebersbergen *et al.* underlined the superiority of advanced algorithms for CAC scoring on CTA. These algorithms are accurate, reproducible and provide a patient specific approach, adaptive to luminal contrast attenuation.

### **Clinical implications**

#### **Risk classifications.**

The prognostic value of CAC score has been extensively studied.<sup>10, 23, 38, 39</sup> For this purpose the CAC score is usually stratified into risk categories.<sup>23, 39</sup> An increase in mortality was observed per increment in CAC score risk category.<sup>10, 38, 39</sup> For clinical purpose, accurate determination of the CAC score risk category is sufficient for risk classification of patients (i.e. the exact CAC score is less important). In this study, a good agreement within the Agatston CAC risk categories was observed. This indicates that quantifying the Agatston CAC score on contrast CTA is sufficiently accurate for clinical decision making. In addition to the clinical value of the CAC score, the prognostic value of CAC progression has been established.<sup>40, 41</sup> However, in the present

study, no serial CAC-score or CTA were available. Therefore, the accuracy of the assessment of CAC progression could not be established.

### **Radiation exposure reduction.**

The risk of cancer per 10.000 CAC scans in female patients of 50 years old is 3/10,000.<sup>42</sup> Even though this number seems relatively small, it is estimated that the incidence of cancer induced by non-contrast CT for CAC score in the United States is around 80-400 per year. In the present patient cohort there is potential for 20% radiation dose reduction, if the non-contrast CT scans are excluded from the protocol. Recently, modifications to contrast CTA scan protocol have resulted in decreased radiation dose, thus reducing CTA radiation exposure.<sup>43</sup> These radiation dose reduction advances could not contribute to less radiation exposure by the non-contrast CT scan because the Agatston CAC score requires a fixed scan protocol. Therefore, with the current low-dose scan protocols the radiation dose of the non-contrast CT is relatively high and the gain of omitting the non-contrast CT from the scan protocol even greater.

### **Limitations**

Some limitations of the present study need to be considered. For this analysis, patients with poor quality images were excluded for the detection and quantification of Agatston CAC score on contrast CTA. It is unclear how the software tool would perform in datasets with high noise levels or severe motion artifacts. In this study the algorithm performed suboptimal in the RCA. This coronary artery is most affected by motion during the cardiac cycle and therefore more prone for motion artefacts.<sup>44</sup> Moreover, the relative lower correlation for LM calcifications could be due to low number of patients (n=38) with a positive CAC score in the LM. The observer variability for the assessment of the CAC-score on non-contrast CT was not assessed in this study. However, this method is widely used and accepted as a robust measurement. The observer variability for the contrast CTA CAC-score could not be assessed since this was a fully automatic method. All cardiac CTA datasets were performed with either a 64-slice CT scanner or a 320-row volumetric scanner from one vendor. Therefore, the applicability of this algorithm to datasets acquired on other vendor machines needs to be further studied. Differences in the detection of the Agatston CAC score between non-contrast CT and contrast CTA could have been caused by the difference in image slice thickness.<sup>45</sup> CAC in non-contrast CT is visually detected in the axial plane in 3.0 mm reconstructed images, whereas CAC in the contrast CTA scan was detected on MPRs based on images with a 0.5 mm slice thickness. Due to this difference, calcified spots located in-between slices of the non-contrast CT are detected on the contrast CTA, resulting in an overestimation of CAC score on contrast CTA. In clinical prac-

tice, observers could perform an additionally manual verification of the contrast CTA Agatston CAC scores, thereby reducing the number of false positive/negative results. For the present study a predefined conversion factor was applied based on a previous study.<sup>19</sup> It is expected that a conversion factor specific for the present algorithm would have provided even higher correlations and better agreement.

## **Conclusion**

A fully automatic detection and quantification of Agatston CAC score on contrast CTA is feasible and shows an excellent correlation with the Agatston CAC score derived from non-contrast CT. Furthermore, a good agreement was obtained between the non-contrast CT and the contrast CTA within the Agatston CAC score risk categories. Importantly, the accuracy to rule-out CAC on contrast CTA compared to non-contrast CT was excellent. By virtue of the excellent correlation between both methods, this fully automatic system could be applied in future clinical practice, thereby saving time on manual interpretation and potentially reduce radiation exposure, by obviating the need for a separate non-contrast CT scan.

## References

- (1) Roger VL, Go AS, Lloyd-Jones DM *et al.* Executive summary: heart disease and stroke statistics—2012 update: a report from the American Heart Association. *Circulation* 2012 January 3;125(1):188-97.
- (2) Genders TS, Pugliese F, Mollet NR *et al.* Incremental value of the CT coronary calcium score for the prediction of coronary artery disease. *Eur Radiol* 2010 October;20(10):2331-40.
- (3) Greenland P, Bonow RO, Brundage BH *et al.* ACCF/AHA 2007 clinical expert consensus document on coronary artery calcium scoring by computed tomography in global cardiovascular risk assessment and in evaluation of patients with chest pain: a report of the American College of Cardiology Foundation Clinical Expert Consensus Task Force (ACCF/AHA Writing Committee to Update the 2000 Expert Consensus Document on Electron Beam Computed Tomography) developed in collaboration with the Society of Atherosclerosis Imaging and Prevention and the Society of Cardiovascular Computed Tomography. *J Am Coll Cardiol* 2007 January 23;49(3):378-402.
- (4) Agatston AS, Janowitz WR, Hildner FJ, Zusmer NR, Viamonte M, Jr., Detrano R. Quantification of coronary artery calcium using ultrafast computed tomography. *J Am Coll Cardiol* 1990 March 15;15(4):827-32.
- (5) Folsom AR, Kronmal RA, Detrano RC *et al.* Coronary artery calcification compared with carotid intima-media thickness in the prediction of cardiovascular disease incidence: the Multi-Ethnic Study of Atherosclerosis (MESA). *Arch Intern Med* 2008 June 23;168(12):1333-9.
- (6) Budoff MJ, Gul KM. Expert review on coronary calcium. *Vasc Health Risk Manag* 2008;4(2):315-24.
- (7) Detrano R, Guerci AD, Carr JJ *et al.* Coronary calcium as a predictor of coronary events in four racial or ethnic groups. *N Engl J Med* 2008 March 27;358(13):1336-45.
- (8) Polonsky TS, McClelland RL, Jorgensen NW *et al.* Coronary artery calcium score and risk classification for coronary heart disease prediction. *JAMA* 2010 April 28;303(16):1610-6.
- (9) Budoff MJ, Shaw LJ, Liu ST *et al.* Long-term prognosis associated with coronary calcification: observations from a registry of 25,253 patients. *J Am Coll Cardiol* 2007 May 8;49(18):1860-70.
- (10) Greenland P, LaBree L, Azen SP, Doherty TM, Detrano RC. Coronary artery calcium score combined with Framingham score for risk prediction in asymptomatic individuals. *JAMA* 2004 January 14;291(2):210-5.
- (11) Meijboom WB, Meijjs MF, Schuijf JD *et al.* Diagnostic accuracy of 64-slice computed tomography coronary angiography: a prospective, multicenter, multivendor study. *J Am Coll Cardiol* 2008 December 16;52(25):2135-44.
- (12) Hamon M, Biondi-Zoccai GG, Malagutti P *et al.* Diagnostic performance of multislice spiral computed tomography of coronary arteries as compared with conventional invasive coronary angiography: a meta-analysis. *J Am Coll Cardiol* 2006 November 7;48(9):1896-910.
- (13) Meijer AB, YL O, Geleijns J, Kroft LJ. Meta-analysis of 40- and 64-MDCT angiography for assessing coronary artery stenosis. *AJR Am J Roentgenol* 2008 December;191(6):1667-75.
- (14) Mowatt G, Cook JA, Hillis GS *et al.* 64-Slice computed tomography angiography in the diagnosis and assessment of coronary artery disease: systematic review and meta-analysis. *Heart* 2008 November;94(11):1386-93.
- (15) Budoff MJ, Dowe D, Jollis JG *et al.* Diagnostic performance of 64-multidetector row coronary computed tomographic angiography for evaluation of coronary artery stenosis in individuals without known coronary artery disease: results from the prospective multicenter ACCURACY

- (Assessment by Coronary Computed Tomographic Angiography of Individuals Undergoing Invasive Coronary Angiography) trial. *J Am Coll Cardiol* 2008 November 18;52(21):1724-32.
- (16) Miller JM, Rochitte CE, Dewey M *et al.* Diagnostic performance of coronary angiography by 64-row CT. *N Engl J Med* 2008 November 27;359(22):2324-36.
  - (17) Einstein AJ. Effects of radiation exposure from cardiac imaging: how good are the data? *J Am Coll Cardiol* 2012 February 7;59(6):553-65.
  - (18) van der Bijl N, Joemai RM, Geleijns J *et al.* Assessment of Agatston coronary artery calcium score using contrast-enhanced CT coronary angiography. *AJR Am J Roentgenol* 2010 December;195(6):1299-305.
  - (19) Mylonas I, Alam M, Amily N *et al.* Quantifying coronary artery calcification from a contrast-enhanced cardiac computed tomography angiography study. *Eur Heart J Cardiovasc Imaging* 2013 August 13.
  - (20) Glodny B, Helmel B, Trieb T *et al.* A method for calcium quantification by means of CT coronary angiography using 64-multidetector CT: very high correlation with Agatston and volume scores. *Eur Radiol* 2009 July;19(7):1661-8.
  - (21) Hong C, Becker CR, Schoepf UJ, Ohnesorge B, Bruening R, Reiser MF. Coronary artery calcium: absolute quantification in nonenhanced and contrast-enhanced multi-detector row CT studies. *Radiology* 2002 May;223(2):474-80.
  - (22) Bischoff B, Kantert C, Meyer T *et al.* Cardiovascular risk assessment based on the quantification of coronary calcium in contrast-enhanced coronary computed tomography angiography. *Eur Heart J Cardiovasc Imaging* 2012 June;13(6):468-75.
  - (23) van Werkhoven JM, Schuijf JD, Gaemperli O *et al.* Incremental prognostic value of multi-slice computed tomography coronary angiography over coronary artery calcium scoring in patients with suspected coronary artery disease. *Eur Heart J* 2009 November;30(21):2622-9.
  - (24) de Graaf FR, Schuijf JD, van Velzen JE *et al.* Diagnostic accuracy of 320-row multidetector computed tomography coronary angiography in the non-invasive evaluation of significant coronary artery disease. *Eur Heart J* 2010 August;31(15):1908-15.
  - (25) Rutten A, Krul SP, Meijs MF, de Vos AM, Cramer MJ, Prokop M. Variability of coronary calcium scores throughout the cardiac cycle: implications for the appropriate use of electrocardiogram-dose modulation with retrospectively gated computed tomography. *Invest Radiol* 2008 March;43(3):187-94.
  - (26) Valentin J. Managing patient dose in multi-detector computed tomography(MDCT). ICRP Publication 102. *Ann ICRP* 2007;37(1):1-79, iii.
  - (27) Yang G, Kitslaar P, Frenay M *et al.* Automatic centerline extraction of coronary arteries in coronary computed tomographic angiography. *Int J Cardiovasc Imaging* 2012 April;28(4):921-33.
  - (28) Guanyu Yang, Alexander Broersen, Robert Petr *et al.* Automatic coronary artery tree labeling in coronary computed tomographic angiography datasets. *Computing in Cardiology* , 109-102. 18-9-2012.
  - (29) Austen WG, Edwards JE, Frye RL *et al.* A reporting system on patients evaluated for coronary artery disease. Report of the Ad Hoc Committee for Grading of Coronary Artery Disease, Council on Cardiovascular Surgery, American Heart Association. *Circulation* 1975 April;51(4 Suppl):5-40.
  - (30) Rosner B. *Fundamentals of biostatistics.* Belmont CA: Duxbury Press; 2005.
  - (31) Bland JM, Altman DG. Statistical methods for assessing agreement between two methods of clinical measurement. *Lancet* 1986 February 8;1(8476):307-10.
  - (32) Fleiss JL, Levin B, Paik MC. *Statistical methods for rates and proportions* . New York: 1981.

- (33) Dalager MG, Bottcher M, Andersen G *et al.* Impact of luminal density on plaque classification by CT coronary angiography. *Int J Cardiovasc Imaging* 2011 April;27(4):593-600.
- (34) Muhlenbruch G, Wildberger JE, Koos R *et al.* Coronary calcium scoring using 16-row multislice computed tomography: nonenhanced versus contrast-enhanced studies in vitro and in vivo. *Invest Radiol* 2005 March;40(3):148-54.
- (35) Ebersberger U, Eilert D, Goldenberg R *et al.* Fully automated derivation of coronary artery calcium scores and cardiovascular risk assessment from contrast medium-enhanced coronary CT angiography studies. *Eur Radiol* 2013 March;23(3):650-7.
- (36) van der Bijl N, Joemai RM, Geleijns J *et al.* Assessment of Agatston coronary artery calcium score using contrast-enhanced CT coronary angiography. *AJR Am J Roentgenol* 2010 December;195(6):1299-305.
- (37) Akram K, Rinehart S, Voros S. Coronary arterial atherosclerotic plaque imaging by contrast-enhanced computed tomography: fantasy or reality? *J Nucl Cardiol* 2008 November;15(6):818-29.
- (38) Shareghi S, Ahmadi N, Young E, Gopal A, Liu ST, Budoff MJ. Prognostic significance of zero coronary calcium scores on cardiac computed tomography. *J Cardiovasc Comput Tomogr* 2007 December;1(3):155-9.
- (39) Shaw LJ, Raggi P, Schisterman E, Berman DS, Callister TQ. Prognostic value of cardiac risk factors and coronary artery calcium screening for all-cause mortality. *Radiology* 2003 September;228(3):826-33.
- (40) Budoff MJ, Young R, Lopez VA *et al.* Progression of coronary calcium and incident coronary heart disease events: MESA (Multi-Ethnic Study of Atherosclerosis). *J Am Coll Cardiol* 2013 March 26;61(12):1231-9.
- (41) Budoff MJ, Hokanson JE, Nasir K *et al.* Progression of coronary artery calcium predicts all-cause mortality. *JACC Cardiovasc Imaging* 2010 December;3(12):1229-36.
- (42) Berrington de GA, Mahesh M, Kim KP *et al.* Projected cancer risks from computed tomographic scans performed in the United States in 2007. *Arch Intern Med* 2009 December 14;169(22):2071-7.
- (43) Achenbach S, Marwan M, Ropers D *et al.* Coronary computed tomography angiography with a consistent dose below 1 mSv using prospectively electrocardiogram-triggered high-pitch spiral acquisition. *Eur Heart J* 2010 February;31(3):340-6.
- (44) Achenbach S, Ropers D, Holle J, Muschiol G, Daniel WG, Moshage W. In-plane coronary arterial motion velocity: measurement with electron-beam CT. *Radiology* 2000 August;216(2):457-63.
- (45) Mao S, Child J, Carson S, Liu SC, Oudiz RJ, Budoff MJ. Sensitivity to detect small coronary artery calcium lesions with varying slice thickness using electron beam tomography. *Invest Radiol* 2003 March;38(3):183-7.



# Chapter 7

## Automated quantitative coronary computed tomography correlates of myocardial ischaemia on gated myocardial perfusion SPECT

de Graaf MA, El-Naggar HM, Boogers MJ, Veltman CE, Broersen A, Kitslaar PH, Dijkstra J, Kroft LJ, Al Y, I, Reiber JH, Bax JJ, Delgado V, Scholte AJ.

*European Journal of Nuclear Medicine and Molecular Imaging* 2013;40:1171-1180

## Abstract

**Purpose:** Automated software tools have permitted more comprehensive, robust and reproducible quantification of coronary stenosis, plaque burden and plaque location of coronary computed tomography angiography (CTA) data. The independent association between these quantitative CTA parameters and the presence of myocardial ischemia has not been explored. The aim of the present investigation was to evaluate the association between quantitatively assessed parameters of coronary artery lesions (QCT) on CTA and the presence of myocardial ischemia on gated myocardial perfusion single-photon emission computed tomography (SPECT).

**Methods:** Forty patients (mean age  $58.2 \pm 10.9$  years, 27 men) with known or suspected CAD who had undergone multi-detector row CTA and gated myocardial perfusion SPECT within 6 months were included. From CTA datasets, vessel and lesion-based visual analysis was performed. Consecutively, lesion-based QCT was performed to assess plaque length, plaque burden, percentage lumen area stenosis and remodeling index. Subsequently, the presence of myocardial ischemia was assessed using the summed difference score ( $\text{SDS} \geq 2$ ) on gated myocardial perfusion SPECT.

**Results:** Twenty-five (62.5%) patients showed myocardial ischemia in 37 vascular territories. Quantitative significant stenosis and quantitative assessment of lesion length were independently associated with myocardial ischemia (OR 7.72 [2.41 – 24.7],  $P < 0.001$  and OR 1.07 [1.00 – 1.45],  $P = 0.032$ , respectively) after correcting for clinical variables and visually assessed significant stenosis. The addition of quantitative significant stenosis ( $\chi^2 = 20.7$ ) and quantitative assessment of lesion length ( $\chi^2 = 26.0$ ) to the clinical variables and the visual assessment ( $\chi^2 = 5.9$ ) had incremental value in the association with myocardial ischemia.

**Conclusion:** Coronary lesion length and quantitative assessed significant stenosis were independently associated with myocardial ischemia. Both quantitative parameters have incremental value over baseline variables and visual significant stenosis. Potentially, QCT can refine assessment of CAD, which may be of potential use for identification of patients with myocardial ischemia.

## Introduction

Computed tomography angiography (CTA) allows evaluation of coronary artery stenosis with high image quality and diagnostic accuracy when compared to invasive coronary angiography.<sup>1-4</sup> As CTA provides detailed information on coronary anatomy and stenosis, it has been proposed as a suitable rule-out test for the evaluation of low to intermediate risk patients with suspected coronary artery disease (CAD)<sup>5</sup>. Although the degree of coronary luminal narrowing is of importance in patients with CAD, previous studies have shown that coronary stenosis is not an accurate predictor of myocardial ischemia.<sup>6</sup> It has been previously reported that in 50% of patients with a significant stenosis, which was defined as  $\geq 50\%$  luminal narrowing on CTA, myocardial ischemia was not detected on myocardial perfusion single photon emission computed tomography (SPECT).<sup>6</sup> Beyond coronary stenosis, additional coronary plaque parameters such as lesion extent, plaque composition as well as plaque location have shown to be significantly associated with myocardial ischemia.<sup>7, 8</sup> However, these parameters are not systematically assessed in clinical practice and the assessment of CAD is mostly based on quantification of coronary artery calcium score and visual estimation of the luminal narrowing. Recent advances in post-processing MDCT data software have permitted automated quantification of coronary stenosis severity and plaque characteristics.<sup>9</sup> This automated software provides good diagnostic accuracy and reproducibility to assess significant coronary artery stenosis. Currently, the relation between quantitative CTA (QCT) derived parameters and the presence of myocardial ischemia on SPECT data is unknown. Accordingly, the present study aimed to assess the association between QCT parameters and presence of myocardial ischemia as assessed with myocardial perfusion SPECT.

## Methods

### Patient population

Forty patients from an ongoing clinical registry who were referred for multi-detector row CTA and stress-rest gated myocardial perfusion SPECT (performed within 6 months) were included. Only patients with sufficient image quality of both modalities were selected. Cardiovascular risk factors and cardiac medication were derived from medical record data. Known CAD was defined as a history of myocardial infarction, or evidence of CAD on previously performed diagnostic tests. Patients who had undergone prior percutaneous coronary intervention or coronary artery bypass graft surgery were excluded. Patients with atrial fibrillation, renal insufficiency (glomerular filtration rate  $< 30$  mL/min), known allergy to iodine-containing contrast agents or

pregnancy were also excluded. Also, patients with cardiac events or coronary revascularization during the time elapsed between cardiac CTA and myocardial perfusion SPECT were excluded from further analysis.

The number of coronary plaques per vascular territory along with their location and characteristics were assessed visually from CTA. Subsequently, a novel automated post-processing imaging algorithm was applied which permits quantitative assessment of CTA datasets. The most severe coronary lesion was identified in each coronary artery and QCT was performed to assess coronary stenosis parameters as described in Table 1.

Stress-rest myocardial perfusion SPECT with  $^{99m}\text{Tc}$  tetrofosmin was performed to assess the extent and location of myocardial ischemia. Myocardial ischemia was defined as a summed difference score (SDS) of  $\geq 2$ .<sup>10</sup> Clinical data were prospectively entered into the departmental Cardiology Information System (EPD-Vision®, Leiden University Medical Center, the Netherlands) and retrospectively analyzed. The Institutional Review Board of the Leiden University Medical Center approved this retrospective evaluation of clinically collected data, and waived the need for written informed consent.

**Table 1: QCT derived parameters and their corresponding definitions.**

<b>QCT parameter</b>	<b>Definition</b>
Lesion length (mm)	The distance between the proximal and distal ends of the coronary lesion
Mean plaque burden	The sum of ((vessel wall area – lumen area) / vessel wall area) per slice / number of slices
Minimal and maximal plaque thickness (mm)	The minimal and maximal distance between the vessel wall and the lumen
Minimal Lumen Area (MLA) (mm <sup>2</sup> )	The minimal lumen area at the point of maximal obstruction
Percentage lumen area stenosis at the level of the MLA (%)	$1 - (\text{MLA} / \text{corresponding reference lumen area})$
Minimal lumen diameter (mm)	The minimal lumen diameter (mm) at the point of maximal obstruction determined by the MLA
Diameter stenosis (%)	The percentage diameter stenosis at the point of maximal obstruction determined by the MLA
Plaque burden at the MLA	$((\text{vessel wall area} - \text{lumen area}) / \text{vessel wall area}) \times 100\%$ at the level of the MLA
Eccentricity index at the level of the MLA	$(\text{maximum plaque thickness} - \text{minimum plaque thickness}) / \text{maximum plaque thickness}$
Remodeling index at the level of the MLA	Vessel wall area / corresponding reference vessel wall area at the level of the MLA), in which positive remodeling was defined as a remodeling index $> 1.0$ <sup>32</sup>

### **Cardiac CTA examination**

Cardiac CTA imaging was performed using either a 64-detector row helical scanner (n=24) (Aquilion 64, Toshiba Medical Systems, Otawara, Japan) or a 320-detector row volumetric scanner (n=16) (Aquilion ONE, Toshiba Medical Systems, Otawara, Japan).

Patients with a heart rate above 65 beats/min received 50 or 100 mg metoprolol orally one hour before imaging, unless contraindicated. A non-contrast enhanced and contrast-enhanced scan was performed. Reconstructed images were transferred to a remote dedicated workstation with post-processing software (Vitrea FX 1.0, Vital Images, Minnetonka, MN, USA). The non-enhanced scans were used to assess the total amount of coronary artery calcium score according to the Agatston approach<sup>11</sup>. CTA datasets were evaluated according during routine clinical practice independent of the quantitative CTA analysis. Image quality of the CTA scans was classified as: (1) good image quality (scans without motion artifacts), (2) moderate image quality (scans with motion artifacts or increased image noise) and (3) poor image quality (non-diagnostic scans); the last were excluded from the analysis. The number and location of atherosclerotic plaques per vascular territory and plaque morphology were visually evaluated from CTA data sets. Significant coronary obstruction was defined as  $\geq 50\%$  luminal narrowing. Atherosclerotic plaques were morphologically classified as non-calcified (lesions with lower density compared to contrast-enhanced lumen), calcified (lesions with high density) or mixed (lesions having elements of both non-calcified and calcified lesions).

### **Quantitative computed tomography coronary angiography**

Dedicated software (QAngioCT Research Edition, Medis Medical Imaging Systems, Leiden, the Netherlands) was used for automated quantification of all coronary lesions.<sup>9</sup> The software automatically displays the centerline along the vessel and detects the contours of the lumen and vessel wall while allowing the observer to manually correct them if needed. First, a fast vessel-tracking algorithm was used to obtain the 3-dimensional centerline (ranging from the proximal to distal marker) of the coronary artery. Based on this centerline, a straightened multi-planar reformatted (MPR) volume of the segment of interest was created. Consecutively, the lumen border contours and vessel wall borders were detected according to methods described previously.<sup>9</sup> The approach uses spatial first- and second-derivative gradient filters in combination with knowledge of the expected CT intensity values in the arteries; therefore, this method is insensitive to differences in attenuation values between data sets. Automated quantitative processing steps were independent from viewing settings. Next, automated quantification of each coronary lesion was performed. For each coronary lesion, reference lines for both lumen and vessel wall were generated using proximal

and distal non-diseased, non-bifurcated reference regions. The mean lumen or vessel wall area of these regions was used to define the reference slope for lumen and vessel wall contours, respectively. The reference lines for lumen and vessel wall represent an estimate of the normal proximal-to-distal tapering of the coronary artery. The minimal lumen area (MLA), the proximal start of the coronary lesion and the distal end of coronary lesion were automatically defined using the detected lumen contours and the difference with the normal tapering of the artery. A number of QCT parameters, listed in Table 1, were derived for each coronary lesion. In addition to coronary vessels with atherosclerotic lesions, automated quantification of non-diseased coronary vessels was performed in the mid part of the coronary vessel, which was used as the best estimate of coronary luminal narrowing per non-diseased coronary artery. Lesions in diagonal branches were allocated to LAD, lesion in intermediate (IM) branch or marginal (OM) branch were allocated to CX. The reproducibility of QCT has been reported previously,<sup>9</sup> showing good reproducibility of QCT for assessment of minimal lumen area and lumen area stenosis.

### **Stress-rest gated SPECT**

Gated myocardial perfusion SPECT with <sup>99m</sup>technetium tetrofosmin (500 MBq, MYOVIEW, General Electric Healthcare, United Kingdom) was performed according to a 2-day stress-rest protocol. In patients who were able to exercise, a symptom-limited bicycle test was performed. In patients unable to exercise, a pharmacologic stress test was performed with either adenosine or dobutamine infusion. Injection of the radiopharmaceutical was done at peak exercise; in the third minute of pharmacological stress induction for adenosine or at the maximum calculated target heart rate for dobutamine. Data-acquisition was performed with a triple-head SPECT camera system (GCA 9300/HG; Toshiba Corporation, Tokyo, Japan), equipped with low-energy high-resolution collimators, 45 minutes after injection of the radiopharmaceutical. A 20% window was used around the 140-keV energy peak of technetium-99m, after which the SPECT data were stored in a 64x64 matrix.

Post-processing of stress- and rest-SPECT datasets was performed using previously validated automated software.<sup>12</sup> Data-reconstruction was performed in vertical and horizontal long- and short-axis views perpendicular to the heart axis. The myocardial segments were assigned to the different perfusion territories using a 20-segment model.<sup>13</sup> Each segment was visually scored by an experienced observer (AJS) according to the standard scoring scale of 0 to 4 (normal, mild, moderate, severe reduction or absence of tracer uptake).<sup>13, 14</sup> To calculate the summed stress score (SSS) and the summed rest score (SRS), the total segmental perfusion scores during stress and rest were added, respectively. The summed difference score (SDS) was calculated as the

difference between the summed stress score and the summed rest score. Myocardial ischemia was defined as an SDS  $\geq 2$ .<sup>10</sup>

On a vessel basis, the presence of myocardial ischemia was assessed and allocated to the corresponding vascular territory as previously described.<sup>15</sup> Accordingly, myocardial ischemia of the anterior and septal wall was allocated to lesions in the left anterior descending coronary artery (LAD), whereas ischemia in the lateral wall was allocated to lesions in the left circumflex coronary artery (LCX). Furthermore, myocardial ischemia in the (postero) inferior wall was assigned to lesions in the right coronary artery (RCA).

### Statistical analysis

For reasons of uniformity, summary statistics for all continuous variables were presented as mean  $\pm$  standard deviation (SD), whereas categorical variables were presented as frequencies and percentages. Vessel-based analysis was performed based on the most severe lesion per vessel according to the quantitatively assessed percentage lumen area stenosis. Independent-samples T tests were used to compare QCT parameters between patients with and without myocardial ischemia on SPECT. The agreement between both visual and quantitative assessment of significant coronary stenosis and SPECT was evaluated using the weighted kappa ( $k$ ) statistics. Excellent, fair-to-good and poor agreement were defined by a  $k$ -value of  $> 0.75$ , between 0.4 and 0.75, and  $< 0.4$ , respectively.<sup>16</sup> To evaluate the association between baseline characteristics, visual CTA parameters, QCT parameters and the presence of myocardial ischemia, multivariate regression analyses were performed. Myocardial ischemia was introduced as dependent variable. Relevant baseline clinical variables were entered into the first model. Variable selection was performed using a backward conditional method (entry, 0.05; removal, 0.10). Three nested models were subsequently created by introducing separately the following variables: visual significant stenosis (model 2), quantitative significant stenosis (model 3) and quantitative assessed lesion length (model 4). For each variable in the model, an odds ratio (OR) with 95% confidence interval (CI) was calculated. The incremental value of the QCT parameters over clinical risk variables and visual assessed stenosis degree was assessed by comparing the global  $\chi^2$  values. The likelihood-ratio chi-square test was used to assess the significance of the incremental  $\chi^2$  values. All statistical tests were two-sided and a P-value  $< 0.05$  was considered to be statistically significant. All statistical analyses were performed with SPSS software (Version 20.0, SPSS Inc., Chicago, Illinois).

## Results

### Patient population

A total of 40 patients ( $58.2 \pm 10.9$  years, 27 men) with known ( $n=16$ ) or suspected ( $n=24$ ) CAD were included. Of these patients, 16 (40%) presented with atypical chest pain, 12 (30%) with typical chest pain, the remaining 12 (30%) patients had diabetes and were evaluated because of an increased cardiac risk profile. The mean duration between cardiac CTA and gated myocardial perfusion SPECT examinations was  $39.9 \pm 42.2$  days (median 33 days, interquartile range 10-52 days). Patients remained clinically stable and no acute coronary events were recorded between evaluations. The clinical characteristics of the patients are listed in Table 2.

### Computed tomography coronary angiography

#### Visual CTA.

The mean coronary artery calcium score was  $451 \pm 1490$ . In the overall patient population ( $n=40$ ), 83 coronary arteries showed atherosclerosis and a total of 162

**Table 2. Patient characteristics.**

Baseline characteristics	n = 40
Age (years)	$58.2 \pm 10.9$
Male	27 (67.5%)
Known CAD	16 (40.0%)
Cardiovascular risk factors	
Hypertension†	20 (50.0%)
Hypercholesterolemia‡	15 (37.5%)
Diabetes mellitus	21 (52.5%)
Family history of CAD*	17 (42.5%)
Smoking	15 (37.5%)
Body Mass index $\geq 30$ kg/m <sup>2</sup> .	6 (15.0%)
Calcium score	$450 \pm 1490$ 28 (0-8730)
Left ventricular ejection fraction	$61 \pm 13$

Data are represented as mean  $\pm$  SD, median(range) or as number and percentages of patients.

†Defined as systolic blood pressure  $\geq 140$  mm Hg or diastolic blood pressure  $\geq 90$  mm Hg or the use of antihypertensive medication.

‡Serum total cholesterol  $\geq 230$  mg/dL or serum triglycerides  $\geq 200$  mg/dL or treatment with lipid lowering drugs.

\*Defined as the presence of coronary artery disease in first-degree family members at  $<55$  years in men and  $<65$  years in women.

Abbreviations: CAD, coronary artery disease

coronary lesions were identified. Visual CTA analysis showed 57 (35%) non-calcified lesions, 71 (44%) mixed lesions and 34 (21%) calcified lesions. In total, 25 coronary arteries contained a visually assessed significant stenosis of  $\geq 50\%$  luminal narrowing.

### Quantitative CTA.

QCT was performed in all 162 lesions to assess quantitative stenosis parameters as described in Table 1. Subsequently, in the 83 coronary arteries with atherosclerosis, the most severe lesion per main vascular territory (using the quantitatively assessed percentage lumen area stenosis) was determined. In Table 3 the results of the quantitative analyses of all coronary lesions and the most severe lesion per artery is demonstrated. In addition, in the remaining 37 non-diseased coronary arteries, QCT analysis was performed in the mid part of the vessel, which was used as a representative of the coronary artery. In total, 45 coronary arteries contained a quantitative assessed significant stenosis of  $\geq 50\%$  luminal narrowing (defined according the percentage area stenosis).

### Stress-rest gated myocardial perfusion SPECT

Gated myocardial perfusion SPECT showed a mean SRS of  $2.8 \pm 3.9$ , a mean summed stress score of  $5.7 \pm 6.3$ , and a mean SDS of  $3.8 \pm 4.9$ . Myocardial ischemia (SDS of  $\geq 2$ ) was observed in 25 (62.5%) patients. Using a 20-segment model, myocardial ischemia was present in 31% ( $n=37$ ) of the 120 vascular territories. The remaining 69% ( $n=83$ ) vascular territories showed no ischemia. A comparison was made between vascular territories with ischemia versus vascular territories without ischemia. In vascular territories showing myocardial ischemia, lesion length, percentage lumen area stenosis, percentage lumen diameter stenosis, mean plaque burden and maxi-

**Table 3. Quantitative analysis of coronary lesions.**

QCT parameter	All coronary lesions (n = 162)	Most severe lesion per artery (n=83)
Lesion length (mm)	12.10 $\pm$ 8.99	12.48 $\pm$ 9.14
Mean plaque burden (%)	76.12 $\pm$ 7.78	76.90 $\pm$ 7.92
Maximal plaque thickness (mm)	2.33 $\pm$ 0.71	2.39 $\pm$ 0.77
MLA (mm <sup>2</sup> )	2.97 $\pm$ 2.19	2.70 $\pm$ 1.81
Percentage lumen area stenosis (%)	47.80 $\pm$ 18.65	52.76 $\pm$ 19.67
Minimal lumen diameter (mm)	1.84 $\pm$ 0.64	1.76 $\pm$ 0.60
Percentage diameter stenosis (%)	29.10 $\pm$ 13.79	32.90 $\pm$ 14.96
Plaque burden at the MLA (%)	82.30 $\pm$ 8.39	83.29 $\pm$ 8.59
Eccentricity index at the level of the MLA	0.60 $\pm$ 0.15	0.60 $\pm$ 0.16
Remodeling index at the level of the MLA	1.05 $\pm$ 0.21	1.07 $\pm$ 0.23

Abbreviations: MLA, minimal lumen area

mal plaque thickness were significantly higher when compared to vascular territories without myocardial ischemia (Table 4).

### Agreement between visual significant stenosis and quantitative assessed stenosis versus myocardial ischemia

On a vessel-based analysis, the number of significant culprit coronary lesions ( $\geq 50\%$  luminal narrowing) was significantly higher using QCT as compared to visual CT analysis (45 (37.5%) vs. 25 (20.8%),  $P < 0.001$ ). Importantly, myocardial ischemia was present in 22 (48.9%) of those significant lesions assessed with QCT ( $k = 0.30$ ,  $P = 0.001$ ), whereas ischemia was only present in 9 (36.0%) of the significant lesions visually assessed ( $k = 0.06$ ,  $P = 0.53$ ). Figure 2 represents an example of a female patient with an obstructive lesion in the LAD coronary artery and myocardial ischemia on gated myocardial perfusion SPECT.

### Independent association between quantitative coronary CTA parameters and myocardial ischemia on gated myocardial SPECT

To evaluate the independent association between visual CTA, quantitative parameters and myocardial ischemia, 4 nested multivariate models were created. In model 1,

**Table 4. Vessel based comparison of visual and quantitative CTA parameters between coronary arteries of vascular territories with and without myocardial ischemia.**

	Ischemia (37 vascular territories)	No ischemia (83 vascular territories)	<i>P-value</i>
<b>Visual CTA (per vessel (n=120))</b>			
No. of lesions <sup>o</sup>	1.76 ± 1.57	1.17 ± 1.19	0.026
No. of bifurcation lesions <sup>o</sup>	0.46 ± 0.61	0.22 ± 0.44	0.015
No. of non-calcified lesions <sup>o</sup>	0.59 ± 0.72	0.42 ± 0.65	0.195
No. of mixed lesions <sup>o</sup>	0.84 ± 1.32	0.45 ± 0.78	0.045
No. of calcified lesions <sup>o</sup>	0.32 ± 0.71	0.30 ± 0.66	0.863
<b>QCT parameters (per vessel (n=120))</b>			
Lesion length (mm) <sup>‡</sup>	13.41 ± 12.09	6.68 ± 7.32	<0.001
Mean plaque burden (%) <sup>‡</sup>	75.27 ± 11.59	70.98 ± 9.85	0.039
Max. plaque thickness (mm) <sup>‡</sup>	2.31 ± 1.08	1.75 ± 0.83	0.003
Lumen area stenosis (%) <sup>‡</sup>	48.40 ± 27.81	35.04 ± 25.35	0.011
Lumen diameter stenosis (%) <sup>‡</sup>	30.94 ± 20.00	21.17 ± 16.87	0.007
Eccentricity index <sup>‡</sup>	0.54 ± 0.14	0.54 ± 0.18	0.846
Remodeling index <sup>‡</sup>	1.10 ± 0.22	1.03 ± 0.20	0.406

Data are represented as mean ± SD. <sup>o</sup>Total number of lesions, bifurcation lesions, non-calcified, mixed and calcified lesions per vascular territory. <sup>‡</sup>Results of the selected most severe lesion per vascular territory.

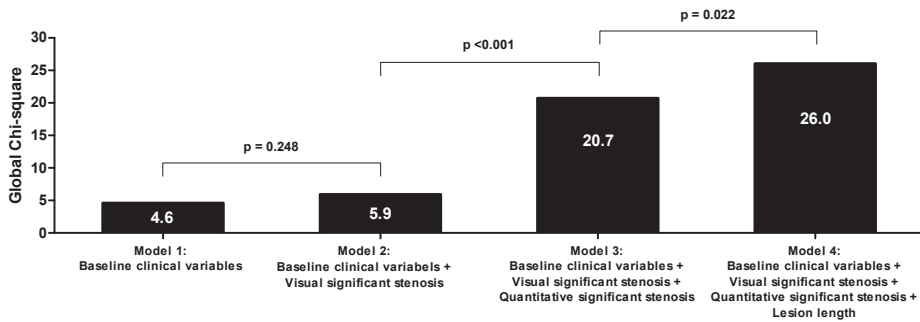


**Figure 1. Bar graph of the multivariable models.**

The bar graph shows the incremental value of quantitative CT parameters over visual CT in the association with myocardial ischemia on gated myocardial perfusion SPECT on a vessel-basis (n=120). The presence of quantitative significant stenosis ( $\geq 50\%$  percentage area stenosis) showed a significant incremental value over conventional clinical risk variables and visual assessed significant stenosis ( $\geq 50\%$  stenosis). Furthermore, lesion length provided a significant incremental value over both clinical risk variables and the presence of a quantitative significant stenosis ( $\geq 50\%$  percentage area stenosis).

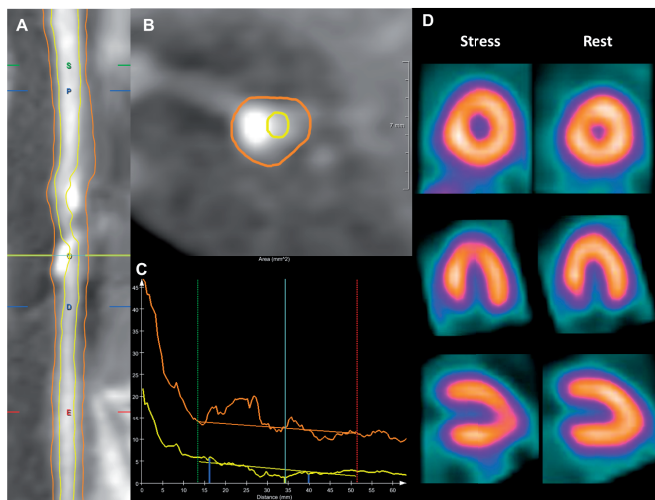


**Figure 2. An example of a 53 year-old female patient with an obstructive lesion in the left anterior descending (LAD) coronary artery.**

The quantitative computed tomography (QCT) processing steps of the culprit lesion are illustrated below. At first, automated QCT was used to detect both lumen (yellow) and vessel wall (orange) contours. Longitudinal lumen and vessel wall contours are shown in panel A, whereas transversal lumen and vessel wall contours at the level of the minimal lumen area (MLA) are shown in panel B. Quantification of the culprit lesion was performed using proximal (green) and distal (red) reference markers as well as lumen (yellow) and vessel wall (orange) reference lines, as illustrated in panel C. Stress-rest gated myocardial perfusion SPECT is shown in panel D. The patient had corresponding myocardial ischemia in the LAD vascular territory on gated myocardial perfusion SPECT. For this patient, summed rest score was 0 and summed stress score was 2, resulting in a summed difference score of 2. QCT showed a lesion length of 23.7 mm, percentage lumen area stenosis of 69.6% and a mean plaque burden of 81.5%.

clinical baseline variables were entered using backward selection. Subsequently, the presence of significant coronary stenosis as assessed with visual CTA was introduced in model 2 and the presence of significant coronary stenosis and lesion length assessed with QCT were included in models 3 and 4, respectively. The results of the 4 nested multivariate models are described in Table 5. Visual CTA assessment of luminal narrowing was not independently associated with the presence of ischemia (OR=1.84, P=0.246). In contrast, the presence of a quantitative assessed significant stenosis and lesion length were independently associated with the presence of myocardial ischemia on gated myocardial SPECT when added to relevant clinical variables (OR=7.36, P<0.01 and OR=1.07, P=0.028).

Furthermore the incremental contribution of all parameters was assessed as shown in Figure 1. Visual significant stenosis provided no significant contribution to the model over relevant baseline risk factors ( $\chi^2$  change from 4.6 in model 1 to 5.9 in model 2, P=0.248). The introduction of quantitative significant stenosis in model 3 provided a significant increase in  $\chi^2$  over model 1 (from 15.9 to 20.8, P<0.01). Additionally, introducing lesion length into model 4 provided significant increment over quantitative stenosis (increase in model  $\chi^2 = 4.2$ , P=0.022).

## Discussion

The present study demonstrated that quantitative derived CTA parameters are associated with the presence of myocardial ischemia on gated myocardial perfusion SPECT. The QCT derived parameters, coronary lesion length, mean plaque burden, maximal plaque thickness, percentage lumen area stenosis, and presence of significant coronary stenosis ( $\geq 50\%$  percentage lumen area stenosis) were significantly higher in coronary artery lesions of vascular territories presenting with myocardial ischemia (Table 4). Furthermore, both coronary lesion length and the presence of quantitative significant coronary stenosis showed a significant incremental value in the association with myocardial ischemia independent of conventional clinical risk variables and the presence of a visual assessed significant stenosis ( $\geq 50\%$  percentage lumen area stenosis).

CTA has a high diagnostic accuracy for the non-invasive detection of coronary atherosclerosis, but a large percentage of lesions are not associated with ischemia on SPECT, since it is considered that non-obstructive coronary stenoses do not induce ischemia.<sup>17</sup> However, various studies have shown that myocardial ischemia is not only dependent on the presence of obstructive CAD, pointing to other potentially important plaque characteristics.<sup>18-20</sup> It has also been reported that diffuse atherosclerosis contributes to myocardial ischemia,<sup>21, 22</sup> in which plaque extent as well as the

Table 5. Multivariate analysis of correlation between, clinical risk factors, visual assessed significant stenosis, quantitative CT parameters and myocardial ischaemia on gated myocardial perfusion SPECT on a vessel-basis (n=120).

Model 1:		Model 2:		Model 3:		Model 4:	
Baseline clinical variables	P-value	Baseline clinical variables + visual significant stenosis	P-value	Baseline clinical variables + visual significant stenosis + quantitative significant stenosis	P-value	Baseline clinical variables + visual significant stenosis + quantitative significant stenosis + lesion length	P-value
OR (95% CI)		OR (95% CI)		OR (95% CI)		OR (95% CI)	
Age	0.219	Age	0.128	Age	0.010	Age	0.005
	(0.94 ; 1.02)		(0.92 ; 1.01)		(0.88 ; 0.98)		(0.87 ; 0.98)
Family History	0.065	Family History	0.055	Family History	0.074	Family History	0.062
	(0.18 ; 1.05)		(0.17 ; 1.02)		(0.16 ; 1.09)		(0.14 ; 1.05)
Diabetes Mellitus	0.194	Diabetes Mellitus	0.127	Diabetes Mellitus	0.071	Diabetes Mellitus	0.060
	(0.23 ; 1.35)		(0.19 ; 1.23)		(0.14 ; 1.08)		(0.12 ; 1.05)
$\chi^2 = 4.6$		Visual significant stenosis	0.246	Visual significant stenosis	0.936	Visual significant stenosis	0.898
			(0.66 ; 5.18)		(0.30 ; 3.04)		(0.33 ; 3.57)
		$\chi^2 = 5.9$		Quantitative significant stenosis	<0.001	Quantitative significant stenosis	0.034
		p = 0.248			(2.45 ; 22.09)		(1.12 ; 13.26)
				$\chi^2 = 20.7$		Lesion length	0.028
				p = <0.0001			(1.01 ; 1.13)
						$\chi^2 = 26.0$	
						p = 0.022	

number of diseased segments have been identified as important parameters for the prediction of myocardial ischemia.<sup>8</sup>

In this perspective, cardiac CTA represents a useful non-invasive imaging technique as it provides information beyond coronary obstruction, including plaque composition, plaque burden, lesion length as well as plaque remodeling. These plaque characteristics have shown to be independently associated with the extent, severity and reversibility of myocardial ischemia,<sup>23</sup> even showing an incremental predictive value for myocardial ischemia over the presence of obstructive CAD.<sup>8</sup>

Quantification of plaque parameters including lesion length, degree of luminal obstruction, plaque burden and remodeling could be more accurate than visual assessment to evaluate the coronary atherosclerosis burden and the risk of ischemic events. In addition, quantitative assessment may provide a more reliable and reproducible approach than visual estimation to evaluate and follow-up patients with coronary atherosclerosis.

Previous attempts in quantifying coronary stenosis using either manual<sup>24</sup> or semi-automated<sup>25,26</sup> approaches have been suboptimal due to the large variability introduced by manual interference as well as difficulties in quantifying heavily calcified lesions.

Thus far, the feasibility of a novel dedicated algorithm for automated quantification of stenosis severity on CTA has been demonstrated in comparison with quantitative coronary angiography showing improved diagnostic accuracy for assessment of significant coronary lesions compared to visual CTA analysis<sup>27</sup>. Furthermore, QCT showed good correlations with quantitative intravascular ultrasound (IVUS) for assessment of coronary stenosis.<sup>9</sup> Although the feasibility of automated QCT analyses has been demonstrated, no study has currently been performed evaluating the value of QCT in the association with the presence of myocardial ischemia on myocardial perfusion SPECT. The current study is the first study that has evaluated the correlates of QCT parameters, derived by a novel algorithm for automated quantification of coronary lesions, with myocardial ischemia. Vessel-based analysis showed that vascular territories with ischemia had a significantly higher number of coronary lesions, bifurcation lesions as well as mixed lesions. QCT plaque parameters including, lesion length, mean plaque burden, maximal plaque thickness, percentage lumen area stenosis and percentage lumen diameter stenosis were significantly higher in vascular territories showing ischemia as compared to vascular territories without ischemia. These results indicate the presence of a significant association between quantitatively derived plaque parameters, representing the extent and severity of atherosclerotic lesions, and the presence of myocardial ischemia. Furthermore, in the present study these quantitatively derived plaque parameters were significantly associated with the presence of myocardial ischemia. Once corrected for clinical

risk variables and visually assessed stenosis degree, both lesion length and the presence of a quantitatively assessed significant stenosis were independently associated with myocardial ischemia. These results are in line with previous studies showing a significant association angiographically assessed lesion length and stenosis severity with myocardial infarction.<sup>28</sup> Additionally, the presence of quantitative significant coronary stenosis (with a cutoff percentage area stenosis of  $\geq 50\%$  luminal narrowing) showed incremental value in a nested multivariate model using myocardial ischemia as the endpoint, whereas, the visual assessment of significant lesions ( $\geq 50\%$  luminal narrowing) did not. This underlines the hypothesis that QCT provides a more accurate lesion analysis as compared to a visual assessment of the CTA images.

Furthermore, lesion length as a representative of diffuse atherosclerosis provided a significant incremental value over the clinical risk variables, visually assessed significant stenosis and quantitative significant stenosis. These results are supported by earlier findings that the additive effect of multiple mild stenoses in series eventually causes perfusion defect.<sup>21</sup> The increase in lesion length represents a more extensive atherosclerotic involvement of the coronary artery, which may lead to considerable more myocardial ischemic damage than might be the case with a short localized obstructive lesion.

In addition, the number of quantitatively assessed significant coronary stenosis was significantly higher compared to the number of visually assessed significant coronary stenosis. Even though the correlation between the presence of myocardial ischemia and stenosis degree assessed using either a visual approach or QCT was poor, there was a significantly improved association between QCT and myocardial ischemia when compared to visual CTA and myocardial ischemia. This discrepancy between visual and QCT for assessment of significant coronary lesions may indicate the importance of using a more accurate quantitative approach for CTA. Accordingly, QCT allows an improved and comprehensive evaluation of coronary plaques which may cause myocardial ischemia.

### **Limitations**

Some limitations need to be considered. In the current study, the prevalence of myocardial ischemia was relatively low on a vessel basis. It would have been preferred to evaluate the performance of QCT in a larger population with higher prevalence of ischemia. However, since CTA is generally performed in low to intermediate risk patients, the present cohort is representative for a general CT population. In addition, QCT was only used in CTA data sets with good or moderate image quality. Furthermore, the present study was subject to selection bias caused by the exclusion criteria for CTA and SPECT. Finally, patients underwent 64- or 320-slice CTA, and currently the diagnostic accuracy of these two techniques has not been evaluated

in a head-to-head comparison; on the other hand, individual 64- and 320-slice CTA studies reported similar diagnostic accuracy for detection of CAD<sup>5</sup>.

### **Clinical implications**

Recent observations have emphasized the discrepancy between coronary artery stenosis (severity) and the presence of ischemia. As recently demonstrated in the FAME trials,<sup>29, 30</sup> fractional flow reserve (FFR) guided coronary revascularization is superior to angiographic stenosis assessment. Also, the DEFACTO trial<sup>31</sup> demonstrated that assessment of FFR from the CTA images provides incremental value over stenosis degree assessment. At present, it is unknown if either stenosis severity or ischemia has the largest influence on prognosis. Possibly, additional characteristics of coronary lesions other than stenosis degree are more related to the presence of myocardial ischemia. As QCT provides an accurate and comprehensive assessment of coronary plaques together with an improved association with myocardial ischemia when compared to visual CT, QCT can be used to improve the diagnostic value of cardiac CTA. Accordingly, it may result in improved risk stratification and less subsequent testing. It has been shown that non-invasive coronary angiography with cardiac CTA allows detection of CAD (i.e. the detection of hemodynamically non-significant CAD) at a much earlier stage than gated myocardial perfusion SPECT. Besides, a normal myocardial perfusion scan does not exclude CAD.<sup>17</sup> Potentially, QCT can facilitate early detection of CAD and accurate identification of patients who may have myocardial ischemia.

### **Conclusion**

Coronary lesion length and the presence of a quantitatively assessed significant stenosis as derived from QCT are significantly correlated with myocardial ischemia on gated myocardial perfusion SPECT. Furthermore, QCT provides incremental value over CTA and baseline clinical risk factors in the association with ischemia on SPECT. Potentially, QCT can refine assessment of CAD, which may be of potential use for identification of patients with myocardial ischemia.

## References

- (1) Hamon M, Biondi-Zoccai GG, Malagutti P *et al.* Diagnostic performance of multislice spiral computed tomography of coronary arteries as compared with conventional invasive coronary angiography: a meta-analysis. *J Am Coll Cardiol* 2006 November 7;48(9):1896-910.
- (2) Hoffmann MH, Shi H, Schmitz BL *et al.* Noninvasive coronary angiography with multislice computed tomography. *JAMA* 2005 May 25;293(20):2471-8.
- (3) Meijboom WB, Meijs MF, Schuijf JD *et al.* Diagnostic accuracy of 64-slice computed tomography coronary angiography: a prospective, multicenter, multivendor study. *J Am Coll Cardiol* 2008 December 16;52(25):2135-44.
- (4) Miller JM, Rochitte CE, Dewey M *et al.* Diagnostic performance of coronary angiography by 64-row CT. *N Engl J Med* 2008 November 27;359(22):2324-36.
- (5) von Ballmoos MW, Haring B, Juillerat P, Alkadhi H. Meta-analysis: diagnostic performance of low-radiation-dose coronary computed tomography angiography. *Ann Intern Med* 2011 March 15;154(6):413-20.
- (6) Hacker M, Jakobs T, Hack N *et al.* Sixty-four slice spiral CT angiography does not predict the functional relevance of coronary artery stenoses in patients with stable angina. *Eur J Nucl Med Mol Imaging* 2007 January;34(1):4-10.
- (7) Naya M, Murthy VL, Blankstein R *et al.* Quantitative relationship between the extent and morphology of coronary atherosclerotic plaque and downstream myocardial perfusion. *J Am Coll Cardiol* 2011 October 18;58(17):1807-16.
- (8) van Velzen JE, Schuijf JD, van Werkhoven JM *et al.* Predictive value of multislice computed tomography variables of atherosclerosis for ischemia on stress-rest single-photon emission computed tomography. *Circ Cardiovasc Imaging* 2010 November 1;3(6):718-26.
- (9) Boogers MJ, Broersen A, van Velzen JE *et al.* Automated quantification of coronary plaque with computed tomography: comparison with intravascular ultrasound using a dedicated registration algorithm for fusion-based quantification. *Eur Heart J* 2012 April;33(8):1007-16.
- (10) Sharir T, Germano G, Kang X *et al.* Prediction of myocardial infarction versus cardiac death by gated myocardial perfusion SPECT: risk stratification by the amount of stress-induced ischemia and the poststress ejection fraction. *J Nucl Med* 2001 June;42(6):831-7.
- (11) Agatston AS, Janowitz WR, Hildner FJ, Zusmer NR, Viamonte M, Jr., Detrano R. Quantification of coronary artery calcium using ultrafast computed tomography. *J Am Coll Cardiol* 1990 March 15;15(4):827-32.
- (12) Germano G, Kavanagh PB, Waechter P *et al.* A new algorithm for the quantitation of myocardial perfusion SPECT. I: technical principles and reproducibility. *J Nucl Med* 2000 April;41(4):712-9.
- (13) Hachamovitch R, Berman DS, Kiat H *et al.* Incremental prognostic value of adenosine stress myocardial perfusion single-photon emission computed tomography and impact on subsequent management in patients with or suspected of having myocardial ischemia. *Am J Cardiol* 1997 August 15;80(4):426-33.
- (14) Berman DS, Kang X, Van Train KF *et al.* Comparative prognostic value of automatic quantitative analysis versus semiquantitative visual analysis of exercise myocardial perfusion single-photon emission computed tomography. *J Am Coll Cardiol* 1998 December;32(7):1987-95.
- (15) Cerqueira MD, Weissman NJ, Dilsizian V *et al.* Standardized myocardial segmentation and nomenclature for tomographic imaging of the heart: a statement for healthcare professionals

- from the Cardiac Imaging Committee of the Council on Clinical Cardiology of the American Heart Association. *Circulation* 2002 January 29;105(4):539-42.
- (16) Fleiss JL. *Statistical methods for rates and proportions*, 2<sup>nd</sup> edn. 2nd ed. New York: 1981.
  - (17) Schuijff JD, Wijns W, Jukema JW *et al*. Relationship between noninvasive coronary angiography with multi-slice computed tomography and myocardial perfusion imaging. *J Am Coll Cardiol* 2006 December 19;48(12):2508-14.
  - (18) Azzarelli S, Galassi AR, Foti R *et al*. Accuracy of 99mTc-tetrofosmin myocardial tomography in the evaluation of coronary artery disease. *J Nucl Cardiol* 1999 March;6(2):183-9.
  - (19) Benoit T, Vivegnis D, Lahiri A, Itti R, Braat S, Rigo P. Tomographic myocardial imaging with technetium-99m tetrofosmin. Comparison with tetrofosmin and thallium planar imaging and with angiography. *Eur Heart J* 1996 April;17(4):635-42.
  - (20) Sacchetti G, Inglese E, Bongo AS *et al*. Detection of moderate and severe coronary artery stenosis with technetium-99m tetrofosmin myocardial single-photon emission tomography. *Eur J Nucl Med* 1997 October;24(10):1230-6.
  - (21) De Bruyne B, Hersbach F, Pijls NH *et al*. Abnormal epicardial coronary resistance in patients with diffuse atherosclerosis but "Normal" coronary angiography. *Circulation* 2001 November 13;104(20):2401-6.
  - (22) Marcus ML, Harrison DG, White CW, McPherson DD, Wilson RF, Kerber RE. Assessing the physiologic significance of coronary obstructions in patients: importance of diffuse undetected atherosclerosis. *Prog Cardiovasc Dis* 1988 July;31(1):39-56.
  - (23) Lin F, Shaw LJ, Berman DS *et al*. Multidetector computed tomography coronary artery plaque predictors of stress-induced myocardial ischemia by SPECT. *Atherosclerosis* 2008 April;197(2):700-9.
  - (24) Leber AW, Knez A, von ZF *et al*. Quantification of obstructive and nonobstructive coronary lesions by 64-slice computed tomography: a comparative study with quantitative coronary angiography and intravascular ultrasound. *J Am Coll Cardiol* 2005 July 5;46(1):147-54.
  - (25) Cheng V, Gutstein A, Wolak A *et al*. Moving beyond binary grading of coronary arterial stenoses on coronary computed tomographic angiography: insights for the imager and referring clinician. *JACC Cardiovasc Imaging* 2008 July;1(4):460-71.
  - (26) Raff GL, Gallagher MJ, O'Neill WW, Goldstein JA. Diagnostic accuracy of noninvasive coronary angiography using 64-slice spiral computed tomography. *J Am Coll Cardiol* 2005 August 2;46(3):552-7.
  - (27) Boogers MJ, Schuijff JD, Kitslaar PH *et al*. Automated quantification of stenosis severity on 64-slice CT: a comparison with quantitative coronary angiography. *JACC Cardiovasc Imaging* 2010 July;3(7):699-709.
  - (28) Meimoun P, Sayah S, Luyckx-Bore A *et al*. Comparison between non-invasive coronary flow reserve and fractional flow reserve to assess the functional significance of left anterior descending artery stenosis of intermediate severity. *J Am Soc Echocardiogr* 2011 April;24(4):374-81.
  - (29) Tonino PA, De BB, Pijls NH *et al*. Fractional flow reserve versus angiography for guiding percutaneous coronary intervention. *N Engl J Med* 2009 January 15;360(3):213-24.
  - (30) De BB, Pijls NH, Kalesan B *et al*. Fractional Flow Reserve-Guided PCI versus Medical Therapy in Stable Coronary Disease. *N Engl J Med* 2012 August 27.
  - (31) Min JK, Leipsic J, Pencina MJ *et al*. Diagnostic Accuracy of Fractional Flow Reserve From Anatomic CT Angiography. *JAMA* 2012 August 26;1-9.
  - (32) Mintz GS, Nissen SE, Anderson WD *et al*. American College of Cardiology Clinical Expert Consensus Document on Standards for Acquisition, Measurement and Reporting of Intravas-

cular Ultrasound Studies (IVUS). A report of the American College of Cardiology Task Force on Clinical Expert Consensus Documents. *J Am Coll Cardiol* 2001 April;37(5):1478-92.



# Chapter 8

## Feasibility of an automated quantitative computed tomography angiography-derived risk score for risk stratification of patients with suspected coronary artery disease

de Graaf MA, Broersen A, Ahmed W, Kitslaar PH, Dijkstra J, Kroft LJ, Delgado V, Bax JJ, Reiber JH, Scholte AJ.

*American Journal of Cardiology* 2014;113:1947-1955

## Abstract

**Purpose:** Computed tomography coronary angiography (CTA) has important prognostic value. Additionally, quantitative CTA (QCT) provides a more detailed, accurate assessment of coronary artery disease (CAD) on CTA. Potentially, a risk score incorporating all quantitative stenosis parameters allows for accurate risk stratification. Therefore, the purpose of this study was to determine if an automatic, quantitative assessment of CAD using QCT combined into a CTA risk score allows risk stratification of patients.

**Methods:** In 300 patients QCT was performed to automatically detect and quantify all lesions in the coronary tree. Using QCT, a novel CTA risk score was calculated based on plaque extent, severity, composition and location on a segment basis. During follow-up the composite endpoint of all-cause mortality, revascularization and non-fatal infarction was recorded.

**Results:** In total, 10% of patients experienced an event during a median follow-up of 2.14 years. The CTA risk score was significantly higher in patients with an event (12.5(IQR8.6–16.4) versus 1.7(IQR0–8.4),  $P<0.001$ ). Among 127 patients with obstructive CAD ( $\geq 50\%$  stenosis), 27 events were recorded, all in patients with a high CTA risk score.

**Conclusion:** The present study demonstrated that a fully automatic QCT analysis of CAD is feasible and can be applied for risk stratification of patients with suspected CAD. Furthermore, a novel CTA risk score incorporating location, severity and composition of coronary lesion was developed. This score may improve risk stratification but needs to be confirmed in larger studies.

## Introduction

The aim of the present study was to evaluate patients with suspected CAD undergoing CTA and: 1) perform a fully automatic quantitative assessment of coronary CTA datasets to assess the location, severity and composition of CAD, and 2) to incorporate all these variables into one risk score. Further aims were: 3) to assess the value of this integrated score for risk stratification and 4) to compare the risk classification according to this new score as compared to existing risk scores.

## Methods

### Patients

The population consisted of 300 patients, referred for the evaluation of (a)typical chest pain or dyspnea. Patients with previous percutaneous coronary intervention (PCI) or coronary artery bypass graft (CABG) were excluded. Clinical data were prospectively entered into the departmental Cardiology Information System (EPD-Vision©, Leiden University Medical Center, the Netherlands) and retrospectively analyzed. The Institutional Review Board of the Leiden University Medical Center approved this retrospective evaluation of clinically collected data, and waived the need for written informed consent.

### CTA acquisition

Patients were scanned either with a 64-slice CT scanner (Aquilion 64, Toshiba Medical System, Otowara, Japan) or a 320-row volumetric scanner (Aquilion ONE, Toshiba Medical System, Otowara, Japan). Coronary CTA was performed according to standard clinical practice as previously described.<sup>1</sup> Only patients with clinical diagnostic image quality of the coronary CTA were included.

### Quantitative computed tomography

QCT was performed in five automatic steps, as depicted in Figure 1.

1) The coronary tree was automatically extracted from the coronary CTA dataset.<sup>2</sup> Using a tree labeling algorithm, the segments of the coronary tree were automatically labeled according the American Heart Association (AHA) 17-segements model.<sup>3;4</sup> 2) Curved multi-planar reformations (CMPR) of each coronary vessel and side-branch were created.<sup>2</sup> 3) The lumen and vessel wall were automatically segmented using a previously validated software tool (QAngio CT Research Edition version 1.3.6, Medis Medical Imaging Systems, Leiden, the Netherlands).<sup>5</sup> 4) Coronary plaque constitution was assessed using a dedicated tissue characterization algorithm as previously

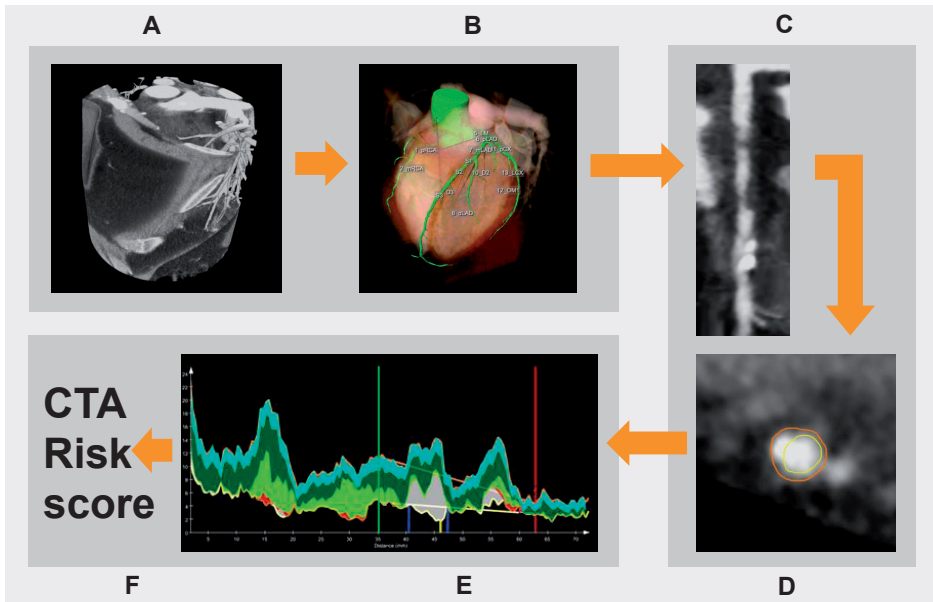


**Figure 1. Schematic overview of the automatic quantitative CT algorithm.**

The 3-dimensional coronary tree was extracted from the coronary CTA data set (Panel A). Using an automatic labeling algorithm the coronary tree was labeled according to the AHA 17-segment model (Panel B). Of each coronary artery a curved multiplanar reformation (CMPR) was constructed (Panel C). Next, a fully automatic detection of the lumen and vessel wall was performed (Panel D). Finally, each atherosclerotic lesion was automatically detected based on the lumen and vessel wall contours as well as the corresponding reference lines (estimate of normal tapering of the coronary artery), as shown in panel E. Stenosis parameters were calculated at the level of the minimal lumen area (MLA, vertical yellow marker). Additionally, plaque volumes and plaque types were derived for the whole coronary artery lesion, ranging from the proximal to the distal lesion marker (blue vertical markers). Fibrotic tissue was labeled in dark green, fibro-fatty tissue in light green, dense calcium in white and necrotic core in red. Finally, the CTA risk score per patient is automatically generated (Panel F).

described.<sup>6</sup> This tissue characterization algorithm allows for the differentiation into four different plaque types. Currently, it is unclear how this should be translated to the commonly used classification of non-calcified, partially calcified and calcified plaque. For this analysis, the percentage ratio between dense calcium (DC) and necrotic core (NC) ( $DC/(NC + DC) \times 100$ ) was used to differentiate between partially calcified, non-calcified and calcified plaques. Lesions with a ratio  $<10\%$  were considered non-calcified plaque as well as lesion without NC or DC, lesions with a ratio  $>75\%$  were classified as calcified plaque. Coronary plaques with ratios  $\geq 10\%$  and  $\leq 75\%$  were classified as partially calcified plaque. 5) Coronary lesions were automatically detected. Within each segment, a regression analysis is performed on the lumen area graph to define a lumen reference line. A lesion is defined on the region surrounding the minimal lumen area (MLA) where the lumen area is smaller than this

reference. If needed, this lesion is enlarged to include calcified spots located near the MLA (within 50 mm and  $>1 \text{ mm}^3$ ). Lesions with negative stenosis degree and steep reference slopes ( $<-0.35 \text{ mm}^2/\text{mm}$ ) were removed as well as short lesions ( $<1.5 \text{ mm}$ ), lesions in segments with small vessel and lumen areas ( $<8 \text{ mm}^2$  and  $<1.5 \text{ mm}^2$  respectively), and distally located lesions ( $>150 \text{ mm}$  from ostium).

The automatic lesion detection was confirmed by an experienced observer. The software allows the observer to override the automatic lesion detection. If needed, small adjustments were made.

### **CTA risk score**

A novel comprehensive risk score was created to combine the information on location, extent, severity and composition of each coronary lesion. As described in Figure 2, the score consists of three components for each segment; a segment location weight factor, a stenosis severity weight factor and a plaque weight factor. 1) The location of each lesion is represented by a segment weight factor based on the Leaman score.<sup>4,7</sup> A different set of weight factors is applied to left or right dominant coronary artery systems. 2) Stenosis severity was described by the stenosis severity weight factor. A previous meta-analysis reported a hazard ratio (HR) of 1.35 (1.09 – 1.67) for each significant stenosis in each segment of the coronary tree.<sup>8</sup> Therefore 1.4 was chosen as the weight factor for a significant stenosis ( $\geq 50\%$  area stenosis). 3) In a study performed by Gaemperli *et al.*, stratifying the diseased segments according to plaque composition, the authors reported a HR of 1.21 (1.11 – 1.32) for segments with calcified plaques, 1.57 (1.38-1.79) for segments with partially calcified plaques and 1.71 (1.14-2.56) for segments with non-calcified plaques.<sup>9</sup> This was translated in the score by a weight factor of 1.2 for calcified plaque, 1.6 for partially calcified plaque and 1.7 for non-calcified plaque.

The CTA risk score is automatically calculated using QCT. When coronary plaque is absent ( $<30\%$  area stenosis) the score is 0. When a stenosis is present, a score is given according to the location of the lesion in the coronary artery tree, this score is multiplied by the stenosis weight factor and multiplied by the plaque weight factor. The final score is calculated by summation of the individual segment scores (range 0-55) (Figure 2).

### **Modified Duke prognostic CAD index**

In addition, the modified Duke prognostic CAD index was applied to the QCT results.<sup>10,11</sup> The score consist of 6 categories; 1:  $<50\%$  stenosis, 2:  $\geq 2$  stenoses 30% to 49% (including 1 artery with proximal disease or 1 vessel with 50% to 69% stenosis, 3: 2 stenoses 50% to 69% or 1 vessel with  $\geq 70\%$  stenosis, 4: 3 stenoses 50% to 69% or 2 vessels with  $\geq 70\%$  stenosis or proximal left anterior descending stenosis  $\geq 70\%$ ,

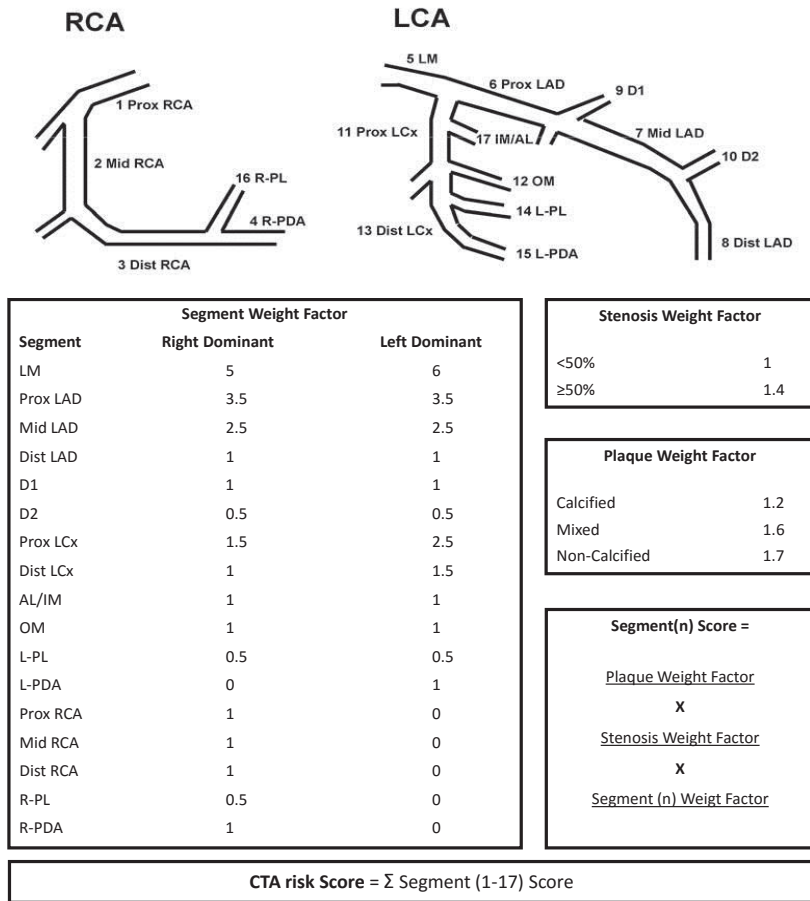


**Figure 2. Schematic overview of the CTA risk score.**

The CTA risk score is calculated by the summation of the individual segment scores, which are obtained by multiplying the segment weight factor, the stenosis weight factor and the plaque weight factor.

AL: anterolateral segment; D1: diagonal 1; D2: diagonal 2; IM: intermediate segment; LAD: left anterior descending coronary artery; LCA: left coronary artery; LCx: left circumflex coronary artery; LM: left main segment; L-PDA: left posterior descending artery; L-PL: left posterolateral segment; OM: obtuse marginal segment; RCA: right coronary artery; R-PDA: right posterior descending artery; R-PL: right posterolateral segment.

5: 3 vessels ≥70% stenoses or 2 vessels ≥70% stenosis with proximal left anterior descending, 6: Left main stenosis ≥50%. Subsequently, the distribution of the novel CTA risk score within the Duke CAD categories was assessed.

**Follow-up and event definition**

Patient follow-up data were gathered using clinical visits or standardized telephone interviews. A composite endpoint was constructed using all-cause mortality, revascularization after 30-days and non-fatal myocardial infarction. This 30-day interval was

used to exclude coronary CTA-driven events (referral for angiography mainly based on coronary CTA findings).<sup>12</sup> Non-fatal myocardial infarction was defined based on criteria of typical chest pain, elevated cardiac enzyme levels, and typical ECG changes.<sup>13</sup>

### Statistical analysis

Continuous data are presented as mean  $\pm$  SD if normally distributed or as median (interquartile range, IQR) if non-normally distributed. Categorical data are presented as absolute numbers and percentages. First, the QCT parameters were compared between both patients groups (with versus without events). Second, both the novel CTA risk score and the modified Duke prognostic CAD index were compared between both groups. Third, the ability of the CTA risk score for risk stratification of patients was assessed. For this purpose, the CTA risk score was stratified into a low and high risk category based on receiver operating characteristic (ROC) curve analysis, ensuring the highest negative predictive value. First, the distribution of the risk score in patients with and without obstructive CAD ( $\geq 50\%$  area stenosis in QCT) was assessed; and correlated to the occurrence of an event. In a similar fashion, the distribution within the Duke CAD categories was assessed. For this purpose, the Duke CAD categories were divided in three groups: Mild CAD, defined as Duke CAD category 1; Moderate CAD, defined as Duke CAD category 2-3; Severe CAD, defined by the three most severe categories. Fourth, to evaluate the independent predictive value of the CTA risk score, univariate and multivariate Cox-regression analyses were performed. All baseline or univariate significant clinical variables were entered into the multivariate model. All statistical tests were two-sided and a P-value  $< 0.05$  was considered statistically significant. All statistical analyses were performed with SPSS software (Version 20.0, SPSS Inc., Chicago, Illinois).

## Results

The patient population consisted of 300 patients referred for the evaluation of chest pain during the period January 2008 - May 2010. Baseline characteristics are summarized in Table 1. The median follow-up duration was 2.14 years (IQR 1.07-3.48); 28(9%) patients were lost to follow-up. During the follow-up period the composite endpoint occurred in 29 patients (event rate 10%) ; 25 (8%) patients underwent revascularization (23 PCI and 2 CABG) after 30-day of CTA acquisition. Death occurred in 4 patients (1%). In patients with an event, mean age was higher and diabetes and hypertension were more often prevalent.

**Table 1. Patient characteristics.**

Variable	Total (300)	Event		P- value
		No (N=271)	Yes (N=29)	
Age (years)	55±11.5	54±11.6	60±8.5	<b>&lt;0.001</b>
Men	180(60%)	161(59%)	19(66%)	0.526
Diabetes Mellitus	90(30%)	76(28%)	14(48%)	<b>0.024</b>
Hypertension†	111(37%)	95(35%)	16(55%)	<b>0.034</b>
Hypercholesterolemia‡	100(33%)	88(32%)	12(41%)	0.334
Smoker	52(17%)	47(17%)	5(17%)	0.988
Obesity*	56(19%)	49(18%)	7(24%)	0.432
Calcium score	146±420 1(0-86)	118±388 1(0-54)	407±596 148(30-514)	<b>&lt;0.001</b>

Data are represented as mean ± SD, median (interquartile range) or as number and percentages of patients.

†Defined as systolic blood pressure ≥140 mm Hg and/or diastolic blood pressure ≥90 mmHg or the use of antihypertensive medication.

‡Defined as serum total cholesterol ≥230 mg/dL or serum triglycerides ≥200 mg/dL or treatment with lipid lowering medication.

\* Defined as a body mass index of ≥ 30 Kg/m<sup>2</sup>

### QCT characteristics

The results of the QCT lesion analysis on a patient basis are depicted in Table 2. In patients with an event, significant obstructive lesions were more frequently observed. Furthermore, in patients with an event the mean number of partially calcified or calcified lesions was higher compared to patients without events.

**Table 2. Comparison of quantitative computed tomography coronary angiography results between patients with and without events.**

Variable	Event		P-value
	No (N=271)	Yes (N=29)	
No of plaques ≥30%	1.54±2.14	3.83±2.04	<b>&lt;0.001</b>
No of plaques 30-50%	0.82±1.17	1.45±1.12	<b>&lt;0.001</b>
No of obstructive lesions ≥50%	0.51±0.87	1.83±0.97	<b>&lt;0.001</b>
No of severe lesions ≥70%	0.17±0.92	0.69±1.07	<b>&lt;0.001</b>
No of calcified lesions	0.95±1.67	2.66±2.10	<b>&lt;0.001</b>
No of partially calcified lesions	0.31±0.73	0.76±0.87	<b>&lt;0.001</b>
No of non-calcified lesions	0.29±0.60	0.41±0.63	0.189

**Table 2. (Continued)**

Variable	Event		P-value
	No (N=271)	Yes (N=29)	
No of narrowed coronary arteries	0.51±0.87	1.83±0.97	<b>&lt;0.001</b>
Left main lesion	6(2%)	4(13%)	<b>0.001</b>
Right coronary artery lesion	45(16%)	11(37%)	<b>0.005</b>
Left anterior descending artery lesion	63(23%)	24(82%)	<b>&lt;0.001</b>
Left circumflex artery lesion	25(9%)	13(44%)	<b>&lt;0.001</b>
Lesions in proximal segments	0.34±0.68	1.07±1.0	<b>&lt;0.001</b>
Lesions only in distal segments	0.38±0.89	1.31±1.17	<b>&lt;0.001</b>
Percentage of proximal lesions	52±37	48±37	0.961

### CTA risk score

In the overall population, the median CTA risk score was 3.0(IQR0.0-9.8). The median CTA risk score was significantly higher in patients with an event as compared to event-free patients (12.5(IQR8.6-16.4) versus 1.7(IQR0-8.4),  $P<0.001$ ). Accordingly, in patients with a CTA risk score of 0, the event rate was <1% (1 of 130). Based on ROC curve analysis, a CTA risk score of 7 was defined as a cut-off value between low and high CTA risk score to ensure the highest negative predictive value. Figure 3 provides a patient example of the QCT analysis. The distribution of patients with a high and low CTA risk score between patients with and without obstructive CAD is depicted in Figure 4. Of interest, in the 112 patients with obstructive CAD, all events occurred in patients with a high CTA risk score.

### Reclassification according to the presence of obstructive CAD and modified Duke prognostic CAD index

The results of the modified Duke prognostic CAD index calculation based on the QCT results are summarized in Figure 5. The majority of the patients were categorized in Duke CAD category 1. Indeed, all events in patients within Duke CAD category 2 or 3 occurred in patients with a high CTA risk score. Only one event occurred in a patient with a low CTA risk score, this patient was classified in Duke CAD category 1.

### Cox-regression analysis

In the univariate Cox-regression analysis (Table 3), age and CTA risk score were significantly associated with the occurrence of an event. In the multivariate analysis, adjusted for significant baseline characteristics, the CTA risk score was independently associated with events.

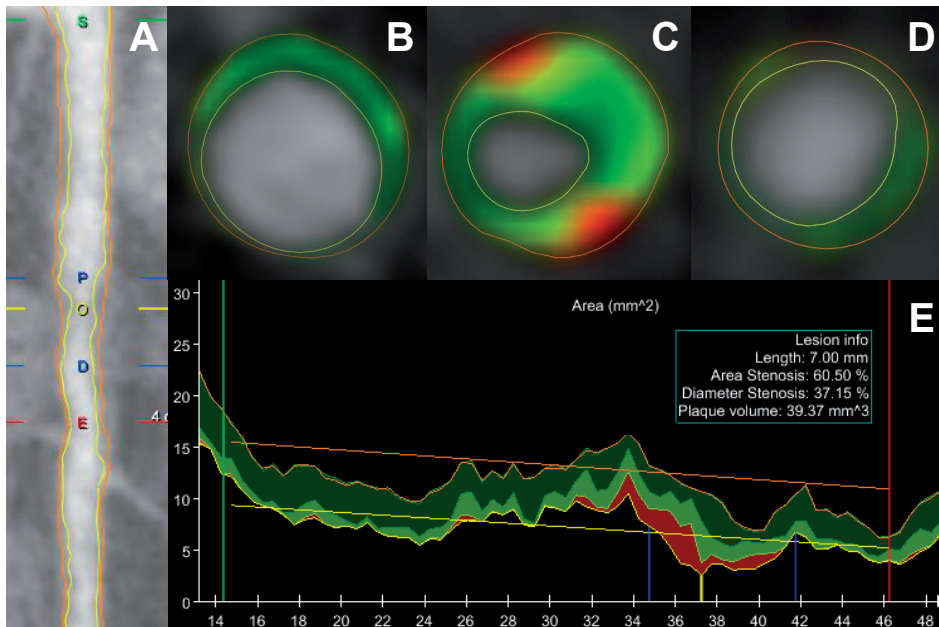


**Figure 3. Patient example of the QCT analysis.**

An example of a 54-year old man with a CTA risk score of 8.3. Panel A shows the MPR of the LAD of this patient in which a significant non-calcified plaque was present. In panel C, the cross-section at the minimal lumen area with corresponding proximal and distal reference regions is shown (Panels B and D). The lesion was automatically detected and quantified (panel E) by the algorithm as depicted in Figure 1. The stenosis degree was 61% and the lesion was characterized as non-calcified plaque. Three months after the coronary CTA, the patient underwent invasive coronary angiography for progressive chest pain, followed by PCI of the LAD.

## Discussion

The present study assessed the feasibility of a novel, fully automatic QCT algorithm to quantify the location, severity and composition of coronary artery atherosclerosis on a patient basis. Particularly, differences in QCT derived CAD parameters were shown between patients with and without subsequent events. Second, a novel CTA risk score was developed, enabling to express the location, extent, severity and composition of CAD in a number for each individual patient. This score was significantly higher in patients who experienced an adverse event. Finally, the distribution of the CTA risk according to the presence of obstructive CAD and within the Duke CAD score categories was established.

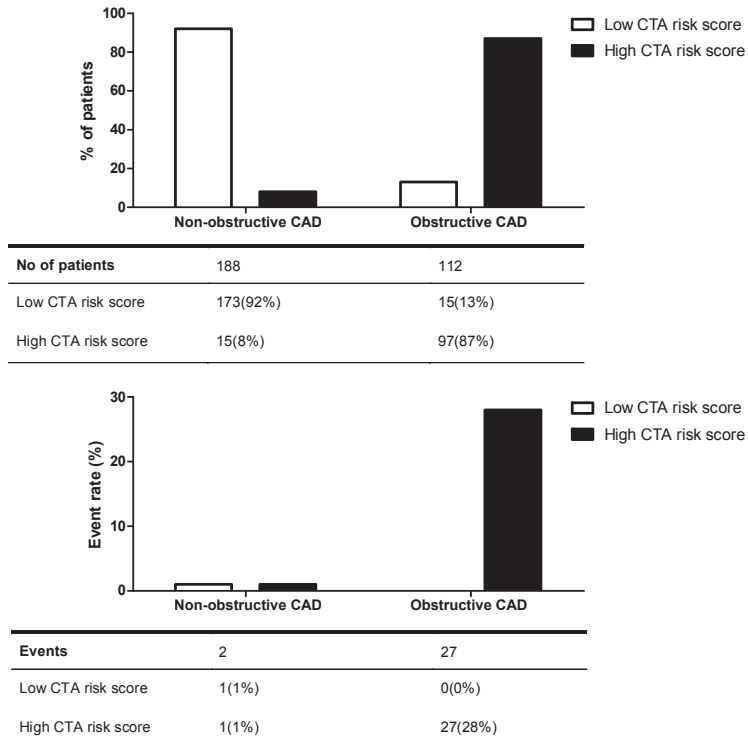


**Figure 4. Distribution of the CTA risk score according to the presence of a significant stenosis.**

Upper panel: Bar graph representing the distribution of patients with a low or high CTA risks score. Lower panel: Bar graph representing the event rates in patients with a low or high CTA risk score in patients with and without obstructive CAD. In the patients with obstructive CAD, all events occurred in patients with a high CTA risk score.

### Quantitative computed tomography coronary angiography (QCT)

The assessment of CAD on CTA images is mainly performed visually. However, the accuracy and reproducibility of visually analysed CTA images is limited.<sup>14</sup> This may result in misclassification of obstructive or non-obstructive CAD; for example, in the multi-centre ACCURACY study a visually assessed obstructive CAD on CTA was confirmed in only 64% of patients using quantitative coronary angiography (QCA).<sup>15</sup>

These observations underscore the need for a robust, reproducible method for quantification of CAD on CTA. Novel software tools have been designed allowing quantitative assessment of CTA datasets similarly to QCA.<sup>5;6;16;17</sup> Leber *et al.* performed a quantitative analysis of CAD on CTA and compared the results to ICA and IVUS.<sup>17</sup> In total, 798 segments were analyzed, illustrating a clear relation between plaque burden as quantified on CTA and IVUS. However, for quantification of stenosis severity only modest correlations between CTA and ICA were shown. Voros *et al.* included 50

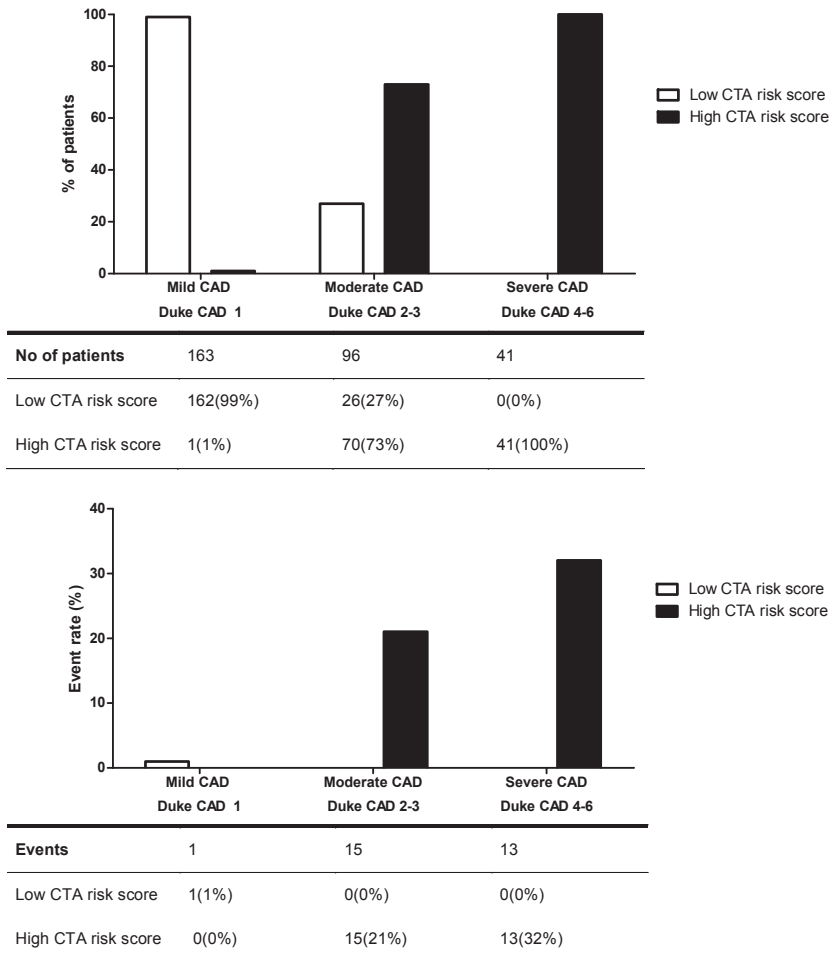


**Figure 5. Distribution of the CTA risk score according to the grouped Duke CAD category.**

Upper panel: Bar graph representing the distribution of patients with a low or high CTA risk score in the three groups. In the patients with mild CAD, a large proportion of patients (73%) were reclassified by a high CTA risk score.

Lower panel: Bar graph representing the event rates in patients with a low or high CTA risk score in the three Duke CAD groups. In the patients with Duke CAD category 2- 3, all events occurred in patients with a high CTA risk score.

patients who underwent cardiac CTA, ICA and IVUS.<sup>16</sup> In this study, stenosis severity as derived from QCT correlated well with stenosis severity on QCA. Moreover, QCT and IVUS correlated significantly in the assessment of lumen and vessel area. These different findings between the study by Leber *et al.*<sup>18</sup> and Voros *et al.*<sup>16</sup>, can be explained by the fact that Voros *et al.* used an automated method for assessment of the coronary artery lumen and vessel wall. The reproducibility of QCT has also been

**Table 3. Univariate and multivariate Cox-regression analysis for the prediction of events.**

Variable	Univariate HR (95%CI)	P-value	Multivariate HR (95%CI)	P-value
Age	1.05(1.01;1.09)	<b>0.008</b>	1.02(0.98;1.07)	0.238
Gender	1.30(0.61;2.80)	0.499		
Diabetes Mellitus	1.86(0.90;3.86)	<b>0.095</b>	2.02(0.95;4.29)	0.067
Hypertension	2.13(1.02;4.42)	<b>0.044</b>	1.07(0.48;2.38)	0.866
Hypercholesterolemia	1.19(0.57;2.50)	0.640		
Family history of CAD	1.41(0.68;2.92)	0.354		
Smoking	0.95(0.36;2.48)	0.910		
Obesity	1.41(0.60;3.29)	0.432		
CTA risk score	1.12(1.07;1.16)	<b>&lt;0.001</b>	1.10(1.01;1.15)	<b>&lt;0.001</b>

CAD: coronary artery disease; CI: confidence interval; CTA: computed tomography angiography; HR: hazard ratio

addressed by Papadopoulou *et al.* illustrating high inter- and intra-observer agreement for assessment of geometrical measurements of coronary atherosclerosis<sup>19</sup>

Quantitative assessment of coronary artery atherosclerosis and plaque constitution is clinically relevant. Versteyleen *et al.* performed a semi-quantitative analysis of CTA data and demonstrated that the 21 patients who developed an ACS more often presented with larger (non-calcified) plaque volumes and higher plaque burden as compared to control patients.<sup>20</sup> Importantly, the authors demonstrated incremental predictive value of semi-quantitative coronary CTA analysis over visual CTA interpretation and Framingham risk score.

For complete analysis of coronary artery atherosclerosis, not only quantitative analysis of stenosis severity and plaque burden is needed but also assessment and quantification of plaque constitution. Earlier studies have shown the agreement between plaque constitution on QCT as compared with IVUS Virtual Histology (IVUS VH). Brodoefel *et al.* compared QCT and IVUS VH in 22 coronary lesions, showing good correlations for assessment of overall plaque volume and non-calcified plaque volume, but the agreement between the 2 techniques for assessment of plaque constitution was limited.<sup>21</sup> The more sophisticated software for quantification of plaque constitution that was used in the current study has been shown to correlate well with IVUS VH in 57 patients (108 coronary lesions).<sup>6</sup> Particularly, distinction and quantification of coronary plaque volume and plaque constitution is feasible with this software.

### Novel CTA risk score

In the present study, a novel CTA risk score was developed. This score consists of three components per coronary lesion (i.e. plaque location, severity and composition).

Each component has been demonstrated to provide important prognostic information for risk stratification of patients with CAD.

**Stenosis location.** The location of a coronary atherosclerotic lesion has important prognostic value. Patients with lesions located proximally in the coronary arteries have a worse prognosis as compared to patients with distally located lesions.<sup>10</sup> In the early 1980s, the Leaman score was developed to provide weight factors for each segment in the coronary artery tree based on the amount of myocardium at risk per coronary segment.<sup>7</sup> This score was thereafter implemented in the angiographic SYNTAX-score, designed to quantify the complexity of CAD and its value has been established in clinical studies.<sup>22-24</sup> The same Leaman weight factors were directly incorporated in the novel score used in the present study.

**Stenosis severity.** Currently, the assessment of CAD on coronary CTA is mainly targeting the detection or exclusion of obstructive CAD. However, the presence of non-obstructive CAD on coronary CTA is also associated with worse prognosis. In the CONFIRM registry, Chow *et al.* demonstrated a 3-fold increase in annual mortality rate for patients with non-obstructive CAD as compared to patients without atherosclerosis.<sup>25</sup> To account for the clinical value of atherosclerotic burden and non-obstructive CAD, previously proposed scores have focused on the number of lesions and the extent of CAD. Min *et al.* for example applied the Duke modified CAD index to CTA images.<sup>16</sup> In this score, patients were categorized according to the extent of CAD. The prognostic value of these scoring systems has recently been reported.<sup>10;26</sup> However, in these scores only rough estimates are implemented, whereas in the present CTA risk score established values from literature were applied per coronary segment.<sup>8</sup>

More recently, a novel score was designed based on the CONFIRM data.<sup>27</sup> This score combines both clinical and CTA data. Similar to the CTA risk score, more weight is assigned to proximal lesions. In contrast, in the CONFIRM score non-calcified plaque was not incorporated, whereas in the CTA risk score this score was weighted a higher risk than calcified plaque.

**Plaque constitution.** Next to assessment of stenosis severity, CTA permits assessment of plaque constitution, which provides additional prognostic value; Hou *et al.* showed in 4,425 patients that the presence of partially calcified and non-calcified plaques was associated with worse prognosis as compared to calcified plaques.<sup>28</sup> These results may suggest that non-calcified and partially calcified plaques represent a more vulnerable stadium of CAD, whereas calcified plaques may reflect more stable CAD. To account for this difference in prognosis, in the present score, different weight factors were applied for the different plaque constitutions.

**Limitations**

Some limitations need to be considered. The current evaluation should be considered a feasibility study, to demonstrate the potential use of QCT, and to introduce the concept of a novel CTA risk score. Further studies in larger populations are needed to confirm the current observations. In addition, although QCT was automatically performed, still limited user input was needed to confirm the automatic lesion detection, which may potentially have introduced observer bias. Moreover, only scans with clinical diagnostic image quality were included.

**Conclusion**

The CTA risk score only includes CTA derived information and no details on patients risk factors or symptoms. For clinical decision making the risk score should be considered in combination with the patients history.

## References

- (1) van Werkhoven JM, Schuijff JD, Gaemperli O, Jukema JW, Kroft LJ, Boersma E, Pazhenkottil A, Valenta I, Pundziute G, de RA, van der Wall EE, Kaufmann PA, Bax JJ. Incremental prognostic value of multi-slice computed tomography coronary angiography over coronary artery calcium scoring in patients with suspected coronary artery disease. *Eur Heart J* 2009;30:2622-2629.
- (2) Yang G, Kitslaar P, Frenay M, Broersen A, Boogers MJ, Bax JJ, Reiber JH, Dijkstra J. Automatic centerline extraction of coronary arteries in coronary computed tomographic angiography. *Int J Cardiovasc Imaging* 2012;28:921-933.
- (3) Guanyu Yang, Alexander Broersen, Robert Petr, Pieter Kitslaar, Michiel A de Graaf, Jeroen J Bax, Johan HC Reiber, Jouke Dijkstra. Automatic coronary artery tree labeling in coronary computed tomographic angiography datasets. *Computing in Cardiology* 2012;38:109-102.
- (4) Austen WG, Edwards JE, Frye RL, Gensini GG, Gott VL, Griffith LS, McGoon DC, Murphy ML, Roe BB. A reporting system on patients evaluated for coronary artery disease. Report of the Ad Hoc Committee for Grading of Coronary Artery Disease, Council on Cardiovascular Surgery, American Heart Association. *Circulation* 1975;51:5-40.
- (5) Boogers MJ, Broersen A, van Velzen JE, de Graaf FR, El-Naggar HM, Kitslaar PH, Dijkstra J, Delgado V, Boersma E, de RA, Schuijff JD, Schalij MJ, Reiber JH, Bax JJ, Jukema JW. Automated quantification of coronary plaque with computed tomography: comparison with intravascular ultrasound using a dedicated registration algorithm for fusion-based quantification. *Eur Heart J* 2012;33:1007-1016.
- (6) de Graaf MA, Broersen A, Kitslaar PH, Roos CJ, Dijkstra J, Lieveveldt BP, Jukema JW, Schalij MJ, Delgado V, Bax JJ, Reiber JH, Scholte AJ. Automatic quantification and characterization of coronary atherosclerosis with computed tomography coronary angiography: cross-correlation with intravascular ultrasound virtual histology. *Int J Cardiovasc Imaging* 2013;29:1177-1190.
- (7) Leaman DM, Brower RW, Meester GT, Serruys P, van den Brand M. Coronary artery atherosclerosis: severity of the disease, severity of angina pectoris and compromised left ventricular function. *Circulation* 1981;63:285-299.
- (8) Bamberg F, Sommer WH, Hoffmann V, Achenbach S, Nikolaou K, Conen D, Reiser MF, Hoffmann U, Becker CR. Meta-analysis and systematic review of the long-term predictive value of assessment of coronary atherosclerosis by contrast-enhanced coronary computed tomography angiography. *J Am Coll Cardiol* 2011;57:2426-2436.
- (9) Gaemperli O, Valenta I, Schepis T, Husmann L, Scheffel H, Desbiolles L, Leschka S, Alkadhi H, Kaufmann PA. Coronary 64-slice CT angiography predicts outcome in patients with known or suspected coronary artery disease. *Eur Radiol* 2008;18:1162-1173.
- (10) Min JK, Shaw LJ, Devereux RB, Okin PM, Weinsaft JW, Russo DJ, Lippolis NJ, Berman DS, Callister TQ. Prognostic value of multidetector coronary computed tomographic angiography for prediction of all-cause mortality. *J Am Coll Cardiol* 2007;50:1161-1170.
- (11) Mark DB, Nelson CL, Califf RM, Harrell FE, Jr., Lee KL, Jones RH, Fortin DF, Stack RS, Glower DD, Smith LR, . Continuing evolution of therapy for coronary artery disease. Initial results from the era of coronary angioplasty. *Circulation* 1994;89:2015-2025.
- (12) Rubinshtein R, Halon DA, Gaspar T, Peled N, Lewis BS. Cardiac computed tomographic angiography for risk stratification and prediction of late cardiovascular outcome events in patients with a chest pain syndrome. *Int J Cardiol* 2009;137:108-115.
- (13) Steg PG, James SK, Atar D, Badano LP, Blomstrom-Lundqvist C, Borger MA, Di MC, Dickstein K, Ducrocq G, Fernandez-Aviles F, Gershlick AH, Giannuzzi P, Halvorsen S, Huber K, Juni P,

- Kastrati A, Knuuti J, Lenzen MJ, Mahaffey KW, Valgimigli M, van 't HA, Widimsky P, Zahger D. ESC Guidelines for the management of acute myocardial infarction in patients presenting with ST-segment elevation. *Eur Heart J* 2012;33:2569-2619.
- (14) Hoffmann H, Frieler K, Hamm B, Dewey M. Intra- and interobserver variability in detection and assessment of calcified and noncalcified coronary artery plaques using 64-slice computed tomography: variability in coronary plaque measurement using MSCT. *Int J Cardiovasc Imaging* 2008;24:735-742.
  - (15) Budoff MJ, Dowe D, Jollis JG, Gitter M, Sutherland J, Halamert E, Scherer M, Bellinger R, Martin A, Benton R, Delago A, Min JK. Diagnostic performance of 64-multidetector row coronary computed tomographic angiography for evaluation of coronary artery stenosis in individuals without known coronary artery disease: results from the prospective multicenter ACCURACY (Assessment by Coronary Computed Tomographic Angiography of Individuals Undergoing Invasive Coronary Angiography) trial. *J Am Coll Cardiol* 2008;52:1724-1732.
  - (16) Voros S, Rinehart S, Qian Z, Vazquez G, Anderson H, Murrieta L, Wilmer C, Carlson H, Taylor K, Ballard W, Karpaliotis D, Kalynych A, Brown C, III. Prospective validation of standardized, 3-dimensional, quantitative coronary computed tomographic plaque measurements using radiofrequency backscatter intravascular ultrasound as reference standard in intermediate coronary arterial lesions: results from the ATLANTA (assessment of tissue characteristics, lesion morphology, and hemodynamics by angiography with fractional flow reserve, intravascular ultrasound and virtual histology, and noninvasive computed tomography in atherosclerotic plaques) I study. *JACC Cardiovasc Interv* 2011;4:198-208.
  - (17) Leber AW, Knez A, von ZF, Becker A, Nikolaou K, Paul S, Wintersperger B, Reiser M, Becker CR, Steinbeck G, Boekstegers P. Quantification of obstructive and nonobstructive coronary lesions by 64-slice computed tomography: a comparative study with quantitative coronary angiography and intravascular ultrasound. *J Am Coll Cardiol* 2005;46:147-154.
  - (18) Leber AW, Knez A, Becker A, Becker C, von ZF, Nikolaou K, Rist C, Reiser M, White C, Steinbeck G, Boekstegers P. Accuracy of multidetector spiral computed tomography in identifying and differentiating the composition of coronary atherosclerotic plaques: a comparative study with intracoronary ultrasound. *J Am Coll Cardiol* 2004;43:1241-1247.
  - (19) Papadopoulou SL, Garcia-Garcia HM, Rossi A, Girasis C, Dharampala AS, Kitslaar PH, Krestin GP, de Feyter PJ. Reproducibility of computed tomography angiography data analysis using semiautomated plaque quantification software: implications for the design of longitudinal studies. *Int J Cardiovasc Imaging* 2012.
  - (20) Versteulen MO, Kietselaer BL, Dagnelie PC, Joosen IA, Dedic A, Raaijmakers RH, Wildberger JE, Nieman K, Crijns HJ, Niessen WJ, Daemen MJ, Hofstra L. Additive value of semiautomated quantification of coronary artery disease using cardiac computed tomographic angiography to predict future acute coronary syndrome. *J Am Coll Cardiol* 2013;61:2296-2305.
  - (21) Brodoefel H, Burgstahler C, Heuschmid M, Reimann A, Khosa F, Kopp A, Schroeder S, Claussen CD, Clouse ME. Accuracy of dual-source CT in the characterisation of non-calcified plaque: use of a colour-coded analysis compared with virtual histology intravascular ultrasound. *Br J Radiol* 2009;82:805-812.
  - (22) Sianos G, Morel MA, Kappetein AP, Morice MC, Colombo A, Dawkins K, van den Brand M, Van DN, Russell ME, Mohr FW, Serruys PW. The SYNTAX Score: an angiographic tool grading the complexity of coronary artery disease. *EuroIntervention* 2005;1:219-227.
  - (23) Wykrzykowska JJ, Garg S, Girasis C, de VT, Morel MA, van Es GA, Buszman P, Linke A, Ischinger T, Klauss V, Corti R, Eberli F, Wijns W, Morice MC, Di MC, van Geuns RJ, Juni P,

- Windecker S, Serruys PW. Value of the SYNTAX score for risk assessment in the all-comers population of the randomized multicenter LEADERS (Limus Eluted from A Durable versus ERodable Stent coating) trial. *J Am Coll Cardiol* 2010;20;56:272-277.
- (24) Kappetein AP, Feldman TE, Mack MJ, Morice MC, Holmes DR, Stahle E, Dawkins KD, Mohr FW, Serruys PW, Colombo A. Comparison of coronary bypass surgery with drug-eluting stenting for the treatment of left main and/or three-vessel disease: 3-year follow-up of the SYNTAX trial. *Eur Heart J* 2011;32:2125-2134.
- (25) Chow BJ, Small G, Yam Y, Chen L, Achenbach S, Al-Mallah M, Berman DS, Budoff MJ, Cademartiri F, Callister TQ, Chang HJ, Cheng V, Chinnaiyan KM, Delago A, Dunning A, Hadamitzky M, Hausleiter J, Kaufmann P, Lin F, Maffei E, Raff GL, Shaw LJ, Villines TC, Min JK. Incremental prognostic value of cardiac computed tomography in coronary artery disease using CONFIRM: COroNary computed tomography angiography evaluation for clinical outcomes: an InteRnational Multicenter registry. *Circ Cardiovasc Imaging* 2011;4:463-472.
- (26) Rana JS, Dunning A, Achenbach S, Al-Mallah M, Budoff MJ, Cademartiri F, Callister TQ, Chang HJ, Cheng VY, Chinnaiyan K, Chow BJ, Cury R, Delago A, Feuchtner G, Hadamitzky M, Hausleiter J, Kaufmann P, Karlsberg RP, Kim YJ, Leipsic J, Labounty TM, Lin FY, Maffei E, Raff G, Villines TC, Shaw LJ, Berman DS, Min JK. Differences in prevalence, extent, severity, and prognosis of coronary artery disease among patients with and without diabetes undergoing coronary computed tomography angiography: results from 10,110 individuals from the CONFIRM (COroNary CT Angiography EvaluatioN For Clinical Outcomes): an InteRnational Multicenter Registry. *Diabetes Care* 2012;35:1787-1794.
- (27) Hadamitzky M, Achenbach S, Al-Mallah M, Berman D, Budoff M, Cademartiri F, Callister T, Chang HJ, Cheng V, Chinnaiyan K, Chow BJ, Cury R, Delago A, Dunning A, Feuchtner G, Gomez M, Kaufmann P, Kim YJ, Leipsic J, Lin FY, Maffei E, Min JK, Raff G, Shaw LJ, Villines TC, Hausleiter J. Optimized prognostic score for coronary computed tomographic angiography: results from the CONFIRM registry (COroNary CT Angiography EvaluatioN For Clinical Outcomes: An InteRnational Multicenter Registry). *J Am Coll Cardiol* 2013;62:468-476.
- (28) Hou ZH, Lu B, Gao Y, Jiang SL, Wang Y, Li W, Budoff MJ. Prognostic value of coronary CT angiography and calcium score for major adverse cardiac events in outpatients. *JACC Cardiovasc Imaging* 2012;5:990-999.





# Chapter 9

## Feasibility of automated quantitative assessment of serial computed tomography angiography to detect changes in coronary atherosclerosis

de Graaf MA, Ahmed W, de Graaf FR, Sieders A, Broersen A, Kitslaar PH, Dijkstra J, Bax JJ, Reiber JH, Scholte AJ.

*Submitted International Journal of Cardiovascular Imaging*

## Abstract

**Purpose:** The aim of this study was to evaluate the feasibility of quantitative computed tomography angiography (QCT) for the assessment of coronary atherosclerosis changes over time on serial coronary computed tomography angiography (CTA) in patients with stable chest pain.

**Methods:** The patient population consists of 53 patients clinically referred for the evaluation of chest pain who underwent a coronary CTA. After a minimum of 2 years CTA was repeated to evaluate changes in coronary atherosclerosis over time. For accurate and reproducible assessment of coronary artery disease (CAD) changes, all CTAs were quantitatively analysed using QAngioCT. All parameters of dimension and composition of CAD were compared between patients to assess possible regression and progression of CAD.

**Results:** Of the 53 patients, 32(60%) showed regression of coronary total atheroma volume (TAV) whereas 21(40%) showed progression of coronary atheroma. In patients with progression of coronary atheroma, median TAV<sub>indexed</sub> increase was 117.73(56.76; 236.01)mm<sup>3</sup> compared to -82.49(-114.17; -42.58)mm<sup>3</sup> for patients with regression. Patients with progression of coronary atheroma had progression of all four plaque types. However, patients with regression demonstrated a regression of all plaque components except for dense calcium, for which progression was observed.

**Conclusion:** The assessment of changes in CAD with QCT is feasible. In patients with stable chest pain syndrome both regression and progression of coronary atheroma is observed. Potentially QCT could be applied to assess the efficacy of anti-atherosclerotic therapy.

## Introduction

Progression of coronary atherosclerosis is of clinical importance. Serial intravascular ultrasound (IVUS) or invasive coronary angiography (ICA) studies have been used to assess progression of atherosclerosis over time, mostly as part of an evaluation on the efficacy of anti-atherosclerotic therapy.<sup>1</sup> However, these methods are invasive, time consuming and expensive. Computed tomography coronary angiography (CTA) is a suitable method for non-invasive assessment of coronary atherosclerosis. Its value in clinical practice has been extensively established.<sup>2,3</sup> For accurate and robust assessment of coronary atherosclerosis, novel quantitative computed tomography (QCT) algorithms are available which allow quantification of coronary atherosclerosis dimensions and composition.<sup>4,5</sup> The accuracy and reproducibility of these tools have been previously validated.<sup>6</sup> Potentially, these algorithms can be applied to quantify coronary atherosclerosis in serial CTA studies. Therefore, the aim of this study was to evaluate the feasibility of QCT for the assessment of coronary atherosclerosis changes over time on serial coronary CTA in patients with stable chest pain.

## Methods

### Patients

This prospective study included 137 patients clinically referred for the evaluation of chest pain to the Rijnland Hospital between July 2009 and June 2011. Patients underwent a non-contrast computed tomography (CT) scan for coronary artery calcium (CAC) score and coronary CTA. By protocol, after a minimum of 2 years CAC-score and CTA were repeated to evaluate changes in coronary atherosclerosis over time. Patients who had undergone prior, myocardial infarction, percutaneous coronary intervention (PCI) or coronary artery bypass graft surgery (CABG) were excluded. The clinical data were prospectively entered into the hospital's electronic patient file and retrospectively analysed. The Institutional Review Board approved this clinical study. Informed consent was obtained in all patients.

### CTA acquisition

All patients underwent a non-contrast and contrast coronary CTA. Contra-indications for CTA were, 1) impaired renal function (glomerular filtration rate  $<30$  ml/min/1.73m<sup>2</sup>), 2) pregnancy, 3) (supra-) ventricular arrhythmias, 4) known allergy to contrast agent, 5) severe claustrophobia. CTA was performed according to standard clinical practice using a Philips Brilliance 64-slice CT scanner. Prior to CTA examination, beta-blocking medication was administered if the heart rate was  $\geq 65$  beats

per minute, unless contra-indicated. Scan parameters were as follows: tube voltage 120kV, automated tube current modulation 250–400mA, pitch 0.2–0.3, collimation  $64 \times 0.625\text{mm}$ , and gantry rotation time 420ms. Images were acquired prospectively and reconstructed at 75% and at the best phase of the R-R interval. All data were stored for offline analysis. The CAC-score was calculated by the Agatston approach. Contrast CTA image quality was classified as: (1) good image quality (scans without motion artefacts), (2) moderate image quality (scans with motion artefacts or increased image noise) and (3) poor image quality (non-diagnostic scans); the last were excluded from the analysis.

### **Quantitative CTA**

For accurate and reproducible assessment of CAD changes, all CTAs were quantitatively analysed using QAngioCT Research Edition version 1.3.6 (Medis medical imaging systems, Leiden, The Netherlands). This software allows for quantitative assessment of both dimension and composition of coronary atherosclerosis. QCT was performed as previously described.<sup>4</sup> In brief, the following automatic processing steps were performed. The 3-dimensional coronary tree was automatically extracted from the coronary CTA dataset. Using an automatic tree labelling algorithm, the segments of the coronary tree were automatically labelled according to the American Heart Association (AHA) 17-segment model. The extracted and labelled coronary tree was verified by an experienced observer. Next, of each coronary, multiplanar reformations (MPRs) were constructed based on the centrelines of the detected coronaries. Thereafter, the lumen and vessel wall were automatically segmented using a previously validated software tool and coronary artery atherosclerosis dimension quantified.<sup>5</sup> If necessary, limited manual input was used to improve the automatic processing steps. With the help of a dedicated tissue characterization algorithm, coronary plaque composition was determined. This algorithm allows differentiating the detected coronary plaque into four different plaque types: fibrotic (FI) plaque, fibro-fatty (FF) plaque, necrotic core (NC) and dense calcium (DC). For the present study, a previously validated method using adaptive HU thresholds was used.<sup>5</sup>

The four major coronaries were studied (i.e. right coronary artery (RCA), left main (LM) artery, left anterior descending (LAD) artery and left circumflex (LCx) artery). Moreover, segments with cross-sectional lumen areas ( $<1.5\text{mm}^2$ ) were excluded as well as segments shorter than 10 mm. The reproducibility of this algorithm has been previously addressed.<sup>6</sup> The reported inter-observer concordance correlation coefficient was 0.96 for plaque burden and plaque area.

## Quantitative CTA atherosclerosis parameters

Figure 1 depicts the definitions of the quantitative derived CTA parameters of atherosclerosis dimensions and composition used in this study. For all four plaque types (i.e. FI, FF, NC, DC0) volumes and percentages were derived from the software. All parameters were indexed to the mean segment length of the total population to account for different segment lengths per patient and per scan providing the possibility to compare these parameters over time.<sup>1</sup> This was performed by calculating:

$$\text{Total volume}_{\text{indexed}(i)} = \frac{\text{total volume}}{\text{total segment length}} \times \text{mean segment length population}$$

To compare patients with regression and progression of coronary atheroma,  $\Delta\text{TAV}_i$  was calculated by subtracting  $\text{TAV}_{i \text{ baseline}}$  from  $\text{TAV}_{i \text{ follow-up}}$ . There is limited data in the literature to serve as a cut-off to define progression or regression of coronary atheroma volume on coronary CTA. To be as sensitive and accurate as possible, we prospectively determined that any change in  $\Delta\text{TAV}_i$  was considered as a change in coronary atheroma volume. Thus,  $\Delta\text{TAV}_i < 0 \text{ mm}^3$  was classified as regression and  $\Delta\text{TAV}_i > 0 \text{ mm}^3$  as progression of coronary atheroma volume. Subsequently, the change over time in volume of the different coronary plaque types in relation to  $\Delta\text{TAV}_i$  was established.

## Statistical analysis

For reasons of clarity, all continuous parameters are reported as mean  $\pm$  SD and median (interquartile range (IQR)). Categorical data are presented as absolute numbers and percentages. All analyses were performed on a patient-basis. First, both baseline and follow-up plaque characteristics were described. Moreover, the changes over time in these parameters were assessed. Second, a comparison was made between patients with progression or regression of coronary atheroma volume. The change over time in the different atherosclerosis parameters (dimension and composition)

Parameter	Definition
Segment length (mm)	Total distance between the proximal and distal point of the extracted segment.
Lumen volume (mm <sup>3</sup> )	Total volume of the vessel lumen of the extracted segment
Vessel wall volume (mm <sup>3</sup> )	Total volume of the vessel wall of the extracted segment
Total atheroma volume (TAV <sub>i</sub> ) (mm <sup>3</sup> )	Total vessel volume – total lumen volume.
Percentage atheroma volume (PAV) (%)	[(Total vessel volume – total lumen volume) / total vessel volume] x 100%.
Total (FI/FF/NC/DC) volume (mm <sup>3</sup> )	Total volume per plaque type
Percentage (FI/FF/NC/DC) (%)	[(Volume of plaque type – plaque volume) / total plaque volume] x 100%

Figure 1. Definitions of QCT plaque parameters.

was compared between patients with regression or progression of coronary atheroma volume. The baseline patient characteristics were compared between patients with regression or progression of coronary atheroma volume. Lastly, the difference in baseline plaque characteristics was compared between patients with regression or progression of coronary atheroma volume. All statistical tests were two-sided and a P-value <0.05 was considered statistically significant. All statistical analyses were performed with SPSS software (Version 20.0, SPSS Inc., Chicago, Illinois).

## Results

### Patient population

For this study, 137 consecutive patients were included with diagnostic qualitative CTA images. The flow diagram in Figure 2 illustrates the selection of patients eligible for inclusion as well as the reasons for exclusion. Of these patients, 65 did not have a follow-up appointment scheduled for logistic reasons or were lost to follow-up. Moreover, 7 patients only had a CAC-score at baseline. The remaining 65 patients completed the study with a CTA scan at baseline and follow-up. In 10 of the 65 patients, the CTA image quality was insufficient. Furthermore, 2 of the remaining 55 patients underwent revascularization between the two studies and were also excluded. In total, 53 patients with 377 segments were analysed. The median time between baseline and follow-up CTA was 25 (IQR 24-26) months. The patient characteristics at baseline and follow-up are listed in Table 1. Mean age was  $54 \pm 8.7$  years and 28 (52.8%) of the patients were male. At baseline, 30% of patients received

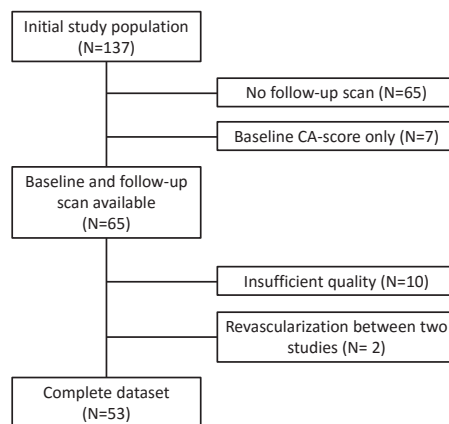


**Figure 2. Flowchart of the study population.**

**Table 1. Patient characteristics.**

<b>Patient characteristics (n=53)</b>	<b>Baseline</b>	<b>Follow-up</b>
Age (yrs.)	54 ± 8.7	N/A
Gender (% male)	28 (52%)	N/A
Non AP complaints	8 (15%)	9 (17%)
AP Complaints	45 (85%)	44 (83%)
Atypical AP complaints	32 (60%)	29 (55%)
Typical AP complaints	12 (22%)	14 (26%)
Typical and Atypical AP complaints	1 (2%)	1 (2%)
Cardiovascular risk factors		
Hypertension†	18 (34%)	17 (32%)
Hypercholesterolemia ‡	6 (11%)	6 (11%)
Diabetes Mellitus	4 (8%)	5 (9%)
Family history of CAD*	37 (70%)	N/A
Current Smoking	12 (23%)	12 (23%)
Ex-Smoker	9 (17%)	9 (17%)
Obesity (BMI ≥ 30 kg/m <sup>2</sup> )	2 (4%)	2 (4%)
Medication		
ACE/ATII	8 (15%)	8 (15%)
Calcium channel blockers	4 (8%)	7(13%)
NTG	7 (13%)	9 (17%)
Beta blockers	20 (38%)	16 (30%)
Diuretics	7 (13%)	7 (13%)
Asprin	19 (36%)	20 (38%)
Statines	16 (30%)	22 (42%)
Triglycerides	1.31 ± 0.59	1.20 ± 0.50
Cholesterol	5.53 ± 0.84	5.02 ± 1.38
HDL Cholesterol	1.61 ± 0.57	1.54 ± 0.61
LDL Cholesterol	3.44 ± 0.80	2.90 ± 1.04
VLDL Cholesterol	0.44 ± 0.50	0.42 ± 0.50
Creatinine	82.54 ± 13.03	79.58 ± 16.72
Agatston CAC score	35 ± 60 1.00 (IQR 0 – 51)	51 ± 77 18 (0 – 73)
Increase in Agatston CAC score		15 ± 25 5 (0 – 20)

Data are represented as mean ± SD, median (interquartile range) or as number and percentages of patients.

†Defined as systolic blood pressure ≥140 mmHg or diastolic blood pressure ≥90 mmHg or treatment for hypertension

‡Serum total cholesterol ≥230 mg/dL or serum triglycerides ≥200 mg/dL or treatment with lipid lowering drugs.

\*Defined as the presence of coronary artery disease in first-degree family members at <55 years in men and <65 years in women.

Abbreviations: ACE: Angiotensin Converting Enzyme, AP: Angina pectoris, BMI: body mass index, CAC: coronary artery calcium, IQR: Interquartile Range, NTG: Nitro-glycerine

statins, compared to 42% at follow-up. The mean Agatston CAC-score at baseline was  $35 \pm 60$  compared to  $51 \pm 77$  at follow-up.

### Comparison of QCT parameters between baseline and follow-up

Both baseline and follow-up coronary artery plaque characteristics were reported on a patient-basis (Table 2). The percentage atheroma volume (PAV) was 34.6(32.6-39.3)% at baseline and 36.1(32.5-41.2)% at follow-up, ( $P=0.241$ ). The  $TAV_i$  significantly increased from  $737.6(629.1-901.5)\text{mm}^3$  at baseline, to  $812.7(687.9-951.6)\text{mm}^3$  at follow-up ( $P=0.043$ ). Overall, the median increase in  $TAV_i$  was 5.10(-6.32-16.71)%. Overall both  $NC_i$  and  $DC_i$  were significantly increased at follow-up.  $NC_i$  had increased from  $20.33(6.45-41.30)\text{mm}^3$  to  $29.66(11.45-49.09)\text{mm}^3$ ,  $DC_i$  had increased from  $5.36(2.07-12.75)\text{mm}^3$  to  $9.63(2.79-24.00)\text{mm}^3$ . Figure 3 presents a case example with progression of atherosclerosis.

**Table 2. QCT plaque characteristics.**

Baseline and follow-up plaque quantitative parameters	Baseline	Follow-Up	Change	P-Value
Percent atheroma volume (PAV) (%)				
Mean $\pm$ SD	$36.0 \pm 5.31$	$37.1 \pm 5.51$	$1.10 \pm 4.52$	
Median (IQR)	34.6 (32.6-39.3)	36.1 (32.5-41.2)	0.33 (-1.97-3.63)	0.241
Total atheroma volume ( $TAV_i$ ) ( $\text{mm}^3$ )				
Mean $\pm$ SD	$768.1 \pm 182.8$	$832.8 \pm 237.4$	$64.78 \pm 208.65$	
Median (IQR)	737.6 (629.1-901.5)	812.7 (687.9-951.6)	34.80 (-58.95-175.91)	<0.043
% Change in total atheroma volume				
Mean $\pm$ SD			$8.49 \pm 22.08$	
Median (IQR)			5.10 (-6.32-16.71)	
Total fibrotic tissue volume ( $FI_i$ ) ( $\text{mm}^3$ )				
Mean $\pm$ SD	$285.18 \pm 89.07$	$308.25 \pm 109.57$	$23.07 \pm 85.60$	
Median (IQR)	270.81 (222.68-332.13)	303.19 (227.81-367.70)	17.80 (-41.42-77.25)	0.079
Total fibro-fatty tissue volume ( $FF_i$ ) ( $\text{mm}^3$ )				
Mean $\pm$ SD	$89.32 \pm 48.96$	$100.49 \pm 50.60$	$11.17 \pm 49.98$	
Median (IQR)	69.23 (47.16-128.50)	94.56 (57.10-128.46)	5.66 (-14.70-22.12)	0.186
Total necrotic core volume ( $NC_i$ ) ( $\text{mm}^3$ )				
Mean $\pm$ SD	$24.75 \pm 19.38$	$36.18 \pm 35.43$	$11.42 \pm 36.15$	

**Table 2. (Continued)**

<b>Baseline and follow-up plaque quantitative parameters</b>	<b>Baseline</b>	<b>Follow-Up</b>	<b>Change</b>	<b>P-Value</b>
Median (IQR)	20.33. (6.45-41.30)	29.66 (11.45-49.09)	5.08 (-0.14-14.14)	<0.001
Total dense calcium volume (DC <sub>i</sub> ) (mm <sup>3</sup> )				
Mean ± SD	10.51 ± 11.59	17.25 ± 22.40	6.74 ± 13.73	
Median (IQR)	5.36 (2.07-12.75)	9.63 (2.79-24.00)	2.23 (-0.29-9.99)	<0.001
% fibrotic tissue				
Mean ± SD	36.77 ± 4.33	36.53 ± 4.38	-0.25 ± 4.22	
Median (IQR)	36.10 (34.20-39.65)	36.49 (33.58-39.35)	0.06 (-3.58-2.95)	0.821
% fibro-fatty tissue				
Mean ± SD	11.00 ± 4.13	11.59 ± 3.39	0.59 ± 3.87	
Median (IQR)	10.06 (7.67-14.60)	12.10 (8.27-14.59)	-0.01 (-1.49-1.58)	0.767
% necrotic core				
Mean ± SD	2.95 ± 1.99	3.93 ± 2.61	0.98 ± 2.65	
Median (IQR)	2.69 (1.03-4.63)	3.79 (1.93-5.17)	0.57 (-0.09-1.79)	<0.001
% dense calcium				
Mean ± SD	1.34 ± 1.34	2.04 ± 2.36	0.70 ± 1.44	
Median (IQR)	0.90 (0.29-1.93)	1.27 (0.34-2.63)	0.28 (-0.22-1.07)	<0.001

### **Patients with regression vs. progression of coronary atheroma volume**

Of the 53 patients, 32(60%) showed regression of coronary atheroma volume ( $\Delta TAV_i < 0 \text{ mm}^3$ ) whereas 21(40%) showed progression of coronary atheroma volume ( $\Delta TAV_i > 0 \text{ mm}^3$ ). In 29 (55%) patients an increase in PAV was observed, whereas 24 (45%) patients showed a decrease in PAV. Moreover, 26 (49%) patients had an increase in PAV >1%, which is considered a relevant threshold for significant change under intensive lipid-lowering therapy in clinical studies.<sup>7, 8</sup> A decrease in PAV >1% was observed in 22 (42%) patients. As depicted in Table 3, in patients with progression of coronary atheroma volume, median  $TAV_i$  increase was 117.73(56.76; 236.01)mm<sup>3</sup>. Patients with regression of coronary atheroma volume presented with a median decrease in  $TAV_i$  of -82.49(-114.17; -42.58) mm<sup>3</sup>. Of particular interest, in patients with regression of coronary atheroma volume an increase in total DC<sub>i</sub> volume was observed 0.42(-0.96; 5.50) mm<sup>3</sup>. The other plaque types showed regression in these patients. In contrast, patients with progression of coronary atheroma volume,

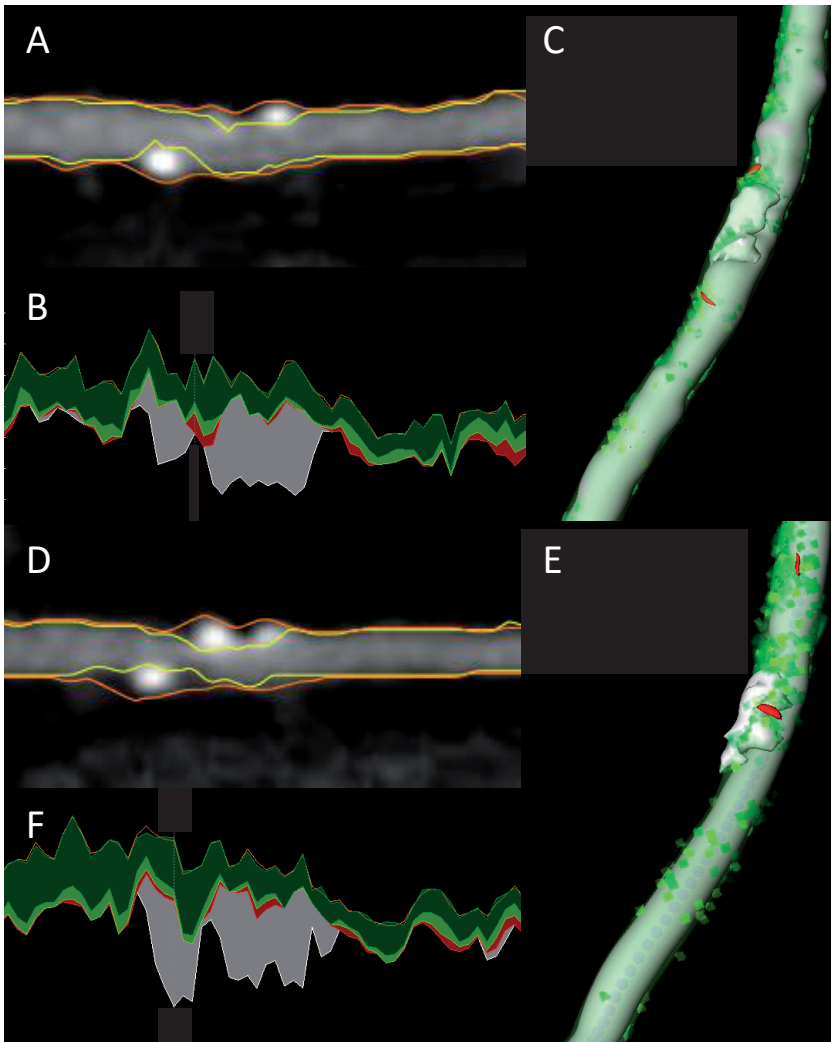


**Figure 3. Case example of a case with progression of coronary atherosclerosis.**

Example of a the left anterior descending (LAD) artery of 48 years old female with stable angina. Panel A show the multiplanar reformation (MPR) of the LAD at baseline. Panel B demonstrated the corresponding quantitative computed tomography data; the lower part of the graphs represents the lumen cross-sectional area, the upper part the vessel wall cores sectional area. The part between the graphs represents the plaque area. Dark-green represent fibrotic plaque, the light-green represent fibro-fatty plaque, red marks necrotic core and white marks dense calcium. Panel C shows a 3D-representation of the coronary vessel with the same color coding. Panel D-F represent the same vessel but after two year follow-up. Overall, progression of atherosclerosis is observed, specifically of calcified plaque.

**Table 3. Comparison of change in coronary plaque dimension and composition over time between patients with regression vs. progression of coronary atheroma volume.**

Change in plaque quantitative parameters	Regression of coronary atheroma volume (n=21)	Progression of coronary atheroma volume (n=32)	P-Value
Change in PAV			
Mean ± SD	-2.63 ± 1.88	4.19 ± 3.63	
Median (IQR)	-2.18 (-3.60; -1.10)	3.08 (1.08; 7.81)	NA
Change TAV <sub>i</sub>			
Mean ± SD	-104.81 ± 101.12	176.07 ± 184.82	
Median (IQR)	-82.49 (-114.17; -42.58)	117.73 (56.76; 236.01)	NA
Change in total fibrotic tissue volume (F <sub>i</sub> ) (mm <sup>3</sup> )			
Mean ± SD	-46.00 ± 49.07	68.40 ± 73.38	
Median (IQR)	-49.09 (-64.74; -10.48)	59.11 (24.60; 107.86)	NA
Change in total fibro-fatty tissue volume (FF <sub>i</sub> ) (mm <sup>3</sup> )			
Mean ± SD	-20.35 ± 33.06	31.86 ± 48.68	
Median (IQR)	-15.68 (-28.43; 2.20)	14.13 (2.08; 47.13)	NA
Change in total necrotic core volume (NC <sub>i</sub> ) (mm <sup>3</sup> )			
Mean ± SD	-4.92 ± 17.69	22.15 ± 41.11	
Median (IQR)	0.53 (-8.12; 6.50)	10.55 (3.68; 26.55)	NA
Change in dense calcium volume (DC <sub>i</sub> ) (mm <sup>3</sup> )			
Mean ± SD	3.29 ± 14.27	9.00 ± 13.10	
Median (IQR)	0.42 (-0.96; 5.50)	6.29 (0.41; 14.72)	NA

showed an increase in volume of all four plaque types. The differences in baseline characteristics between patients with regression and patients with progression of coronary atheroma volume were assessed. Besides hypercholesterolemia, there were no significant differences between the two patients groups. Worth mentioning, there was no difference in increase in CAC-score between patients with regression or progression of coronary atheroma volume. Table 4 demonstrates the difference in baseline coronary atherosclerosis dimensions and composition between patients with regression or progression of coronary atheroma volume. Patients with regression of coronary atheroma had significantly higher baseline PAV compared to patients with progression of disease (36.64% (33.72; 40.62) vs 33.44% (31.50; 37.58), P=0.040). Both groups had comparable baseline composition of coronary atherosclerosis.

**Table 4. Comparison of baseline coronary plaque dimensions and composition between patients with regression vs. progression of coronary atheroma volume.**

Baseline plaque quantitative parameters	Regression of coronary atheroma volume (n=21)	Progression of coronary atheroma volume (n=32)	P-Value
Baseline PAV (N)			
Mean $\pm$ SD	37.80 $\pm$ 5.88	34.76 $\pm$ 4.60	
Median (IQR)	36.64 (33.72; 40.62)	33.44 (31.50; 37.68)	0.040
Baseline TAV <sub>i</sub> (N)			
Mean $\pm$ SD	801.09 $\pm$ 132.59	746.38 $\pm$ 208.59	
Median (IQR)	810.78 (697.84; 905.59)	695.04 (570.18; 856.84)	0.102
Baseline % fibrotic tissue (FI)			
Mean $\pm$ SD	69.88 $\pm$ 8.38	72.13 $\pm$ 9.80	
Median (IQR)	69.69 (64.00; 76.20)	73.82 (63.28; 78.11)	0.536
Baseline % fibro-fatty tissue (FF)			
Mean $\pm$ SD	21.83 $\pm$ 5.16	20.02 $\pm$ 7.07	
Median (IQR)	21.70 (17.51; 25.81)	18.77 (15.46; 25.54)	0.335
Baseline % necrotic core (NC)			
Mean $\pm$ SD	5.96 $\pm$ 3.34	5.10 $\pm$ 3.55	
Median (IQR)	5.97 (2.92; 8.06)	3.75 (2.08; 8.49)	0.383
Baseline % dense calcium (DC)			
Mean $\pm$ SD	2.32 $\pm$ 2.71	2.75 $\pm$ 2.52	
Median (IQR)	1.21 (0.38; 2.83)	2.16 (0.85; 4.04)	0.317

## Discussion

The present study addressed the feasibility of a novel CTA quantification tool to assess changes of coronary atherosclerosis in a CTA population evaluated for stable chest pain. In addition to the assessment of progression of coronary atheroma volume, the change in specific coronary plaque components was assessed. In 40% of the patients progression of coronary atheroma volume was observed, whereas 60% showed regression of atheroma volume. Patients with progression of coronary atheroma had progression of all four plaque types. However, patients with regression of atheroma demonstrated a regression of all plaque components except for dense calcium, for which progression was observed.

## Assessments of coronary atherosclerosis progression

Currently, the standard for evaluating coronary atherosclerosis changes is IVUS. This method allows evaluation of lumen and vessel wall dimensions as well as assessment of coronary atheroma volume. By applying radiofrequency backscatter analysis, IVUS Virtual Histology (VH) allows for assessment of coronary plaque components. IVUS VH has been validated against histopathology.<sup>9</sup> Both IVUS and IVUS VH are often used in studies assessing coronary atherosclerosis progression or regression.<sup>1, 10-13</sup> However, since IVUS is an invasive and costly method, new research has focused on the value of CTA for the assessment of coronary atherosclerosis progression. By applying novel imaging quantification tools, coronary atherosclerosis dimension can be quantified on CTA and used to follow-up changes of atherosclerosis in patients.<sup>4, 6</sup> The validity of these tools has been established and QCT has become accepted as a research tool. More recently, using a Hounsfield Unit (HU) threshold, different plaque components can be individually assessed and quantified using QCT.<sup>5</sup> This allows for a more advanced assessment of coronary atherosclerosis, similar to IVUS VH. Especially with decreasing radiation exposures for CTA, QCT techniques become more available for serial evaluation of coronary atherosclerosis. Another advantage of CTA over IVUS is that CTA allows for visualization of the entire coronary artery tree, whereas IVUS only allows assessment of large coronaries in which a catheter can be introduced. However, a major advantage of IVUS is the higher spatial resolution as compared to CTA. This allows for assessment of more subtle changes in coronary atherosclerosis.<sup>14</sup>

## Quantification of CAD progression on CTA

Previous studies have focussed on the validity of quantifying CAD progression with CTA and quantification software. Papadopoulou *et al.* studied the natural history of coronary atherosclerosis in 32 patients with acute coronary syndrome.<sup>8</sup> Patients were serially scanned with a mean interval of 39 months. Overall, the mean change in TAV was 6.7% and 34% of the patients demonstrated regression of coronary atherosclerosis, whereas 44% showed progression of disease. More recent investigations have addressed the feasibility of CTA to study plaque progression or regression as influenced by statin therapy. Hoffman *et al.* performed a second CTA in 63 patients who had 18-36 month earlier been clinically referred to CTA.<sup>15</sup> Using commercially available software coronary atherosclerosis was quantified in a volumetric approach. It was demonstrated that statin therapy induced a decrease in the growth rate of non-calcified plaque but not of plaques containing calcium (i.e. mixed or calcified plaque). Similarly, Zeb *et al.* included 100 patients who underwent serial CTA with a mean interval of 13 months.<sup>16</sup> In statin users, total plaque progression was significantly reduced compared to non-statin users ( $33.3 \text{ mm}^3 \pm 90.5$  vs.  $31.0 \text{ mm}^3 \pm 84.5$ ).

Moreover, a significantly larger reduction in non-calcified plaque was observed in statin users compared to non-statin users. However, in both groups an increase in calcium was noted on the CTA. It seems that anti-atherosclerotic therapy leads to a reduction of non-calcified plaque without affecting the growth-rate of calcified plaque. Similarly, in the present study, in patients with regression of coronary atheroma volume over time, an increase in calcium volume was observed. This has previously been shown in several IVUS VH studies that investigated the change in coronary plaque composition over time influenced by statin therapy.<sup>10-13</sup> In the majority of these studies, the volume and relative percentage of NC, FI or FF changed over time in patients receiving statin therapy. However, in none of the studies a significant change in DC was noted neither in patients receiving statin therapy, nor in the control cases.

### **Limitations**

The study is hampered by some limitations. First, the study included a limited number of patients. Therefore the lack of significant differences in baseline characteristics between patient groups should be considered with care. Second, the patients were relatively disease free (mean CAC-score 35) and the results cannot be extrapolated to a population with a higher disease burden. Moreover, in current literature there is limited evidence for standard procedures for serial plaque imaging on coronary CTA. We have used a very sensitive parameter to define regression or progression of coronary atherosclerosis, namely any change in TAV. However, establishing standard procedures for assessing changes on CTA is needed. Additionally there was no reference data to compare the quantification results with (i.e. no IVUS or ICA); therefore the present study should be seen as a feasibility study.

### **Conclusion**

The assessment of changes in CAD with QCT is feasible. In patients with stable chest pain both regression and progression of coronary atheroma is observed. Potentially QCT could be applied to assess the efficacy of anti-atherosclerotic therapy.

## References

- (1) Nicholls SJ, Sipahi I, Schoenhagen P, Crowe T, Tuzcu EM, Nissen SE. Application of intravascular ultrasound in anti-atherosclerotic drug development. *Nat Rev Drug Discov* 2006 June;5(6):485-92.
- (2) von Ballmoos MW, Haring B, Juillerat P, Alkadhi H. Meta-analysis: diagnostic performance of low-radiation-dose coronary computed tomography angiography. *Ann Intern Med* 2011 March 15;154(6):413-20.
- (3) Bamberg F, Sommer WH, Hoffmann V *et al.* Meta-analysis and systematic review of the long-term predictive value of assessment of coronary atherosclerosis by contrast-enhanced coronary computed tomography angiography. *J Am Coll Cardiol* 2011 June 14;57(24):2426-36.
- (4) de Graaf MA, Broersen A, Ahmed W *et al.* Feasibility of an automated quantitative computed tomography angiography-derived risk score for risk stratification of patients with suspected coronary artery disease. *Am J Cardiol* 2014 June 15;113(12):1947-55.
- (5) de Graaf MA, Broersen A, Kitslaar PH *et al.* Automatic quantification and characterization of coronary atherosclerosis with computed tomography coronary angiography: cross-correlation with intravascular ultrasound virtual histology. *Int J Cardiovasc Imaging* 2013 June;29(5):1177-90.
- (6) Papadopoulou SL, Garcia-Garcia HM, Rossi A *et al.* Reproducibility of computed tomography angiography data analysis using semiautomated plaque quantification software: implications for the design of longitudinal studies. *Int J Cardiovasc Imaging* 2013 June;29(5):1095-104.
- (7) Nissen SE, Nicholls SJ, Sipahi I *et al.* Effect of very high-intensity statin therapy on regression of coronary atherosclerosis: the ASTEROID trial. *JAMA* 2006 April 5;295(13):1556-65.
- (8) Papadopoulou SL, Neefjes LA, Garcia-Garcia HM *et al.* Natural history of coronary atherosclerosis by multislice computed tomography. *JACC Cardiovasc Imaging* 2012 March;5(3 Suppl):S28-S37.
- (9) Nasu K, Tsuchikane E, Katoh O *et al.* Accuracy of in vivo coronary plaque morphology assessment: a validation study of in vivo virtual histology compared with in vitro histopathology. *J Am Coll Cardiol* 2006 June 20;47(12):2405-12.
- (10) Kawasaki M, Sano K, Okubo M *et al.* Volumetric quantitative analysis of tissue characteristics of coronary plaques after statin therapy using three-dimensional integrated backscatter intravascular ultrasound. *J Am Coll Cardiol* 2005 June 21;45(12):1946-53.
- (11) Prasad A, Cipher DJ, Prasad A *et al.* Reproducibility of intravascular ultrasound virtual histology analysis. *Cardiovasc Revasc Med* 2008 April;9(2):71-7.
- (12) Ogasawara D, Shite J, Shinke T *et al.* Pioglitazone reduces the necrotic-core component in coronary plaque in association with enhanced plasma adiponectin in patients with type 2 diabetes mellitus. *Circ J* 2009 February;73(2):343-51.
- (13) Hong MK, Park DW, Lee CW *et al.* Effects of statin treatments on coronary plaques assessed by volumetric virtual histology intravascular ultrasound analysis. *JACC Cardiovasc Interv* 2009 July;2(7):679-88.
- (14) Kruk M, Wardziak L, Mintz GS *et al.* Accuracy of coronary computed tomography angiography vs intravascular ultrasound for evaluation of vessel area. *J Cardiovasc Comput Tomogr* 2014 March;8(2):141-8.

## Chapter 9

- (15) Hoffmann H, Frieler K, Schlattmann P, Hamm B, Dewey M. Influence of statin treatment on coronary atherosclerosis visualised using multidetector computed tomography. *Eur Radiol* 2010 December;20(12):2824-33.
- (16) Zeb I, Li D, Nasir K *et al.* Effect of statin treatment on coronary plaque progression - a serial coronary CT angiography study. *Atherosclerosis* 2013 December;231(2):198-204.





# Part 2

Clinical aspects coronary CTA in high risk diabetic patients without chest pain syndrome



# Chapter 10

Changes in ischaemia as assessed with single-photon emission computed tomography myocardial perfusion imaging in high-risk patients with diabetes without cardiac symptoms: relation with coronary atherosclerosis on computed tomography coronary angiography

de Graaf MA, Roos CJ, Mansveld JM, Kharagjitsingh AV, Dibbets-Schneider P, Kroft LJ, Jukema JW, Ficarò EP, Bax JJ, Scholte AJ.

European Heart Journal Cardiovascular Imaging 2015;16:863-870

## Abstract

**Purpose:** The study aims 1) to evaluate changes in myocardial ischemia on single photon emission computed tomography (SPECT) myocardial perfusion imaging (MPI) after 2 years in a cohort of high risk patients with diabetes without cardiac symptoms or known coronary artery disease (CAD) and 2) to assess the value of baseline computed tomography coronary angiography (CTA) derived coronary atherosclerosis parameters to predict changes in myocardial ischemia.

**Methods:** The population consisted of 100 high risk patients with diabetes without cardiac symptoms referred for cardiovascular risk stratification. All patients underwent coronary artery calcium (CAC) scoring, CTA and SPECT MPI. After 2 years follow-up, SPECT MPI was repeated to evaluate potential progression of ischemia.

**Results:** In total, 20% of patients presented with ischemia at baseline. Of these 20 patients, 7 (35%) still had ischemia at follow-up, whereas 13 (65%) showed resolution and 4(20%) showed progression of ischemia at follow-up. Of the 80 patients without ischemia at baseline, 65 (81%) had a normal MPI at follow-up and 15 patients (19%) presented with new ischemia. There were no significant differences in the CAC score or the extent, severity and composition of CAD on CTA between patients with and without ischemia at baseline. Similarly, no differences could be demonstrated between patients with and without ischemia at follow-up or between patients with and without progression of ischemia.

**Conclusion:** The rate of progression of ischemia in high risk patients with diabetes without cardiac symptoms is limited. Few patients presented with new ischemia, whereas some patients show resolution of ischemia. Atherosclerosis parameters on CTA were not predictive of new onset ischemia or progression of ischemia.

## Introduction

Cardiovascular death is the main cause of death in patients with diabetes mellitus (DM).<sup>1</sup> Moreover, patients with DM often have silent myocardial ischemia on single photon emission tomography (SPECT) myocardial perfusion imaging (MPI) and coronary artery disease (CAD) in an advanced stage on coronary computed tomography angiography (CTA).<sup>2-8</sup> After 2-3 years of follow-up, a limited number of patients present with new ischemia.<sup>9</sup> However, no clinical variables predictive of new ischemia have yet been established. Potentially, atherosclerotic plaque characteristics on CTA could be associated with the onset of new ischemia. Therefore, the aim of this study was to: 1) evaluate changes in myocardial ischemia after 2 years in a cohort of high risk patients with diabetes without cardiac symptoms and 2) to assess the value of baseline CTA derived coronary atherosclerosis parameters to predict changes in myocardial ischemia on SPECT MPI in these patients.

## Methods

### Patients

The patient population consisted of 159 high risk patients with diabetes without cardiac symptoms referred from a diabetic out-patient clinic for cardiovascular risk stratification as previously described.<sup>10, 11</sup> Inclusion criteria for the study were: confirmed diagnosis of type 2 DM, normal resting electrocardiogram (ECG), absence of cardiac symptoms. Patients with known CAD or treated with anti-anginal medication were excluded, as well as patients with a previous stress test or coronary angiography. All patients underwent clinical evaluation, including laboratory testing, coronary artery calcium (CAC) scoring, coronary CTA and SPECT MPI between May 2005 and January 2006. After 2 years follow-up, SPECT MPI was repeated as prospectively scheduled to evaluate myocardial ischemia as indicated in the guidelines that were applicable at that time.<sup>12</sup> Patients were treated according standard clinical care and based on test results.

The patient's medical records were evaluated to assess if the patient underwent coronary revascularization between the 2 SPECT MPI studies. Clinical data were prospectively entered into the departmental Cardiology Information System (EPD-Vision©, Leiden University Medical Center, the Netherlands) and retrospectively analysed. The Institutional Review Board of the Leiden University Medical Center approved this retrospective evaluation of clinically collected data, and waived the need for written informed consent.

## **SPECT myocardial perfusion imaging**

### **Image acquisition.**

ECG-gated technetium-99m sestamibi ( $^{99m}\text{Tc}$ -sestamibi; 1000MBq) SPECT MPI was performed using a 2-day stress and rest protocol. Patients had to refrain from caffeine-containing products 24-hours before testing. Vasodilator stress was performed using adenosine (140 $\mu\text{g}/\text{kg}/\text{minute}$ , intravenous for 6 minutes) with simultaneous handgrip exercise. Blood pressure and 12-lead ECG were recorded during adenosine stress. SPECT imaging was performed, 120 minutes after injection of the radiopharmaceutical, using a triple-head SPECT gamma camera (GCA 9300/HG, Toshiba Corporation, Tokyo, Japan). Images were acquired using a circular 360 degrees orbit in 64 projections and 20 second per projection.<sup>13</sup> Attenuation correction was not performed.

### **Quantification of myocardial ischemia.**

The SPECT MPI datasets were sent to an independent, dedicated core-lab (INVIA, Ann Arbor, Michigan, USA), blinded of patients' history or scan order. By using Corridor4DM (INVIA, Ann Arbor, Michigan, USA), myocardial perfusion and reversibility (ischemia) was quantified as follows.<sup>14, 15</sup> First, the stress dataset was normalized to the maximum pixel intensity within the myocardium; all values were multiplied by 100/value of the maximum pixel. Second, the rest dataset was normalized in the same manner using the peak in the location of the peak intensity in the stress map. The extent of hypoperfusion in the stress study was expressed as a percentage of the entire left ventricle. Comparing the rest and the stress study, allowed for assessment of reversibility by comparing the areas of hypoperfusion on the stress study to the same areas in the rest study; a  $\geq 10\%$  increase in tracer uptake was used to define reversibility. Reversibility was expressed as percentage of the entire left ventricle. Change in ischemia was calculated as the differences in reversibility between the baseline and follow-up study. To facilitate the analysis, patients were stratified into two groups based on differences in reversibility between the baseline and follow-up study. Any increase in ischemia was defined as progression, whereas a decrease in ischemia was defined as regression.

## **Coronary computed tomography angiography**

### **Image acquisition.**

Patients were scanned with either a 64-slice CT scanner (Aquilion 64, Toshiba Medical System, Otowara, Japan) or a 320-row volumetric scanner (Aquilion ONE, Toshiba Medical System, Otowara, Japan). Contra-indications for CTA were, 1) impaired renal function (glomerular filtration rate  $< 60 \text{ ml}/\text{min}/1.73\text{m}^2$ ), 2) pregnancy, 3) (supra-

ventricular arrhythmias, 4) known allergy to contrast agent, 5) severe claustrophobia. Non-contrast CT and contrast CTA were performed according to standard clinical practice. Prior to CT examination, beta-blocking medication was administered if the heart rate was  $\geq 65$  beats per minutes, unless contra-indicated. Datasets were sent to a remote workstation for analysis.

### **Image analysis.**

Evaluation of the CTA was performed on a dedicated workstation (Vitrea FX, Vital Images, Minnetonka, MN, USA). For each patient the Agatston CAC score was measured. Thereafter, the CTA datasets were evaluated for the presence, severity and composition of coronary atherosclerosis as previously described.<sup>16</sup> In brief, each segment of the coronary tree was scored as normal ( $<30\%$ ), non-obstructive ( $30-50\%$ ) or obstructive ( $\geq 50\%$ ) CAD. Coronary plaque composition was assessed as non-calcified, calcified or mixed-plaque. Per patient, the number of segments with atherosclerosis and the number of each type of plaque were assessed. Significant coronary artery disease was defined by the presence of a coronary lesion with  $\geq 50\%$  stenosis.

### **Statistical analysis**

For reasons of uniformity summary statistics for all continuous data are presented as mean  $\pm$  SD. Normality of the data was confirmed by comparing the histogram with a normal probability curve. Categorical data are presented as absolute numbers and percentages. First, clinical patient characteristics were compared between patients with and without ischemia at baseline. Second, in a similar fashion, patients with and without ischemia at follow-up were compared. Third, patients with and without progression of ischemia were compared likewise. Thereafter, the CTA parameters of the extent, severity and composition of coronary atherosclerosis were compared between all patient groups. Statistical significance was assessed using non-parametric tests for continuous data with a non-normal distribution and t-test for data with a normal distribution. Chi-square tests were applied to categorical data. All statistical tests were two-sided and a P-value  $<0.05$  was considered statistically significant. All statistical analyses were performed with SPSS software (Version 20.0, SPSS Inc., Chicago, Illinois).

## **Results**

### **Patient characteristics**

The population consisted of 159 patients. In 36 patients, one of the two SPECT MPI studies was not performed (for logistical reasons). The datasets of the remaining

123 patients were sent to an independent core-lab for quantification of myocardial ischemia. In 16 patients quantitative analysis could not be performed due to protocol violations or insufficient image quality. The results of 107 patients were available for analysis, 7 patients underwent planned revascularization between the two studies and were therefore excluded. The final patient cohort consisted of 100 patients. Table 1 demonstrates the baseline characteristics of the population. In total, 62 patients were male, half of the patients presented with hypertension or hypercholesterolemia. Mean diabetes duration was  $113 \pm 87$  months. In Table 1, the medical therapy at baseline is described. In total, 52 patients received statin therapy, 17 aspirin and 31 ACE-inhibitors. At follow-up, in 23 patients statin therapy was added and 8 patients received additional ACE-inhibitors. Aspirin was added in 22 patients. At follow-up, 19 patients received anti-angina medication (i.e. beta-blockers, calcium-antagonists or nitrates).

### **SPECT MPI results**

Median time between the 2 SPECT MPI studies was 30 (IQR 27-33) months. As shown in Figure 1, 20% of patients presented with ischemia at baseline, without need of revascularization. Of these 20 patients, 7 (35%) patients still had ischemia at follow-up, whereas 13 (65%) patients showed resolution of ischemia and 4 showed progression of ischemia at follow-up. Of the 80 of patients without ischemia at baseline, 65 (81%) had a normal study at follow-up and 15 patients (19%) presented with new ischemia. Figure 2 demonstrates the rate of progression of ischemia. In patients with a normal baseline SPECT MPI, 19% of the patients presented with progression of ischemia. In Table 1, the baseline results stratified according to the presence of baseline ischemia are demonstrated. Except for family history and low-density lipoprotein (LDL)-cholesterol, there were no significant differences between patients with or without myocardial ischemia at baseline. In Table 2, the difference in characteristics between patients with and without ischemia at follow-up is shown. Remarkably, there were no significant differences between both patients groups. Table 3 summarizes the differences between baseline characteristics between patients with and without progression of ischemia. DM duration was significantly longer among patients who showed progression of ischemia ( $180 \pm 97$  vs.  $135 \pm 83$  months,  $P=0.049$ ). The remaining baseline characteristics were comparable between patients with and without progression of ischemia. At follow-up, 5 patients presented with onset of chest-pain, of which 1 had progression of ischemia and 4 presented without new ischemia. Of the 19 patients in whom anti-anginal medication was added, 2 presented with progression of ischemia ( $P=0.295$ ). There was no relation between the onset of symptoms and new ischemia or progression of ischemia.

**Table 1. Clinical characteristics of the population in relation to baseline ischemia.**

	<b>Total ( N=100)</b>	<b>Ischemia (n=20)</b>	<b>No ischemia (n=80)</b>	<b>P- value</b>
Age(years)	53 ± 10	54 ± 11	53 ± 10	0.791
Gender(% male)	62 (62%)	15 (75%)	47 (59%)	0.181
Hypertension† n(%)	52 (52%)	7 (35%)	45 (56%)	0.089
Hypercholesterolemia‡ n(%)	51 (51%)	11 (55%)	40 (50%)	0.689
Family history of CAD* n(%)	56 (65%)	5 (25%)	51 (64%)	<b>0.002</b>
Smoking n(%)	19 (19%)	6 (30%)	13 (13%)	0.161
<b>Diabetes-related factors</b>				
Age at time of diagnosis(years)	43 ± 12	45 ± 15	43 ± 11	0.443
Diabetes duration(months)	113 ± 87	99 ± 95	117 ± 85	0.409
HbA <sub>1c</sub> (%)	7.5 ± 1.6	7.7 ± 1.5	7.5 ± 1.7	0.633
<b>Diabetes-related complications</b>				
PVD n(%)	9 (9%)	2 (10%)	7 (9%)	0.857
PNP n(%)	23 (23%)	6 (30%)	17 (21%)	
PVD and PNP n(%)	10 (10%)	2 (10%)	8 (10%)	
<b>Diabetes-related treatment</b>				
Oral	61 (61%)	14 (70%)	47 (59%)	0.617
Insulin	19 (19%)	2 (10%)	17 (21%)	
Oral and insulin	17 (17%)	3 (15%)	14 (17%)	
<b>Medication at baseline</b>				
Aspirin n(%)	17 (17%)	6 (30%)	11 (14%)	0.084
ACE-inhibitors n(%)	31 (31%)	7 (35%)	24 (30%)	0.665
ARB	26 (26%)	5 (25%)	21 (26%)	0.909
Statins n(%)	52 (52%)	14 (70%)	38 (48%)	0.072
<b>Serum markers at baseline</b>				
Total cholesterol(mmol/l)	4.8 ± 1.1	4.4 ± 1.0	3.9 ± 1.3	0.074
LDL(mmol/l)	3.1 ± 1.1	2.7 ± 0.9	3.3 ± 1.1	<b>0.049</b>
HDL(mmol/l)	1.4 ± 0.6	1.3 ± 0.4	1.4 ± 0.6	0.401
Cholesterol/HDL ratio	3.9 ± 1.4	3.9 ± 1.5	3.9 ± 1.3	0.971
Triglycerides(mmol/l)	2.0 ± 1.3	1.9 ± 0.8	2.1 ± 1.3	0.602

Abbreviations: ACE, angiotensin converting enzyme; ARB, angiotensin receptor blocker; CAD, coronary artery disease; DM, diabetes mellitus; HDL, high density lipoprotein; LDL, low density lipoprotein; PNP, polyneuropathy; PVP, peripheral vessel disease

†Blood pressure ≥140/90 mmHg or treatment with antihypertensive medication; ‡ total cholesterol level >5.0mmol/L or use of cholesterol lowering medication; \*defined as the presence of coronary artery disease in first-degree family members at age <55 years in men and <65 years in women; #body mass index ≥30

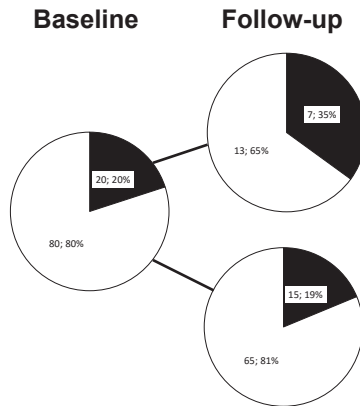


**Figure 1. Distribution of myocardial ischemia on SPECT MPI at baseline and after 2 years follow-up.** Pie charts of the distribution of myocardial ischemia on SPECT MPI stratified according to baseline ischemia. Black represents ischemia, white represents a normal SPECT MPI.

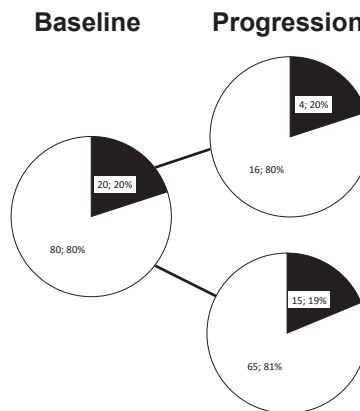


**Figure 2. Distribution of progression of myocardial ischemia on SPECT MPI at baseline and after 2 years follow-up.** Pie charts of the distribution of progression myocardial ischemia on SPECT MPI stratified according to baseline ischemia. At baseline black marks ischemia, white represents a normal SPECT MPI. For follow-up, black marks progression of ischemia.

### CTA results

93 of the 100 patients underwent coronary CTA and 98 patients CAC scoring. The median time between the first SPECT MPI and CTA was 22 (IQR 4 - 46) days. In Table 4 the CTA results are demonstrated, stratified according to the presence of baseline and follow-up ischemia. A comparison was made for the presence, extent and composition of coronary atherosclerosis on CTA. For all parameters, there were no significant differences between patients with and without ischemia at baseline.

**Table 2. Clinical characteristics of the population in relation to follow-up ischemia.**

	<b>FU ischemia (n=22)</b>	<b>FU no ischemia (n=78)</b>	<b>P- value</b>
Age(years)	54 ± 12	53 ± 9	0.641
Gender(% male)	13 (59%)	49 (62%)	0.750
Hypertension† n(%)	11 (50%)	41 (53%)	0.832
Hypercholesterolemia‡ n(%)	11 (50%)	40 (51%)	0.915
Family history of CAD* n(%)	10 (46%)	46 (59%)	0.259
Smoking n(%)	4 (18%)	15 (19%)	0.912
<b>Diabetes-related factors at FU</b>			
Age at time of diagnosis(years)	43 ± 15	43 ± 10	0.912
Diabetes duration(months)	136 ± 99	113 ± 85	0.300
HbA <sub>1c</sub> (%)	7.7 ± 1.8	7.7 ± 1.5	0.876
<b>Diabetes-related complications at FU</b>			
			0.571
PVD n(%)	2 (9%)	7 (9%)	
PNP n(%)	6 (27%)	18 (23%)	
PVD and PNP n(%)	7(32%)	4 (5%)	
<b>Diabetes-related treatment at FU</b>			
			0.224
Oral	9 (41%)	42 (54%)	
Insulin	3 (14%)	18 (23%)	
Oral and insulin	9 (41%)	16 (21%)	
<b>Medication at FU</b>			
Aspirin n(%)	12 (55%)	25 (32%)	0.054
ACE-inhibitors n(%)	10 (45%)	28 (36%)	0.415
ARB n(%)	6 (27%)	22 (28%)	0.931
Statins n(%)	17 (77%)	57 (73%)	0.692
Beta-blockers n(%)	2 (9%)	6 (8%)	0.831
Calcium-antagonists n(%)	1 (5%)	12 (15%)	0.182
Nitrates n(%)	0 (0%)	1 (1%)	0.594
<b>Serum markers at FU</b>			
Total cholesterol(mmol/l)	4.2 ± 1.1	4.5 ± 1.0	0.382
LDL(mmol/l)	2.6 ± 0.9	2.7 ± 0.9	0.548
HDL(mmol/l)	1.2 ± 0.3	1.3 ± 0.4	0.432
Cholesterol/HDL ratio	3.6 ± 1.0	3.7 ± 1.2	0.645
Triglycerides(mmol/l)	2.0 ± 1.7	1.9 ± 1.0	0.751

Abbreviations and definitions as in Table 1.

Similarly, no differences could be demonstrated between patients with and without ischemia at follow-up or between patients with and without progression of ischemia. Overall, 24 (26%) patients presented with obstructive CAD on CTA (of note: patients who underwent revascularization between the two SPECT MPI studies were

**Table 3. Clinical characteristics of the population in relation to progression of ischemia.**

	<b>Progression (n=19)</b>	<b>No progression /regression (n=81)</b>	<b>P- value</b>
Age(years)	53 ± 12	53 ± 10	0.794
Gender(% male)	10 (53%)	52 (64%)	0.350
Hypertension† n(%)	9 (47%)	43 (53%)	0.653
Hypercholesterolemia‡ n(%)	9 (47%)	42 (52%)	0.725
Family history of CAD* n(%)	10 (53%)	46 (57%)	0.742
Smoking n(%)	4 (21%)	15 (19%)	0.800
<b>Diabetes-related risk factors at FU</b>			
Age at time of diagnosis(years)	41 ± 13	44 ± 11	0.320
Diabetes duration(months)	180 ± 97	135 ± 83	<b>0.049</b>
HbA <sub>1c</sub> (%)	8.1 ± 1.5	7.7 ± 1.6	
<b>Diabetes-related complications at FU</b>			
			0.455
PVD n(%)	2 (11%)	7 (9%)	
PNP n(%)	4 (21%)	20 (25%)	
PVD and PNP n(%)	4 (21%)	7 (9%)	
<b>Diabetes-related treatment at FU</b>			
			0.249
Oral	8 (42%)	43 (53%)	
Insulin	3 (16%)	18 (22%)	
Oral and insulin	8 (42%)	17 (21%)	
<b>Medication at FU</b>			
Aspirin n(%)	10 (53%)	27 (33%)	0.117
ACE-inhibitors n(%)	9 (47%)	29 (36%)	0.350
ARB n(%)	5 (26%)	23 (29%)	0.856
Statins n(%)	16 (84%)	58 (73%)	0.260
Beta-blockers n(%)	2 (11%)	6 (32%)	0.652
Calcium-antagonists n(%)	0 (0%)	13 (16%)	0.061
Nitrates n(%)	0 (0%)	1 (1%)	0.626
<b>Serum markers at FU</b>			
Total cholesterol(mmol/l)	4.3 ± 1.0	4.5 ± 1.0	0.469
LDL(mmol/l)	2.6 ± 0.9	2.7 ± 0.9	0.653
HDL(mmol/l)	1.2 ± 0.25	1.3 ± 1.2	0.435
Cholesterol/HDL ratio	3.7 ± 1.2	3.7 ± 1.2	0.154
Triglycerides(mmol/l)	1.9 ± 1.7	1.9 ± 1.0	0.435

Abbreviations and definitions as in Table 1.

excluded). In patients with ischemia at baseline, more had obstructive CAD (33% vs. 24%, P=0.476) but these differences were not significant. These patients also had a higher mean CAC score (19 (IQR 0-115) vs. 4 (IQR 0-101), P=0.390), but the

Table 4. Coronary atherosclerosis on CTA in relation to the SPECT MPI results.

Abbreviations: CAC, coronary artery calcium; CAD, coronary artery disease

	All patients (n=93)	BL ischemia (N=18)	BL no ischemia (N=75)	P-value	FU ischemia (N=19)	FU no ischemia (N=74)	P-value	Progression (N = 17)	No progression /regression (N=76 )	P-value
<b>Coronary stenosis</b>										
No. of plaques $\geq 30\%$	3.6 $\pm$ 3.8	4.1 $\pm$ 3.7	3.5 $\pm$ 3.9	0.542	4.2 $\pm$ 3.4	3.4 $\pm$ 4.0	0.196	3.8 $\pm$ 3.3	3.5 $\pm$ 4.0	0.452
No. of non-obstructive lesions $< 50\%$	3.0 $\pm$ 3.2	3.1 $\pm$ 2.9	3.0 $\pm$ 3.3	0.762	3.1 $\pm$ 2.4	3.0 $\pm$ 3.4	0.441	2.8 $\pm$ 2.5	3.0 $\pm$ 3.4	0.714
No. of obstructive lesions $\geq 50\%$	0.6 $\pm$ 1.3	0.9 $\pm$ 1.8	0.5 $\pm$ 1.1	0.361	1.16 $\pm$ 1.9	0.42 $\pm$ 1.0	0.131	1.0 $\pm$ 1.7	0.5 $\pm$ 1.1	0.250
No. of patients with obstructive CAD	24 (26%)	6 (33%)	18 (24%)	0.476	7 (37%)	17 (23%)	0.434	6 (35%)	18 (24%)	0.546
<b>Coronary plaque type</b>										
No. of calcified lesions	0.9 $\pm$ 2.0	0.7 $\pm$ 1.8	1.0 $\pm$ 2.0	0.330	1.0 $\pm$ 1.6	1.4 $\pm$ 2.2	0.424	0.7 $\pm$ 1.0	1.0 $\pm$ 2.1	0.614
No. of mixed lesions	1.1 $\pm$ 1.9	1.7 $\pm$ 2.4	0.9 $\pm$ 1.7	0.144	1.8 $\pm$ 2.5	0.9 $\pm$ 1.6	0.159	1.6 $\pm$ 2.3	1.0 $\pm$ 1.8	0.249
No. of non-calcified lesions	1.3 $\pm$ 2.1	1.4 $\pm$ 1.9	1.3 $\pm$ 2.2	0.445	1.2 $\pm$ 1.7	1.4 $\pm$ 2.2	0.842	1.2 $\pm$ 1.8	1.3 $\pm$ 2.2	0.760
<b>Coronary artery calcium (CAC)</b>										
CAC score	170 $\pm$ 451 10 (0-104)	211 $\pm$ 378 19 (0-115)	160 $\pm$ 468 4 (0-101)	0.390	295 $\pm$ 792 47 (0-164)	136 $\pm$ 299 0 (0-100)	0.118	236 $\pm$ 812 16 (0-81)	154 $\pm$ 316 4 (0-112)	0.408
No. patients with CAC score = 0	45 (46%)	7 (37%)	38 (48%)	0.377	6 (28%)	39 (51%)	0.072	6 (32%)	39 (49%)	0.162

difference was not statistically different. In patients presenting with progression of ischemia, obstructive CAD occurred more often (35% vs. 24%,  $P=0.546$ ) and CAC scores were slightly higher (16 (IQR 0-81) vs. 4 (IQR 0-112),  $P=0.408$ ), but these differences were also not significant.

## Discussion

The present study demonstrated a low rate of progression of ischemia after 2 years in high risk patients with diabetes without cardiac symptoms. Moreover, no relation between atherosclerosis parameters on CTA and changes of ischemia was observed.

Previous studies have investigated the role of screening with SPECT MPI for silent ischemia in asymptomatic diabetic patients.<sup>17</sup> Most importantly, in the Detection of Ischemia in Asymptomatic Diabetics (DIAD) study, 1123 diabetic patients without any suspicion of CAD were randomized between screening with SPECT MPI and no screening.<sup>18</sup> Of the 522 patients who underwent SPECT MPI, 133 (22%) presented with an abnormal study, the majority (73%) of which were regional perfusion abnormalities.<sup>9</sup> Except for gender, diabetes duration and heart rate response to Valsalva (performed as part of cardiac autonomic function testing), no clinical characteristics or laboratory markers could accurately predict the presence of silent ischemia in these patients. Second, Lorenzo *et al.* included 180 asymptomatic diabetic patients who underwent SPECT MPI and were followed for a mean period of 36 months.<sup>19</sup> In total, 46 patients (26%) of the patients presented with an abnormal MPI. No differences in characteristics were observed between patients with and without myocardial ischemia. However, at present only one study has focused on progression of ischemia in these patients. In DIAD-2, 358 of the initial 522 patients underwent a second SPECT MPI study to evaluate the change in myocardial perfusion after a 3 year interval.<sup>9</sup> Similar to the present study, of the 71 (20%) patients who presented with an abnormal SPECT MPI study at baseline, 56 (79%) showed resolution of ischemia after 3 years, whereas only a limited number of patients (10%) with a normal baseline examination presented with new ischemia. Likely this resolution of ischemia was caused by intensified medical therapy after recommendations in the American Diabetes Association (ADA) guidelines.<sup>20</sup> Similarly, in the present report medical therapy was intensified at follow-up. However, no relation between added anti-anginal medication and ischemia progression could be established. Comparable to the present report, in DIAD-2 the value of clinical characteristics to predict the risk of new ischemia was limited. Only peripheral vessel disease (PVD) and elevated LDL-cholesterol levels were associated with new onset of ischemia.

Presumably, the relative low rate of progression of ischemia is caused by accurate medical therapy. If these diabetic patients are treated according guidelines based on the outcomes of testing, the clinical follow-up is prosperous. It seems that medical treatment outweighs the potential negative effect of other clinical characteristics. It would however have been unethical to refrain patients from appropriate medical therapy.

In the present report, there was no significant difference between the median CAC score in patients with and without baseline ischemia. In contrast, Anand *et al.* showed a significant association between the CAC score and myocardial ischemia in 510 asymptomatic diabetic patients.<sup>21</sup> MPI was performed in all patients with a CAC score >100 and in a random sample of patients with a CAC score ≤100. The CAC score was significantly associated with the presence of myocardial ischemia. Of particular interest, all patients with a CAC score ≤10 presented with a normal SPECT MPI. Furthermore, in the current report, no correlation was demonstrated between coronary atherosclerosis parameters of the extent, severity or composition of coronary atherosclerosis on CTA and baseline ischemia on SPECT MPI. Indeed, several studies have previously demonstrated the limited correlation between the coronary stenosis severity on CTA and ischemia on SPECT MPI, both in patients with stable angina and asymptomatic diabetic patients.<sup>11, 22</sup> However, for the present study, it was hypothesized that CTA could be able to identify different coronary atherosclerotic plaque characteristics which could predict changes in myocardial ischemia on SPECT MPI. The relation between coronary plaque type and the presence of myocardial ischemia has previously been studied.<sup>23-25</sup> Lin *et al.* included 163 low-to-intermediate risk symptomatic patients who underwent both CTA and SPECT MPI.<sup>25</sup> Besides stenosis severity, mixed plaque was significantly associated with the presence of myocardial ischemia. Moreover, van Velzen *et al.* evaluated 514 patients with SPECT MPI and coronary CTA.<sup>23</sup> The presence of mixed or calcified plaque independently predicted myocardial ischemia. In contrast, Bauer *et al.* focused on the relation between non-calcified CAD on CTA and myocardial ischemia in 72 patients.<sup>24</sup> It was demonstrated that coronary arteries with a perfusion defect in the corresponding vascular territory had significantly larger non-calcified plaque volumes, but there was no difference in calcified plaque volume. The underlying pathophysiological relation between coronary plaque composition and myocardial ischemia is unknown. Possible, mixed plaques with a relatively large plaque burden are prone to rupture, causing myocardial ischemia, whereas the more advanced stage of calcified plaque is relatively stable. Especially in a patient without baseline ischemia, rupture of a hemodynamically non-significant plaque could cause onset of ischemia. However, the relation between CTA atherosclerosis parameters and progression of atherosclerosis has not been described earlier. Moreover, in the present study, no association could be established between

CTA coronary atherosclerosis and changes in myocardial ischemia. There was no significant difference in the different plaque types between patients with and without onset of new ischemia or progression of ischemia. Nor could a difference in the presence of non-obstructive CAD between both patient groups be established. Moreover, the CAC score was similar in both groups. The relative disagreement between atherosclerosis on CTA and ischemia on SPECT MPI could be caused by the fact that the two different modalities evaluate different manifestations of CAD. CTA only allows assessment of coronary artery stenosis in the major epicardial coronary arteries. On the other hand, SPECT MPI visualizes perfusion defects which could be caused by either stenosis in a major epicardial coronary artery and/or by microvascular disease and endothelial dysfunction. However, it is well known that especially in diabetic patients, microvascular disease plays an important role in the onset of myocardial ischemia.<sup>6</sup>

### **Limitations**

Some limitations need to be considered. First, a limited number of patients is included. Second, patients who underwent revascularization were excluded, which may have affected results. And furthermore, additional SPECT parameters such as left ventricular ejection fraction, transient ischemic dilatation or ECG abnormalities were not incorporated in the current analysis.

### **Conclusions**

The rate of progression of ischemia in high risk patients with diabetes without cardiac symptoms is limited. Few patients presented with new ischemia, whereas some patients show resolution of ischemia. Atherosclerosis parameters on CTA were not predictive of new onset ischemia or progression of ischemia. Neither baseline characteristics, CAC score nor atherosclerosis parameters on CTA were predictive of the onset of new ischemia or were correlated with progression of ischemia.

## References

- (1) Morrish NJ, Wang SL, Stevens LK, Fuller JH, Keen H. Mortality and causes of death in the WHO Multinational Study of Vascular Disease in Diabetes. *Diabetologia* 2001 September;44 Suppl 2:S14-S21.
- (2) Miller TD, Rajagopalan N, Hodge DO, Frye RL, Gibbons RJ. Yield of stress single-photon emission computed tomography in asymptomatic patients with diabetes. *Am Heart J* 2004 May;147(5):890-6.
- (3) Seven-year outcome in the Bypass Angioplasty Revascularization Investigation (BARI) by treatment and diabetic status. *J Am Coll Cardiol* 2000 April;35(5):1122-9.
- (4) Prevalence of unrecognized silent myocardial ischemia and its association with atherosclerotic risk factors in noninsulin-dependent diabetes mellitus. Milan Study on Atherosclerosis and Diabetes (MiSAD) Group. *Am J Cardiol* 1997 January 15;79(2):134-9.
- (5) Zeina AR, Odeh M, Rosenschein U, Zaid G, Barmeir E. Coronary artery disease among asymptomatic diabetic and nondiabetic patients undergoing coronary computed tomography angiography. *Coron Artery Dis* 2008 February;19(1):37-41.
- (6) Marwick TH. Diabetic heart disease. *Heart* 2006 March;92(3):296-300.
- (7) Scholte AJ, Schuijf JD, Kharagjitsingh AV *et al.* Prevalence of coronary artery disease and plaque morphology assessed by multi-slice computed tomography coronary angiography and calcium scoring in asymptomatic patients with type 2 diabetes. *Heart* 2008 March;94(3):290-5.
- (8) Bourque JM, Patel CA, Ali MM, Perez M, Watson DD, Beller GA. Prevalence and predictors of ischemia and outcomes in outpatients with diabetes mellitus referred for single-photon emission computed tomography myocardial perfusion imaging. *Circ Cardiovasc Imaging* 2013 May 1;6(3):466-77.
- (9) Wackers FJ, Chyun DA, Young LH *et al.* Resolution of asymptomatic myocardial ischemia in patients with type 2 diabetes in the Detection of Ischemia in Asymptomatic Diabetics (DIAD) study. *Diabetes Care* 2007 November;30(11):2892-8.
- (10) Scholte AJ, Schuijf JD, Kharagjitsingh AV *et al.* Prevalence and predictors of an abnormal stress myocardial perfusion study in asymptomatic patients with type 2 diabetes mellitus. *Eur J Nucl Med Mol Imaging* 2009 April;36(4):567-75.
- (11) Scholte AJ, Schuijf JD, Kharagjitsingh AV *et al.* Different manifestations of coronary artery disease by stress SPECT myocardial perfusion imaging, coronary calcium scoring, and multislice CT coronary angiography in asymptomatic patients with type 2 diabetes mellitus. *J Nucl Cardiol* 2008 July;15(4):503-9.
- (12) Brindis RG, Douglas PS, Hendel RC *et al.* ACCF/ASNC appropriateness criteria for single-photon emission computed tomography myocardial perfusion imaging (SPECT MPI): a report of the American College of Cardiology Foundation Quality Strategic Directions Committee Appropriateness Criteria Working Group and the American Society of Nuclear Cardiology endorsed by the American Heart Association. *J Am Coll Cardiol* 2005 October 18;46(8):1587-605.
- (13) Hansen CL, Goldstein RA, Berman DS *et al.* Myocardial perfusion and function single photon emission computed tomography. *J Nucl Cardiol* 2006 November;13(6):e97-120.
- (14) Ficaro EP, Corbett JR. Advances in quantitative perfusion SPECT imaging. *J Nucl Cardiol* 2004 January;11(1):62-70.
- (15) Ficaro EP, Lee BC, Kritzman JN, Corbett JR. Corridor4DM: the Michigan method for quantitative nuclear cardiology. *J Nucl Cardiol* 2007 July;14(4):455-65.

- (16) van Werkhoven JM, Schuijff JD, Gaemperli O *et al.* Incremental prognostic value of multi-slice computed tomography coronary angiography over coronary artery calcium scoring in patients with suspected coronary artery disease. *Eur Heart J* 2009 November;30(21):2622-9.
- (17) Scholte AJ, Bax JJ, Wackers FJ. Screening of asymptomatic patients with type 2 diabetes mellitus for silent coronary artery disease: combined use of stress myocardial perfusion imaging and coronary calcium scoring. *J Nucl Cardiol* 2006 January;13(1):11-8.
- (18) Wackers FJ, Young LH, Inzucchi SE *et al.* Detection of silent myocardial ischemia in asymptomatic diabetic subjects: the DIAD study. *Diabetes Care* 2004 August;27(8):1954-61.
- (19) De Lorenzo A, Lima RS, Siqueira-Filho AG, Pantoja MR. Prevalence and prognostic value of perfusion defects detected by stress technetium-99m sestamibi myocardial perfusion single-photon emission computed tomography in asymptomatic patients with diabetes mellitus and no known coronary artery disease. *Am J Cardiol* 2002 October 15;90(8):827-32.
- (20) American Diabetes Association. Clinical practice recommendations 2001. Position statement: management of dyslipidemia in adults with diabetes. 24 , S58-S61. 2001.
- (21) Anand DV, Lim E, Hopkins D *et al.* Risk stratification in uncomplicated type 2 diabetes: prospective evaluation of the combined use of coronary artery calcium imaging and selective myocardial perfusion scintigraphy. *Eur Heart J* 2006 March;27(6):713-21.
- (22) Schuijff JD, Wijns W, Jukema JW *et al.* Relationship between noninvasive coronary angiography with multi-slice computed tomography and myocardial perfusion imaging. *J Am Coll Cardiol* 2006 December 19;48(12):2508-14.
- (23) van Velzen JE, Schuijff JD, van Werkhoven JM *et al.* Predictive value of multislice computed tomography variables of atherosclerosis for ischemia on stress-rest single-photon emission computed tomography. *Circ Cardiovasc Imaging* 2010 November;3(6):718-26.
- (24) Bauer RW, Thilo C, Chiamida SA, Vogl TJ, Costello P, Schoepf UJ. Noncalcified atherosclerotic plaque burden at coronary CT angiography: a better predictor of ischemia at stress myocardial perfusion imaging than calcium score and stenosis severity. *AJR Am J Roentgenol* 2009 August;193(2):410-8.
- (25) Lin F, Shaw LJ, Berman DS *et al.* Multidetector computed tomography coronary artery plaque predictors of stress-induced myocardial ischemia by SPECT. *Atherosclerosis* 2008 April;197(2):700-9.





# Chapter 11

## Prognostic value of coronary computed tomography angiography in high risk diabetic patients without chest pain syndrome

de Graaf MA, van den Hoogen IJ, Roos CJ, Leen AC, Kharagjitsingh AV, Wolterbeek R, Kroft LJ, J. Wouter Jukema, Bax JJ, Scholte AJ.

(Shared first authorship)

Journal of Nuclear Cardiology 2015;23:24-36

## Abstract

**Purpose:** Diabetic patients with coronary artery disease (CAD) are often free of chest pain syndrome. A useful modality for non-invasive assessment of CAD is coronary computed tomography angiography (CTA). However, the prognostic value of CAD on coronary CTA in diabetic patients without chest pain syndrome is relatively unknown. Therefore, the aim was to investigate the long term prognostic value of coronary CTA in a large population diabetic patients without chest pain syndrome.

**Methods:** Between 2005 and 2013, 525 diabetic patients without chest pain syndrome were prospectively included to undergo coronary artery calcium (CAC)-scoring followed by coronary CTA. During follow-up the composite endpoint of all-cause mortality, non-fatal myocardial infarction (MI) and late revascularization (>90 days) was registered.

**Results:** In total, CAC-scoring was performed in 410 patients and coronary CTA in 444 patients (431 interpretable). After median follow-up of 5.0(IQR 2.7-6.5) years the composite endpoint occurred in 65(14%) patients. Coronary CTA demonstrated a high prevalence of CAD (85%), mostly non-obstructive CAD (51%). Furthermore, patients with a normal CTA had an excellent prognosis (event-rate 3%). An incremental increase in event-rate was observed with increasing CAC-risk category or coronary stenosis severity. Finally, obstructive (50-70%) or severe CAD (>70%) was independently predictive of events (HR=11.10[2.52;48.79](P=0.001), HR=15.16[3.01;76.36] (P=0.001)). Obstructive (50-70%) or severe CAD (>70%) provided increased value over baseline risk factors.

**Conclusion:** Coronary CTA provided prognostic value in diabetic patients without chest pain syndrome. Most importantly, the prognosis of patients with a normal CTA was excellent.

## Introduction

Diabetes mellitus (DM) is a major and rapidly growing global health problem. In 2013 DM was responsible for 8.4% of all-cause mortality in patients between 20-79 years old and 10.8% of total health expenditure worldwide.<sup>1</sup> Cardiovascular complications are the leading cause of mortality in diabetic patients.<sup>2</sup> Accordingly, the European Society of Cardiology (ESC) classifies patients with DM as high risk for coronary artery disease (CAD).<sup>3</sup> However, not all patients with DM have CAD and also diabetic patients with CAD are often free of chest pain syndrome.<sup>4</sup> Coronary computed tomography angiography (CTA) is a useful modality for non-invasive assessment of CAD. Indeed, in diabetic patients without chest pain syndrome a high prevalence of CAD is present on coronary CTA.<sup>5-7</sup> Potentially CTA could be used to risk stratify DM patients. However, the prognostic value of CAD on coronary CTA in these patients is relatively unknown. As a consequence, the value of coronary CTA for risk stratification of these patients is unestablished.<sup>8,9</sup> Therefore, the aim of this study is to investigate the long term prognostic value of coronary CTA in a large population of diabetic patients without chest pain syndrome.

## Methods

### Patients

The study population consisted of 525 diabetic patients without chest pain syndrome, referred from an outpatient diabetic clinic for assessment of cardiovascular risk between May 2005 and August 2013. The cardiovascular assessment include coronary artery calcium (CAC) score and CTA to evaluate the presence and severity of CAD.<sup>5, 10</sup> After enrolment in the prospective clinical registry, patients underwent a non-contrast CT for CAC-scoring followed by a contrast coronary CTA. Inclusion criteria consisted of confirmed diagnosis of DM type 1 or 2 (fasting plasma glucose level  $\geq 126$  mg/dL, use of oral glucose lowering medication or insulin) and absence of chest pain syndrome.<sup>11</sup> Exclusion criteria were known or suspected coronary artery disease (CAD), previous coronary revascularization, cardiac arrhythmias, pregnancy and contraindications for the use of iodinated contrast media.

Clinical data were prospectively entered into the departmental Cardiology Information System (EPD-Vision©, Leiden University Medical Center, the Netherlands) and retrospectively analyzed. The Institutional Review Board of the Leiden University Medical Center approved this evaluation of clinically collected data, and waived the need for written informed consent.

### **Coronary CTA acquisition**

Patients were scanned using a 64-slice or 320-row multidetector scanner (64-slice: Aquillon 64, Toshiba Medical Systems, Otawara, Japan; 320-row: Aquillon ONE, Toshiba Medical System, Otawara, Japan). Scan-protocol was followed as previously described.<sup>12, 13</sup> Post-processing of scans was performed with application of dedicated software (Vitrea FX 1.0, Vital Images, Minnetonka, MN, USA). Uninterpretable scans were excluded from the analysis.

### **CAC-scoring**

CAC-scoring was performed according to the algorithm of Agatston. CAC-score was stratified into four risk categories: 0, 1-99, 100-399,  $\geq 400$ .<sup>12</sup>

### **Coronary CTA**

All coronary CTAs were analysed by consensus of experienced observers according to the modified 17 segments American Heart Association (AHA) classification.

First, each segment was assessed for interpretability. Segments were defined as uninterpretable in case of severe motion artefacts or low contrast resolution. Additionally, segments with a diameter  $\leq 1.5$  mm were excluded.<sup>5</sup> Second, interpretable segments were evaluated for stenosis. Stenosis was stratified into four categories: normal if no plaques were present on CTA, non-obstructive if the plaque covered  $< 50\%$ , obstructive if the plaque covered 50-70%, severe if the plaque covered  $> 70\%$  of the coronary artery lumen. If plaque was present, plaque composition was determined (calcified, mixed, and non-calcified). One type of plaque composition was assigned per segment.

### **Follow-up**

Follow-up data were retrospectively gathered by review of electronic medical records, blinded from CTA results, between December 2013 and February 2014, both the medical records of the department of cardiology and of the referring outpatient diabetic clinic have been analysed. Three endpoints were registered: all-cause mortality, non-fatal myocardial infarction (MI), late revascularization. Non-fatal MI was defined based on criteria of typical chest pain, elevated cardiac enzyme levels and typical changes on the ECG.<sup>14</sup> Late revascularization was defined as percutaneous coronary intervention (PCI) or coronary artery bypass grafting (CABG) after 90 days of scan acquisition.<sup>15</sup> All revascularization procedures within 90 days were considered coronary CTA-driven. For the analysis a composite endpoint was constructed of all three endpoints.

## Statistical analysis

All continuous data (normally distributed, non-normally distributed) are presented as mean  $\pm$ SD for reasons of uniformity. Categorical data are presented as absolute numbers and percentages.

First, baseline characteristics were compared between patients with and without obstructive CAD ( $\geq 50\%$ ), similarly between patients with and without events. Second, results of both CAC-scoring and coronary CTA were compared between patients with and without events. Third, survival analyses were performed by the Kaplan-Meier method. Cumulative event rates for CAC-score and coronary stenosis were obtained by this method, using the composite endpoint. Note that these survival analyses were crude, because no corrections for baseline characteristics were performed. Fourth, the independent prognostic value of baseline characteristics, CAC-scoring and coronary CTA was assessed. For this purpose univariate and multivariate Cox-regression analyses were performed. To avoid over fitting of the model a selection of univariate significant variables was entered into the multivariate model.

All statistical tests were two-sided. Comparisons between groups were performed with the Independent-Samples T test or Mann-Whitney U test for continuous data and the  $\chi^2$  test for categorical data. Comparisons of Kaplan-Meier curves were performed with the Log-Rank test. To compare the model fit of the multivariate Cox-regression models for CTA and CAC-score the -2 log likelihood was used. However, it should be noted that for non-nested models (i.e Model 2 vs Model 4), this only provides a crude comparison for which no P-values could be calculated. All statistical analyses were performed with SPSS software (Version 22.0, SPSS IBM Corp., Armonk, New York). A P-value  $< 0.05$  was considered statistically significant.

## Results

### Patients

The study population consisted of 525 patients. As depicted in Figure 1, 76(14%) patients were excluded from this analysis because of logistical reasons (i.e. patients who did not attend appointment). The results of 449 patients were available for the present analysis: 405 patients underwent both CAC-scoring and coronary CTA, 5 patients underwent only CAC-scoring, 39 patients underwent only coronary CTA. In total, CAC-scoring was performed in 410 patients and coronary CTA in 444 patients. Mean age was  $54 \pm 11$  years, 265(59%) patients were male and median DM duration was 12(IQR 6-22) years. Baseline characteristics of the population are depicted in Table 1.

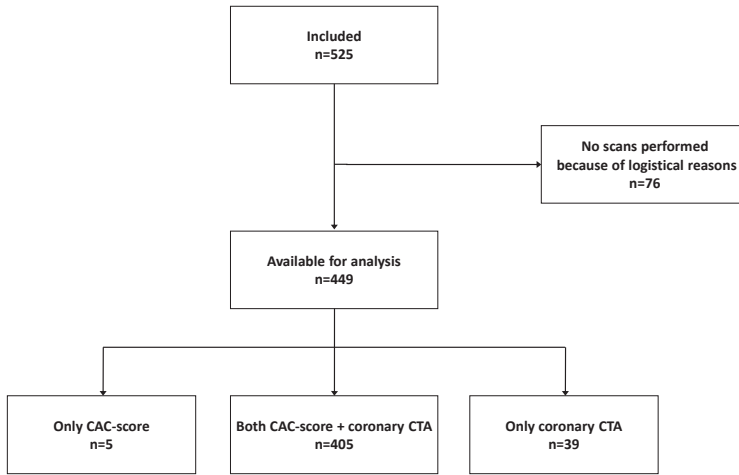


Figure 1. Flowchart of the study population.

Table 1. Baseline characteristics stratified according to coronary CTA results and events.

Baseline	Obstructive CAD (≥50%)			P-value	Events		P-value
	Total (n=449)	Yes (n=147)	No (n=284)		Yes (n=65)	No (n=384)	
Age(years)	54±11	60±9	50±11	<0.001	59±10	53±11	<0.001
Male n(%)	265(59%)	101(69%)	154(54%)	0.004	47(72%)	218(57%)	0.018
BMI(kg/m <sup>2</sup> )	28.6±5.7	28.5±5.0	28.5±6.0	0.942	28.7±5.3	28.6±5.8	0.912
Hypertension† n(%)	145(33%)	65(44%)	72(26%)	<0.001	28(43%)	117(31%)	0.051
Hypercholesterolemia‡ n(%)	162(36%)	68(46%)	85(30%)	0.001	33(51%)	129(34%)	0.009
Family history of CAD* n(%)	190(43%)	60(41%)	125(45%)	0.448	29(45%)	161(42%)	0.735
Smoker n(%)	101(23%)	41(28%)	59(21%)	0.114	23(35%)	78(21%)	0.008
<b>DM-related risk factors</b>							
DM type 2 n(%)	312(70%)	111(76%)	185(65%)	0.028	51(79%)	261(68%)	0.089
DM duration(years)	15±13 12(IQR 6-22)	18±14 15(IQR 9-24)	14±12 10(IQR 5-20)	<0.001	17±14 14(IQR 8-22)	15±12 12(IQR 5-22)	0.240
<b>HbA<sub>1c</sub></b>							
NGSP (%)	7.8±1.5	7.9±1.6	7.7±1.5	0.211	8.0±1.7	7.7±1.5	0.287
IFCC (mmol/mol)	62±16	63±18	61±16	0.211	64±19	61±16	0.287
Serum creatinine	78±19	82±19	76±19	0.002	83±21	77±18	0.012
eGFR (MDRD)	76±22	70±20	79±22	<0.001	69±21	77±22	0.006
<b>DM-related complications</b>							
PVD n(%)	20(5%)	12(8%)	7(3%)		7(11%)	13(3%)	
PNP n(%)	97(22%)	41(28%)	50(18%)	<0.001	20(31%)	77(20%)	0.002

Table 1. (Continued)

Baseline	Obstructive CAD ( $\geq 50\%$ )			P-value	Events		P-value
	Total (n=449)	Yes (n=147)	No (n=284)		Yes (n=65)	No (n=384)	
PVD and PNP n(%)	26(6%)	14(10%)	12(4%)		6(9%)	20(5%)	
<b>DM-related treatment</b>				0.578			0.083
Oral	131(29%)	47(32%)	79(28%)		21(32%)	110(29%)	
Insulin	170(38%)	50(34%)	116(41%)		18(28%)	152(40%)	
Oral and insulin	99(22%)	33(22%)	58(20%)		21(32%)	78(20%)	
<b>Medication</b>							
Aspirin n(%)	99(22%)	47(32%)	46(16%)	<b>&lt;0.001</b>	27(42%)	72(19%)	<b>&lt;0.001</b>
ACE-inhibitors n(%)	155(35%)	73(50%)	73(26%)	<b>&lt;0.001</b>	34(52%)	121(32%)	<b>0.001</b>
ARB n(%)	36(8%)	10(7%)	25(9%)	0.464	6(9%)	30(8%)	0.715
Statins n(%)	248(56%)	97(66%)	138(49%)	<b>0.001</b>	45(69%)	203(53%)	<b>0.018</b>
Beta-blockers n(%)	41(9%)	20(14%)	19(7%)	<b>0.018</b>	11(17%)	30(8%)	<b>0.018</b>
Calcium-antagonists n(%)	14(3%)	9(6%)	5(2%)	<b>0.015</b>	6(9%)	8(2%)	<b>0.002</b>
<b>Serum markers</b>							
Total cholesterol(mmol/l)	4.7 $\pm$ 1.1	4.6 $\pm$ 1.2	4.7 $\pm$ 1.0	0.183	4.9 $\pm$ 1.2	4.6 $\pm$ 1.0	0.051
LDL(mmol/l)	2.9 $\pm$ 1.0	2.8 $\pm$ 1.1	2.9 $\pm$ 1.0	0.503	3.0 $\pm$ 1.1	2.8 $\pm$ 1.0	0.176
HDL(mmol/l)	1.4 $\pm$ 0.5	1.4 $\pm$ 0.5	1.5 $\pm$ 0.5	0.062	1.4 $\pm$ 0.5	1.4 $\pm$ 0.5	0.729
Cholesterol/HDL ratio	3.6 $\pm$ 1.5	3.7 $\pm$ 1.4	3.6 $\pm$ 1.6	0.594	3.8 $\pm$ 1.3	3.6 $\pm$ 1.5	0.310
Triglycerides(mmol/l)	1.7 $\pm$ 1.2	1.7 $\pm$ 1.1	1.6 $\pm$ 1.2	0.462	1.8 $\pm$ 1.2	1.6 $\pm$ 1.1	0.262

Abbreviations: ACE, angiotensin converting enzyme; ARB, angiotensin receptor blocker; BMI, body mass index; CAD, coronary artery disease; DM, diabetes mellitus; eGFR, estimated glomerular filtration rate; HDL, high density lipoprotein; IFCC, International Federation of Clinical Chemistry; LDL, low density lipoprotein; MDRD, Modification of Diet in Renal Disease; NGSP, National Glycohemoglobin Standardization Program; PNP, polyneuropathy; PVD, peripheral vessel disease.

Definitions: † Blood pressure  $\geq 140/90$  mmHg or treatment with antihypertensive medication; ‡ total cholesterol level  $>5.0$ mmol/L or use of cholesterol lowering medication; \* presence of coronary artery disease in first-degree family members at age  $<55$  years in men and  $<65$  years in women.

## Events

The composite endpoint of all-cause mortality, non-fatal MI and late revascularization occurred in 65(14%) patients. All-cause mortality occurred in 13(3%) patients and late revascularization in 52(12%) patients (PCI: 30 patients, CABG: 22 patients). Of the 52 patients who underwent revascularization, 27(52%) patients were referred to invasive coronary angiography because of new-onset angina, 20 (38%) patients had documented ischemia on a SPECT myocardial perfusion imaging (MPI) performed after CTA and 5 (10%) patients presented with new ischemia on SPECT MPI during follow up. Non-fatal MI did not occur. Early revascularization, which was excluded from the composite endpoint, occurred in 16(4%) patients (PCI: 13 patients, CABG:

3 patients). Median follow-up was 5.0(IQR 2.7-6.5) years. No patients were lost to follow-up.

Patients with events demonstrated a higher mean age ( $59\pm 10$  vs.  $53\pm 11$  ( $P<0.001$ )) and number of males (47(72%) vs. 218(57%) ( $P=0.018$ )) compared to patients without events. Furthermore, hypercholesterolemia (33(51%) vs. 129(34%) ( $P=0.009$ )), smoker (23(35%) vs. 78(21%) ( $P=0.008$ )) and overall DM-related complications ( $P=0.002$ ) were more frequently observed in this group (Table 1).

### **CAC-scoring**

CAC-scoring was performed in 410 patients. Median CAC-score was 29(IQR 0-294). The distribution within the CAC-risk categories was as follows: CAC-score=0 in 144(35%) patients, CAC-score=1-99 in 106(26%) patients, CAC-score=100-399 in 67(16%) patients, CAC-score $\geq$ 400 in 93(23%) patients. In total, CAC-score=0 and CAC-score $\geq$ 1 were observed in respectively 35% and 65% of patients (Table 2).

The results of CAC-scoring, stratified according to events, are depicted in Table 2. Patients with events demonstrated a higher median CAC-score compared to patients without events (543(IQR 141-1310) vs. 13(IQR 0-177) ( $P<0.001$ )). Moreover, patients with events were more often classified in a higher CAC-risk category ( $P<0.001$ ).

### **Coronary CTA**

Coronary CTA was performed in 444 patients, of which 13 were uninterpretable. The remaining results of 431 patients were used for the present analysis. A high prevalence of CAD (85%) was demonstrated on coronary CTA: non-obstructive CAD (<50%) in 219(51%) patients, obstructive CAD (50-70%) in 117(27%) patients, severe CAD (>70%) in 30(7%) patients. A normal CTA was observed in 65(15%) patients (Table 2).

The baseline characteristics, stratified according to coronary CTA results, are depicted in Table 1. Patients with obstructive CAD ( $\geq 50\%$ ) demonstrated a higher mean age ( $60\pm 9$  vs.  $50\pm 11$  ( $P<0.001$ )), number of males (101(69%) vs. 154(54%) ( $P=0.004$ )) and median diabetes duration (15(IQR 9-24) vs. 10(IQR 5-20) ( $P<0.001$ )) compared to patients with no or non-obstructive CAD (<50%). Furthermore, hypertension (65(44%) vs. 72(26%) ( $P<0.001$ )), hypercholesterolemia (68(46%) vs. 85(30%) ( $P=0.001$ )) and overall DM-related complications ( $P<0.001$ ) were more frequently observed in this group.

The results of coronary CTA, stratified according to events, are depicted in Table 2. Patients with events presented with more severe coronary stenosis compared to patients without events ( $P<0.001$ ). Moreover, a higher mean number of plaques ( $9.7\pm 4.4$  vs.  $7.7\pm 5.7$  ( $P=0.002$ )), mean number of obstructive lesions ( $2.8\pm 2.8$  vs.  $0.6\pm 1.4$  ( $P<0.001$ )) and mean number of severe lesions ( $0.3\pm 0.8$  vs.  $0.1\pm 0.4$  ( $P=0.009$ ))

**Table 2. Results of CAC-scoring and coronary CTA stratified according to events.**

CAC-scoring	Events			P-value
	Total (n=410)	Yes (n=59)	No (n=351)	
<b>CAC-score</b>	355±800 29(IQR 0-294)	1043±1449 543(IQR 141-1310)	239±554 13(IQR 0-177)	<b>&lt;0.001</b>
<b>CAC-risk category</b>				<b>&lt;0.001</b>
CAC-score=0	144(35%)	5(9%)	139(40%)	
CAC-score=1-99	106(26%)	7(12%)	99(28%)	
CAC-score=100-399	67(16%)	12(20%)	55(16%)	
CAC-score≥400	93(23%)	35(59%)	58(17%)	
<b>Coronary CTA</b>	<b>Total (n=431)</b>	<b>Yes (n=64)</b>	<b>No (n=367)</b>	<b>P-value</b>
<b>Coronary stenosis</b>				<b>&lt;0.001</b>
No. of patients with normal CTA n(%)	65(15%)	2(3%)	63(17%)	
No. of patients with non-obstructive CAD (<50%) n(%)	219(51%)	11(17%)	208(57%)	
No. of patients with obstructive CAD (50-70%) n(%)	117(27%)	39(61%)	78(21%)	
No. of patients with severe CAD (>70%) n(%)	30(7%)	12(19%)	18(5%)	
<b>Coronary plaques (stenosis)</b>				
No. of plaques	8.0±5.6	9.7±4.4	7.7±5.7	<b>0.002</b>
No. of non-obstructive lesions	7.0±5.3	6.9±4.1	7.1±5.4	0.724
No. of obstructive lesions	1.0±1.9	2.8±2.8	0.6±1.4	<b>&lt;0.001</b>
No. of severe lesions	0.1±0.5	0.3±0.8	0.1±0.4	<b>0.009</b>
<b>Coronary plaques (composition)</b>				
No. of calcified lesions	1.1± 2.2	2.6±3.5	0.8±1.8	<b>&lt;0.001</b>
No. of mixed lesions	1.5±2.4	3.0±3.0	1.3±2.1	<b>&lt;0.001</b>
No. of non-calcified lesions	0.9±1.5	1.3±2.2	0.8±1.4	0.067

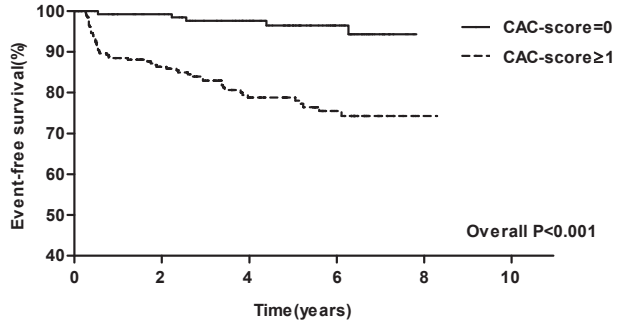
Abbreviations: CAC, coronary artery calcium; CAD, coronary artery disease; CTA, computed tomography coronary angiography.

were observed in this group. In addition, a higher mean number of calcified lesions (2.6±3.5 vs. 0.8±1.8(P<0.001)) and mixed lesions (3.0±3.0 vs.1.3±2.1(P<0.001)) were present in patients with events.

### Kaplan-Meier analysis

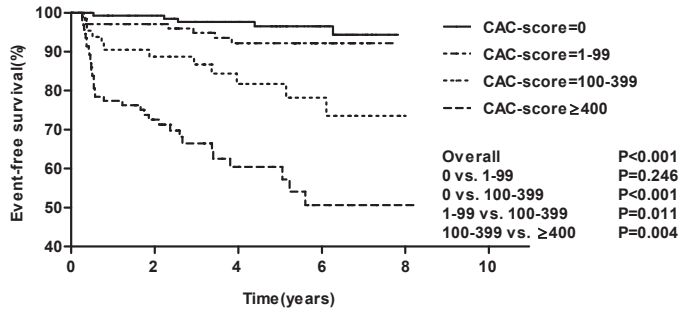
The results of the Kaplan-Meier survival analyses, stratified according to CAC-score, are depicted in Figure 2 Panel A and B. Crude event-rate was lower in patients with CAC-score=0 compared to patients with CAC-score≥1 (5/144(3%) vs. 54/266(20%)

# A



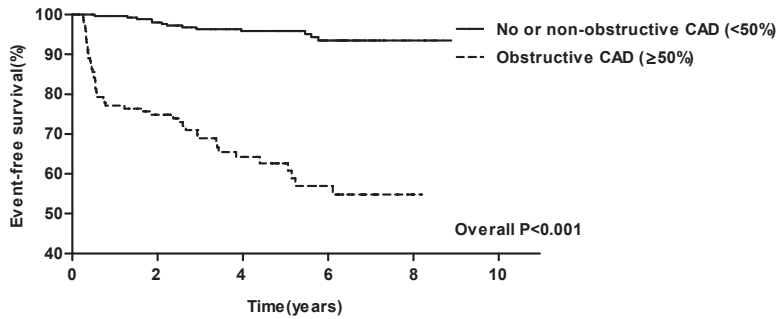
No. of patients at risk	410	317	221	111	1
CAC-score=0	144	124	97	49	1
CAC-score≥1	266	193	124	62	1

# B



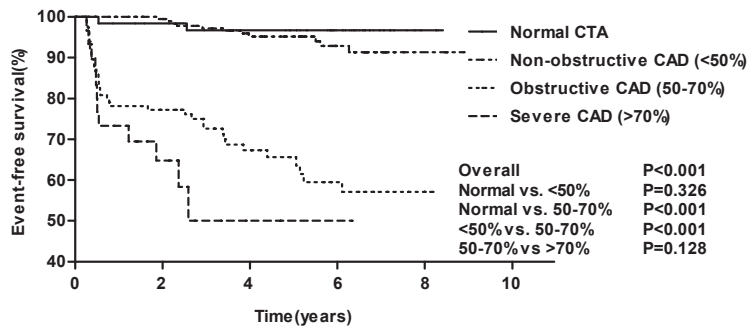
No. of patients at risk	410	317	221	111	1
CAC-score=0	144	124	97	49	1
CAC-score=1-99	106	90	66	35	
CAC-score=100-399	67	48	31	17	
CAC-score≥400	93	55	27	10	1

C



No. of patients at risk	431	337	234	126	14
CAD <50%	284	247	184	99	13
CAD ≥50%	147	90	50	27	1

D



No. of patients at risk	431	337	234	126	14
Normal CTA	65	60	52	35	4
CAD <50	219	187	132	64	9
CAD 50-70	117	77	48	26	1
CAD >70	30	13	2	1	

**Figure 2. Kaplan-Meier curves for the composite endpoint (all-cause mortality, non-fatal MI, late revascularization) according to CAC-score and coronary stenosis.**

Panel A: event-free survival difference between patients with CAC-score=0 and CAC-score≥1 Panel B: event-free survival difference between patients with CAC-score=0, CAC-score=1-99, CAC-score=100-399 and CAC-score≥400 Panel C: event-free survival difference between patients with no or non-obstructive CAD (<50%) and obstructive CAD (≥50%). Panel D: event-free survival difference between patients with normal CTA, non-obstructive CAD (<50%), obstructive CAD (50-70%) and severe CAD (>70%).

( $P < 0.001$ ) (Panel A). Additionally, an incremental increase in event-rate was observed with increasing CAC-risk category: 5/144(3%) for CAC-score=0, 7/106(7%) for CAC-score=1-99, 12/67(18%) for CAC-score=100-399, 35/93(38%) for CAC-score $\geq$ 400 ( $P < 0.001$ ). Thus, event-rate was highest in patients with CAC-score $\geq$ 400 (Panel B).

The results of the Kaplan-Meier survival analyses, stratified according to coronary stenosis, are depicted in Figure 2 Panel C and D. Crude event-rate was lower in patients with no or non-obstructive CAD ( $< 50\%$ ) compared to patients with obstructive CAD ( $\geq 50\%$ ) (13/284(5%) vs. 51/147(35%)( $P < 0.001$ )) (Panel C). An excellent prognosis was observed in patients with a normal CTA (event-rate 2/65(3%)). Of note, the 2 patients with a normal CTA presented with complications not related to diabetes and died of a (presumably) non-cardiac course. Additionally, an incremental increase in event-rate was observed with increasing coronary stenosis severity: 11/219(5%) for non-obstructive CAD ( $< 50\%$ ), 39/117(33%) for obstructive CAD (50-70%), 12/30(40%) for severe CAD ( $> 70\%$ ) ( $P < 0.001$ ). Event-rate was highest in patients with severe CAD ( $> 70\%$ ) (Panel D).

### Cox-regression analysis

The results of univariate Cox-regression analyses for the prediction of events are depicted in Table 3 and Table 4. CAC-score $\geq$ 100, obstructive (50-70%) or severe CAD ( $> 70\%$ ), total number of plaques, number of plaques stratified to stenosis (obstructive, severe) and number of plaques stratified to plaque composition (calcified, mixed, non-calcified) were all significant univariate predictors of the composite endpoint (Table 4).

The results of the multivariate Cox-regression analyses for the prediction of events are depicted in Table 5. To avoid over fitting of the model (limited number of events,  $n=65$ ) only a selection of the univariate significant variables was entered into the multivariate model (i.e. age, male gender, smoker, CAC-risk category, coronary stenosis grade). The variable smoker was selected over hypertension and hypercholesterolemia, assuming it correlated less with age and male gender. Moreover, replacing smoking with either hypertension or hypercholesterolemia did not have a strong influence on the results. In the multivariate analyses, corrected for the selected baseline variables (Model 2), CAC-score $\geq$ 100 was independently predictive of events. Moreover, CAC-score $\geq$ 400 provided incremental prognostic value over CAC-score=100-399 (HR=12.52 [95%CI 4.29;36.54]( $P < 0.001$ ) vs. HR=5.13 [95%CI 1.68;15.60]( $P=0.004$ )). Accordingly, obstructive (50-70%) or severe CAD ( $> 70\%$ ) remained an independent predictor of events. The presence of severe CAD ( $> 70\%$ ) provided incremental prognostic value over obstructive CAD (50-70%) (HR=15.16 [95%CI 3.01;76.36] ( $P=0.001$ ) vs. HR=11.10 [95%CI 2.52;48.79]( $P=0.001$ )). Adding the CTA results to Model 2 (including baseline variables and CAC-score) resulted in a significant change

**Table 3. Univariate Cox-regression analyses of baseline characteristics for the prediction of events.**

<b>Baseline</b>	<b>Univariate HR [95%CI]</b>	<b>P-value</b>
Age	1.06[1.04;1.09]	<b>&lt;0.001</b>
Male	1.97[1.14;3.38]	<b>0.015</b>
BMI	1.00[0.96;1.04]	0.959
Hypertension	1.79[1.10;2.93]	<b>0.020</b>
Hypercholesterolemia	2.15[1.32;3.51]	<b>0.002</b>
Family history of CAD	0.95[0.58;1.56]	0.846
Smoker	1.98[1.19;3.30]	<b>0.008</b>
<b>DM-related risk factors</b>		
DM type 2	1.58[0.87;2.85]	0.132
DM duration	1.00[1.00;1.00]	0.160
HbA <sub>1c</sub>	1.08[0.92;1.27]	0.326
<b>DM-related complications</b>		
PVD	3.01[1.37;6.60]	<b>0.006</b>
PNP	1.66[0.98;2.82]	0.058
PVD and PNP	1.77[0.76;4.10]	0.184
<b>DM-related treatment</b>		
Oral	1.13[0.67;1.90]	0.646
Insulin	0.60[0.35;1.04]	0.069
Oral and insulin	1.79[1.06;3.01]	<b>0.028</b>
<b>Medication</b>		
Aspirin	2.78[1.69;4.55]	<b>&lt;0.001</b>
ACE-inhibitors	2.39[1.47;3.89]	<b>&lt;0.001</b>
ARB	1.03[0.44;2.39]	0.946
Statins	1.97[1.16;3.34]	<b>0.012</b>
Beta-blockers	2.29[1.20;4.39]	<b>0.012</b>
Calcium-antagonists	3.94[1.70;9.14]	<b>0.001</b>
<b>Serum markers</b>		
Total cholesterol	1.23[0.99;1.54]	0.067
LDL	1.13[0.89;1.43]	0.317
HDL	0.92[0.55;1.54]	0.756
Cholesterol/HDL ratio	1.06[0.93;1.22]	0.364
Triglycerides	1.09[0.91;1.31]	0.364

Abbreviations and definitions as in Table 1.

in -2 log likelihood (17.60, P 0.001) (Model 3). Moreover, adding the CTA results to the baseline model resulted in a larger increase in the -2 log likelihood compared to the adding of the CAC-score (43.78 vs. 36.30) (Model 4).

**Table 4. Univariate Cox-regression analyses of CAC-scoring and coronary CTA for the prediction of events.**

<b>CAC-scoring</b>	<b>Univariate HR [95%CI]</b>	<b>P-value</b>
<b>CAC-risk category</b>	Overall	<b>&lt;0.001</b>
CAC-score=0	Ref. category	
CAC-score=1-99	1.92[0.61;6.05]	0.265
CAC-score=100-399	6.11[2.15;17.35]	<b>0.001</b>
CAC-score≥400	15.79[6.16;40.50]	<b>&lt;0.001</b>
<b>Coronary CTA</b>	<b>Univariate HR [95%CI]</b>	<b>P-value</b>
<b>Coronary stenosis</b>	Overall	<b>&lt;0.001</b>
Normal CTA	Ref. category	
Non-obstructive CAD (<50%)	1.92[0.43;8.67]	0.397
Obstructive CAD (50-70%)	16.18[3.90;67.21]	<b>&lt;0.001</b>
Severe CAD (>70%)	29.03[6.40;131.73]	<b>&lt;0.001</b>
<b>Coronary plaques (stenosis)</b>		
No. of plaques	1.09[1.04;1.14]	<b>&lt;0.001</b>
No. of non-obstructive lesions	1.02[0.98;1.07]	0.375
No. of obstructive lesions	1.40[1.31;1.51]	<b>&lt;0.001</b>
No. of severe lesions	2.42[1.77;3.30]	<b>&lt;0.001</b>
<b>Coronary plaques (composition)</b>		
No. of calcified lesions	1.22[1.14;1.30]	<b>&lt;0.001</b>
No. of mixed lesions	1.24[1.16;1.33]	<b>&lt;0.001</b>
No. of non-calcified lesions	1.17[1.04;1.31]	<b>0.007</b>

Abbreviations and definitions as in Table 2

## Discussion

The present study assessed the long term prognostic value of coronary CTA in a large prospective registry of diabetic patients without chest pain syndrome. Coronary CTA demonstrated high prevalence of CAD (85%), mostly non-obstructive. Most importantly, patients with a normal CTA had an excellent prognosis. Furthermore, an incremental increase in event-rate was observed with increasing coronary stenosis severity. Finally, obstructive (50-70%) or severe CAD (>70%) was independently predictive of events, with increased value over baseline risk factors (i.e. age, male gender, smoker). Moreover, the CAC-score demonstrated a similar independent predictive value for the occurrence of events. However, the model including CTA performed better than the model with CAC-score, and CTA provided some additional value over the CAC-score. Although it should be noted that this was a crude analysis

Table 5. Multivariate Cox-regression analyses of selected significant univariate variables for the prediction of events.

Variable	Model 1			Model 2			Model 3			Model 4		
	Multivariate HR [95%CI]	P-value		Multivariate HR [95%CI]	P-value		Multivariate HR [95%CI]	P-value		Multivariate HR [95%CI]	P-value	
Age	1.06[1.04;1.09]	<b>&lt;0.001</b>		1.01[0.98;1.04]	0.541		1.00 [0.97;1.04]	0.809		1.03[1.00;1.05]	0.094	
Male	1.80[1.05;3.12]	<b>0.033</b>		1.33[0.74;2.39]	0.339		1.00 [0.97;1.04]	0.273		1.40[0.79;2.46]	0.246	
Smoker	2.23[1.34;3.73]	<b>0.002</b>		1.67[0.97;2.88]	0.065		1.40 [0.77;2.57]	0.139		1.84[1.09;3.13]	<b>0.024</b>	
CAC-risk category				Overall	<b>&lt;0.001</b>		Overall	0.069				
CAC-score=0				Ref. category			Ref. category					
CAC-score=1-99				1.74[0.54;5.56]	0.352		1.37 [0.38;4.93]	0.630				
CAC-score=100-399				5.13[1.68;15.60]	<b>0.004</b>		2.54 [0.70;9.29]	0.158				
CAC-score≥400				12.52[4.29;36.54]	<b>&lt;0.001</b>		4.06 [1.11;14.82]	<b>0.034</b>				
Coronary stenosis							Overall	<b>0.002</b>		Overall	<b>&lt;0.001</b>	
Normal CTA				Ref. category			Ref. category			Ref. category		
Non-obstructive CAD (<50%)							0.98 [0.18;5.36]	0.978		1.60[0.35;7.34]	0.549	
Obstructive CAD (50-70%)							4.70 [0.82;26.99]	0.082		11.10[2.52;48.79]	<b>0.001</b>	
Severe CAD (>70%)							5.54 [0.85;36.07]	0.074		15.16[3.01;76.36]	<b>0.001</b>	
Change in -2 log likelihood				36.30	<b>&lt;0.001±</b>		17.60	<b>0.001*</b>		43.78	<b>&lt;0.001±</b>	

Model 1: Baseline characteristics

Model 2: Baseline characteristics + coronary artery calcium score

Model 3: Baseline characteristics + coronary artery calcium score + coronary computed tomography coronary angiography

Model 4: Baseline characteristics + coronary computed tomography coronary angiography

Abbreviations and definitions as in Table 2.

± compared to Model 1

\* compared to Model 2

and that the present study was not designed to assess the difference in performance between CTA and CAC-score.

### **CAC-score**

Previous studies widely established the prevalence of CAC in diabetic patients without chest pain syndrome.<sup>16-18</sup> The present study assessed the prognostic value of CAC by demonstrating CAC-score $\geq$ 100 as independent predictor of events in diabetic patients without chest pain syndrome. Prior to our study, Raggi *et al.* investigated the prognostic value of CAC-scoring for all-cause mortality in asymptomatic individuals.<sup>19</sup> In this study 10377 asymptomatic individuals were prospectively included to undergo electron beam computed tomography (EBCT): 903(9%) individuals with DM, 9474(91%) individuals without DM. This study, with mean follow-up of 5 years, demonstrated CAC as independent predictor of all-cause mortality in both diabetic and non-diabetic asymptomatic individuals. Moreover, Anand *et al.* investigated the prognostic value of EBCT for short term events in 510 asymptomatic patients with DM type 2.<sup>20</sup> This study, with median follow-up of 2.2 years, demonstrated CAC-score $\geq$ 100 as independent predictor of cardiac death, MI, acute coronary syndrome (ACS), late coronary revascularization (>60 days after EBCT) and non-haemorrhagic stroke over established cardiovascular risk factors. Additionally, the PREDICT (prospective evaluation of diabetic ischemic disease by computed tomography) study investigated the prognostic value of EBCT for cardiovascular events in 589 asymptomatic patients with DM type 2.<sup>21</sup> Cardiovascular events, which were defined as death due to MI or other cardiovascular causes, non-fatal MI, unstable angina, other objective evidence of CAD and stroke, occurred in 66(11%) patients after median follow-up of 4 years. In the multivariate analyses CAC-score $\geq$ 101 was independently predictive of cardiovascular events. These findings were in line with the present study. Moreover, similar to the present study, incremental prognostic value was provided with increasing CAC-risk category.

### **Coronary stenosis on CTA**

Several large cohort studies assessed the prevalence of CAD in the specific setting of diabetic patients without chest pain syndrome.<sup>6, 17, 22, 23</sup> Similar to the present study, in these studies the majority of asymptomatic diabetic patients presented with CAD on coronary CTA (64-93 %). Accordingly, non-obstructive CAD (<50%) was most frequently observed (44-64%), whereas obstructive CAD ( $\geq$ 50%) was less prevalent (17-29%).

Only a few studies assessed the prognostic value of coronary CTA in diabetic patients without chest pain syndrome.<sup>15, 22, 24</sup> From the CONFIRM (coronary CT angiography evaluation for clinical outcomes: an international multicentre) registry

of 27125 patients, Min *et al.* selected 400 asymptomatic diabetic patients who underwent coronary CTA.<sup>15</sup> The prognostic value of CTA was investigated using the same composite endpoint as in the present study. Events occurred in 33(8%) patients after mean follow-up of  $2.4 \pm 1.1$  years: all-cause mortality in 13(3%) patients, non-fatal MI in 8(2%) patients, late revascularization in 12(3%) patients. In the multivariate analyses, corrected for selected variables (i.e. age, male gender, CAC-score), maximal stenosis severity, number of vessels with obstructive CAD ( $\geq 50\%$ ) and segment stenosis score (a marker of overall atherosclerosis extent) were independently predictive of events. Indeed, obstructive (50-70%) or severe ( $>70\%$ ) CAD provided prognostic value in the present study. Also Faustino *et al.* investigated the prognostic value of coronary CTA for cardiovascular events in 85 asymptomatic patients with DM type 2.<sup>24</sup> Cardiovascular events occurred in 10(11.8%) patients after median follow-up of 48(IQR 18-68) months: cardiovascular death in 2(2.4%) patients, unstable angina in 1(1.2%) patients, stroke 7(8.4%) in patients. In the multivariate analyses, corrected for univariate significant variables, absence of obstructive CAD ( $\geq 50\%$ ) was independently protective of events. Indeed, no or non-obstructive CAD ( $<50\%$ ) was not associated with increased risk for events in the present study. Most importantly, patients with a normal CTA had an excellent prognosis. Last, Park *et al.* investigated the prognostic value of coronary CTA for cardiovascular events in 557 asymptomatic Korean patients with DM type 2.<sup>22</sup> Cardiovascular events were defined as cardiovascular death, non-fatal MI, ACS requiring hospitalization and late revascularization ( $>6$  months after coronary CTA). More cardiovascular events and lower 3 year event-free survival rates were observed in patients with obstructive CAD ( $\geq 50\%$ ) compared to patients without obstructive CAD ( $<50\%$ ). Accordingly, in the present study a higher crude event-rate was observed in patients with obstructive CAD ( $\geq 50\%$ ) compared to patients with no or non-obstructive CAD ( $<50\%$ ).

### **Coronary plaque composition on CTA**

Multiple studies assessed plaque composition on coronary CTA in diabetic patients without chest pain syndrome. Comparable to the present study, the majority of these studies described an increased prevalence of mixed lesions in asymptomatic diabetic patients.<sup>6, 17, 25</sup>

The prognostic value of coronary plaque composition on coronary CTA for cardiovascular events in the specific setting of diabetic patients without chest pain syndrome has not been previously established. The present study demonstrated all coronary plaque compositions (calcified, mixed, non-calcified) as univariate significant predictors of events. The prognostic value of calcified and mixed lesions was highest. These findings suggest an independent association between plaque composition and events.

However, the role of coronary plaque composition remains controversial. Gaemperli *et al.* demonstrated the prognostic value of coronary plaque composition in 220 symptomatic patients.<sup>26</sup> In contrast to the present study, mixed and non-calcified demonstrated highest predictive value for events. On the other hand, in the CONFIRM registry, including both symptomatic and asymptomatic patients with and without DM, calcified and mixed plaque provided the strongest predictive value.<sup>27</sup> Further research is needed to understand the underlying pathophysiological mechanism of the different coronary plaque compositions.

### **Single positron Emission Tomography (SPECT) Myocardial perfusion imaging (MPI)**

The role of SPECT MPI for screening for silent ischemia in asymptomatic diabetic patients has been previously addressed.<sup>28,29</sup> Anand *et al.* included 510 asymptomatic diabetic patients of whom 180 patients underwent SPECT MPI.<sup>29</sup> In those patients, the event-rate was significantly increased with increasing ischemic burden on SPECT MPI demonstrating the value for risk stratification. The most important study in this field was the DIAD (detection of Ischemia in Asymptomatic Diabetics) study.<sup>28</sup> In this randomized controlled trial 1123 asymptomatic diabetic participants were randomized to SPECT MPI or no screening. After a mean follow-up of 4.8 years the incidence of cardiac events was higher in patients with significant MPI abnormalities. However, there was no significant prognostic benefit of screening.

### **Clinical implications**

The present observations demonstrate the prognostic value of CTA in diabetic patients without chest pain syndrome. Recent ESC guidelines indicate patients with DM as high risk for CAD (or very high risk if  $\geq 1$  cardiovascular risk factor was present) irrespective of chest pain symptoms. Indeed, in the present study a great majority of patients presented with CAD on coronary CTA and the presence of obstructive (50-70%) or severe CAD (>70%) was associated with an impaired prognosis. Still, CAD was ruled-out in 15% of patients based on a normal CTA. Most importantly, the prognosis of these patients was excellent.

The value of screening for CAD in high risk diabetic patients without chest pain syndrome was recently addressed by Muhlestein *et al.*<sup>30</sup> In this trial, 900 asymptomatic patients were randomized to CAD screening using coronary CTA or optimal medical treatment (OMT). The trial demonstrated no survival benefit from screening with coronary CTA. Therefore, this study does not support screening in all diabetic patients. Similarly, the American Diabetes Association position statement on cardiovascular disease and risk management only recommend screening using advanced cardiac testing in patients with cardiac symptoms or ECG abnormalities.<sup>31</sup> However,

as also demonstrated in the present study, a large proportion of the patients had CAD on CTA and coronary CTA could identify patients with excellent prognosis. This supports the need to enrich the screening population to a high risk population who will mostly benefit from screening using coronary CTA. Especially since coronary CTA may lead to radiation exposure and may result in unnecessary invasive testing such as coronary angiography and revascularization procedures.<sup>31</sup> Potentially, coronary CTA can provide a pivotal role in tailored therapy in these diabetic patients. Patients with a normal CTA have an excellent prognosis and could be treated conservatively (OMT), whereas patients with an abnormal CTA may benefit from additional non-invasive or invasive evaluation.

### **Limitations**

Several limitations of the present study need to be considered. First, the present study was a single centre study. Second, the composite event-rate was relatively low. As a consequence, the study was underpowered to include all baseline risk factors into the multivariate model. Second, the endpoint mainly consisted of late revascularization, therefore conclusions regarding hard endpoints are not justified based on this study. We cannot rule out that, despite the wide time interval, some referral bias has occurred in the patients who underwent late revascularization. Moreover, it is possible that events that have occurred in other medical centres were missed in the analysis. Third, coronary CTA only visualizes coronary atherosclerosis and provides no information on the hemodynamic significance of coronary stenosis.

### **Conclusion**

Coronary CTA provided prognostic value in a large prospective registry of diabetic patients without chest pain syndrome. Most importantly, the prognosis of patients with a normal CTA was excellent. In addition, an incremental increase in event-rate was observed with increasing CAC-risk category and coronary stenosis severity. The highest event rate was observed in patients with severe CAD (>70%). Both CAC-score and coronary stenosis severity were independently predictive of events, after correction for baseline risk factors.

## References

- (1) International Diabetes Federation. Diabetes e-Atlas. <http://www.idf.org/e-atlas/home> . 2013. 20-6-2014.
- (2) Morrish NJ, Wang SL, Stevens LK, Fuller JH, Keen H. Mortality and causes of death in the WHO Multinational Study of Vascular Disease in Diabetes. *Diabetologia* 2001 September;44 Suppl 2:S14-S21.
- (3) Ryden L, Grant PJ, Anker SD *et al.* ESC guidelines on diabetes, pre-diabetes, and cardiovascular diseases developed in collaboration with the E. *Diab Vasc Dis Res* 2014 May;11(3):133-73.
- (4) Zellweger MJ, Hachamovitch R, Kang X *et al.* Prognostic relevance of symptoms versus objective evidence of coronary artery disease in diabetic patients. *Eur Heart J* 2004 April;25(7):543-50.
- (5) Scholte AJ, Schuijff JD, Kharagiitsingh AV *et al.* Prevalence of coronary artery disease and plaque morphology assessed by multi-slice computed tomography coronary angiography and calcium scoring in asymptomatic patients with type 2 diabetes. *Heart* 2008 March;94(3):290-5.
- (6) Zeina AR, Odeh M, Rosenschein U, Zaid G, Barmeir E. Coronary artery disease among asymptomatic diabetic and nondiabetic patients undergoing coronary computed tomography angiography. *Coron Artery Dis* 2008 February;19(1):37-41.
- (7) Djaberi R, Beishuizen ED, Pereira AM *et al.* Non-invasive cardiac imaging techniques and vascular tools for the assessment of cardiovascular disease in type 2 diabetes mellitus. *Diabetologia* 2008 September;51(9):1581-93.
- (8) Perrone-Filardi P, Achenbach S, Mohlenkamp S *et al.* Cardiac computed tomography and myocardial perfusion scintigraphy for risk stratification in asymptomatic individuals without known cardiovascular disease: a position statement of the Working Group on Nuclear Cardiology and Cardiac CT of the European Society of Cardiology. *Eur Heart J* 2011 August;32(16):1986-93, 1993a, 1993b.
- (9) Taylor AJ, Cerqueira M, Hodgson JM *et al.* ACCF/SCCT/ACR/AHA/ASE/ASNC/NASCI/SCAI/SCMR 2010 appropriate use criteria for cardiac computed tomography. A report of the American College of Cardiology Foundation Appropriate Use Criteria Task Force, the Society of Cardiovascular Computed Tomography, the American College of Radiology, the American Heart Association, the American Society of Echocardiography, the American Society of Nuclear Cardiology, the North American Society for Cardiovascular Imaging, the Society for Cardiovascular Angiography and Interventions, and the Society for Cardiovascular Magnetic Resonance. *J Am Coll Cardiol* 2010 November 23;56(22):1864-94.
- (10) Djaberi R, Schuijff JD, Boersma E *et al.* Differences in atherosclerotic plaque burden and morphology between type 1 and 2 diabetes as assessed by multislice computed tomography. *Diabetes Care* 2009 August;32(8):1507-12.
- (11) Diagnosis and classification of diabetes mellitus. *Diabetes Care* 2008 January;31 Suppl 1:S55-S60.
- (12) van Werkhoven JM, Schuijff JD, Gaemperli O *et al.* Incremental prognostic value of multi-slice computed tomography coronary angiography over coronary artery calcium scoring in patients with suspected coronary artery disease. *Eur Heart J* 2009 November;30(21):2622-9.
- (13) de Graaf FR, Schuijff JD, van Velzen JE *et al.* Diagnostic accuracy of 320-row multidetector computed tomography coronary angiography in the non-invasive evaluation of significant coronary artery disease. *Eur Heart J* 2010 August;31(15):1908-15.

- (14) Steg PG, James SK, Atar D *et al.* ESC Guidelines for the management of acute myocardial infarction in patients presenting with ST-segment elevation. *Eur Heart J* 2012 October;33(20):2569-619.
- (15) Min JK, Labounty TM, Gomez MJ *et al.* Incremental prognostic value of coronary computed tomographic angiography over coronary artery calcium score for risk prediction of major adverse cardiac events in asymptomatic diabetic individuals. *Atherosclerosis* 2014 February;232(2):298-304.
- (16) Khaleeli E, Peters SR, Bobrowsky K, Oudiz RJ, Ko JY, Budoff MJ. Diabetes and the associated incidence of subclinical atherosclerosis and coronary artery disease: Implications for management. *Am Heart J* 2001 April;141(4):637-44.
- (17) Rivera JJ, Nasir K, Choi EK *et al.* Detection of occult coronary artery disease in asymptomatic individuals with diabetes mellitus using non-invasive cardiac angiography. *Atherosclerosis* 2009 April;203(2):442-8.
- (18) Choi EK, Chun EJ, Choi SI *et al.* Assessment of subclinical coronary atherosclerosis in asymptomatic patients with type 2 diabetes mellitus with single photon emission computed tomography and coronary computed tomography angiography. *Am J Cardiol* 2009 October 1;104(7):890-6.
- (19) Raggi P, Shaw LJ, Berman DS, Callister TQ. Prognostic value of coronary artery calcium screening in subjects with and without diabetes. *J Am Coll Cardiol* 2004 May 5;43(9):1663-9.
- (20) Anand DV, Lim E, Hopkins D *et al.* Risk stratification in uncomplicated type 2 diabetes: prospective evaluation of the combined use of coronary artery calcium imaging and selective myocardial perfusion scintigraphy. *Eur Heart J* 2006 March;27(6):713-21.
- (21) Elkeles RS, Godsland IF, Feher MD *et al.* Coronary calcium measurement improves prediction of cardiovascular events in asymptomatic patients with type 2 diabetes: the PREDICT study. *Eur Heart J* 2008 September;29(18):2244-51.
- (22) Park GM, Lee SW, Cho YR *et al.* Coronary computed tomographic angiographic findings in asymptomatic patients with type 2 diabetes mellitus. *Am J Cardiol* 2014 March 1;113(5):765-71.
- (23) Silva JD, Mota P, Coelho A, Catarino R, Leitao-Marques A. Incidence of subclinical atherosclerosis in asymptomatic type-2 diabetic patients: the potential of multi-slice computed tomography coronary angiography. *Coron Artery Dis* 2011 January;22(1):26-31.
- (24) Faustino A, Providencia R, Mota P *et al.* Can cardiac computed tomography predict cardiovascular events in asymptomatic type-2 diabetics?: results of a long term follow-up. *BMC Cardiovasc Disord* 2014;14:2.
- (25) Pundziute G, Schuijff JD, Jukema JW *et al.* Type 2 diabetes is associated with more advanced coronary atherosclerosis on multislice computed tomography and virtual histology intravascular ultrasound. *J Nucl Cardiol* 2009 May;16(3):376-83.
- (26) Gaemperli O, Valenta I, Schepis T *et al.* Coronary 64-slice CT angiography predicts outcome in patients with known or suspected coronary artery disease. *Eur Radiol* 2008 June;18(6):1162-73.
- (27) Hadamitzky M, Achenbach S, Al-Mallah M *et al.* Optimized prognostic score for coronary computed tomographic angiography: results from the CONFIRM registry (COronary CT Angiography Evaluation For Clinical Outcomes: An International Multicenter Registry). *J Am Coll Cardiol* 2013 July 30;62(5):468-76.

- (28) Young LH, Wackers FJ, Chyun DA *et al.* Cardiac outcomes after screening for asymptomatic coronary artery disease in patients with type 2 diabetes: the DIAD study: a randomized controlled trial. *JAMA* 2009 April 15;301(15):1547-55.
- (29) Anand DV, Lim E, Hopkins D *et al.* Risk stratification in uncomplicated type 2 diabetes: prospective evaluation of the combined use of coronary artery calcium imaging and selective myocardial perfusion scintigraphy. *Eur Heart J* 2006 March;27(6):713-21.
- (30) Muhlestein JB, Lappe DL, Lima JA *et al.* Effect of Screening for Coronary Artery Disease Using CT Angiography on Mortality and Cardiac Events in High-Risk Patients With Diabetes: The FACTOR-64 Randomized Clinical Trial. *JAMA* 2014 November 17.
- (31) (8) Cardiovascular disease and risk management. *Diabetes Care* 2015 January;38 Suppl:S49-S57.





# Chapter 12

Summary and conclusions



The aim of this thesis was to explore the value of coronary computed tomography angiography in clinical practice. Specifically, the thesis focuses on the feasibility of quantitative assessment of coronary atherosclerosis on CTA. Additionally, the clinical value of coronary CTA in the specific setting of high risk diabetic patients without chest pain syndrome was established.

The general introduction in **Chapter 2** of this thesis discusses the evolving role of cardiac CT in the diagnosis of patients with suspected CAD. An overview is provided of the performance of cardiac CTA and CAC score in the specific setting of patients with stable angina and patients presenting with acute chest pain at the emergency department. Furthermore, novel applications as myocardial perfusion and CT derived fractional flow reserve are discussed.

## Part 1

Part 1 of this thesis established the value of quantitative assessment of coronary atherosclerosis on coronary CTA in clinical practice.

**Chapter 3** provides an overview of the different imaging modalities for quantitative assessment of coronary atherosclerosis and progression of coronary plaque. The clinical value of progression of atherosclerosis and corresponding medical therapy is discussed.

The value of QCT to assess coronary plaque constitution is assessed in **Chapter 4-6**. For this purpose the QCT datasets were registered based on anatomical landmarks with IVUS VH as reference standard.

In **Chapter 4** the ability of QCT to assess coronary plaque composition was assessed. For this purpose 57 patients who had undergone CTA prior to IVUS VH were included. QCT was performed in all patients. CTA plaque volume was differentiated in 4 different plaque types: necrotic core, dense calcium, fibrotic and fibro-fatty tissue. The same parameters were derived from IVUS VH and compared. The performance of two different approaches for tissue characterization was evaluated. The first used fixed Hounsfield unit (HU) cut-off values to differentiate the different components. The second used a dynamic threshold model, for which the HU threshold were adapted to the lumen HU intensity. The different plaque types on QCT were well-correlated with IVUS VH. The dynamic threshold approach performed better, compared to the fixed threshold approach, as demonstrated by more narrow limits of agreement on the Bland–Altman analyses. Based on these results it was concluded that automatic, quantitative CTA tissue characterization is feasible using a dedicated software tool.

The relation between coronary atherosclerosis on QCT as compared to IVUS VH is further explored in **Chapter 5**. A major limitation of IVUS VH is the inability of the echo signal to penetrate coronary calcium. As a result, tissue located in the acoustic shadow behind calcium is difficult to classify. Using a novel algorithm this shadow can be automatically detected and quantified. The quantified volumes were added to the total volume of calcium to compensate for the expected underestimation of calcium by IVUS VH. Indeed, by applying the novel algorithm, the agreement between IVUS VH and QCT for the assessment of coronary calcium improved.

In **Chapter 6** the ability of QCT to assess the Agatston coronary artery calcium score (CAC) was investigated. For this purpose 100 patients, 20 patients for each CAC category (i.e. 0, 1–99, 100–399, 400–999,  $\geq 1,000$ ), were randomly selected. The Agatston CAC score on non-contrast CT was calculated manually, while the novel algorithm was used to automatically detect and quantify Agatston CAC score in contrast CTA images. The resulting Agatston CAC scores were validated against the non-contrast images. The automatically computed CAC score showed a high correlation and intra-class correlation with non-contrast CT CAC score. Moreover, agreement within the CAC categories was good. It was concluded that fully automatic detection of Agatston CAC score on contrast CTA is feasible and showed high correlation with the non-contrast CT CAC score. This could imply a radiation dose reduction and time saving by omitting the non-contrast scan.

Previous studies have demonstrated the disagreement between significant stenosis on CTA and ischemia on SPECT MPI. Potentially, QCT can improve the correlation between stenosis severity and the presence of ischemia. Therefore, the aim of **Chapter 7** was to evaluate the association between QCT parameters of coronary artery lesions and the presence of myocardial ischemia on gated myocardial perfusion SPECT. Forty patients were included with known or suspected coronary artery disease who had undergone CTA and gated myocardial perfusion SPECT within 6 months. From the CTA datasets, vessel-based and lesion-based visual analyses were performed. Consecutively, lesion-based QCT was performed to assess plaque length, plaque burden, percentage lumen area stenosis and remodelling index. Subsequently, the presence of myocardial ischemia was assessed using the summed difference score ( $\text{SDS} \geq 2$ ) on gated myocardial perfusion SPECT. Myocardial ischemia was seen in 25 patients (62.5%) in 37 vascular territories. Coronary lesion length and quantitatively assessed significant stenosis were independently associated with myocardial ischemia. Both quantitative parameters had incremental value over baseline variables and traditional visual assessment of significant stenosis. It was concluded that QCT can possibly enhance assessment of CAD, which may be of potential use for identification of patients with myocardial ischemia.

To evaluate the prognostic value of the severity, location and composition of CAD combined in a CTA risk score, the study of **Chapter 8** was designed. The hypothesis was that a risk score incorporating all quantitative stenosis parameters allows for accurate risk stratification. Therefore, the purpose of this study was to determine if an automatic quantitative assessment of CAD using QCT combined into a single CTA risk score allows risk stratification of patients. In 300 patients QCT was performed to automatically detect and quantify all lesions in the coronary tree. Using QCT, the novel CTA risk score was calculated based on plaque extent, severity, composition, and location on a segment basis. During follow-up, the composite end point of all-cause mortality, revascularization, and nonfatal infarction was recorded. In 127 patients with obstructive CAD ( $\geq 50\%$  stenosis), 27 events were recorded, all in patients with a high CTA risk score. In conclusion, the present study demonstrated that a fully automatic QCT analysis of CAD is feasible and can be applied for risk stratification of patients with suspected CAD. The novel CTA risk score incorporating location, severity, and composition of coronary lesion may improve risk stratification, but this needs to be confirmed in larger studies.

The aim of the study in **Chapter 9** was to evaluate the feasibility of QCT for the assessment of coronary atherosclerosis changes over time on serial CTA in patients with stable chest pain. For this study 53 patients clinically referred for the evaluation of chest pain who underwent a coronary CTA at the Rijnland Hospital. After a minimum of 2 years CTA was repeated to evaluate changes in coronary atherosclerosis over time. For accurate and reproducible assessment of CAD changes, all CTAs were quantitatively analysed using QCT. All parameters of dimension and composition of CAD were compared between patients to assess possible regression and progression of CAD. It was demonstrated that 32(60%) showed regression of coronary total atheroma volume whereas 21(40%) showed progression of coronary atheroma. Patients with progression of coronary atheroma had progression of all four plaque types. However, patients with regression demonstrated a regression of all plaque components except for dense calcium, for which progression was observed. This study demonstrated that the assessment of changes in CAD with QCT is feasible. Potentially QCT could be applied to assess the efficacy of anti-atherosclerotic therapy.

## Part 2

Part 2 of this thesis discusses the value of CTA in high risk diabetic patients without chest pain syndrome.

**Chapter 10** primarily evaluated changes in myocardial ischemia on SPECT myocardial perfusion imaging after 2 years in a cohort of high-risk patients with diabetes

without cardiac symptoms or known CAD. Secondly, this chapter assessed the value of baseline CTA-derived coronary atherosclerosis parameters to predict changes in myocardial ischemia. The population consisted of 100 high-risk patients with diabetes without cardiac symptoms referred for cardiovascular risk stratification. All patients underwent CAC scoring, CTA, and SPECT MPI. After 2 years of follow-up, SPECT MPI was repeated to evaluate potential progression of ischemia. The rate of progression of ischemia in high-risk patients with diabetes without cardiac symptoms is limited. Few patients presented with new ischemia, whereas some patients showed resolution of ischemia. Atherosclerosis parameters on CTA were not predictive of new-onset ischemia or progression of ischemia.

**Chapter 11** aims to investigate the long term prognostic value of coronary CTA in a large population of high risk diabetic patients without chest pain syndrome. 525 diabetic patients without chest pain syndrome were prospectively included to undergo coronary artery calcium (CAC)-scoring followed by coronary CTA. During follow-up the composite endpoint of all-cause mortality, non-fatal myocardial infarction and late revascularization (>90 days) was registered. After median follow-up of 5.0(IQR 2.7-6.5) years the composite endpoint occurred in 65(14%) patients. Coronary CTA demonstrated a high prevalence of CAD (85%), mostly non-obstructive CAD (51%). Furthermore, patients with a normal CTA had an excellent prognosis (event-rate 3%). An incremental increase in event-rate was observed with increasing CAC-risk category or coronary stenosis severity. Finally, obstructive (50-70%) or severe CAD (>70%) was independently predictive of events. It was concluded that coronary CTA provided prognostic value in high risk diabetic patients without chest pain syndrome. Most importantly, the prognosis of patients with a normal CTA was excellent.

## Conclusions

The objective of this dissertation was to establish the value of QCT to further enhance the clinical applicability and accuracy of coronary CTA. The automatic characterization of coronary atherosclerosis with QCT is feasible and correlates well with IVUS VH. However, further work is needed to provide quantification of coronary stents and coronary blood flow. In the near future, the parameters of dimension and composition of coronary atherosclerosis will likely gain more clinical interest. It appears that coronary CTA can provide more clinically relevant information than the mere presence of coronary atherosclerosis or obstructive stenosis. Therefore, a novel CTA risk score was created incorporating detailed information on the location, severity and composition of atherosclerosis as assessed with QCT. This CTA risk score allows

accurate risk stratification of patients with suspected CAD. The work on this CTA risk score is continued to further validate the CTA risk score in external patient cohorts.

In this thesis the feasibility of QCT to assess changes over time in coronary atherosclerosis on CTA was explored. For clinical practice, disease progression (or regression) is an important variable which could be used to evaluate the efficacy of drugs, but also provide a more detailed insight in the natural history of coronary atherosclerosis on CTA.

A drawback of coronary CTA is the fact that the hemodynamic significance of a lesion cannot be evaluated. In this thesis it was demonstrated that QCT provided better correlation with the presence of myocardial ischemia on SPECT MPI as compared to current visual assessment of coronary CTA.

With regards to the specific setting of high risk diabetic patients without chest pain syndrome several conclusion can be derived from this thesis. First, if treated with optimal medical therapy, very few patients present with progression of myocardial ischemia. Second, the prognosis of these patients is good; the overall long-term event-rate is limited. Especially diabetic patients without CAD on coronary CTA have an excellent prognosis. Even though the prognostic value of CTA was demonstrated in this thesis, it is unclear if screening using cardiac imaging influences the outcome of these patients. Additionally, cardiac CTA or CAC-score could help tailor medical therapy in this challenging patient population.



# Chapter 13

Samenvatting en conclusies



Het doel van dit proefschrift was het bestuderen van de rol van computer tomografie (CT) coronairangiografie in de klinische praktijk. Het onderzoek van de thesis richt zich met name op de toepasbaarheid van een kwantitatieve analyse van coronairatherosclerose op CT coronairangiografie. Daarnaast wordt in dit proefschrift de klinische waarde van CT coronairangiografie in hoog-risico diabetes patiënten zonder angina pectoris klachten onderzocht.

De algemene introductie in **Hoofdstuk 2** bespreekt de rol van cardiale CT in de diagnostiek van patiënten met verdenking op coronairlijden. Er wordt een overzicht geschetst van de waarde van cardiale CT en de coronair calcium score, in zowel patiënten met stabiele pijn op de borst, als patiënten met acute cardiale klachten die zich presenteren op de spoedeisende hulp. Daarnaast wordt ingegaan op nieuwe toepassingen van CT zoals myocardperfusie CT en 'fractional flow reserve' bepalingen op CT.

## Deel 1

Deel 1 van dit proefschrift legt zich toe op de klinische toepasbaarheid van kwantitatieve analyse van atherosclerose op CT coronairangiografie.

In **hoofdstuk 3** wordt een overzicht geschetst van de verschillende beeldvormingstechnieken voor kwantificatie van coronairatherosclerose. Daarnaast wordt besproken hoe progressie van ziekte bepaald kan worden en wat de relatie is met medicamenteuze therapie.

De waarde van QCT voor het bepalen van plaquecompositie werd bestudeerd in **Hoofdstuk 4-6**. Hiervoor werden de QCT datasets geregistreerd met de IVUS VH datasets op basis van anatomische herkenningspunten.

In **Hoofdstuk 4** wordt gekeken naar de mogelijkheid om middels QCT de compositie van coronairatherosclerose op CT te bepalen. Hiervoor werden 57 patiënten geïncludeerd die zowel CT coronairangiografie als IVUS VH hadden ondergaan.

In alle patiënten werd QCT verricht. Plaquevolume werd gedifferentieerd in 4 verschillende plaquetypes: necrotische plaque, 'dense calcium', fibreuze plaque en fibreus-vet weefsel. Dezelfde parameters werden bepaald in IVUS VH en vergeleken. Er werden twee verschillende algoritmes voor plaquedifferentiatie gebruikt. De eerste methode gebruikt vaste ('fixed') HU afkapwaardes. De tweede methode gebruikt een dynamisch algoritme, waarbij de HU afkapwaardes worden aangepast aan de intens-

iteit van het lumen. De differentiatie tussen de verschillende plaquetypes middels QCT toonde een goede correlatie met IVUSVH. Het dynamische algoritme presteerde beter, zoals bleek uit smallere Bland-Altman 'limits of agreement'. Op basis van deze resultaten werd geconcludeerd dat middels QCT, automatische kwantificatie van verschillende plaquetypes mogelijk is.

De relatie tussen coronairatherosclerose op QCT en op IVUS VH wordt verder onderzocht in **Hoofdstuk 5**. Een belangrijke beperking van IVUS VH is het feit dat het echosignaal niet doordringt door coronair calcium. Hierdoor ontstaat een akoestische schaduw, waarbinnen plaquekarakterisatie moeilijk is. Middels een nieuw algoritme werd deze akoestische schaduw gedetecteerd en gekwantificeerd. Deze gekwantificeerde volumina werden meegenomen met de totale hoeveelheid calcium. Hiermee werd getracht te compenseren voor de verwachte onderschatting van coronair calcium op IVUS VH. Het bleek dat het toepassen van dit akoestische schaduwalgoritme de overeenkomst tussen IVUS VH en QCT voor het bepalen van coronair calcium verbeterde.

In **Hoofdstuk 6** wordt de mogelijkheid om met QCT de Agatston coronair calcium (CAC) score te bepalen in contrast-CT datasets onderzocht. Hiervoor werden 100 patiënten random geselecteerd uit verschillende CAC score categorieën (0, 1–99, 100–399, 400–999,  $\geq 1,000$ ). Een nieuw algoritme werd gebruikt om automatisch de CAC score te detecteren en kwantificeren in contrast-CT datasets. Deze CAC score werd gevalideerd met de Agatston CAC-score bepaald uit non-contrast CT datasets, zoals nu klinisch gebruikt wordt. De automatisch bepaalde CAC score uit contrast CT had een hoge correlatie en intra-class correlatie met de CAC score uit non-contrast CT. Daarnaast was er een goede overeenstemming binnen de verschillende CAC categorieën. Op basis hiervan werd geconcludeerd dat automatische detectie van de CAC score op contrast CT mogelijk is en een goede correlatie heeft met de non-contrast CAC score. Mogelijk leidt het klinisch toepassen van dit algoritme tot een reductie van de stralingbelasting voor de patiënt en tijdswinst omdat het verrichten van een non-contrast scan niet langer nodig is.

Eerdere studies hebben laten zien dat er een beperkte overeenkomst is tussen de aanwezigheid van een obstructieve stenose op CT en de aanwezigheid van myocardischemie op 'single-photon emission CT' SPECT. Mogelijkerwijs kan QCT deze correlatie verbeteren.

In **hoofdstuk 7** wordt daarom de relatie onderzocht tussen QCT parameters van coronairatherosclerose en de aanwezigheid van myocardischemie op SPECT. Veertig patiënten werden geïncludeerd die zowel CT coronairangiografie als SPECT hadden

ondergaan, binnen een tijdsinterval van 6 maanden. De CT coronairangiografie datasets werden eerst visueel geanalyseerd, per vat en per laesie. Vervolgens werd QCT verricht van elke laesie in de coronairvaatboom, om plaque lengte, 'plaqueburden', percentage stenosegraad en 'remodellingindex' te bepalen. Daarnaast werd de aanwezigheid van myocardischemie bepaald aan de hand van de 'summed difference score'. In totaal presenteerde 25 (62.5%) patiënten zich met myocardischemie in 37 stroomgebieden. Zowel stenosegraad als plaque-lengte was onafhankelijk gecorreleerd aan de aanwezigheid van myocardischemie. Beide kwantitatieve parameters hadden toegevoegde waarde bovenop baseline patiëntkarakteristieken en visueel bepaalde stenosegraad. Geconcludeerd werd dat QCT mogelijk een verbeterde bepaling van atherosclerose op CT mogelijk maakt en dus mogelijk geschikt kan zijn voor het beter identificeren van patiënten met myocardischemie.

In **hoofdstuk 8** wordt gekeken naar de prognostische waarde van een CTA-risicoscore die de ernst, locatie en compositie van coronairlijden op CTA combineert in één getal. De hypothese was dat een dergelijke score die meerdere kwantitatieve atherosclerose parameters samenvoegt in een getal, gebruikt kan worden voor risicostratificatie van patiënten. Het doel van deze studie was om te bepalen of een CTA risico score op basis van automatische kwantitatieve analyse van coronairlijden met QCT, risicostratificatie van patiënten mogelijk maakt. In 300 patiënten werd QCT verricht voor het automatisch detecteren en kwantificeren van alle coronarstenosen in de coronairvaatboom. Een nieuwe CTA-risicoscore werd gecreëerd die een weergave geeft van de totale atherosclerose belasting van een patiënt. Deze score is de optelsom van de locatie, ernst en compositie van atherosclerose per coronairsegment. Gedurende follow-up werden de volgende eindpunten geregistreerd: sterfte, myocardinfarct en late-revascularisatie (>90 dagen). In de 27 patiënten met obstructief coronairlijden ( $\geq 50\%$  stenose) vonden 27 events plaats, allen in patiënten met een hoge CTA risico score. Deze studie liet zien dat een volledig automatische analyse van coronairlijden op CT coronair angiografie middels QCT mogelijk is en gebruikt kan worden voor risicostratificatie van patiënten. Daarnaast toonde deze studie aan dat een nieuwe CTA-risicoscore die verschillende parameters van atherosclerose in één getal samenvat, nauwkeurige risicostratificatie van patiënten mogelijk maakt. De exacte klinische waarde van deze score moet echter nog worden bevestigd in grotere studies.

In de studie beschreven in **Hoofdstuk 9**, wordt gekeken naar de mogelijkheid om middels QCT veranderingen in coronairatherosclerose op seriële CT coronair angiografie te meten. Hiervoor werden 53 patiënten met stabiele angina geïncludeerd. Deze patiënten waren verwezen voor klinische evaluatie van pijn op de borst middels CT in het Rijnlandziekenhuis. Na minimaal 2 jaar werd de CT coronair angiografie

herhaald, om de verandering in coronairatherosclerose in de tijd te bepalen. Om de veranderingen zo accuraat mogelijk te bepalen werd alle CT data geanalyseerd met QCT. Parameters van dimensie en compositie van atherosclerose werden vergeleken om te bepalen of er progressie of regressie van atherosclerose was. In 32 patiënten (60%) was er regressie van het totale atheromavolume, terwijl 21 patiënten (40%) progressie van atheroma hadden. Patiënten met progressie hadden progressie van alle vier verschillende plaque componenten. Patiënten met regressie van ziekten hadden regressie van alle plaquecomponenten, behalve calcium. Middels deze studie werd aangetoond dat het bepalen van progressie van atherosclerose mogelijk is met QCT. Mogelijk kan QCT in de toekomst worden gebruikt voor het bepalen van de effectiviteit van anti-atherosclerose therapie.

## Deel 2

Deel 2 van deze thesis bespreekt de waarde van CT coronair angiografie in hoog-risico diabetespatiënten zonder angina pectoris klachten.

**Hoofdstuk 10** is een evaluatie van veranderingen in myocardischemie op SPECT in 2 jaar tijd, in een cohort diabetes patiënten zonder cardiale klachten of bekend coronairlijden. Daarnaast wordt in dit hoofdstuk gekeken naar de waarde van parameters van atherosclerose op CT om veranderingen in myocardischemie te voorspellen. De patiënten populatie bestond uit 100 hoog risico patiënten zonder cardiale klachten die waren verwezen voor cardiovasculaire risico analyse. Alle patiënten kregen een CAC-score, CT coronairangiografie en SPECT myocardperfusie scintigrafie op baseline. Na 2 jaar werd SPECT myocardperfusie scintigrafie herhaald om eventuele progressie van myocardischemie vast te stellen. Het aantal patiënten met toename van ischemie was zeer beperkt. Slechts weinig patiënten presenteerden zich met nieuwe ischemie, terwijl andere patiënten afname van ischemie lieten zien. Atherosclerose parameters op CT coronairangiografie waren niet gerelateerd aan veranderingen in myocardischemie.

**In hoofdstuk 11** wordt de prognostische waarde onderzocht van CT coronair angiografie in een groot cohort diabetes patiënten zonder cardiale klachten. In totaal werden 525 patiënten geïncludeerd, die zowel een CAC score als een CT coronairangiografie ondergingen. Gedurende follow-up werd gekeken naar sterfte, myocardinfarct en late-revascularisatie (>90dagen). Na een mediane follow-up van 5 (IQR 2.7-6.5) jaar, trad een event op in 65(14%) patiënten. CT coronairangiografie toonde een hoge prevalentie van coronairlijden (85%), met name niet obstructief (51%). De

prognose van patiënten met een normale CT was zeer gunstig (incidentie 3%). Er was een toename in incidentie van events met toenemende CAC-score of ernst van coronairstenose. Daarnaast had de aanwezigheid van obstructief of ernstig coronairlijden onafhankelijke voorspellende waarde voor het optreden van events. Op basis hiervan werd geconcludeerd dat CT coronairangiografie voorspellende waarde heeft in diabetes patiënten zonder cardiale klachten. Met name de prognose van patiënten zonder coronairlijden op CT is uitstekend.

## Conclusies

Dit proefschrift onderzoekt de waarde van QCT voor het verder verbreden van klinische toepasbaarheid en verhogen van diagnostische waarde van CT coronairangiografie. Automatisch karakterisatie van coronairatherosclerose is mogelijk en toont een goede correlatie met IVUS VH. In de toekomst is meer onderzoek nodig om ook kwantificatie van stents en coronaire bloedstroom mogelijk te maken.

Waarschijnlijk krijgen kwantitatieve parameters van afmetingen en plaque samenstelling in de toekomst meer klinische waarde. CT coronairangiografie faciliteert meer dan alleen analyse van de aanwezigheid van atherosclerose of obstructieve stenose. Daarom werd in dit proefschrift een nieuwe CT risico score ontwikkelend op basis van QCT, welke informatie over de locatie, compositie en ernst van coronairatherosclerose samenvoegt in een score. Deze CTA risico score kan gebruikt worden voor risicostatificatie van patiënten met verdenking op coronairlijden. Verder onderzoek zal worden gedaan om de klinische waarde van deze CT risico score verder te bevestigen in externe patiëntcohorten.

In deze dissertatie is ook gekeken naar de mogelijkheid om met QCT veranderingen in atherosclerose over de tijd te kwantificeren. Dit zou in de toekomst klinisch goed toepasbaar zijn voor het meten van de effectiviteit van antiarteriosclerose therapie. Ook zou deze techniek meer inzicht kunnen verschaffen over het natuurlijk beloop van coronairatherosclerose.

Een nadeel van CT coronairangiografie is het feit dat deze techniek geen inzicht verschaft in thermodynamische consequenties van coronairstenosen. Dit proefschrift laat zien dat QCT een betere correlatie heeft met de aanwezigheid van myocardischemie op SPECT in vergelijking tot reguliere visuele analyse van CT coronairangiografie.

Met betrekking tot de klinische setting van hoog risico diabetes patiënten zonder angina pectoris kunnen op basis van dit proefschrift twee dingen worden geconcludeerd. Ten eerste: indien patiënten met diabetes een accurate farmacologische behandeling krijgen, is het aantal patiënten dat zich presenteert met toename van myocardischemie zeer beperkt. Ten tweede is de prognose van deze patiënten goed.

De lange termijn overleving, laat weinig events zien. Met name diabetes patiënten zonder coronairlijden op CT coronairangiografie hebben een goede prognose. Hoewel dit proefschrift de prognostische waarde van CTA heeft bevestigd, is vooralsnog niet duidelijk of het doen van beeldvorming in deze patiënten groep invloed heeft op overleving en uitkomst. Mogelijk kan CT coronairangiografie of coronair calcium score in de toekomst worden gebruikt voor het individualiseren van medicamenteuze therapie in deze uitdagende patiëntenpopulatie.

## List of publications

As on August 15<sup>th</sup> 2016

van Velzen J. E., de Graaf F. R., de Graaf M. A., Schuijf J. D., Kroft L. J., de Roos A., Reiber J. H., Bax J. J., Jukema J. W., Boersma E., Schalij M. J., van der Wall E. E. Comprehensive assessment of spotty calcifications on computed tomography angiography: comparison to plaque characteristics on intravascular ultrasound with radiofrequency backscatter analysis. *J Nucl Cardiol* 2011;18:893-903.

de Graaf M. A., Jager K. J., Zoccali C., Dekker F. W. Matching, an appealing method to avoid confounding? *Nephron Clin Pract* 2011;118:c315-8.

van Velzen J. E., de Graaf M. A., Ciarka A., de Graaf F. R., Schalij M. J., Kroft L. J., de Roos A., Jukema J. W., Reiber J. H., Schuijf J. D., Bax J. J., van der Wall E. E. Non-invasive assessment of atherosclerotic coronary lesion length using multi-detector computed tomography angiography: comparison to quantitative coronary angiography. *Int J Cardiovasc Imaging* 2012;28:2065-71.

de Graaf M. A., Jukema J. W. High coronary plaque load: a heavy burden. *Eur Heart J* 2013;34:3168-70.

Roos C. J., Witkowska A. J., de Graaf M. A., Veltman C. E., Delgado V., de Grooth G. J., Jukema J. W., Bax J. J., Scholte A. J. Association of atherosclerosis in the descending thoracic aorta with coronary artery disease on multi detector row computed tomography coronary angiography in patients with suspected coronary artery disease. *Int J Cardiovasc Imaging* 2013;29:1829-37.

Kirisli H. A., Schaap M., Metz C. T., Dharampal A. S., Meijboom W. B., Papadopoulou S. L., Dedic A., Nieman K., de Graaf M. A., Meijs M. F., Cramer M. J., Broersen A., Cetin S., Eslami A., Florez-Valencia L., Lor K. L., Matuszewski B., Melki I., Mohr B., Oksuz I., Shahzad R., Wang C., Kitslaar P. H., Unal G., Katouzian A., Orkisz M., Chen C. M., Precioso F., Najman L., Masood S., Unay D., van Vliet L., Moreno R., Goldenberg R., Vucini E., Krestin G. P., Niessen W. J., van Walsum T. Standardized evaluation framework for evaluating coronary artery stenosis detection, stenosis quantification and lumen segmentation algorithms in computed tomography angiography. *Med Image Anal* 2013;17:859-76.

## List of publications

de Graaf M. A., El-Naggar H. M., Boogers M. J., Veltman C. E., Broersen A., Kitslaar P. H., Dijkstra J., Kroft L. J., Al Younis I., Reiber J. H., Bax J. J., Delgado V., Scholte A. J. Automated quantitative coronary computed tomography correlates of myocardial ischaemia on gated myocardial perfusion SPECT. *Eur J Nucl Med Mol Imaging* 2013;40:1171-80.

de Graaf M. A., Broersen A., Kitslaar P. H., Roos C. J., Dijkstra J., Lelieveldt B. P., Jukema J. W., Schalij M. J., Delgado V., Bax J. J., Reiber J. H., Scholte A. J. Automatic quantification and characterization of coronary atherosclerosis with computed tomography coronary angiography: cross-correlation with intravascular ultrasound virtual histology. *Int J Cardiovasc Imaging* 2013;29:1177-90.

Bruschke A. V., Veltman C. E., de Graaf M. A., Vliegen H. W. Myocardial bridging: what have we learned in the past and will new diagnostic modalities provide new insights? *Neth Heart J* 2013;21:6-13.

de Graaf M. A., van Velzen J. E., de Graaf F. R., Schuijf J. D., Dijkstra J., Bax J. J., Reiber J. H., Schalij M. J., van der Wall E. E., Jukema J. W. The maximum necrotic core area is most often located proximally to the site of most severe narrowing: a virtual histology intravascular ultrasound study. *Heart Vessels* 2013;28:166-72.

Veltman C. E., Hoogslag G. E., Kharbanda R. K., de Graaf M. A., van Zwet E. W., van der Hoeven B. L., Delgado V., Bax J. J., Scholte A. J. Relation between coronary arterial dominance and left ventricular ejection fraction after ST-segment elevation acute myocardial infarction in patients having percutaneous coronary intervention. *Am J Cardiol* 2014;114:1646-50.

Daniels L. A., Krol S. D., de Graaf M. A., Scholte A. J., van 't Veer M. B., Putter H., de Roos A., Schalij M. J., van de Poll-Franse L. V., Creutzberg C. L. Impact of cardiovascular counseling and screening in Hodgkin lymphoma survivors. *Int J Radiat Oncol Biol Phys* 2014;90:164-71.

de Graaf M. A., Broersen A., Ahmed W., Kitslaar P. H., Dijkstra J., Kroft L. J., Delgado V., Bax J. J., Reiber J. H., Scholte A. J. Feasibility of an automated quantitative computed tomography angiography-derived risk score for risk stratification of patients with suspected coronary artery disease. *Am J Cardiol* 2014;113:1947-55.

Daniels L. A., Krol A. D., de Graaf M. A., Scholte A. J., Van't Veer M. B., Putter H., de Roos A., Schalij M. J., Creutzberg C. L. Screening for coronary artery disease after

mediastinal irradiation in Hodgkin lymphoma survivors: phase II study of indication and acceptance. *Ann Oncol* 2014;25:1198-203.

Kamperidis V., de Graaf M. A., Broersen A., Ahmed W., Sianos G., Delgado V., Dijkstra J., Bax J. J., Scholte A. J. Prognostic value of aortic and mitral valve calcium detected by contrast cardiac computed tomography angiography in patients with suspicion of coronary artery disease. *Am J Cardiol* 2014;113:772-8.

Kirisli H. A., Gupta V., Shahzad R., Al Younis I., Dharampal A., Geuns R. J., Scholte A. J., de Graaf M. A., Joemai R. M., Nieman K., van Vliet L., van Walsum T., Lelieveldt B., Niessen W. J. Additional diagnostic value of integrated analysis of cardiac CTA and SPECT MPI using the SMARTVis system in patients with suspected coronary artery disease. *J Nucl Med* 2014;55:50-7.

van Ginkel A., Sorgdrager B., de Graaf M. A., Karalis I., Ajmone Marsan N. ST-segment elevation associated with allergic reaction to echocardiographic contrast agent administration. *Neth Heart J* 2014;22:77-9.

Caselli C., De Graaf M. A., Lorenzoni V., Rovai D., Marinelli M., Del Ry S., Gianni D., Bax J. J., Neglia D., Scholte A. J. HDL cholesterol, leptin and interleukin-6 predict high risk coronary anatomy assessed by CT angiography in patients with stable chest pain. *Atherosclerosis* 2015;241:55-61.

van Rosendaal A. R., de Graaf M. A., Scholte A. J. Myocardial CT perfusion for the prediction of obstructive coronary artery disease, valuable or not? *Cardiovasc Diagn Ther* 2015;5:63-6.

Neglia D., Rovai D., Caselli C., Pietila M., Teresinska A., Aguade-Bruix S., Pizzi M. N., Todiere G., Gimelli A., Schroeder S., Drosch T., Poddighe R., Casolo G., Anagnostopoulos C., Pugliese F., Rouzet F., Le Guludec D., Cappelli F., Valente S., Gensini G. F., Zawaideh C., Capitano S., Sambuceti G., Marsico F., Perrone Filardi P., Fernandez-Golfín C., Rincon L. M., Graner F. P., de Graaf M. A., Fiechter M., Stehli J., Gaemperli O., Reyes E., Nkomo S., Maki M., Lorenzoni V., Turchetti G., Carpeggiani C., Marinelli M., Puzzuoli S., Mangione M., Marcheschi P., Mariani F., Gianni D., Nekolla S., Lombardi M., Sicari R., Scholte A. J., Zamorano J. L., Kaufmann P. A., Underwood S. R., Knutti J. Detection of significant coronary artery disease by noninvasive anatomical and functional imaging. *Circ Cardiovasc Imaging* 2015;8.

## List of publications

de Graaf M. A., Roos C. J., Mansveld J. M., Kharagjitsingh A. V., Dibbets-Schneider P., Kroft L. J., Jukema J. W., Ficaro E. P., Bax J. J., Scholte A. J. Changes in ischaemia as assessed with single-photon emission computed tomography myocardial perfusion imaging in high-risk patients with diabetes without cardiac symptoms: relation with coronary atherosclerosis on computed tomography coronary angiography. *Eur Heart J Cardiovasc Imaging* 2015;16:863-70.

Kooij M., Vliegen H. W., de Graaf M. A., Hazekamp M. G. Surgical treatment of aberrant aortic origin of coronary arteries. *Eur J Cardiothorac Surg* 2015;48:724-30; discussion 30-1.

van Rosendael A. R., de Graaf M. A., Scholte A. J. Cardiac arrest during vigorous exercise: coronary plaque rupture or myocardial ischaemia? *Neth Heart J* 2015;23:130-2.

Katsanos S., Debonnaire P., van der Kley F., van Rosendael P. J., Joyce E., de Graaf M. A., Schalijs M. J., Scholte A. J., Bax J. J., Ajmone Marsan N., Delgado V. Position of Edwards SAPIEN transcatheter valve in the aortic root in relation with the coronary ostia: implications for percutaneous coronary interventions. *Catheter Cardiovasc Interv* 2015;85:480-7.

Ahmed W., de Graaf M. A., Broersen A., Kitslaar P. H., Oost E., Dijkstra J., Bax J. J., Reiber J. H., Scholte A. J. Automatic detection and quantification of the Agatston coronary artery calcium score on contrast computed tomography angiography. *Int J Cardiovasc Imaging* 2015;31:151-61.

Veltman C. E., van der Hoeven B. L., Hoogslag G. E., Boden H., Kharbanda R. K., de Graaf M. A., Delgado V., van Zwet E. W., Schalijs M. J., Bax J. J., Scholte A. J. Influence of coronary vessel dominance on short- and long-term outcome in patients after ST-segment elevation myocardial infarction. *Eur Heart J* 2015;36:1023-30.

Gao X., Kitslaar P. H., Budde R. P., Tu S., de Graaf M. A., Xu L., Xu B., Scholte A. J., Dijkstra J., Reiber J. H. Automatic detection of aorto-femoral vessel trajectory from whole-body computed tomography angiography data sets. *Int J Cardiovasc Imaging* 2016;32:1311-22.

van Rosendael A. R., de Graaf M. A., Dimitriu-Leen A. C., van Zwet E. W., van den Hoogen I. J., Kharbanda R. K., Bax J. J., Kroft L. J., Scholte A. J. The influence of clinical and acquisition parameters on the interpretability of adenosine stress myocardial computed tomography perfusion. *Eur Heart J Cardiovasc Imaging* 2016.

Liga R., Vontobel J., Rovai D., Marinelli M., Caselli C., Pietila M., Teresinska A., Aguade-Bruix S., Pizzi M. N., Todiere G., Gimelli A., Chiappino D., Marraccini P., Schroeder S., Drosch T., Poddighe R., Casolo G., Anagnostopoulos C., Pugliese F., Rouzet F., Le Guludec D., Cappelli F., Valente S., Gensini G. F., Zawaideh C., Capitanio S., Sambuceti G., Marsico F., Filardi P. P., Fernandez-Golfin C., Rincon L. M., Graner F. P., de Graaf M. A., Stehli J., Reyes E., Nkomo S., Maki M., Lorenzoni V., Turchetti G., Carpeggiani C., Puzzuoli S., Mangione M., Marcheschi P., Giannessi D., Nekolla S., Lombardi M., Sicari R., Scholte A. J., Zamorano J. L., Underwood S. R., Knuuti J., Kaufmann P. A., Neglia D., Gaemperli O. Multicentre multi-device hybrid imaging study of coronary artery disease: results from the EVAluation of INtegrated Cardiac Imaging for the Detection and Characterization of Ischaemic Heart Disease (EVINCI) hybrid imaging population. *Eur Heart J Cardiovasc Imaging* 2016.

Caselli C., Prontera C., Liga R., De Graaf M. A., Gaemperli O., Lorenzoni V., Ragusa R., Marinelli M., Del Ry S., Rovai D., Giannessi D., Aguade-Bruix S., Clemente A., Bax J. J., Lombardi M., Sicari R., Zamorano J., Scholte A. J., Kaufmann P. A., Knuuti J., Underwood S. R., Clerico A., Neglia D. Effect of Coronary Atherosclerosis and Myocardial Ischemia on Plasma Levels of High-Sensitivity Troponin T and NT-proBNP in Patients With Stable Angina. *Arterioscler Thromb Vasc Biol* 2016;36:757-64.

Koenraadt W. M., Tokmaji G., DeRuiter M. C., Vliegen H. W., Scholte A. J., Siebelink H. M., Gittenberger-de Groot A. C., de Graaf M. A., Wolterbeek R., Mulder B. J., Bouma B. J., Schalij M. J., Jongbloed M. R. Coronary anatomy as related to bicuspid aortic valve morphology. *Heart* 2016;102:943-9.

van Rosendaal A. R., Kroft L. J., Broersen A., Dijkstra J., van den Hoogen I. J., van Zwet E. W., Bax J. J., de Graaf M. A., Scholte A. J. Relation between quantitative coronary CTA and myocardial ischemia by adenosine stress myocardial CT perfusion. *J Nucl Cardiol* 2016.

Dimitriu-Leen A. C., Scholte A. J., van Rosendaal A. R., van den Hoogen I. J., Kharagjitsingh A. V., Wolterbeek R., Knuuti J., Kroft L. J., Delgado V., Jukema J. W., de Graaf M. A., Bax J. J. Value of Coronary Computed Tomography Angiography in Tailoring Aspirin Therapy for Primary Prevention of Atherosclerotic Events in Patients at High Risk With Diabetes Mellitus. *Am J Cardiol* 2016;117:887-93.

Dedic A., Ten Kate G. J., Roos C. J., Neefjes L. A., de Graaf M. A., Spronk A., Delgado V., van Lennep J. E., Moelker A., Ouhlous M., Scholte A. J., Boersma E., Sijbrands

#### List of publications

E. J., Nieman K., Bax J. J., de Feijter P. J. Prognostic Value of Coronary Computed Tomography Imaging in Patients at High Risk Without Symptoms of Coronary Artery Disease. *Am J Cardiol* 2016;117:768-74.

de Graaf M. A., van Rosendaal A. R., Kroft L. J., Vliegen H. W., Hazekamp M. G., Bax J. J., Scholte A. J. An anomalous left coronary artery with a malignant course: coronary angiography and myocardial perfusion imaging with computed tomography. *Neth Heart J* 2016;24:154-5.

Broersen A., de Graaf M. A., Eggermont J., Wolterbeek R., Kitslaar P. H., Dijkstra J., Bax J. J., Reiber J. H., Scholte A. J. Enhanced characterization of calcified areas in intravascular ultrasound virtual histology images by quantification of the acoustic shadow: validation against computed tomography coronary angiography. *Int J Cardiovasc Imaging* 2016;32:543-52.

van den Hoogen I. J., de Graaf M. A., Roos C. J., Leen A. C., Kharagjitsingh A. V., Wolterbeek R., Kroft L. J., Wouter Jukema J., Bax J. J., Scholte A. J. Prognostic value of coronary computed tomography angiography in diabetic patients without chest pain syndrome. *J Nucl Cardiol* 2016;23:24-36.

# Dankwoord

Het onderzoek, zoals beschreven in dit proefschrift, is uitgevoerd op de afdeling Cardiologie van het Leids Universitair Medisch Centrum (LUMC). Hierbij is nauw samengewerkt met het Laboratorium voor Klinische en Experimentele Beeldverwerking (LKEB) en de afdeling Nucleaire Geneeskunde van het LUMC. Ik wil een ieder die direct of indirect een bijdrage heeft geleverd aan mijn onderzoek heel hartelijk bedanken. Een aantal mensen wil ik hierbij in het bijzonder noemen.

Arthur, ik ben je zeer dankbaar voor alle hulp tijdens mijn onderzoek. Ik kijk dan ook met veel genoegen terug op de congresbezoeken, het opzetten van perfusie CT en het Evinci-project. Ik heb je humor en betrokkenheid erg gewaardeerd, je was altijd zeer benaderbaar en laagdrempelig bereid tot overleg.

Prof. Bax, Jeroen. Van jouw inzicht in het veld en je talent om nieuwe richtingen te zien heb ik erg veel geleerd. Dank voor je altijd kritische blik en het streven naar perfectie.

Prof Jukema, Wouter. Dank voor je betrokkenheid en de uitnodiging om samen stukken te schrijven. Met veel plezier kijk ik terug op de vele uren CT-scans beoordelen.

Victoria, thank you for all your help with difficult statistics and complicated projects. I have really appreciated your critical opinion during our meetings.

Greetje, dank voor alle tijd die je hebt geïnvesteerd in het beoordelen van CT-scans en de prettige samenwerking hierbij.

De mensen van het LKEB: Hans, Boudewijn, Jouke, Pieter en Alex. Dank voor de boeiende samenwerking. Samen konden we de klinische en technische aspecten van CT coroniarangiografie samenvoegen tot nieuwe klinisch toepasbare software. Steeds meer gingen we “dezelfde taal” spreken.

Alex, bijzonder veel dank voor onze intensieve, prettige samenwerking en de vele uren die je hebt gestoken in de technische ondersteuning van de projecten. Het was een zeer waardevolle band.

De afdeling Nucleaire Geneeskunde, in het bijzonder Petra. Veel dank voor de ondersteuning bij het verwerken van de SPECT beelden. Zonder jouw hulp was het niet gelukt.

Ron Wolterbeek, dank voor alle statistische hulp en de bereidheid altijd weer dingen uit te leggen.

Het oude-CT-team: Joanne, Joella, Fleur, Mark, Noor. Mijn onderzoekscarrière is bij jullie begonnen. Dank voor alle dingen die ik van jullie heb geleerd en voor jullie werk waarop ik kon voortborduren.

Het nieuwe-CT-team: Carolien, Kees, Marieke, Philippe, Ibtihal, Maaïke, Sanjay, Madelien, Aukelien, Alexander. Met veel plezier kijk ik terug op de vele uren achter de Vitrea, de CT-etentjes en de congressen. Ook veel dank aan alle andere “tuincollega’s” waarmee ik een hele leuke tijd heb gehad.

“Mijn” wetenschapsstage studenten Wehab, Inge en Josanne. Veel dank voor jullie enthousiasme en inzet. Ik heb bewondering voor jullie doorzettingsvermogen en talent om al zo vroeg in je studie zo zelfstandig onderzoek te doen. Het was een genoegen om aan de basis van jullie verdere carrière te staan.

Jeroen, al mijn gehele studietijd ben jij mijn beste maatje. Dank voor je luisterend oor, je hulp bij het lezen van mijn stukken en je gewaardeerde adviezen, maar vooral voor alle etentjes en de gezellig uitjes. Dank dat je mijn paranimf wilt zijn

Banne, met jou deel ik de liefde voor het koude. Het is begonnen met skiën en heeft uiteindelijk geleid tot de oprichting van de ‘Scheve Schaats’. Veel dank voor je organisatorische talent en je inzet. Dank dat ook jij mijn paranimf wilt zijn.

Alle andere vrienden van Faust, Huize Hooi, het 96<sup>e</sup> bestuur van de M.F.L.S., de Scheve Schaats en alle anderen. “Zonder ontspanning geen inspanning”. Dank voor alle gezelligheid, mooie reizen en de gezamenlijke sportieve prestaties.

Lieve pap, lieve mam (moeders). Dank, onvoorstelbaar veel dank! Jullie betrokkenheid en vertrouwen waardeer ik zeer. Pap, dank voor alle gesprekken en je adviezen. Met jou deel ik de liefde voor het vak. Ik hoop later iets van jouw communicatieve en sociale talenten als arts te mogen bezitten. Mam, dank voor al je lieve mails en berichtjes. Ik hoop iets van jouw hartelijkheid en attentheid te hebben meegekregen.

Lieve omi en in herinnering, lieve opa. Ook aan jullie veel dank. We hebben een hechte band en jullie spelen een belangrijke rol in mijn leven. Mijn communicatieve vaardigheden heb ik zonder twijfel aan mijn grootvader te danken. Ik heb er elke dag profijt van en ben je heel erg dankbaar.

Lieve Iris. De laatste loodjes wegen het zwaarst en die kon ik gelukkig delen met jou. Ik ben je dankbaar voor je begrip en je geduld. Je maakt mijn leven waardevoller en door jou voelt ons huis als een thuis.

## Curriculum Vitae

Michiel Alexander de Graaf werd geboren op 27 juli 1988 te Woerden. Hij behaalde in 2006 zijn VWO diploma (cum laude) aan het Kalsbeek College in Woerden. In datzelfde jaar begon hij zijn studie Geneeskunde aan het Leids Universitair Medisch Centrum. Gedurende zijn studie maakte hij deel uit van diverse onderwijscommissie, waaronder de opleidingscommissie en de curriculumherzieningscommissie. In het collegejaar 2008-2009 was hij lid van het bestuur van de studievereniging van Geneeskunde, de Medische Faculteit der Leidse Studenten (M.F.L.S.) waar hij de functie van Lid Onderwijs Geneeskunde vervulde. In de zomer 2009 begon hij als student-onderzoeker bij de afdeling Cardiologie in het LUMC waar hij werkte onder leiding van dr. J.E. van Velzen en dr. J.D. Schuijf. Het doctoraal diploma werd behaald in augustus 2011. Voor dat hij startte met de coschappen, begon hij in mei 2011 met zijn promotieonderzoek bij de afdeling Cardiologie onder leiding van prof. dr. J.J. Bax, prof dr. Jukema en dr. A.J.H.A. Scholte. De resultaten hiervan staan beschreven in dit proefschrift. In november 2014 vervolgde hij zijn studie Geneeskunde en startte met de coschappen, welke hij in september 2016 cum laude afronde. Aansluitend startte hij met de cardiologie opleiding in het MCH-Bronovo (dr Y.W.J. Sijpkens en dr P.R.M. van Dijkman), deze zal worden vervolgd in het Leids Universitair Medisch Centrum (prof. dr. M.J. Schalij).